REPORT DOCUMENTATION PAGE

1. Recipient's Reference	2. Originator's Reference	3. Further Reference	4. Security Classification of Document
	AGARD-AG-292	ISBN 92-835-0341-4	UNCLASSIFIED

5. Originator

Advisory Group for Aerospace Research and Development
North Atlantic Treaty Organization
7 rue Ancelle, 92200 Neuilly sur Seine, France

6. Title

HELICOPTER FATIGUE DESIGN GUIDE

7. Presented at

8. Author(s)/Editor(s)	9. Date
Edited by F.Liard	November 1983
10. Author's/Editor's Address	11. Pages
	278

12. Distribution Statement

13. Keywords/Descriptors

Helicopters
Design
Fatigue (materials)

14. Abstract

In the course of the past few years the Structures and Materials Panel of AGARD has considered a number of aspects the of fatigue problem as it affects helicopters. The present publication constitutes a review document in which is distilled the experience of specialists from amongst the helicopter manufacturing nations of NATO. It is aimed expecially at those in design offices and test houses who undertake rotary wing aircraft design and who need information by which to determine fatigue strength and behaviour.

This AGARDograph was sponsored by the Structures and Materials Panel of AGARD.

AGARD-AG-292

AGARD-AG-292

AGARD

ADVISORY GROUP FOR AEROSPACE RESEARCH & DEVELOPMENT

7 RUE ANCELLE 92200 NEUILLY SUR SEINE FRANCE

AGARDograph No. 292

Helicopter Fatigue Design Guide

NORTH ATLANTIC TREATY ORGANIZATION

NORTH ATLANTIC TREATY ORGANIZATION

ADVISORY GROUP FOR AEROSPACE RESEARCH AND DEVELOPMENT, Paris

(ORGANISATION DU TRAITE DE L'ATLANTIQUE NORD)

AGARDograph No.292

HELICOPTER FATIGUE DESIGN GUIDE

Edited by

F.Liard

This AGARDograph was sponsored by the Structures and Materials Panel of AGARD.

THE MISSION OF AGARD

The mission of AGARD is to bring together the leading personalities of the NATO nations in the fields of science and technology relating to aerospace for the following purposes:

- Exchanging of scientific and technical information;
- Continuously stimulating advances in the aerospace sciences relevant to strengthening the common defence posture;
- Improving the co-operation among member nations in aerospace research and development;
- Providing scientific and technical advice and assistance to the North Atlantic Military Committee in the field of aerospace research and development;
- Rendering scientific and technical assistance, as requested, to other NATO bodies and to member nations in connection with research and development problems in the aerospace field;
- Providing assistance to member nations for the purpose of increasing their scientific and technical potential;
- Recommending effective ways for the member nations to use their research and development capabilities for the common benefit of the NATO community.

The highest authority within AGARD is the National Delegates Board consisting of officially appointed senior representatives from each member nation. The mission of AGARD is carried out through the Panels which are composed of experts appointed by the National Delegates, the Consultant and Exchange Programme and the Aerospace Applications Studies Programme. The results of AGARD work are reported to the member nations and the NATO Authorities through the AGARD series of publications of which this is one.

Participation in AGARD activities is by invitation only and is normally limited to citizens of the NATO nations.

Published November 1983

ISBN 92-835-0341-4

Printed by Specialised Printing Services Limited
40 Chigwell Lane, Loughton, Essex IG10 3TZ

PREFACE

The fatigue strength of the main mechanical components of the helicopter (i.e. rotor assembly, transmission systems) and of the primary structural elements in its airframe has always constituted an area of major concern for manufacturers as well as for airworthiness authorities and users.

At the same time, the increasing utilisation of helicopters in the array of modern weapon systems, together with the introduction of new materials or technologies, has accentuated the need for NATO forces to master the problems of fatigue phenomena related to helicopters.

In the course of the last eight years, the Structures and Materials Panel of AGARD has undertaken, successively, a set of working activities which has resulted in publications on the following topics:

(1) Helicopter Design Mission Load Spectra:
Proceedings of a Specialists' Meeting held in Ottawa in the Spring of 1976

(2) Survey of Present Regulations and Substantiation Procedures:
Proceedings of an experts' meeting held in Florence in September 1978

(3) Helicopter Fatigue Life Prediction:
Proceedings of a Specialists' Meeting held in Aix-en-Provence in September 1980.

The present publication constitutes a review document which assembles the experience of specialists from helicopter producing NATO countries; it is intended for those design department and test laboratory personnel who carry responsibility for rotary wing design and who need to determine fatigue strength and behaviour.

This Preface would not be complete without a few words of acknowledgement to the experts who agreed to contribute to the writing of the various chapters of this Manual. I would especially like to express thanks to Mr F.Liard, a former engineer at "Aerospatiale", who undertook the difficult task of ensuring that degree of coordination which the preparation of this document involved.

J.M.FEHRENBACH
Chairman, Sub-Committee
on Helicopter Fatigue

* * *

PREFACE

La résistance en fatigue des composants mécaniques principaux (ensemble rotor, systèmes de transmission) et des éléments de la structure primaire des cellules d'hélicoptères a toujours constitué un domaine majeur de préoccupation tant pour les industriels constructeurs que pour les services officiels chargés de la règlementation et les organismes utilisateurs de ces matériels.

Par ailleurs, l'utilisation croissante des hélicoptères dans la panoplie des systèmes d'armes modernes, conjuguée avec l'introduction de nouveaux matériaux ou technologies accentue l'importance que présente pour les forces de l'O.T.A.N. ce problème de la maitrise des phénomènes de fatigue intéressant les hélicoptères.

La commission Structures et Matériaux de l'AGARD a été conduite à proposer et développer une série de réflexions dans ce domaine au cours des huit dernières années, matérialisées successivement par:

– une réunion de spécialistes en avril 1976 à Ottawa sur le thème:
(1) Spectres de charges pour la conception des hélicoptères

– une réunion d'experts en septembre 1978 à Florence sur le thème:
(2) Revue des règlements actuels et des méthodes de démonstration

– une réunion de spécialistes en septembre 1980 à Aix-en-Provence sur le thème:
(3) Justification de la durée de vie en fatigue des hélicoptères.

La présente publication constitue un document de synthèse qui rassemble l'expérience des spécialistes des pays de l'O.T.A.N. producteurs d'hélicoptères à l'attention des personnels des bureaux d'études et des laboratoires d'essais qui

ont la responsabilité de concevoir des matériels à voilure tournante et d'en justifier la résistance et le comportement en fatigue.

Qu'il me soit permis, au terme de cette préface de remercier tous les experts qui ont accepté de contribuer à la rédaction des différents chapitres de ce manuel et plus particulièrement Mr F.Liard, ancien ingénieur à l'Aérospatiale, qui a bien voulu assurer la coordination du travail difficile que constituait l'élaboration de ce document.

J.M.FEHRENBACH
Président du sous-comité pour
la Fatigue des Hélicoptères

CONTENTS

CHAPTER 1
INTRODUCTION

by

Ferdinand F.Liard
Former Scientific Department Head
Société Nationale Industrielle Aérospatiale
B.P.13 – 13725 Marignane CEDEX
France

CONTENTS

1.1 BACKGROUND

Although the modern helicopter only came in the thirties, its designers have had to face, among other difficult problems, high cycle fatigue causing a number of serious accidents.

Of course, fatigue has already been studied by automotive engineers in the 19th century, but its contingent nature was not understood. Even some thirty years back a few project engineers still considered that the test of a single part - unbroken at twice the desired life under flight loads - was the proof of its safety.

During the last decades a tremendous amount of work has been done on fatigue, in the research laboratories as well as at industrial facilities. Unfortunately there is a lack of uniformity, as each country and sometimes each manufacturer develops its own methods.

The Structures and Material Panel of AGARD has been contributing to the exchange of knowledge on fatigue evaluation of helicopters by organising Symposia and Specialists Meetings and by creating a working group on the subject.

This working group has the task of defining the contents and organizing the publication by AGARD of a handbook on helicopter fatigue. It was decided eventually not to duplicate the wide general knowledge on fatigue which can be found in many books and to keep to what was particular to the helicopter. The handbook was then more modestly entitled «helicopter fatigue design guide».

1.2 SCOPE

Fatigue prevention is one of the most important aspects of aircraft safety and unfortunately the proof of an improper design may come after several years when a large number of flying hours have been accumulated on an important fleet.

In addition, it is known that the different methods in use do not give an equivalent level of safety.

The aim of this guide is to provide, at each step of the design, recommendations in order to get the best possible fatigue behaviour of every part of the helicopter : dynamic components gear boxes and airframes and to cover conventional materials and composites.

The presence of working group members and authors from the fixed-wing side is a good opportunity to suggest to helicopter designers, more familiar with the safe life approach, to profit, from the important work done for airplanes in the field of fracture mechanics.

The recommendations contained in this guide are by no means considered rules but it is hoped that, together with the analysis of the substantiation methods in use, they will help the manufacturers and the official services do their jobs in the best possible conditions.

1.3 LAYOUT

This Guide is divided into six sections and one appendix of which a short description is given thereafter.

Section 2 : General survey and evaluation of current procedures :

This section describes the broad phases of the fatigue design process and summarizes the actions to be taken at each step.

Section 3 : Spectra development :

This section gives a survey of the best existing methods to establish mission and load spectra considering, for both flight parameters and loads, the two usual steps of estimation or calculations and measurements.

For the difficult problem of rotor loads prediction, the comparison with flight test results shows the effect of the various possible refinements. This work is completed by the status of measurement techniques and a suggestion of counting methods in order to allow the automatic processing of test results for fatigue purposes.

Section 4 : Fatigue design data

This section covers both aspects of the crack initiation phase very familiar to helicopter specialists and of crack propagation phase. As the latter, commonly used in the fixed wing field, is becoming of great interest to helicopter manufacturers, a thorough analysis of theory and experiments has been made for metallic structures which opens the way to the very promissing field of composites.

It includes in addition a few considerations on the causes of variation of fatigue strength and covers the important aspect of statistical analysis of data processing.

Section 5 : Development and qualification procedures :

This chapter gives a survey of the rules and current methods used for fatigue development and qualification of military and civil helicopters in NATO countries. Using the load spectra and fatigue data of the previous chapters, it covers both the safe life and damage tolerant approaches for airframe and dynamic system at the various stages of development of the helicopter.

It also gives some comments on the tolerance to extreme environmental conditions.

Section 6 : Service load monitoring and structural integrity evaluation :

Service load monitoring allows to individualize the life of costly parts of each individual helicopter or at least, of the fleets of helicopters performing the same types of missions. Although little has been done yet, this chapter studies the different means towards achieving this goal and analyses the causes of errors in the structural integrity evaluation.

Appendix : HELIX and FELIX spectra

Following the line of the work already done for fighters, a Dutch - English - German team is working on the definition of the shape of simplified load spectra applicable to the dynamic components of any articulated (HELIX) or rigid (FELIX) rotor heads.

If applied systematically to specimens for fatigue testing its allows the direct comparison of the results coming from different laboratories and the selection of the best solutions without using MINER's hypothesis.

CHAPTER 2

GENERAL SURVEY AND EVALUATION OF CURRENT PROCEDURES

by

A.D. Hall

Westland Helicopters Limited
Yeovil, Somerset
England

CONTENTS

2.1. GENERAL SURVEY

The helicopter is a unique form of aircraft that provides lift by means of a system of rotating aerofoils. The classic, or "conventional", helicopter not only provides this lift from a large single main rotor but also uses that rotor to propel the aircraft in any chosen direction - forwards, backwards or sideways as well as up and down. Provision has to be made to react the torque applied to the main rotor and again, on the conventional helicopter, this is provided by an auxiliary rotor system mounted on the tail of the aircraft and applying thrust in the horizontal plane. This tail rotor also has a dual function, because it provides directional control as well.

Fatigue loadings on the helicopter are generated from many sources but the major inputs (at high frequency) arise from the asymmetrical airflows through the main and tail rotors in forward flight. Manoeuvring conditions produce additional low frequency loadings.

This chapter will describe in general terms, the procedure of design and fatigue substantiation of the helicopter and its components under all the fatigue load inputs that are recognised by the current "state of the art". Four broad phases of fatigue assessment are addressed as follows:

The Design Phase

The Development Phase

The Production Phase

The In-Service Phase

2.2. THE DESIGN PHASE

2.2.1. OPERATIONAL REQUIREMENTS AND SPECIFICATIONS

The helicopter is a remarkably versatile aircraft and its military utilisation may cover a wide range of operations, for example:

Navy: Anti-submarine Warfare
Commando Transport

Army: Utility
Tactical
Troop Carrying
Heavy Lift

Air Force: Transport
Search and Rescue

The sheer scale of the costs of designing and developing a modern helicopter mean that the manufacturer must endeavour to provide a common basic aircraft at a particular weight band that will be adaptable to as wide a range of uses as is possible. Economic common sense also dictates that in many cases commonality with a Civil type will also be sought.

It is essential in the initial phase to have a "Statement of intent", or its equivalent, from all the interested operators. This in turn will lead to the development of usage spectra for all the proposed roles that find a place in the Aircraft Specification.

The Aircraft Specification is the legal basis of the contract between the Manufacturer and Customer and, from our fatigue point of view, must state the fatigue lives to be achieved, the design requirements to be met and, as already mentioned, the spectrum, or spectra, of use.

In addition, the performance aims of speed, altitude, weight, e.g., climb rate etc. form part of the Aircraft Specification and the fatigue substantiation is based upon these "envelopes".

It may be pointed out at this stage that although "safe" fatigue life must form a legal basis of the aircraft specification, it is desirable that achieved lives should be very long or preferably unlimited for economic and logistic reasons. Even more desirable is the introduction of "Damage Tolerance" principles into mechanical systems of the helicopter which have hitherto been substantiated to "safe life" procedures. This philosophy will be discussed in depth later in the design guide.

2.2.2. SOURCES OF VIBRATORY LOADS

Fatigue loading on the helicopter and its components originates to a very large extent from the rotors themselves. Certainly the so-called "high frequency" loadings (3 - 4 Hz upwards) correspond to integral multiples of main and tail rotor rotational frequencies.

"Low-cycle" fatigue is also present in many components both from aircraft manoeuvring and gust loadings and also rotor stop-start cycles.

It is convenient to group components of the helicopter in respect of types of fatigue loading and the following is suggested:

(a) Rotor Systems

(b) Transmission

(c) Airframe

2.2.2.(a) Rotor Systems

The components included under this heading comprise the rotor blades, hubs and controls of both the main and tail rotor systems.

The main rotor blades generate lift by means of collective pitch application and translational flight, in any direction, is achieved by means of cyclic pitch. Collective pitch is the application of equal pitch increments to all blades to produce vertical thrust whereas cyclic pitch produces a variation of pitch in a specific relation to the azimuth position of each blade. Cyclic pitch produces a tilt of the rotor disc and hence a horizontal thrust vector to achieve the translational flight speed required.

In translational flight, the airflow through the rotor produces unequal aerodynamic lift distributions on the "advancing" and "retreating" blades and the effect is to generate fluctuating loads on any individual blade dependent upon its azimuth position.

The blade itself is, in effect, a rotating beam subjected to these vibratory load inputs and also the tension due to centrifugal load. The beam has a series of natural modes and frequencies of response in bending (in the plane of the rotor and also at 90° to the plane of the rotor) and torsion. Coupling between these modes is also present.

The blade response is therefore a complex one and, in terms of fatigue, it is clear that all sections of each blade require an in depth evaluation to determine their criticality.

Furthermore, at the root end attachment of the blades to the hub, residual shears apply vibratory loads to hub, gearbox and the airframe itself.

As mentioned previously, part of the blade response is torsional from lag - flap couplings and centre of pressure fluctuation. This produces a reaction at the blade pitch control horn generating fatigue loads in the control system. Predominant loads are usually at once rotor rotational speed in the rotating control system and "n" times rotor rotational speed in the fixed parts of the control system.

2.2.2.(b) Transmission

In the "conventional" helicopter, the transmission system consists of a main gearbox with power inputs from one or more engines. Outputs from this gearbox are to the main rotor, tail rotor and, usually, to accessories such as hydraulic and electrical systems etc. The drive to the main rotor involves a large reduction of rotational speed from the engine inputs and a similarly large increase in torque.

The main gearbox usually has to transfer the full lift, shears and bending moments from the main rotor hub to the airframe in addition to its fundamental purpose of torque transmission.

The drive to the tail rotor includes one or two further gearboxes that are required to change the direction of the drive and sometimes speed changes are made at these gearboxes.

The fatigue loadings in the power transmission system can thus come from many sources as follows:

Pulsed bending of the gear teeth (Reversed bending on "idler" gear teeth).

Aircraft manoeuvre loads and moments on the gear casing.

Gear tooth frequency loads on the casings.

High frequency rotor loads on the casings.

Rotating bending and fluctuation torsional loads on the gear shafts.

Fluctuating torsion on tail drive transmission shafts and couplings during directional manoeuvres.

Rolling loads on ball and roller bearings.

In addition the whole transmission system will respond to vibratory torsional loading of the main and tail rotors dependent on its natural torsional frequencies.

2.2.2.(c) Airframe

The major fatigue loadings on the airframe can come from the following sources:

Manoeuvring and "g" loadings.

Gust loads on the rotor.

Fin, tail plane and tail rotor loads.

Undercarriage loads.

Rotor order frequency loadings from main and tail rotor. The magnitude of these loads is very dependent on the dynamic natural frequencies of the fuselage in bending and torsion.

2.2.3. COMPONENTS TO BE CONSIDERED

In order to establish a list of the components of the helicopter to be the subject of the full fatigue substantiation it is necessary to understand the consequences of failure of those components.

The usual procedure is to categorise such parts both in terms of the severity of the failure consequences and also in terms of the loads and stresses to which they are subjected.

The highest such category is commonly called "Vital" or "Critical", and parts in this category may be described as "Components subject to significant fatigue loading and whose failure would cause catastrophe".

This category will contain many parts of the main and tail rotor system and controls etc. which are not redundant or duplicated, and which have limited damage tolerance necessitated by the "state of the art" of the helicopter design.

It is usually necessary to ensure integrity of these parts by an extensive fatigue testing programme as pure calculation is frequently unreliable at present.

The loading on such parts will eventually come from direct flight measurement.

The fatigue substantiation will be described in more detail later in this survey and in the Design Guide. Furthermore, parts in the "Vital" category will be subjected to the strictest possible control in manufacture such that variability in strength is minimised. All such parts must be identifiable and the ability to trace manufacture back through all processes to material source is essential.

It is hardly necessary to emphasise that the "Vital" parts category should be kept, by design, as small as possible. However, at the current state of helicopter design there still may be a hundred or more components involved.

At the other end of the scale of categorisation are components such as the fuselage itself which may consist largely of conventional fixed wing aircraft type of structure and as such may well have reasonably good damage tolerant qualities. Here the problem is less one of direct aircraft safety but one of economics and logistics involving "cost of ownership" to the customer by minimising repair during its normal life expectation.

Fuselage components are therefore often subject to forms of fatigue testing to demonstrate their "fail safeness" on the one hand and that they have a long life without major fatigue cracking on the other.

2.2.4. DERIVATION OF DESIGN LOAD SPECTRA

In the early days of the design phase it is necessary to estimate the fatigue load spectra on all structural components both in the rotor systems and in the transmission and also on fuselage components. For the Vital components described above the fatigue loading is frequently the criteria of design, and often overrules static loading considerations.

The design load spectra will be derived from consideration of the operational role usage of the aircraft and to this end it is important to obtain from the intended customer a "Statement of Intent" or similar. This will enable the designer to establish the expected manoeuvring pattern in the various roles intended and the percentage of aircraft life to be spent in these manoeuvre conditions. In a similar manner power spectra for the transmission need to be estimated.

The estimation of vibratory loading in the various components for the steady flight and manoeuvre conditions is a fairly difficult process. There are many extensive computer programmes that will estimate the dynamic response of the rotor blades to the aerodynamic inputs. But these usually only give accurate results under steady hover or forward flight conditions. The Stress Office generally has to utilise data from previous aircraft to establish a parametric read-across in the transient manoeuvre state.

Having determined the loading in the rotor system the effect on the fuselage needs to be understood. This, again, is a problem, the current approach to which involves the establishment of stiffness characteristics of the proposed fuselage configurations from such models as "NASTRAN" and determination of the response to inputs from the main rotor. At the current state of the art the main aim is to avoid resonances in the fuselage structure at the major rotor frequencies.

Having established load, power and bending moment spectra in the various components for all known roles of the aircraft, it becomes necessary to condense this into simplified loading for design purposes. One of the most important aspects of this is to establish whether a particular role is causing an unacceptable bias in the design, i.e. excess weight. In this case consideration may need to be given to restricting fatigue lives in such a role, whereas the overall aim should be unlimited life whenever possible. Basic Training comes to mind as a role where the usage may be more severe than in normal operation.

2.2.5. DESIGN ALLOWABLES

In order to "size" fatigue critical components to meet the loading spectra derived above it is necessary to have knowledge of the intrinsic fatigue strength of the materials used and to be able to make allowances for geometric effects, i.e. stress concentrations, and also the effect of the various manufacturing processes used and surface finishes.

It is also necessary to understand the effect of fretting. Although this must be minimised wherever possible, by the use of surface treatments, interfacing layers etc., it is unlikely that components containing joints etc. will ever be completely free of this form of degradation.

In general, basic design data is generated by small scale coupon tests of the materials in use to establish alternating Stress/No. of cycles (S/N) curves under a variety of steady stress conditions. These tests are usually supplemented by larger scale testing involving components representative of the proposed design. These latter tests are normally essential where new features form part of the design or where new materials, processes and complex geometry are involved.

In many cases the designer has at his command data from previous tests on full scale components from earlier designs that are sufficiently similar to be utilised. This data often provides the very best source of information.

Using all these sources of design strength estimates together with the derived load spectra and using conventional stressing methods, the designer is then in a position to establish the design of the prototype aircraft and components.

2.3. THE DEVELOPMENT PHASE

The objective of the Development Phase is to bring the prototype design to its introduction into service as a full Production concept. During this phase complete components are fatigue tested, prototype aircraft are flown to establish actual flight loads and the preliminary fatigue substantiation is undertaken to provide an interim fatigue lives list.

2.3.1. DEVELOPMENT TESTING

During this phase the prototype components are subjected to a searching series of fatigue tests. The aim is to establish the potential fatigue strengths of the parts and relate them to the knowledge of loads becoming available from flight test.

The mode of testing may vary dependent upon type of loading and complexity of the component. Where possible the most realistic knowledge of fatigue strength would come from a loading programme that is related to actual flight loads. In these cases a simple multi-level, repetitive load programme should be used. This should take into account variation of mean load (perhaps due to centrifugal loading) where applicable. In other cases the load pattern may be sufficiently simple to allow a constant amplitude type of loading to be used. This often has the advantage of getting quick results but may not necessarily reveal representative modes of failure in complex items.

Whichever form of testing is chosen at this stage, it is a considerable advantage to aim for failure of the part rather than a "non-break". Apart from the obvious reason of knowing how to modify a part that is found to be understrength from this testing, there is very real value in knowing the strength potential of a part at this stage as the design will inevitably be "stretched" in the future.

If this testing indicates that the chosen design is under strength re-design has to take place and re-testing is necessary. Some designs may need minor modification during this stage to accommodate desirable long term production processes and the effect of these must be assessed.

2.3.2. FLIGHT TESTING

A number of prototype aircraft are built during the development phase for various tasks and one of these will usually be dedicated to a flight test programme of load measurement.

Fundamental areas where load measurements must be taken are as follows:

Main and Tail Rotor Blades - Bending and torsional stress surveys along the span of the blade.

Main and Tail Rotor Control System - Load measurements in the rotating and stationary control rods, levers and actuators.

Main Rotor Hub - plate bending (depends on hub geometry).

Main Rotor Transmission - input and output mean and vibratory torque.

Tail Drive Transmission - mean and vibratory torque.

In addition to these major areas many ad hoc measurements are made for specific purposes, for example, undercarriage loads, fuselage vibration, fin and tailplane vibratory loading etc. These are usually subsidiary to the major programme on the dynamic components and are aimed at solving specific problems.

Loads are usually measured by means of strain gauges mounted on the critical areas of the components where possible. Calibration of the gauges would be undertaken by both mechanical and electrical methods when practical. In some cases, for example, fuselage vibration, accelerometers may need to be utilised when strain gauge location is difficult. Generally speaking however it can be difficult to relate accelerometer readings to loads and stresses and the direct methods are preferred.

Recording of the strain gauge outputs can be undertaken by a number of methods. In the past it has been common practice to record directly onto paper trace but this has proved unwieldy for both analysis and storage purposes. Modern practice utilises analogue or digital recording onto magnetic tape and thus can have the advantage of being input directly into a computerised analysis to establish load or stress spectra and indeed, component life.

The Flight Programme itself is designed to establish loadings in the critical components under all critical combinations of aircraft weight, centre of gravity positions and altitudes at all forward speeds appropriate rotor speeds and in all manoeuvring conditions such as banked turns, pull ups, transitions to hover, sideways and rearwards flight etc.

Although the basic aim of the flight programme will be to establish loading spectra for substantiation purposes it is quite probable that a considerable amount of exploratory flying will be carried out at the same time to establish the optimum performance characteristics of the helicopter. This work will require constant interfacing of the flight test, performance and stress engineers as in many cases component fatigue strength will determine the flight envelope boundaries. Modern methods of telemetering the flight loading to a ground station so that critically stressed components can be monitored during flight have assisted such exploratory work very considerably.

Towards the end of the Development Phase the flight envelopes of speed, altitude weight etc. will have been established. Now the fatigue loadings appropriate to all flight conditions can, in association with flight manoeuvre spectra, be used to establish the fatigue load spectra ready for the production substantiation.

2.4. THE PRODUCTION PHASE

The Production Phase is concerned with the final fatigue substantiation processes in order to provide a comprehensive promulgation of fatigue lives on all "safe-life" components, and inspection periods and procedures on other fatigue critical areas where damage tolerance has been established.

Fatigue testing of the production standard component from the production line is required in this phase and this is used in conjunction with the flight load spectrum derived from the strain-gauge flying of the Development Phase.

2.4.1. PRODUCTION FATIGUE TESTING

Now that the design and manufacturing processes associated with the production components have been defined it is necessary to obtain assurance of their fatigue strength.

A number of components are selected from the production lines (inevitably in the early stages of production) at random, for testing. The information required from these tests is an estimate of the average fatigue strength (usually stated in the form of an S/N curve over the range of endurances appropriate to the life and load frequencies experienced by the part) and also some confirmation of the degree of scatter of strength or life of the part about the average value.

In most cases at least six components (blades, hub components, control items etc.) should be chosen to give a reasonable level of confidence.

The fatigue tests may be carried out under constant amplitude conditions, or under a multi-level programme of loading to represent the variation in load levels during flight. In either case the load levels are chosen in excess of the flight loading by a factor of safety that will be discussed in the next section.

Constant amplitude tests are usually made at a series of load levels and may assist in the definition of the S/N curve shape and the scatter of strength of the part. However, it is not usually possible with the limited number of components tested (for economic reasons) to obtain a high level of confidence in these results. It is preferable to obtain information upon S/N curve shape and scatter from test on large numbers of specimens of similar material and geometry that have been tested previously, using the test results solely to establish mean strength.

The representation of flight loads by means of a fatigue test programme is considered to give a more realistic estimate of strength by reducing the dependence on Cumulative Damage assumptions. However, it is clear that the test loading can only represent the flight loads from a specific type of flying and all roles may not be covered. The method is to use the programme test to establish the vertical location of an S/N curve, of a pre-determined shape, using cumulative damage methods. Subsequent life calculations will again use the same cumulative damage methods which are then acting only as a "transfer function" between test loads and flight loads. It is considered that such multi-level testing will be more likely to expose realistic failure modes of a complex component than constant amplitude testing. Certainly the effect of large fluctuation of mean load, such as the on-off centrifugal loads on a rotor blade, can be effectively included in such a test.

If we now turn to a consideration of the actual components to be tested it is possible to separate these into the following sections as in para.2.2.2.

(a) Rotor Systems

(b) Transmission

(c) Airframe

2.4.1.(a) Rotor Systems

The main components that we are concerned with here are main and tail rotor blades, hubs and the control linkages for these items. In addition the actuating jacks for the controls also require test clearance.

All these items can be tested in conventional ways as described above. Account should be taken of mean loads and fluctuation of mean load and all vibratory loading actions should be as closely represented as possible. The items under test should be mounted completely representatively in the rig as the stiffness of the mounting can have a considerable influence on the stress distribution within the test component. This usually means that the component under test would be assembled to its adjacent aircraft parts.

Items such as main rotor blades have a considerable variation of flatwise and chordwise bending moments along the span and the centrifugal loads decrease from root to tip. It may be necessary with such components to test individual sections in separate tests, such as a root end and an outboard section. Again, it may be necessary to introduce props or resonant weight systems to test sections deemed to be critical (from prior calculation or development tests) without unrepresentative failure in other parts of the component.

Nowadays it is becoming common practice to manufacture major items such as rotor blades of composite materials, for example, glass and carbon fibre reinforced plastics. The general principles behind the substantiation procedures for these materials are similar to those of metallic materials. However, there are some aspects that must be given special attention. Epoxy resin systems are subject to moisture pick-up which is accelerated at high ambient temperatures. There is some evidence that this can degrade the strength properties to some extent and this has to be taken into account. Programmes of coupon specimens can estimate the effects for design procedure but it may be necessary to adopt a process of exposure of full scale specimens to climatic conditions and then fatigue test. The exposure may be to natural or artificially produced hot/wet climates. This is inevitably long term but until our knowledge is more complete on effects of environment, these procedures have to be faced. Another problem is the definition of failure in such materials. It is possible that stiffness deterioration may become the basis but this is not agreed by all manufacturers.

Items such as control rods often have simple end loads with no mean load and these can be tested in simple rigs or, in some cases, in universal test machines.

Hydraulic actuator jacks are a more difficult proposition as they are subject to feed back loads from the rotor system coupled with internal pressure fluctuations both from the feedback and from actuation pressures. All these must be represented in a full fatigue test.

2.4.1(b) Transmission

The consequences of failure of many parts of the main and tail transmission systems can be catastrophic, or hazardous at the least, and fatigue testing and substantiation is just as important as for main rotor components.

Referring back to 2.2.2.(b), testing usually has to be carried out on the gear teeth in all major gear trains, transmission shafts and couplings and the main gearbox casing itself.

Fatigue loading on gear teeth takes the form of a pulsed load at once per gear wheel rotational frequency. The magnitude of this load is dependent on the power or torque being transmitted. The test will usually take the form of an overload or factored torque test in a test rig with the gearbox running at normal speeds. Full representation of external loadings, in order to obtain representative casing deflections, should be applied during the test if possible. Although such a test may be undertaken at a constant load level there are benefits of realism to be obtained by applying a programme of loads representing aircraft power usage.

The transmission shafts and couplings would normally be tested by means of applied repetitive torque applications representing the major changes of mean torque or power in the system. The influence of high frequency torsional fluctuations must be accounted for but as these can usually be shown to be non-damaging by calculation, they may not need to be represented on the test.

The casing of the main gearbox provides a difficult challenge from the test point of view. It is necessary to establish a load sequence that will cover major manoeuvre loadings from the main rotor, i.e. lift, moments and shears. The box should be assembled with the major gear trains and repetitive application of drive torque need to be applied during the test. Consideration has to be given to high frequency loaded components although it may be possible to show by calculation that such loads are not significant. Additional loads that may need to be considered if control jacks are mounted on the gearbox are those fed back from the rotor at rotor order frequencies. These may be covered by separate local tests.

2.4.1(c) Airframe

Conventionally the airframe of a modern helicopter is built on the principles comparable to those in current use on fixed wing aircraft. Typically this may be of stressed skin and stringer construction. This construction has a certain amount of inherent fail safeness and may be subject to "Damage Tolerance" methods of assessment.

Current assessment methods vary and may range from calculation (together with localised testing of critical areas) to fatigue tests on a full scale fuselage. In general, however, it is most difficult to assess the fatigue loading on a fuselage. The manoeuvre loadings at relatively low frequency can be established without too much difficulty and these would form the fundamental fatigue loading pattern for any test series. However, superimposed upon this basic loading pattern is the high frequency vibration transmitted to the fuselage from the rotor systems. This latter is often the initiating cause of many minor (and sometimes major) cracks that can lead to expensive repair, even though they may not immediately cause a safety hazard.

It is necessary to establish that the fuselage will have a satisfactory economic life without major repair on the one hand and also that the probability of major catastrophe from fatigue failure is "extremely remote" on the other.

There can be no doubt that the initial design assessment is critical in leading to the above desirable state although it is difficult if not impossible to make predictions of the high frequency loadings and arbitrary estimates must be made.

To substantiate the fuselage for fatigue, the best approach is probably to subject major critical parts to a realistic programme of manoeuvre loads together with a vibratory environment which will representatively produce fretting conditions at joint and rivet holes.

The test would establish the lives at which fuselage cracking takes place, the locations of such cracks and their inspectability and also the rates of crack propagation to establish the damage tolerance characteristics of the fuselage. Further discussion of this subject will be found in section 5.4. of this Design Guide.

There are other parts of the fuselage which have single load paths and damage tolerance cannot be established, such as the main rotor gearbox pick-up points. These have to be substantiated in the same way as other "Vital" components and must have full fatigue test programmes as described in 2.4.1.(a) above.

2.4.2. FACTORS

Fatigue testing of components shows that a considerable amount of scatter on strength or life is always present. If S/N curves representative of the average strength were utilised in the fatigue life estimation calculations then in service there would be a 50% failure rate at the calculated life. This is of course quite unacceptable.

In practice, Vital Parts (i.e. those parts, the failure of which would cause catastrophe) must be demonstrated to have a chance of failure that is "Extremely Improbable". This has been quantified by some authorities as a failure probability of 10^{-9} at the specified life.

Clearly to demonstrate such safety levels demands a knowledge of the distribution of strength of a component which cannot be established by any practical test series. Limited work on large samples seems to indicate that in many cases there may be lower limits to fatigue strength distribution functions. The record of past experience suggests that factors based upon three standard deviations below the mean strength will produce substantiated fatigue lives leading to satisfactory levels of safety in the complete helicopter.

Having determined the guide lines upon which factors should be based, it is next necessary to obtain scatter measurements. Ideally these would be based upon a very large sample of the actual production component under consideration but this is invariably prohibitively expensive and a less costly approach usually has to be made. One possibility is to carry out tests on a limited number of components, perhaps six, and, indeed, this is normal when establishing mean strength. Unfortunately, however, it becomes necessary to introduce "factors of confidence" of a significant size when predicting scatter with small samples and this can lead to rather pessimistic overall factors. Alternatively, factors pre-determined from previous testing of large samples, with similar materials and surface finishes to the production components, may be used and this does at least lead to a conformity of approach which can be measured against in-service failure statistics.

In an ideal world common factors would be agreed by all Authorities and would find their way into the various Requirements providing a universal basis of substantiation. However, there is no common approach at this stage and actual factors do not always feature in requirements. It is often left to the designer to come to a local agreement with his Certifying Authority on the factors to be used. This is an area where standardisation should be considered.

2.4.3. FINAL FATIGUE SUBSTANTIATION

At this stage all the information that we have gathered during the development and production phases must be brought together to produce the fully substantiated fatigue lives for the in-service aircraft.

This information consists of the manoeuvre spectra appropriate to all predicted roles of the aircraft, the measured flight loads, the fatigue strength of actual production components and the life or strength scatter factors appropriate to the required safety levels.

For all Vital Parts it will be necessary to establish the safe fatigue life after which the part will be discarded. The number of parts in this category should be minimised by design and the aim should be to achieve unlimited lives wherever possible on such parts. This will have a very significant effect on the "cost of ownership" of the aircraft.

With regard to the fuselage itself the design should aim to achieve a "fail-slow" type of structure and damage tolerance analyses and tests should be used to demonstrate that this has been successful. It is essential that fuselage structure will have a long life free of cracking wherever possible. The structure must be inspectable so that any cracking can be found at an early stage and repaired easily and economically.

The methods of fatigue life estimation of the safe life parts are reasonably uniform amongst contractors. Production fatigue tests, whether carried out at constant amplitude loading or programmed loading aims at the establishment of a mean S/N curve for the component. This is reduced using strength and/or life factors to a "Working Curve". A spectrum of fatigue loads is produced for each component, these may be based upon each individual role or may in some cases be covered by a simple "umbrella" spectrum. Cumulative Damage methods are used to link the load spectra and working curve to give the fatigue life of the components.

Finally, it is necessary to ensure that the manufacturing qualities achieved in the early production stage is maintained throughout the entire length of the production run. "Quality Control" testing uses a sampling technique whereby items are withdrawn at regular intervals during the production run and fatigue tests them to failure. Acceptance bands to cover scatter are set to decide whether production is continuing satisfactorily.

2,5. IN SERVICE PHASE AND EVALUATION OF CURRENT PROCEDURES

2.5.1. IN SERVICE EXPERIENCE

Fatigue evaluation does not stop at entry into service of the type. There must be feedback from the operator on the fatigue performance and a full defect reporting procedure has to be instigated.

Current procedures have led, in general, to reasonably satisfactory performance of Vital components in service and catastrophic incidents due to fatigue failure are rare. However, there can be no cause for complacency as such failures have happened and no doubt will continue to do so. It is always necessary to increase our understanding of the fatigue process.

One area where careful control must be exercised is in maintenance. It is normal on most critical components that, on overhaul, a crack detection is carried out. Should a crack be found this will, of course, be cause for rejection of the part. However, it is not enough to merely put the part in the scrap-box, it must be reported and the part returned for investigation. Only in this way can the designer have assurance that his procedures are maintaining the required levels of safety.

During the course of fatigue substantiation attention was drawn to the importance of the assumed flight spectrum. In some cases the operator may be able to assist by recording significant features of his operation that can lead to an updating of spectrum information. This can in many cases lead to in-service extension of fatigue life and hence lower operating costs. Obviously the reverse could (but should not) happen and here a safety issue may be highlighted. Several parameters that the operator could record come to mind. For example, flight duration, time spent at high speed, time spent in hover, time spent at high power levels. All these can lead to a first order revision of the original assumptions of flight envelope and can make significant changes in the life predictions for expensive components. It may be that these parameters, and others, could be recorded continuously on a sample or even a fleet of aircraft leading to much more realistic re-estimates of usage. This latter is one of the aspects of "Health Monitoring" which is now assuming increasing significance in the field of rotorcraft operation.

2.5.2. CHANGES IN SERVICE USAGE

Finally we come to the maintenance of safety levels over the service life of the aircraft. It is necessary now to know whether the original assumptions made regarding the use of the aircraft remain valid over the years. The helicopter is a very versatile machine and changes in use can be frequent. The onus in on the operator to inform the design authority of changes in use so that re-estimates of fatigue life can take place. The "Statement of Intent" is the best way of transmitting this information and this should be updated regularly.

For the future it can be expected that advances in micro-electronic technology will lead, as part of a health monitoring system, to a continuous monitoring of changes in usage and a protection of fatigue lives of Vital Parts.

It is our belief however that the way ahead for the helicopter is in the development of fail safe and damage tolerant approaches to design that will eventually lead to the elimination of the safe-life component.

CHAPTER 3
SPECTRA DEVELOPMENT

CONTENTS

SUB.CHAPTER 3.1
MISSION SPECTRA

by

Gérard STIEVENARD

Société Nationale Industrielle Aérospatiale
B.P. 1 – 13725 MARIGNANE CEDEX
FRANCE

CONTENTS

3.1 MISSION SPECTRA

3.1.0 Introduction

It is essential that the mission spectra are known when calculating the service life of «vital» helicopter components.

Two different methods of approach may be applied when establishing these spectra. The first involves establishing the spectrum so that it guarantees flight safety irrecpective of the aircraft's role and the component in question. This type of spectrum is obviously not realistic, but provides an additional safety margin to that which should exist between flight stress levels and component strength. This method therefore is conservative, but also has some advantages. By covering all possible types of helicopter utilisation, a single service life figure may be applied to each type of part. When a helicopter is used for a large variety of missions, the spectrum is not invalidated ; this provides for more flexible monitoring of parts with limited service life and a very small risk of error in determining the number of flying hours, which in this case have the same significance irrespective of the mission performed.

The other method of approach, on the other hand, involves dealing as far as possible with the mission specific to a particular operator. This second approach enables fatigue damage to be calculated more realistically ; this is sometimes necessary when the specific operation envisaged leads to excessively severe results if applied to the entire fleet. This method requires the type of mission performed by the operator to be repetitive and the manufacturer must be informed of any significant change in utilisation.

When the aircraft is in its prototype or production development stage, i.e. at a time when it is difficult to obtain statistical data on the missions for which the operators will use the aircraft when it becomes available, estimated figures have to be used to establish the spectrum needed for preliminary calculation of the service lives.

This spectrum can be established either from the type specifications used as a basis for defining the aircraft, or by extrapolation of a spectrum which has already been defined for aircraft types with a similar role. The spectrum should then take into account the differences in the flight envelope likely to exist between the two types of aircraft, particularly with respect to differences in weight and balance, airspeed, load factors, etc.

If no actual data measured on an operational aircraft exist , the mission spectrum used for preliminary life calculations must incorporate safety margins large enough to ensure both flight safety and sufficient service life to all vital parts prior to the start of full scale production. This is essential to ensure the aircraft being a commercial success.

When the aircraft are delivered to the operators, it is possible to determine a realistic spectrum by continuous recording of some flight parameters on several aircraft for a flying time long enough to be representative of the future life of the aircraft, and then to perform a statistical interpretation of the recorded data.

3.1.1 Key mission spectrum parameters

The flight parameters to be considered when determining a mission spectrum are those likely to cause changes in loads leading to fatigue damage.

Two types of fatigue are to be sought : vibration fatigue which corresponds to low amplitude dynamic stressing likely to cause component failure after a large number of cycles, and low cycle fatigue which, on the contrary, produces stresses with large changes in amplitude but with few cycles. The stress variations generally found on helicopters may be represented by the following diagram.

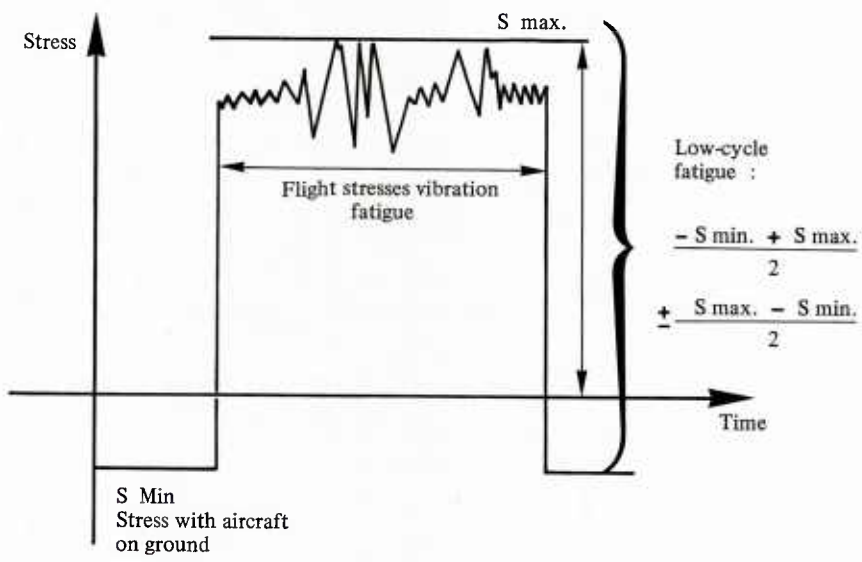

For rotor components, vibration fatigue generally corresponds to dynamic stresses whose amplitude varies for each flight configuration, and low cycle fatigue corresponds to the ground- air -ground load variations.

For the transmission components, the types of stresses are the same except that power variations may also produce low fatigue cycles at a higher frequency than once per flight. More particular attention should be paid to certain missions due to the large power fluctuations involved in the transmissions. These are aerial work missions where loads are carried on the sling and where each rotation involving picking up and setting down the load is also a low fatigue cycle. The same applies to the rotors for training type missions which generally involve a large number of take-offs and landings together with main rotor overspeed to simulate engine failure with an autorotative landing.

The parameters which enable one to identify the flight configurations leading to the load variations described, above are set out in the following list. This list is obviously not exhaustive and may be optimised with respect to the characteristics of the aircraft for which the mission spectrum is to be examined. These parameters may be associated with the helicopter itself and its performance, but they should be related in particular to the use the operator makes of the aircraft.

Parameters to be recorded or extracted from recordings.

Aircraft weight

Longitudinal and lateral center of gravity location

Rotation speeds for main and tail rotors

Helicopter airspeeds (in level flight, climb and descent)

Load factors (aircraft attitude)

Altitude with atmospheric conditions (temperature, pressure)

Control positions :

- Collective pitch
- Longitudinal cyclic pitch
- Lateral cyclic pitch
- Tail rotor.

Power :

- Engines
- Gearboxes (main, intermediate, tail)
- Main rotor
- Tail rotor .

Torque :

- Engines
- Gearboxes (main, intermediate, tail)
- Main rotor
- Tail rotor.

Flying time :

- Number of take-offs and landings per hour of flying time.

3.1.2 Analysis of parameter variations

As already indicated, representative statistical data are needed if the mission spectra are to be determined correctly. This requirement can be met firstly by using several aircraft for the recordings to allow for intrinsic variations in the helicopter itself. At least three aircraft are needed for each type of mission. The measurement methods used may be selected from those listed in paragraph 3.3.1. These aircraft must obviously not be affected by temporary flight envelope limitations. Emphasis should also be placed on an important psychological aspect : the crews responsible for recording the parameters must be perfectly aware of the established objective. The recorders must never be thought of as «spies» and the flights must take place as though these recorders were not fitted.

The «type of mission» refers to the mission which being repeated throughout the entire life of the aircraft, will make the calculated spectrum representative of the aircraft use.

Depending on the operator, the missions may, for example, be of a military nature (tactical flights, anti-tank flights, anti-submarine flights, etc.) or of a civil nature (passenger transport, aerial work, off-shore work, etc .). Each of these types of mission may be covered by a specific mission spectrum giving different service lives.

The duration of the recording should be such that the sampling for statistical processing will be representative of the flight configurations distribution on a time basis. One method of optimising the duration of the recording is to calculate the percentage of operation in each configuration for different recording times. When the calculation results stabilise, i.e. when the percentages do not alter appreciably with the duration of the recording, this duration period may be considered adequate.

Generally about 100 hours flying time per aircraft gives the anticipated result.

3.1.3 Processing and analysis of results

When the key parameters have been recorded using suitable equipment (e.g. magnetic tape) they can be processed and analysed. It should be noted that it is not absolutely necessary to make a continuous recording of all the parameters given in the list in paragraph 3.1.1. If the weight and C of G of the aircraft are known on take-off, the change in these two parameters can be calculated for a given flight by using the hourly fuel consumption figures which are known by other means. For the power, torque and RPM parameters, the third one can be derived from the other two. By knowing the kinematics of the aircraft, the number of recording points may also be reduced.

When analysing the key spectrum parameters, the first task is to establish analysis levels, e.g. for aircraft weight, analysis in stages of 50 kg seems appropriate, and stages of 1 cm for balance, 10 km/h for speed, 0.1 g for load factors, etc. When the parameters have been processed in this way, the flight configurations can be identified by simultaneous examination of the values obtained.

For example :

for IAS = 0 $Hp \simeq 10$ m Max. power the configuration corresponds to hover flight in ground effect.

Since the results are processed by a computer, code factors may be entered enabling the configurations to be identified with respect to the various parameter ranges.

The time period for each configuration is then to be established enabling the corresponding utilisation percentage to be determined with respect to the total time.

$$pi = \frac{ti}{T} \text{ (time period in this configuration)} \times 100$$

pi : percentage for the configuration

T : total recording time

For the power spectra, it is not essential to identify the configurations since only the power level distribution on a time basis is important when calculating damage to the gearboxes.

For the main rotor (hub + blade) the configurations generally representing the most damaging conditions are those involving high load factors and so the latter must be analysed in detail for each speed and weight of the aircraft.

3.1.4 Examples of results obtained

Several mission spectra examples are given in the appendix. The first is a civil spectrum corresponding to passenger transport operations. In this spectrum it is clearly seen that the percentage figures for helicopter utilisation in level flight are high, whereas those for turns with load factors are very low. This is quite logical since this type of utilisation involves flying as quickly as possible between two points and ensuring that the passengers remain comfortable.

The second example is a tactical flight spectrum obtained from recordings made on three machines over 750 hours (3 x 250 hours).

From this spectrum, however, we can see that the operator is trying to obtain maximum benefit from the velocity of the aircraft close to the ground. An extremely detailed evaluation of the load factors was made for this spectrum as can be seen in table 3.1.2.b. This figure shows that the values may reach 2.0 g.

The third spectrum given as an example is a military anti-tank mission spectrum. The feature which stands out is the large percentage of hover flight configurations associated with large control movements.

For the aircraft involved, spectrum No. 1 led to limited service life for the suspension components due to their vulnerability to damage at high speeds. Spectrum No. 2 led to limitations being applied to the control system whereas spectrum No. 3 led to limitations on the main gearbox due to the power levels used.

Table 3.1 - 1 TRANSPORT SPECTRUM

Configuration	Ho	Hδ = 1500 m	Hδ = 3000 m	Total
Hover IGE	4.450	0.500	0.050	5
Hover OGE	4.450	0.500	0.050	5
Rearwards flight at maximum permitted IAS	0.356	0.040	0.004	0.4
Start of forward flight from rearward flight	0.089	0.010	0.001	0.1
Sideways flight to the right at max. IAS	0.890	0.100	0.010	1
Sideways flight to the left at max. IAS	0.890	0.100	0.010	1
Rudder reversal from turn to right in hover	0.445	0.050	0.005	0.5
Rudder reversal from turn to left in hover	0.445	0.050	0.005	0.5
Transition IAS	2.670	0.300	0.030	3
Turn to right at transition IAS	0.890	0.100	0.010	1
Turn to left at transition IAS	0.890	0.100	0.010	1
0.5 VNE	7.120	0.810	0.070	8
0.7 VNE	6.206	0.724	0.070	7
Turn to right at 0.7 VNE (40^{o})	1.335	0.150	0.015	1.5
Turn to left at 0.7 VNE (40^{o})	1.335	0.150	0.015	1.5
0.85 VNE	15.120	1.710	0.170	17
Turn to right at 0.85 VNE (40^{o})	1.780	0.200	0.020	2
Turn to left at 0.85 VNE (40^{o})	1.780	0.200	0.020	2
0.9 VNE	25.810	2.900	0.290	29
0.95 VNE	1.980	0.498	0.022	2.5
VNE	0.890	0.098	0.012	1
1.11 VNE	0.445	0.050	0.005	0.5
Oblique climb at max. power	2.136	0.240	0.024	2.4
Vertical climb at max. power	2.136	0.240	0.024	2.4
Autorotation at NR min.	0.090	0.009	0.001	0.1
NR max.	0.090	0.009	0.001	0.1
Load factor < 1	0.445	0.050	0.005	0.5
Approach	3.015	0.350	0.035	3.5
Flare	0.356	0.040	0.004	0.4
Quick stop	0.090	0.009	0.001	0.1

Table 3.1 - 2a TACTICAL FLIGHT SPECTRUM

Configuration	Ho	Hσ = 1500 m	Hσ = 3000 m	Total
Hover IGE	7.779	0.699	0.262	8.740
Hover OGE	2.841	0.255	0.096	3.192
Rudder reversal from turn to right in hover	0.002	–	–	0.002
Rudder reversal from turn to left in hover	0.002	–	–	0.002
Start of forward flight and transition IAS				
n < 1 g	0.318	0.029	0.011	0.358
n = 1 g	4.067	0.366	0.137	4.570
n ⩾ 1 g	3.282	0.295	0.111	3.688
Climb (Vz > 10 m/s)	0.151	0.014	0.005	0.170
Descent (Vz < 10 m/s)	0.059	0.005	0.002	0.066
Sideways flight to right	0.077	0.007	0.003	0.087
Sideways flight to left	0.077	0.007	0.003	0.087
Level flight IAS 0.6 VNE	9.429	0.847	0.318	10.594
0.7 VNE	6.974	0.627	0.235	7.836
0.8 VNE	7.137	0.641	0.241	8.019
0.85 VNE	6.413	0.576	0.216	7.205
0.9 VNE	7.181	0.645	0.242	8.068
0.95 VNE	1.773	0.159	0.060	1.992
1 VNE	0.707	0.064	0.024	0.795
Turns in level flight (see table)	7.408	0.666	0.250	8.324
Load factor < 1	1.592	0.143	0.054	1.789
Autorotation	0.322	0.029	0.011	0.362
Obstacle clearance	0.750	0.067	0.025	0.843
Approach	10.020	0.901	0.338	11.259
Flare	4.299	0.386	0.145	4.830
Aircraft on ground	6.390	0.574	0.215	7.180

Table 3.1 - 2b BREAKDOWN OF LOAD FACTORS WITH RESPECT TO SPEED

VNE / g	0.6	0.7	0.8	0.9	0.95	1	1.11
1.1	0.8322	0.6296	0.5626	0.5358	0.1273	0.1273	0
1.2	0.7047	0.5164	0.5362	0.5550	0.1382	0.0445	0
1.3	0.3569	0.2648	0.2401	0.2642	0.0576	0.0161	0
1.4	0.0963	0.0722	0.0727	0.0789	0.0190	0.0060	0
1.5	0.0305	0.0226	0.0233	0.0250	0.0060	0.0017	0
1.6	0.0063	0.0044	0.0060	0.0062	0.0008	0.0003	0
1.7	0.0076	0.0057	0.0054	0.0063	0.0015	0.0002	0
1.8	0.0047	0.0036	0.0026	0.0036	0.0007	0	0
1.9	0.0012	0.0010	0.0008	0.0011	0.0002	0	0
2	0.0034	0.0026	0.0020	0.0028	0.0005	0	0

Table 3.1 - 3 ANTI-TANK MISSION SPECTRUM

Configuration			%
Ground load	1.1	Ground idle (0.3 % taxiing)	2.6
	1.2	Vertical take-off (2 per hour)	0.5
	1.3	Landing (2 per hour)	0.5
Steady hover	2.1	Hover IGE	1.5
	2.2	Hover OGE	5.2
	2.3	Hover forwards	5
	2.4	Hover rearwards	3.5
	2.5	Hover to right	5
	2.6	Hover to left	5
Steady forward flight			
	3.1	Level flight 0 to 50 km/h	3
	3.2	Level flight 50 to 150 km/h	9.3
	3.3	Level flight cruise speed	20
	3.4	Level flight VNE	3.7
	3.5	Level flight VD	1.3
Other steady flight configurations			
	4.1	Sideways flight to left	1.2
	4.2	Sideways flight to right	1.2
	4.3	Climb at max. continuous power	2.1
	4.4	Vertical climb a take-off power	2
	4.5	Climb at maximum power	1.1
	4.6	Descent at reduced power	3
Transitions	5.1	Transition from forward flight to autorotation	0.250
	5.2	Transition from autorotation to power on flight	0.250
Flight manoeuvers			
	6.1	Cyclic and collective pull-ups	1.000
	6.2	Flare	1.000
	6.3	Quick stop	0.600
	6.4	Turns to left up to 180 km/h	4.500
	6.5	Turns to right up to 180 km/h	4.500
	6.6	Turns to left from 180 km/h to Vmax.	1.025
	6.7	Turns to right from 180 km/h to Vmax.	1.025
	6.8	Change of turn to left 61 to 120 km/h	0.7
	6.9	Change of turn to right 61 to 120 km/h	0.7
	6.10	Change of turn to left 121 to 180 km/h	0.5
	6.11	Change of turn to right 121 to 180 km/h	0.5
	6.12	Rotation to left about yaw axis	0.875
	6.13	Rotation to right about yaw axis	0.875
	6.14	Lateral reversal	1.1
	6.15	Longitudinal reversal	1.1
	6.16	Rudder reversal	1.1
	6.17	Rolling pull-out	0.3

Configuration (continued)			%
Autorotation	7.1	Autorotation descent	0.3
	7.2	Lateral reversal	0.1
	7.3	Longitudinal reversal	0.1
	7.4	Rudder reversal	0.1
	7.5	Turns to left up to 200 km/h	0.150
	7.6	Turns to right up to 200 km/h	0.150
	7.7	Autorotation landing	0.100
Take-off and landing on slopes			
	8.1	Take-off from a 7^{o} slope to left	0.120
	8.2	Take-off from a 7^{o} slope to right	0.060
	8.3	Take-off from a 10^{o} slope to left	0.010
	8.4	Take-off from a 10^{o} slope to right	0.010
	8.5	Take-off from a 7^{o} slope nose down	0.015
	8.6	Take-off from a 7^{o} slope nose up	0.015
	8.7	Take-off from a 12^{o} slope to left	0.010
	8.8	Take-off from a 12^{o} slope to right	0.005
	8.9	Take-off from a 14^{o} slope to left	0.005
	8.10	Landing on a 7^{o} slope to left	0.120
	8.11	Landing on a 7^{o} slope to right	0.060
	8.12	Landing on a 10^{o} slope to left	0.010
	8.13	Landing on a 10^{o} slope to right	0.010
	8.14	Landing on a 7^{o} slope nose down	0.015
	8.15	Landing on a 7^{o} slope nose up	0.015
	8.16	Landing on a 12^{o} slope to left	0.010
	8.17	Landing on a 12^{o} slope to right	0.005
	8.18	Landing on a 14^{o} slope to left	0.005

SUB-CHAPTER 3.2

LOAD PREDICTION

CONTENTS

3.2.1 ROTORS

by

William F.White
Directorate for Development and Qualification
U.S. Army Aviation Research and Development Command
St. Louis, MO 63120, USA

and

Robert L.Tomaine
Directorate for Advanced Systems
U.S. Army Research and Development Command
St. Louis, MO 63120, USA

CONTENTS

3.2.1.1 Introduction

In the design of rotor dynamic components, relationships between the magnitude of flight loads and fatigue strength must be established. It is important then that both the fatigue strength of the components and the oscillatory loads expected in flight be accurately established in the design stage. During the design stage, estimation of fatigue strength is made using fatigue strength data from previous component tests of similar parts. Because of the large amount of fatigue testing that has been accomplished over the years, the estimate of component fatigue strength is done with a relatively high degree of confidence. Accuracies of fatigue life assessment of components, therefore, depend largely on the accuracy of rotor loads predictions.

One method of predicting rotor loads is to extrapolate flight test data from helicopters which are dynamically and aerodynamically similar to the helicopter being designed. This method proved to be simple and economical when metal rotor components were used, high speed computer and modern sophisticated aeroelastic rotor analyses were not available, and desired helicopter vibration levels were not very stringent. The second method is to use analytical predictions. It is recognized that the prediction of rotor loads is one of the most demanding problems in rotary wing technology since it involves a highly nonlinear aeroelastic response problem. Rotor loads, however, are basic to determining fatigue life, reliability, flight envelope limitations, and ride comfort. Ultimately, the accuracy of rotor loads analyses have a large impact on system development cost and productivity. Much effort has been devoted to the development of sophisticated methods for calculating rotor loads, but these methods necessarily depend on approximations and empiricisms because the aerodynamic and structural phenomena involved are not completely understood.

The 1973 AGARD Specialist Meeting on Helicopter Rotor Loads Prediction Methods (Reference 321.1) was a milestone in documenting the state of the art of loads prediction and in defining areas for further research and development. High speed computers had allowed incorporation of the latest generation of aerodynamic and structural technology into analyses which were rapidly evolving into global models. In 1974, Ormiston in Reference 321.2 conducted a unique comparison of loads programs by comparing results for a set of standard cases for a very simple hypothetical rotor system. As noted in Reference 321.2,

large differences existed even at the most fundamental levels such as airfoil data and blade frequencies. Ormiston's paper noted that the large differences may not necessarily reflect on the adequacy and value of these analyses as design tools. In fact, industry experience has shown that with accumulated experience from many calculations for familiar configurations, various empirical factors can be adjusted to provide reasonable results for some parameters. However, the adequacy of these loads analyses as design tools remains undocumented.

Reference 321.3 addresses the progress in rotor loads technology since this 1973-1974 period. As noted in Reference 321.3, there has been continued progress in the fundamental technology areas of structural dynamics and aerodynamics. Structural dynamic modeling in existing operational loads analyses still consists of relatively simplified modal or finite element procedures. In many applications, the structural dynamic representation of the rotor involves relatively simple analyses based on engineering beam theory. In the past decade, as noted in Reference 321.3, considerable emphasis has been placed on application of finite element methods to permit coupling of the complex components of the rotorcraft by automated techniques suitable for assembling finite elements and substructures. These efforts have primarily resulted in exploratory pilot programs.

In the aerodynamics area, Reference 321.3 noted the many advances in basic understanding, but concluded that most of the aerodynamic advances in operational rotor loads programs have involved relatively modest changes. The aerodynamic models used in rotor loads analyses are characterized by heavy reliance on empirical techniques. Lifting line theory with two-dimensional airfoil data as a function of angle of attack and Mach number is almost universally used for blade aerodynamic loads. Many analyses incorporate approximate or semi-empirical corrections for the effects of dynamic stall, yawed flow, three-dimensional flow, and vortex/blade interactions. Empirical techniques are used either because existing aerodynamic theories are not able to model the complex viscous and compressible flow of the rotor blade or because a rigorous application of the theory leads to an impractical numerical problem. There have been substantial improvements in understanding and acquiring steady and unsteady airfoil data. Much additional work is required in lifting surface analyses and inflow modeling. Inflow modeling has evolved relatively slowly in the past decade with the most significant progress in the ability to predict the change in inflow velocities due to the flow field generated by the fuselage.

In addition to the basic disciplines of aerodynamic and structural mechanics, numerical solution techniques require additional and perhaps equal emphasis by the rotor loads specialist. The results of numerous studies indicate that accuracy is compromised by numerical techniques and procedures used to solve the equations of motion. Difficulties have been encountered in achieving converged solutions, in reaching the desired rotor lift levels, or in avoiding apparent blade motion instabilities. Considering the complexity of the large number of highly coupled, nonlinear equations, difficulties of this type are not surprising. In the past decade, there has been limited discussion of these problems in the literature, but they appear to be significant.

3.2.1.2 Rotor Operating Environment

As shown in Figure 321.1, a helicopter blade in the process of one revolution encounters a rapidly varying aerodynamic environment due to the relative magnitudes of rotational and forward flight velocities. A complicated flow field is established by the rotor wake which is a primary factor in developing the unsteady flow environment of the rotor blade. At low advance ratios corresponding to the transition region, the induced velocity field of the rotor wake is the major contributor to high vibratory airloads. Flight in this region results in the tendency of the wake to be drawn close or into the plane of the rotor disc. When this occurs, large higher harmonic components of inflow exist and result in high loads. At high advance ratios, blade sections experience rapid variations in the flow environment at various azimuthal locations. Blade sections experience compressible flow into the transonic region and also execute complex unsteady motions into stall. Unsteady wake effects manifest themselves as contributions to higher harmonic airloads and provide the environment for dynamic stall.

Excitation of the rotor blade from this rapidly varying aerodynamic environment is fundamental to the operation of the rotor, and forced response cannot be eliminated. The degree of blade response is governed by its dynamic characteristics and determined by the harmonic content of aerodynamic and inertial loads. The transfer of rotor loads through the shaft to the airframe is one of the two major vibration load paths shown i Figure 321.2. On the basis of very general considerations, it can be demonstrated that the rotor acts as a filter which transmits to the airframe only discrete harmonics of blade loads. Generally, the blade lower harmonics $(N-1)\,\Omega$, $N\,\Omega$, and $(N+1)\,\Omega$ are most significant. As these loads are transmitted from the rotating blade to the airframe, variable hub forces and moments are produced. These varying loads have only the discrete harmonics of $N\,\Omega$ and multiples thereof. If the blades are not identical, other harmonics such as Ω, $2\,\Omega$, $3\,\Omega$, etc., may be present.

The second major load path illustrated in Figure 321.2 is the transfer of loads through wake interactions. As illustrated in Figure 321.3, aerodynamic interaction includes excitation of the fuselage due to rotor downwash, flow disturbances in the plane of the rotor due to the presence of the fuselage, and rotor to rotor wake interference. Thus, wake interactions provide a load path independent of the shaft and may also significantly modify the loads transmitted through the shaft. The problem related to wake interactions are of increasing concern due principally to the requirement that the helicopter be readily transportable. One significant characteristic that results from this requirement has been a narrow gap between the blades and the top of the airframe. Because of this, the surface pressures due to blade proximity can be considerably higher than they are with more conventional separation distances. A reduction of the rotor/airframe separation distance by one blade chord can double the amplitude of vibratory pressure inputs to the fuselage. An additional major source of helicopter fatigue loads involves aerodynamic excitation of the empennage. The sources of aerodynamic excitation include main and tail rotor wakes, fuselage, engine nacelle and pylon/hub flow disturbances. These combined excitations include a broad range of excitation frequencies which causes a formidable problem in designing empennage structural dynamic characteristics to avoid excitation harmonics. In addition to resulting in high empennage fatigue loads, the excitations may excite major fuselage modes causing high cabin area vibratory responses.

The airframe can have a significant effect on the flow field in the plane of the rotor disk. Fuselage upwash increases the blade angle of attack over the forward portion of the rotor disk and can induce blade stall. This results in an impulsive blade loading with each passage through this region and may produce significant response in all the lower flapwise and chordwise bending modes. Since the fuselage of the modern helicopter tends to extend farther and farther forward, relative to the rotor hub, any disturbance it causes is moved farther outboard along the blade, to a region of high dynamic pressure, and the effect is likely to be accentuated. With earlier generations of rotorcraft, this was less critical. Rotors were generally not as heavily loaded, flight speeds were lower, and more importantly, the rotor and airframe were well separated.

3.2.1.3 Summary Of Rotor Loads Analyses

In the past two decades, significant research has focused on the basic disciplines of rotor aerodynamics and structural dynamics. Major advancements have been realized in many areas such as variable inflow, steady and unsteady aerodynamics, airfoil data, and blade aeroelastic coupling effects. The wide range of research has contributed significantly to an improved understanding of the rapidly varying and complex operating environment of the rotor. In the analytical representation of the rotor, the last two decades have been marked by a progressive removal of constraints forced by a combination of a limited computational capability and an imperfect understanding of the realities of the flow field. The latter constraint has been removed somewhat by a steadily growing data base; the result of systematic flight testing and wind tunnel work at model and full scale. The data have provided the guide, and computers have improved both in terms of capacity and speed; and as a result, current analytical capability provides a basic foundation for improving fatigue design methodology. However, improvements in rotor loads analyses have not been commensurate with improvements in the basic disciplines of aerodynamics and structural dynamics. In the past two decades, major helicopter manufacturers initiated these analyses to support development programs and gradually modified and extended their capability with advances in the state of the art. These developments, particularly in industry, have usually been driven by a need to solve a specific problem with limited time and resources available. This section provides a summary definition of existing industry rotor loads analyses. The originating organization and computer program names are identified in Table 321.1. These programs encompass a rather wide variation of sophistication and capability. Several are multi-use "global" programs that include rotor loads prediction as one of several capabilities. Others were developed primarily for predicting rotor loads. Table 321.2 through Table 321.7 defines the functional capability of existing analyses.

Airfoil aerodynamics and induced downwash are determined by a variety of methods. Static airfoil properties are usually based on experimental data, using a table look-up procedure, with unsteady wake effects approximated by Theodorsen theory below stall. Unsteady aerodynamics in the stall regime, i.e., dynamic stall, is treated by several semi-empirical methods (Table 321.3). The effects of yawed flow on lift and drag are included for some methods. The rotor loads programs include a variety of methods for calculating nonuniform induced downwash (Table 321.3). Most are based on a lifting line theory with a finite element (potential vortex filaments) representation of the trailed and shed vorticity. Induced velocities are calculated from the Biot-Savart law.

Modal equations are obtained from the partial differential equations of a rotating beam, and the generalized coordinates of the normal modes are the system degrees of freedom. Finite element equations are based on the force and moment equilibrium of a lumped mass or elemental segment of the blade and each element requires several degrees of freedom. In either the modal or the finite element representation, the coupling between degrees of freedom is important. This is difficult to summarize and the information in Table 321.4 is far from definitive.

The numerical integration solution methods defined in Table 321.5 integrate the equations of motion in time from an arbitrary, assumed initial condition until a suitably converged solution is achieved. A variety of initial conditions, convergence criteria, convergence rates, integration methods, step sizes, etc., is used. The harmonic response solution methods generally calculate structural response using airload harmonics based on previously assumed blade motion and structural response. Iterations between the response and airloads continue until a converged solution is achieved.

The comparative study of Reference 321.2 presents a perspective on the state of the art in rotor loads analyses. A hypothetical rotor was defined and existing loads analyses were used to calculate rotor blade loads, vibratory hub shears, and other parameters. The following conclusions summarize the findings of this study with respect to the relative quantitative accuracy of these analyses:

a. Rotor forces, power, control positions, and blade flappings generally showed small to moderate differences.

b. Flapwise bending moments showed small to moderate differences that increase with advance ratio.

c. Chordwise bending moments showed moderate to large differences for all advance ratios.

d. Torsional response showed moderate to large differences, especially at high advance ratio.

e. Blade root vibratory shears showed large to very large differences.

Reference 321.2 was unique in that all methods were applied to the same set of standard cases for a hypothetical rotor. The results were surprising with respect to the relatively wide variation in loads predicted by the different methods. Figure 321.4 shows, for example, the large range in loads predicted for a typical operating condition. The methods all employed variable inflow and unsteady stall aerodynamics of one form or another. In examining the results, it was clear that differences existed in both the aerodynamic and structural formulation of the methods. Figure 321.5 shows that large differences existed even at the most fundamental level, namely that of steady state airfoil data. Figure 321.6 shows that differences also existed at the fundamental level of predicting in-vacuo blade natural frequencies. The variations seen in aerodynamic pitching moment and torsion natural frequency are

particularly important because the torsional response of the blade couples directly with the aerodynamic loading. Reference 321.2 concluded that: "Difficulties in the results arise from all three basic areas: numerical solution techniques, structural dynamics, and aerodynamics."

3.2.1.4 Status Of Structural Modeling

One of the main results of Reference 321.2 was the large differences in chordwise bending moments and vibratory shears even when nonlinear aerodynamic phenomena were absent or negligible. This indicated that important differences exist in structural dynamic modeling, probably due, in part, to different assumptions and approximations for structural/inertial coupling and, in part, to an inadequate fundamental knowledge of the mechanics of a flexible rotating blade. The results indicated that structural coupling effects are significant, that different approximations and assumptions are in common use, and that the validity of these approximations needs to be examined more closely.

Structural dynamic modeling of the rotor consists of relatively simplified modal or finite element procedures. Modal equations are obtained from the partial differential equations of a rotating blade, and the generalized coordinates of the normal modes are used as the system degrees of freedom. Finite element equations are based on the force and moment equilibrium of an elemental segment of the blade. In many applications, the structural dynamic representation of the rotor involves relatively simple analyses based on engineering beam theory. A recent correlation (Reference 321.4) of several analyses with data from a full-scale rotor blade operating in a vacuum showed reasonable agreement for conditions of minimum structural coupling and relatively simple root boundary conditions. However, the applicability of existing loads analyses for conditions of significant structural coupling from geometric, inertial, or elastic effects is unresolved. In general, operational loads analyses contain an incomplete structural dynamic representation of complex boundary conditions, such as control of kinematic constraints, dampers, and hub flexibility. As compared to state of the art structural dynamic modeling capability, the methods used in the vast majority of operational rotor loads analyses are antiquated techniques with limited versatility to model complex structures. Incomplete structural dynamic modeling influences the accuracy of rotor loads analyses, but more significantly, directly impacts basic rotor blade design. For example, separation of blade frequencies from appropriate harmonics of the excitation is a fundamental fatigue design consideration yet this is a major and recurring problem in recent helicopter development programs.

The aeroelastic nature of the rotor loads problem has focused attention on the rotor blade structural model as an area for introducing improvements. The accurate simulation of the structural and dynamic behavior of a rotor blade is less difficult than the accurate simulation of aerodynamic excitations. On the other hand, even at this time, the requirements for accurate structural simulation are not understood fully. There is a consensus that careful attention has to be paid to factors influencing blade torsional deflections.

Hodges in Reference 321.5 has derived equations valid to second order for homogeneous, isotropic beams undergoing moderate displacements. These equations are the basis of a finite element aeroelastic stability analysis, embodied in the GRASP program, now in development. Progress has been made in identifying some of the considerations for introducing more consistent normal modes coordinates in the blade response equations. References 321.6 and 321.7 discuss additional terms in the blade response equations required when coupled modes are employed to express the equations in normal modes coordinates. It was found in Reference 321.7 that additional stiffness terms arise because the blade pitches at angles different from the distribution used to obtain the coupled modes. Application of this approach described in Reference 321.7 did not lead to an unqualified selection of coupled or uncoupled modes. Nevertheless, these considerations are indicative of the attention being paid to the structural and dynamic representation.

Representations of structural redundancies characteristic of modern rotor blade designs have been introduced in several analyses available or under development. Multiple load path representations are available, for example, in the Boeing-Vertol C-60 and the Sikorsky ET499 analyses. These analyses are based on a Myklestad transfer matrix formulation and are limited to a harmonic balance solution. At present, these analyses are not able to represent transient phenomena. Figure 321.7 shows that moment distributions predicted by the Sikorsky ET499 program agree more closely with test data vibratory amplitude than the results obtained by the Sikorsky normal modes method Y200 of Reference 321.8. While systematic study has not yet been conducted to identify conclusively the causes of the differences, the key assumptions are believed to be the use of uncoupled modes, the assumption of low twist and the use of a modal displacement method to express moments in the modal analysis.

An avenue being followed to represent structural redundancies is a formulation based on the finite element displacement method. The GRASP program (unpublished work by Hodges) mentioned above is an example of such an analysis. An advantage of this approach is its ability to permit coupling of the blade to the airframe, control system, and structural restraints by means of automated techniques suitable for assembling finite elements and substructures in the context of a displacement method.

3.2.1.5 Status Of Two Dimensional Aerodynamic Modeling

The aerodynamic models used in rotor loads analyses are characterized by a heavy reliance on empirical techniques. Lifting line theory with two-dimensional airfoil data as a function of angle of attack and Mach number is almost universally used for blade aerodynamic loads. Many analyses incorporate approximate or semi-empirical corrections for the effects of dynamic stall, yawed flow, three-dimensional and compressible flow at the tip, and vortex/blade interactions. Empirical techniques are used either because existing aerodynamic theories are not able to model the complex viscous and compressible flow of the rotor blade, or because a rigorous application of the theory leads to an impractical numerical problem.

One of the most basic requirements in any rotor loads prediction analysis is the ability to determine the aerodynamic forces and moments at discrete blade sections. This has traditionally been done by calculating the local velocities and angles of attack and yaw (or sweep) and then using the measured

aerodynamic characteristics for two dimensional airfoil sections. As pointed out in Reference 321.2, however, substantial differences are apparent even at this very basic level, e.g., see Figure 321.4. Obviously, if one analysis was capable of precisely predicting the flow conditions and blade dynamic response different load predictions would still result because of uncertainty in airfoil data. It has been demonstrated and known for some time that different characteristics very likely will be obtained for the same airfoil section tested in two or more tunnels. This can be attributed to several factors including model surface quality, the Reynolds number differences, tunnel turbulence level, floor and ceiling interferences, wall interferences, and, to some extent, data acquisition techniques.

The dependency on empiricism for unsteady airfoil characteristics and, in particular, dynamic stall characteristics was also cited in Reference 321.2 as a deficiency in the prediction of rotor loads. While progress has been made in this area, it has predominantly been progress in obtaining additional experimental data and in investigating the basic features of dynamic stall. Reference 321.9 provides a good summary of what has been learned about dynamic stall and the current status of prediction techniques. Several prediction techniques are described and discussed by McCroskey in Reference 321.9 that are empirical in nature and each incorporates certain simplifying assumptions and shortcomings. As pointed out by McCroskey, each method manages to reproduce reasonably well the data sets used in its development, but almost no correlation has been demonstrated in reproducing independent data sets. A new semi-empirical technique has recently been developed by Gangwani in Reference 321.10. This method explicitly accounts for the formation and streamwise movement of the vortex shed from the leading edge. It also incorporates the effects of nonzero sweep angles.

A major contribution to the available data base and the understanding of dynamic stall phenomenon is reported in Reference 321.11. This work included tests of eight airfoils and an attempt to quantify the effects of several aifoil design parameters on the dynamic stall characteristics. Figure 321.8 presents the maximum lift achieved by seven of the sections tested. This figure shows that the lift increment due to deep dynamic stall, i.e., vortex dominated, large airload fluctuations, is not significantly different for the airfoils tested but the lift increment obtained at dynamic stall onset is affected by airfoil shape.

3.2.1.6 Status Of Three-Dimensional Aerodynamic Modeling

The blade element approach has been the traditional method of obtaining blade loads. This method assumes that each blade section behaves as if it were on a two-dimensional wing. The method applies to steady and unsteady conditions, but is not applicable for three-dimensional conditions, e.g., when a vortex passes near a blade or at the tip of a blade. Progress has been made at the fundamental level in developing three-dimensional, quasi-steady and unsteady, subsonic and transonic analyses. These analyses are referred to as blade analyses to imply that thickness effects are considered.

An inviscid, nonconservative, potential flow, quasi-steady lifting blade analysis is described by Arieli and Tauber in Reference 321.12. This method is an extension of a full potential code developed by Jameson (Reference 321.13) for fixed wing applications. The method currently accounts for only a single blade and, therefore, the wake induced flow field is incomplete. It also cannot currently account for tip vortex roll up and makes assumptions regarding the location of the vortex sheet to facilitate the derivation of the solution in transformed space. Results from this method are compared to experimental data and two-dimensional calculations for a station near the tip of a non-lifting rotor blade in Figure 321.9. For this station on the advancing blade, the calculation agrees well with experiment and the three-dimensional effects are significant. The three-dimensional characteristics shown near the tip could have large effects on the predicted blade loads and moments.

Another three-dimensional analysis under development is described in References 321.14 and 321.15. The mathematical model used in this method is a three-dimensional, unsteady (low frequency) small disturbance transonic model. Figure 321.10 shows the correlation of this method from Reference 321.16 with measured non-lifting rotor results at 90% radius and an azimuth of 120^{o}. Good correlation is shown for the unsteady calculation whereas the quasi-steady calculation fails to model the chordwise pressure distribution. This same characteristic was shown by Arieli and Tauber in Reference 321.12 at 120^{o} and indicates that accounting for the flow history is important.

The quasi-steady, lifting blade and the unsteady non-lifting blade analyses discussed have been used to analytically assess the impact of three-dimensional effects on the advancing tip. The results, to date, suggest that these effects on blade loads could be large. Also, practical techniques for modeling these effects in actual load prediction programs are required. An example of a practical lifting surface implementation for the blade vortex encounter problem is contained in the analysis of Reference 321.17.

3.2.1.7 Status Of Inflow Modeling

The ability to determine the aerodynamic loading on the blade requires the ability to predict the flow conditions to which each section of the blade is subjected as well as the blade motions. The history of predicting the induced inflow has evolved from uniform momentum models to longitudinal skewed momentum models to longitudinal/lateral skewed momentum models to discrete vortex models (sometime including the shed wake due to the time dependent lift) and wake distortions. It was shown by Arcidiacomo in Reference 321.1 that the nonuniform inflow associated with the vortex methods was necessary to better represent the airload character at least at some radial locations on the blade. To calculate higher harmonics of aerodynamic loads vortex-wake models are in use. As the computing times are nearly equal for rigid-wake and prescribed-wake analyses, models such as the experimental-prescribed-contracted-wake model shown in Figure 321.11 are preferred (reference 321.18). The blade is represented by a lifting line and the wake is divided into an inboard section and the tip vortex. In the near wake, meshes of trailed and shed vortices form the inboard section, whereas a bundle of trailing vortices forms the tip vortex. In the mid wake the shed vortices are omitted and in the far wake there are only two single tip and root vortices. Wake geometry is taken from experimental investigations of Landgrebe (Reference 321.19).

A more adequate represenation of the wake geometry in forward flight might be obtained by using free-wake analysis such as the free-wake model of Sadler, see Figure 321.12 and Reference 321.20. The blade is again represented by a lifting line and the wake is calculated by a process similar to the start-up of a rotor in a free stream. An array of discrete trailing and shed vortices is generated with vortex strengths corresponding to stepwise radial and azimuthal blade circulations. The array of shed and trailing vortices is limited to the near wake whereas an arbitrary number of trailing vortices form the far wake. The end points of the vortex elements are allowed to be transported by the resultant velocity of the free stream and vortex-induced velocities. Calculation is terminated when the vortices trailing from the blade during the first azimuthwise step no longer influence points of interest near the rotor disc. The results are wake geometry and wake flow data in addition to wake influence coefficients that may be used to calculate blade loads.

Perhaps the most significant progress in predicting the rotor inflow field has been the ability to predict the change in the inflow velocities due to the flow field generated by the fuselage. The use of potential flow panel methods such as that described in Reference 321.21 allows the calculation of the fuselage induced velocities at the rotor blade and the blade aerodynamic analysis can then account for the change produced in local blade loading and the wake strength. Figure 321.13 from Reference 321.22 shows the experimental and calculated differences in the blade flatwise bending moment with and without the fuselage. Certain features of the fuselage effect are reasonably well predicted; however, the effects in the first and second quadrant are poorly represented. Reference 321.22 also describes tests in which the effect of the fuselage on rotor loads is systematically measured.

3.2.1.8 Correlation

Although the verification of an analysis is often based upon correlation results, there are many factors other than accuracy of the analytical methodology employed in the analysis which can cause serious discrepancies in correlation results. These include: inputs to the analysis, measurement accuracy of the experimental data, uncertainties in the vehicle and rotor trim state, atmospheric conditions such as gust and turbulence, and the experience of the user. Perhaps the least investigated of these factors is the vehicle and rotor flight state. In many of the loads analyses, the vehicle trim (fuselage and rotor) is calculated externally and trim state differences can directly and indirectly affect the computation of blade loads and hub loads. In effect, any error or lack of proper theoretical formulations in the analyses are compounded by these factors. In order to verify any analysis through correlation, all of the above factors must be considered.

As is the case of any correlation study, the "best" results are obtained by the originator and most frequent user of the particular analysis. Results are dependent on a thorough knowledge of the program and proper interpretation of the extensive input requirements and output quantities. Thus, as a general rule, when an organization attempts to execute an externally developed analysis, the correlation results are not as "good" as internal users have experienced. The few studies published by other than the originators (see Reference 321.24 and 321.25) tend to be much less favorable. This situation has several possible explanations; the input quantities may be inaccurate, the user may not understand how to use the analysis effectively, or there may be too many empirical inputs which require adjustment to provide favorable correlation results.

In general, rotor loads analyses exhibit relatively poor correlation in low speed translational flight, in high speed level flight where significant blade stall is encountered, and in high load factor maneuvers. Most of the analyses provide acceptable steady state and peak-to-peak flapwise load predictions for moderate flight conditions. Edgewise correlation is consistently less accurate. Torsional bending moments and pitch link loads are normally more difficult to predict, especially at high advance ratios.

The problem associated with predicting rotor loads in low speed translational flight is associated with the inability to accurately estimate rotor inflow. Flight in this region results in the tendency of the wake to be drawn close or into the plane of the rotor disc. When this occurs, large higher harmonic components of inflow exist and result in high vibratory loads. This is illustrated by the flight test measurements of Reference 321.18. Figure 321.14 shows results of harmonic airloads as a function of multiples of the rotating frequency for 30, 50, and 70 kts horizontal flight speeds. A comparison of the results indicates a harmonic decay for the different airspeeds, whereas the absolute magnitudes of amplitudes increase with lower flight speeds. Figure 321.15 shows corresponding harmonics for variations in the vertical speed component, i.e., climb and descent at 30 kts airspeed. In climb the harmonic airloads show a strong decay versus frequency, indicating that nearly no vortex-interactions occur. In contrast to this favorable variation, the curve for the descent case is marked by large amplitudes at high harmonics, indicating severe vortex interactions. Further results from the transient flight conditions are shown in Figure 321.16 comparing the aerodynamic exciting forces during a landing flare condition. Two observations from this figure are: first, the higher harmonic amplitudes evident in the diagram are even exceeding the 1Ω and 2Ω trim loads; and second, that aerodynamic exciting forces change quite rapidly within one second during this flight condition.

Rotor loads analyses generally provide acceptable results for flapwise and edgewise loads at moderate level flight trim conditions. Typical correlation of the Sikorsky Aircraft normal modes Y200 analysis with CH-53A flight test data is shown in Figure 321.17 (from Reference 321.26) using two unsteady aerodynamic models and variable inflow. As can be seen, blade stresses correlated well with both unsteady models. However, push rod loads calculated with the Time Delay Model are much less than values calculated with the α, A, B Method and flight test values. Neither analytical model predicts the initiation of torsional response at approximately 180° azimuth angle. The calculated build up of push rod loads and blade stresses with airspeed is compared with flight test data in Figure 321.18. Both unsteady methods predict satisfactorily the increases in blade moments as stall is penetrated. Best correlation of the rise of control loads in stall is obtained with the α, A, B Method.

Typical correlation (from Reference 321.27) of the Bell Helicopter Textron rotorcraft flight simulation program C81 is shown in Figures 321.19 and 321.20. Calculations were made using unsteady

aerodynamics. Two airspeeds were selected at each CG condition, V_H and 0.8 V_H. Correlation of rotor loads is good at 0.8 V_H for both CG conditions. However, at V_H, C81 underpredicts both beamwise and chordwise moments at forward CG and overpredicts those at aft CG.

Measured and calculated pitch-link-load variation with speed for two different CG's are given in Figures 321.21 and 321.22. The analytical data were obtained using unsteady aerodynamics. Past experience with C81 has shown that in order to achieve oscillatory pitch link loads correlation, the unsteady aerodynamics option must be used. Past experience has also shown that a good definition of airfoil pitching moment characteristics is required for accurate prediction of both steady and oscillatory components of the pitch link load. The importance of using unsteady aerodynamics in pitch-link-load predictions is depicted in Figures 321.23 and 321.24. Shown in these figures are comparisons of flight test pitch link load waveforms with those calculated by C81 with and without unsteady aerodynamics. Both forward and aft CG conditions were analyzed. The data show that the use of the unsteady aerodynamic model not only improves the correlation in phase, but also the one- and two-per-rev magnitudes as evidenced by the time history waveforms.

Typical correlation of the Westland Helicopters Limited coupled mode rotor loads prediction program R150 is shown in Figures 321.25 and 321.26. Good correlation is indicated for flapwise and edgewise bending moments.

It is rare that any analysis correlates with test data on an absolute basis. Rotor loads analyses are no exception in this regard, as indicated by the preceding figures. However, often analyses lacking absolute correlation can be used to predict trends having been anchored to some reference data point. Figures 321.27 and 321.28 and 321.29 from Reference 321.3 show the application of the Sikorsky Normal Mode Analysis Y200 in this manner, Here the analysis is used to predict the effect of tip shape changes tested in Reference 321.22 on key blade loads. The results are normalized in terms of the rectangular tip loads at one gross weight and compared with similarly normalized data taken from Reference 321.22. The beneficial effects of advanced tips on flatwise moments and control loads are predicted. The detailed correlation for these two loads is reasonable but far from perfect even on this normalized basis. Edgewise moment correlation is significantly poorer than either the flatwise moment or the control load correlation. These results, while not unexpected in light of the lack of a rigorous three dimensional aerodynamic model in the analysis, do indicate the problem facing the designer as he tries to evolve more advanced rotors. The value of systematic test data is clear.

3.2.1.9 References

321.1 Specialists Meeting on Helicopter Rotor Loads Prediction Methods, Milan, Italy, AGARD Conference Proceedings No. 122, March 1973.

321.2 Ormiston, R.A., Comparison of Several Methods for Predicting Loads on a Hypothetical Helicopter Rotor, Journal of the American Helicopter Society, Vol 19, No. 4, October 1974.

321.3 Arcidiacono, P.J., and Sopher, R., Review of Rotor Loads Prediction Methods, London, England, AGARD Conference Proceeding No. 334, May 1982.

321.4 Lee, B.L., Experimental Measurement of the Rotating Frequencies and Mode Shapes of a Full Scale Helicopter Rotor in a Vacuum and Correlation with Calculated Results, Reprint 79-18, 35th Annual National Forum of the American Helicopter Society, May 1979.

321.5 Hodges, D.H., and Dowell, E.H., Nonlinear Equations of Motion for the Elastic Bending and Torsion of Twisted Nonuniform Rotor Blades, NASA TN D-7818, December 1974.

321.6 Sopher, R., Derivation of Equations of Motion for Multi-Blade Rotors Employing Coupled Modes and Including High Twist Capability, NASA CR 137810, February 1975.

321.7 Hansford, Robert E., Comparison of Predicted and Experimental Rotor Loads to Evaluate Flap-Lag Coupling with Blade Pitch, Journal of the American Helicopter Society, Vol 24, No. 5, October 1979.

321.8 Arcidiacono, P.J., Prediction of Rotor Instability at High Forward Speeds - Vol 1 - Steady Differential Equations of Motion for a Flexible Helicopter Blade with Chordwise Mass Unbalance, USAAVLABS TR 68-18A, February 1969.

321.9 McCroskey, W.J., The phenomenon of Dynamic Stall, Presented to von Karman Institute Lecture Series on Unsteady Airloads and Aeroelastic Problems in Separated and Transonic Flows, Rhode-Saint-Genese, Belgium, March 1981.

321.10 Gangwani, S.T., Prediction of Dynamic Stall and Unsteady Airloads for Rotor Blades, American Helicopter Society Preprint 81-1, Proceedings of the 37th Annual Forum of the American Helicopter Society, New Orleans, Louisiana, May 1981.

321.11 McCroskey, W.J., et al, Dynamic Stall on Advanced Airfoil Sections, American Helicopter Society Preprint 80-1, 36th Annual Forum of the American Helicopter Society, Washington, DC, May 1980.

321.12 Arieli, R., and Tauber, M., Computation of Subsonic and Transonic Flow About Lifting Rotor Blades, Presented at the AIAA Atmospheric Flight Mechanics Conference, Boulder, Colorado, August 1979.

321.13 Jameson, A., and Caughey, D., Numerical Calculation of the Transonic Flow Past a Swept Wing, Courant Institute of Mathematical Sciences, COO-3077-140, June 1977.

321.14 Carradonna, F.X., and Isom, M.P., Subsonic and Transonic Potential Flow Over Helicopter Rotor Blades, AIAA Journal, Vol IV, No. 12, December 1972.

321.15 Carradonna, F.X., and Steger, J.L., Implicit Potential Methods for the Solution of Transonic Rotor Flows, Presented at the 1980 Army Numerical Analysis and Computers Conference, Moffett Field, California, February 1980.

321.16 Chattot, J.J., Calculation of Three-Dimensional Unsteady Transonic Flows Past Helicopter Blades, NASA Technical Paper 1721, October 1980.

321.17 Johnson, W., Development of a Comprehensive Analysis for Rotor Craft: Aircraft Model Solution Procedure and Applications, Vertica Vol 5, pp 185-216, 1981.

321.18 Huber, H., and Polz, G., Studies on Blade-to-Blade and Rotor-Fuselage-Tail Interferences, London, England, AGARD Conference Proceeding No. 334, May 1982.

321.19 Landgrebe, A.J., An Analytical Method for Predicting Rotor Wake Geometry, Journal of the American Helicopter Society, Vol 14, No. 4, 1969.

321.20 Sadler, S.G., Development and Application of a Method for Predicting Rotor Free Wake Positions and Resulting Rotor Blade Air Loads, NASA CR-1911, 1971.

321.21 Sheehy, R.W., A Simplified Approach to Generalized Helicopter Configuration Modeling and the Predictions of Fuselage Surface Pressures, American Helicopter Society Symposium on Helicopter Aerodynamic Efficiency, Hartford, CT, March 1975.

321.22 Jepson, D., Moffitt, R., Hilzinger, K., Bissell, J., Analysis and Correlation of Test Data from an Advanced Technology Rotor System, NASA CR-152366, July 1980.

321.23 Freeman, C.E., and Wilson, J.C., Rotor-Body Interference (ROBIN) - Analysis and Test, American Helicopter Society 26th Annual Forum Preprint 80-5, May 1980.

321.24 Validation of Rotorcraft Flight Simulation Program Through Correlation with Flight Data for Soft Inplane Hingeless Rotors, USAAMRDL TR 75-50, January 1976.

321.25 Validation of the Rotorcraft Flight Simulation Programs (C81) for Articulated Rotor Helicopter Through Correlation with Flight Data, USAAMDRL TR 75-4, May 1976.

321.26 Blackwell, R.H., and Mirik, P.H., Effect of Blade Design Parameters on Helicopter Stall Boundaries, 30th Annual Nation Forum of the American Helicopter Society, May 1974.

321.27 Yen, J.G., and Glass, M., Helicopter Rotor Load Predictions, Specialist Meeting on Fatigue Methodology, St. Louis, Missouri, March 1980.

321.28 Drees, J.M., A Theory of Airflow Through Rotors and Its Application to Some Helicopter Problems, Journal of the Helicopter Society of West Britain, Vol 3, No. 2, pp 79-104, 1949.

321.29 Carta, F.O., Casellini, L.M., Arcidiacono, P.J., and Elman, H.L., Analytical Study of Helicopter Rotor Stall Flutter, 20th Annual National Forum of the American Helicopter Society, Washington, DC, 1970.

321.30 Harris, F.D., Tarzanin, F.T., Jr., and Fisher, R.K., Jr., Rotor High Speed Performance, Theory vs Test, Journal of the American Helicopter Society, pp 35-44, July 1970.

321.31 Beddoes, T.S., A Synthesis of Unsteady Aerodynamic Effects Including Stall Hysterisis, 1st European Rotorcraft and Powered Lift Aircraft Forum, September 1975.

321.32 Theodorsen, T., General Theory of Aerodynamic Instability and the Mechanics of Flutter, NACA Report 496, 1935.

321.33 Ericsson, L.E., and Reding, J.P., Dynamic Stall of Helicopter Blades, Journal of Americal Helicopter Society, Vol 17, No. 1, January 1972.

321.34 Tarzanin, F.J., Jr., Prediction of Control Loads Due to Blade Stall, Journal of American Helicopter Society, pp 33-46, April 1972.

321.35 Castles, W., Jr., and De Lewis, J.H., The Normal Component of the Induced Velocity in the Vicinity of a Lifting Rotor and Some Examples of its Application, NACA Report 1184, 1954.

321.36 Bielawa, R.L., Synthesized Unsteady Airfoil Data with Applications to Stall Flutter Calculations, 31st Annual National Forum of the Americal Helicopter Society, Washington, DC, May 1975.

321.37 Costes, J.J., Calcul des Forces Aerodynamiques Instation naires sur les Pales d'un Rotor de Helicoptere, AGARD Report No. 595, 1972.

321.38 Hoener, S.F., Aerodynamic Lift, Published by the Author, 1975.

3.2.1.10 Symbols

c	chord
c_p	pressure coefficient
f^p	flat plate area
M	Mach number
r	radial station
R	blade radius
$\bar{r}$	r/R
V	speed
V_H	maximum level flight airspeed
α	angle of attack
β	angles of sideslip
θ	blade pitch angle
Ω	rotor rotational speed
ψ	azimuth angle
μ	advance ratio

TABLE 1 HELICOPTER LOADS ANALYSES

COMPANY	CODE	PROGRAM NAME
BELL HELICOPTER TEXTRON, INC.	BHT	C-81
SIKORSKY AIRCRAFT, INC.	SA	Y200
UNITED AIRCRAFT RESEARCH LABORATORIES	UARL	G400
WESTLAND HELICOPTER LIMITED	WHL	R150
KAMAN AIRCRAFT CORPORATION	KAC	6F
HUGHES HELICOPTERS, INC.	HH	DART, CRFA-1
LOCKHEED AIRCRAFT CORPORATION	LAC	REXOR
COSTRUZIONI AERONAUTICHE AGUSTA	CAA	GRDP80, STAHR
BOEING VERTOL COMPANY	BV	C-60

TABLE 2 ANALYSIS FUNCTIONAL CAPABILITY

		FLIGHT CONDITIONS MODELED				
CODE	ROTOR TYPES	HOVER	FORWARD FLIGHT	STEADY STATE MANEUVERS	TRANSIENT MANEUVERS	OUTPUT CAPABILITIES
BHT C-81	ARTICULATED, HINGELESS, TEETERING	YES	YES	TURNS, PULL-UPS, PUSHOVERS	YES, ARBITRARY CONTROL INPUTS	HUB/BLADE/CONTROL SYSTEM LOADS, PERFORMANCE
SA Y200	ARTICULATED, HINGELESS, TEETERING	YES	YES	NO	VERTICAL GUST RESPONSE	BLADE LOADS, PERFORMANCE
UARL G400	ARTICULATED, HINGELESS, TEETERING	YES	YES	NO	NO	HUB/BLADE LOADS, PERFORMANCE
WHL R150	ARTICULATED, HINGELESS	YES	YES	PITCH & ROLL RATE	NO	HUB/BLADE/CONTROL SYSTEM LOADS, PERFORMANCE
KAC 6F	ARTICULATED, HINGELESS	YES	YES	YES	TRANSIENT RESPONSE TO BLADE INITIAL CONDITIONS	HUB/BLADE/CONTROL SYSTEM LOADS, PERFORMANCE
HH DART	ARBITRARY	YES	YES	YES	YES	HUB/BLADE/CONTROL SYSTEM LOADS, PERFORMANCE
HH CRFA-1	ARBITRARY	YES	YES	YES	NO	HUB/BLADE/CONTROL SYSTEM LOADS, PERFORMANCE
LAC REXOR	ARTICULATED, HINGELESS	YES	YES	YES	YES, ARBITRARY CONTROL INPUTS	HUB/BLADE/CONTROL SYSTEM LOADS, PERFORMANCE
CAA GRDP80	ARBITRARY	YES	YES	YES	YES	HUB/BLADE/CONTROL SYSTEM LOADS, PERFORMANCE
CAA STAHR	ARTICULATED, HINGELESS	YES	YES	YES	NO	HUB/BLADE/CONTROL SYSTEM LOADS, PERFORMANCE
BV C-60	ARTICULATED, HINGELESS TEETERING	YES	YES	YES	NO	HUB/BLADE/CONTROL SYSTEM LOADS, PERFORMANCE

TABLE 3 ROTOR AERODYNAMIC REPRESENTATION

CODE	GENERAL METHOD	AIRFOIL TABLES	TIP LOSS	INFLOW	BLADE VORTEX	UNSTEADY AERO BELOW STALL	DYNAMIC STALL LIFT	DYNAMIC STALL DRAG	DYNAMIC STALL MOMENT	YAWED FLOW
BHT C-81	2D STRIP THEORY	MAX OF 10 $F(\alpha, M)$	PORTION OF OUTBOARD SEG C_l SET TO ZERO	INPUT TABLES OR MOD MOMENTUM REF (28)	EMPIRICAL CORR TO LOCAL INDUCED VELOCITY	CARTA REF (29)	HARRIS REF (30)	HARRIS REF (30)	CARTA REF (29)	DRAG & $C_{l_{max}}$ REF (29)
SA Y200	2D STRIP THEORY	MAX OF 1 $F(\alpha, M)$	EMPIRICAL CORRECTION	UNIFORM OR FUNC OF SHAFT ANGLE	NONE	CARTA REF (29)	CARTA REF (29)	NO	CARTA REF (29)	NONE
UARL G400	2D STRIP THEORY	MAX OF 1 $F(\alpha, M)$	EMPIRICAL CORRECTION	3 OPTIONS: UNIFORM, GLAUERT, INPUT HARMONICS	COUPLED TO FREE WAKE ANALYSIS	NONE	EMPIRICAL	NO	EMPIRICAL	NONE
WHL R150	2D STRIP THEORY	MAX OF 1 $F(\alpha, M)$	C_l SET TO ZERO AT TIP	VORTEX RING MODEL OR GLAUERT OPTION	EMPIRICAL VORTEX CORE POSITIONED TO MODEL LOCAL VORTEX EFFECTS	INDICIAL REF (31)	BEDDOES REF (31)	BEDDOES REF (31)	BEDDOES REF (31)	MOD SWEEP RULE
KAC 6F	2D STRIP THEORY	MAX OF 10 $F(\alpha, M)$	LIFT ON OUTBOARD SEG SET TO ZERO	UNIFORM OR VARIABLE INPUT IN TABULAR FORM	INCL IN INDUCED VELOCITY INPUT	THEODORSEN REF (32)	NONE	NONE	NONE	EMPIRICAL
HH DART	2D STRIP THEORY	MAX OF 2 $F(\alpha, M)$	INCLUDED IN AIRFOIL TABLES	UNIFORM OR PRESCRIBED STEADY AND OSCILLATORY	NONE	THEODORSEN REF (32)	ERICSSON & REDING REF (33)	NONE	ERICSSON & REDING REF (33)	$C_{l_{max}}$ REF (30)
HH CRFA-1	2D STRIP THEORY	MAX OF 3 $F(\alpha, M)$	INCLUDED IN AIRFOIL TABLES	NONUNIFORM - CYLINDRICAL VORTEX THEORY	UNDER DEVELOPMENT	THEODORSEN REF (32)	EMPIRICAL	EMPIRICAL	EMPIRICAL	$C_{l_{max}}$ REF (30)
LAC REXOR	2D STRIP THEORY	MAX OF 2 $F(\alpha, M)$	C_l SET TO ZERO AT TIP	EMPIRICAL MOD OF CASTLE INFLOW MODEL REF (35)	NONE	THEODORSEN REF (32)	TARZANIN REF (34)	TARZANIN REF (34)	HARRIS REF (30)	DRAG & $C_{l_{max}}$ REF (30)
CAA GRDP80	2D STRIP THEORY	YES OR USER INPUT EXPRESSIONS	YES	UNIFORM, GLAUERT, MANGLER-SQUIRE OR ARBITRARY DISTRIBUTION	NONE	QUASI-STATIC OR BIELAWA REF (36)	COSTES REF (37)	COSTES REF (37)	BIELAWA REF (36)	MODIFIED HORNER REF (38)
CAA STAHR	2D STRIP THEORY	ANALYTICAL EXPRESSIONS FROM TEST DATA	NONE	USER PRESCRIBED INPUT	NONE	QUASI-STATIC OR BIELAWA REF (36)	BIELAWA REF (36)	BIELAWA REF (36)	BIELAWA REF (36)	MODIFIED HORNER REF (38)
BV C-60	2D STRIP THEORY	MAX OF 5 $F(\alpha, M)$	YES	LIFTING LINE VORTEX THEORY	EMPIRICAL VORTEX SEGMENTS AT TIP AND ROOT	THEODORSEN REF (32)	TARZANIN REF (34)	TARZANIN REF (34)	HARRIS REF (30)	DRAG & $C_{l_{max}}$ REF (30)

TABLE 4 ROTOR STRUCTURAL DYNAMIC REPRESENTATION

CODE	NO. OF ELASTIC ROTORS	KINEMATIC COUPLING	ELASTIC & INERTIAL PROPERTIES	GEOMETRIC PROPERTIES	EQUATIONS OF MOTION	MAX NO. OF MODES OR FINITE ELEMENTS	COUPLING OF MODES OR FINITE ELEMENTS	DEGREES OF FREEDOM HUB	DEGREES OF FREEDOM SWASHPLATE	DEGREES OF FREEDOM PYLON
BHT C-81	2	LAG DAMPER δ_3, PRECONE, PRELAG, PITCH AXIS OFFSET	ARBITRARY 20 SEG	ARBITRARY 20 SEG	MODAL	11	FULLY COUPLED FLAP/LAG TORSION	FIXED	COLLECTIVE CYCLIC	MAXIMUM 10 MODES
SA Y200	1	LAG DAMPER, δ_3, PRECONE, PRELAG	ARBITRARY 15 SEG	ARBITRARY 15 SEG	MODAL	8	UNCOUPLED FLAP/LAG/TORSION	FIXED	COLLECTIVE CYCLIC	N/A
UARL G400	1	LAG DAMPER, δ_3, PRECONE, PRELAG	ARBITRARY 15 SEG	ARBITRARY 15 SEG	MODAL	10	UNCOUPLED FLAP/LAG/TORSION	6 DOF	COLLECTIVE CYCLIC	N/A
WHL R150	1	LAG DAMPER, δ_3, α_2, TORQUE OFFSET	ARBITRARY 24 SEG	ARBITRARY 24 SEG	MODAL	8	FULLY COUPLED FLAP/LAG TORSION	FIXED	COLLECTIVE CYCLIC, HHC	FIXED
KAC 6F	1	LAG DAMPER, FEATHERING, BENDING, SERVO FLAP, TWIST	ARBITRARY 30 SEG	ARBITRARY 30 SEG	MODAL	7	FULLY COUPLED FLAP/LAG/TORSION SERVO FLAP	FIXED	COLLECTIVE CYCLIC	FIXED
HH DART	1	ARBITRARY REDUNDANT LOAD PATH	ARBITRARY	ARBITRARY	FINITE ELEMENT	11	FULLY COUPLED FLAP/LAG TORSION	6 DOF	COLLECTIVE CYCLIC	6 DOF
HH CRFA-1	1	ARBITRARY	ARBITRARY	ARBITRARY	FINITE ELEMENT	50	FULLY COUPLED FLAP/LAG TORSION	6 DOF	COLLECTIVE CYCLIC	INCLUDED AS HUB IMPEDENCE
LAC REXOR	1	PRECONE, DROOP, SWEEP, PITCH/LAG, PITCH/FLAP	ARBITRARY 20 SEG	ARBITRARY EXCEPT CONST CHORD	MODAL	4	COUPLED FLAP/LAG UNCOUPLED TORSION	6 DOF	COLLECTIVE CYCLIC	FIXED
CAA GRDP80	LIMITED BY CORE ONLY	ARBITRARY	ARBITRARY	ARBITRARY	FINITE ELEMENT	LIMITED BY CORE ONLY	ARBITRARY	ARBITRARY	ARBITRARY	ARBITRARY
CAA STAHR	1	ANY COMB OF SINGLE DOF HINGES	ARBITRARY	ARBITRARY	FINITE ELEMENT	LIMITED BY CORE ONLY	ARBITRARY	FIXED	COLLECTIVE CYCLIC	N/A
BV C-60	1	LAG DAMPER, δ_3, SWEEP, DROOP, PRECONE	ARBITRARY	ARBITRARY	FINITE ELEMENT	25	COUPLED FLAP/TORSION, UNCOUPLED EDGEWISE	6 DOF	COLLECTIVE CYCLIC	FIXED

TABLE 5 NUMERICS AND SOLUTION PROCEDURES

CODE	METHOD OF SOLUTION	INTEGRATION METHOD	CONVERGENCE CRITERIA	INTEGRATION STEP SIZE	NUMBER OF RADIAL POINTS	REVOLUTIONS OR ITERATIONS FOR CONVERGENCE
BHT C-81	NUMERICAL INTEGRATION	4 CYCLE RUNGE-KUTTA	NONE	USER INPUT FUNCTION OF MAX MODAL FREQ	20	N/A
SA Y200	NUMERICAL INTEGRATION	MODIFIED EULER	BLADE ANGLE CONVERGED TO WITHIN .001 RADIAN	INPUT	15	5
UARL G400	NUMERICAL INTEGRATION	ADAMS	DEFINED BY FLAP & LAG MOTION WITHIN INPUT VALVES	INPUT	15	INPUT
WHL R150	NUMERICAL INTEGRATION	Z TRANSFORM ZERO ORDER HOLD	MODAL RESPONSE $<$ 1% BETWEEN REVOLUTIONS	INPUT	13	6-9
KAC 6F	NUMERICAL INTEGRATION	INTEGRATING MATRIX OPERATOR	ROTOR BLADE PERIODICITY FOR STEADY STATE SOLUTION	72	30	N/A
HH DART	NUMERICAL INTEGRATION	NEWMARK	SUBHARMONIC RESPONSE $<$ 1% OF LARGEST HARMONIC	INPUT	11	20
HH CRFA-1	HARMONIC RESPONSE		AIRLOAD DISTRIBUTION $<$ 1% CHANGE		50	
LAC REXOR	NUMERICAL INTEGRATION	ADAMS-BASHFORTH (TIME) TRAPOZODIA	ACCELERATION CORRECTION TERMS WITHIN TOLERANCE	INPUT	20	N/A
CAA STAHR	NUMERICAL INTEGRATION	NEWTON	EUCLIDEAN NORM	24	10	N/A
BV C-60	HARMONIC RESPONSE		NONE	INPUT	20	10-20

TABLE 6 TRIM PROCEDURE

CODE	PROCEDURES	CRITERIA
BHT C-81	Modified Newton-Raphson; 2 body attitudes, 4 rotor controls and rotor long and lat flapping to satisfy requirements on X, Y, and Z force, L, M, N moments and rotor flapping equilibrium for quasi-static.	Within user input rigid body forces and moments and rotor flapping moments for quasi-static. For time-variant assumed after a user input number of rotor revolutions.
SA Y200	Newton-Raphson iteration with rotor controls and rotor shaft angle as independent variables. Order of trim is Z force balance and rotor flapping equilibrium followed by yawing moment and side force.	Main rotor rigid body flapping approaching zero, Z and Y force and yawing moment to within user input values.
UARL G400	Optional trim to either an input shaft angle or propulsive force.	Rotor control angles iterated until input tolerances are met on pitching moment, rolling moment, lift force.
WHL R150	Trim program, with simple rotor model, satisfies inplane and vertical forces and pitch, roll, and yaw moments to define main and tail rotor trim conditions. These conditions are then input, for an isolated rotor, into the Coupled Mode Rotor Performance and Load Prediction Program (R150).	Trim convergence to within user specified force and moment tolerances.
KAC 6F	Servoflap controls, fuselage, and horizontal tail incidences, and tail rotor thrust to satisfy force and moment trim.	Trim within user specified tolerances of forces and moments for aircraft trim.
HH DART	Rotor trim; specify flapping thrust and/or torque. Thrust assumed perpendicular to tip path plane for trim.	Trim within user specified tolerances.
HH CRFA-1	Rotor only trim requiring first harmonic of thrust moment to go to zero.	
LAC REXOR	A set of up to 10 "controlling" and "controlled" variables can be chosen, a one to one relationship is defined and "controlling variables" are iterated on until convergence is obtained.	The "controlling variable" changes are within user input "activity band."
CAA GRDP80	Quasi-static and time variant option.	
CAA STAHR	Quasi-static only.	
BV C-60	External trim program. Trim conditions are then input for an isolated rotor into C-60.	Trim within user specified tolerances. Input hub forces matched and control positions change less than 0.1 degree between iterations.

TABLE 7 AIRFRAME AERODYNAMIC AND DYNAMIC REPRESENTATION

CODE	FUSELAGE AERODYNAMICS	LIFTING SURFACE AERODYNAMICS	AERODYNAMIC INTERACTIONS: ROTOR/FUSELAGE	ROTOR/SURFACES	ROTOR/ ROTOR	FUSELAGE/SURFACES	AIRFRAME DYNAMICS
BHT C-81	INPUT TABLES $F(\alpha, \beta)$ OR NONLINEAR EQUATION OPTION	3D TABLES $F(\alpha, \beta)$ OR 2D EQUATIONS WITH SWEEP AND AR CORRECTIONS	NONE	TABLES OR EQUATIONS	NONE	EMPIRICAL CORRECTIONS	RIGID BODY POINT MASS
SA Y200	LINEAR VARIATION WITH α, β	LINEAR VARIATION WITH α, β	AVERAGE DOWNWASH FACTOR	CORR TO TAIL NORMAL FORCE	NONE	LAG DOWNWASH CORR TO TAIL NORMAL FORCE	RIGID BODY POINT MASS
UARL G400	N/A	N/A	NONE	NONE	NONE	NONE	N/A
WHL R150	INPUTS FROM TEST DATA	INPUTS FROM TEST DATA	FUSELAGE UPWASH, INCLUDING EFFECTS ON WAKE DISPLACEMENT	NONE, INCLUDED IN TRIM PROGRAM	NONE	NONE	SEPARATE PROGRAM FOR CALCULATION OF AIRFRAME DYNAMICS
KAC 6F	2D LINEAR	2D LINEAR	NONE	NONE	NONE	NONE	RIGID BODY POINT MASS
HH DART	NONE	NONE	NONE	NONE	NONE	NONE	NONE
HH CRFA-1	SURFACE SINGULARITY	SURFACE SINGULARITY	NONE	NONE	NONE	NONE	FULLY COUPLED NASTRAN MODEL
LAC REXOR	INPUT TABLES	INPUT TABLES	INPUT TABLES FUNCTION OF WAKE ANGLE	INPUT TABLES FUNCTION OF WAKE ANGLE	NONE	NONE	RIGID BODY POINT MASS
CAA GRDP80	INPUT TABLES	INPUT TABLES	YES	YES	YES	YES	FINITE ELEMENT REPRESENTATION
CAA STAHR	N/A	N/A	N/A	N/A	N/A	N/A	N/A
BV C-60	N/A	N/A	N/A	N/A	TANDEM ROTORS	N/A	N/A

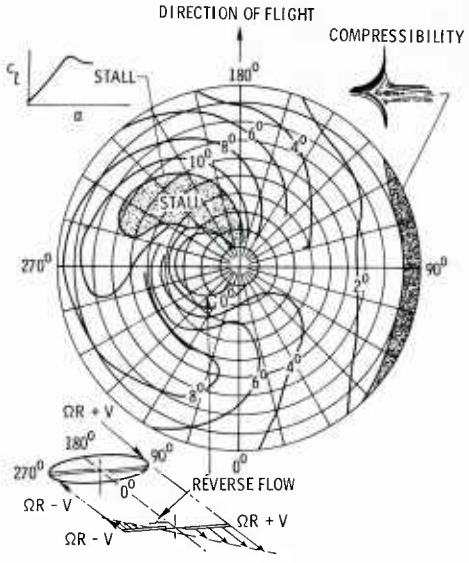

FIG. 321-1

MAIN ROTOR
AERODYNAMIC ENVIRONMENT

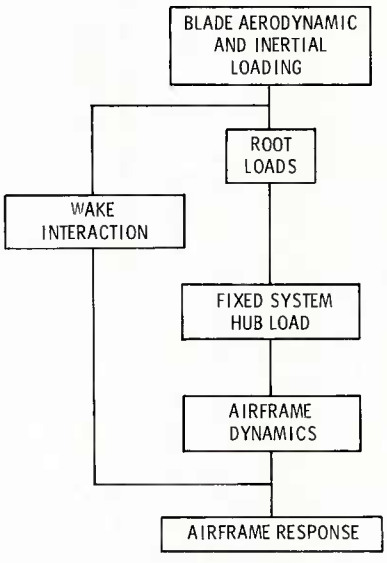

FIG. 321-2

ROTOR LOAD PATHS

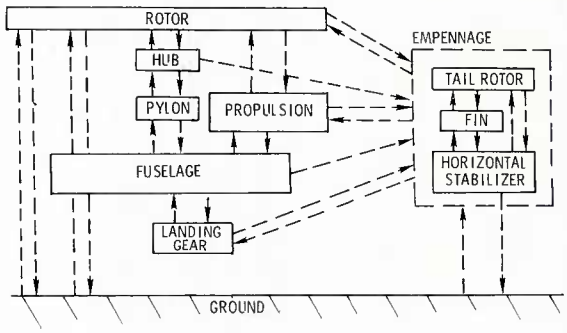

FIG. 321-3

AERODYNAMIC INTERACTIONS
OF A SINGLE MAIN ROTOR HELICOPTER

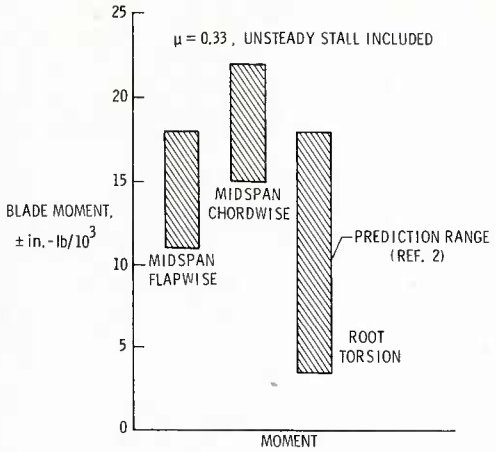

FIG. 321-4

ANALYSES DIFFER WIDELY
IN PREDICTED MOMENTS

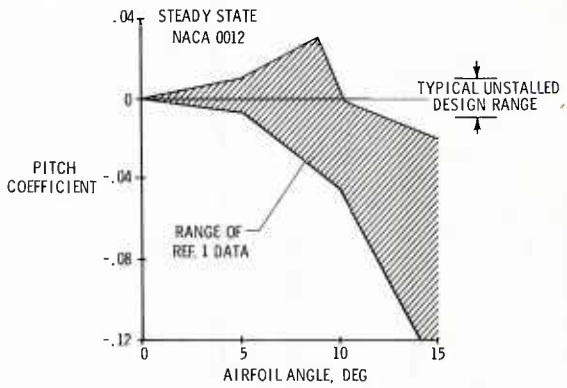

FIG. 321-5

CRITICAL AIRFOIL DATA
SHOW LARGE SCATTER

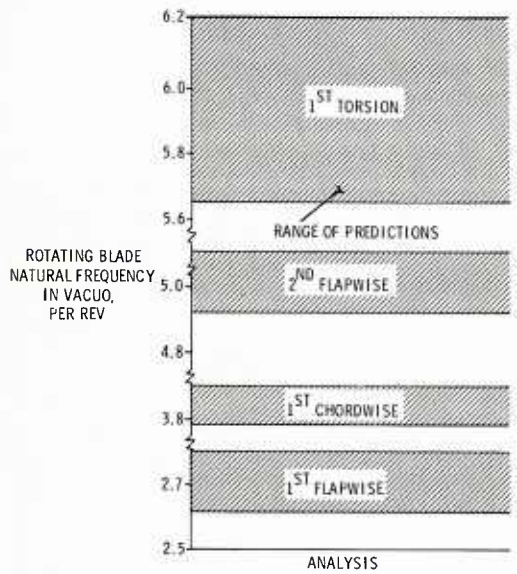

FIG. 321-6

REFERENCE 1 SHOWED
LARGE SCATTER IN PREDICTED
NATURAL FREQUENCIES

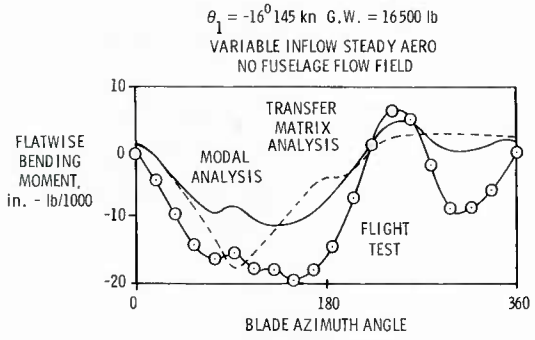

FIG. 321-7

COMPARISON OF MODAL ANALYSIS AND TRANSFER MATRIX ANALYTIC RESULTS WITH FLIGHT TEST

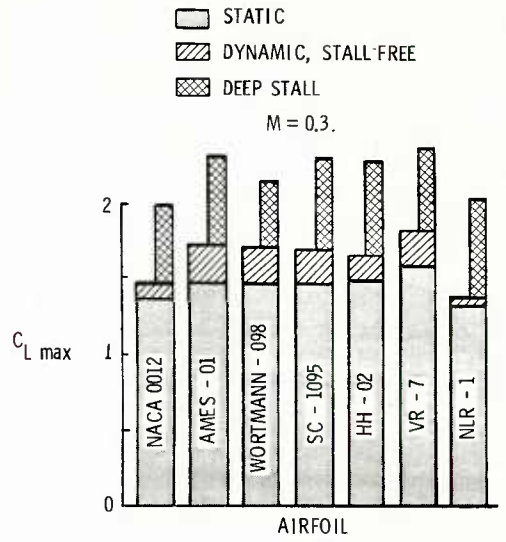

FIG. 321-8

COMPARISON OF AIRFOIL STALL CHARACTERISTICS

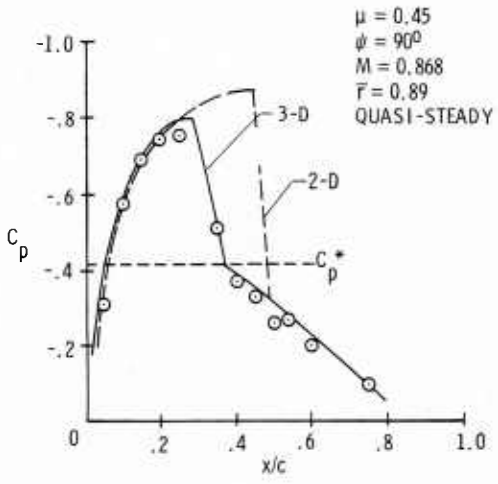

FIG. 321-9

COMPARISON OF TWO AND THREE DIMENSIONAL PRESSURE CALCULATIONS WITH MEASUREMENT

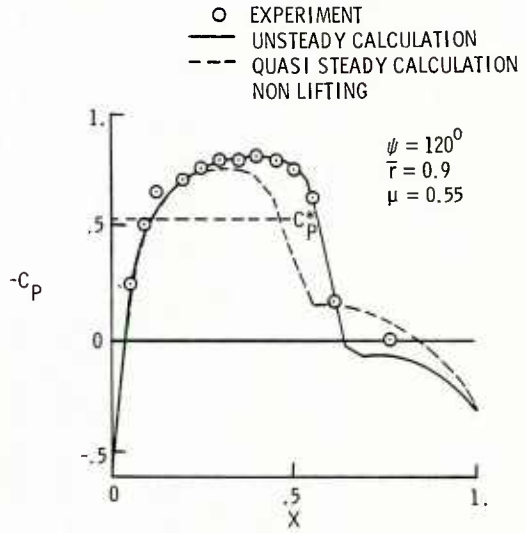

FIG. 321-10

COMPARISON OF UNSTEADY AND QUASI STEADY PRESSURE CALCULATIONS WITH MEASUREMENT

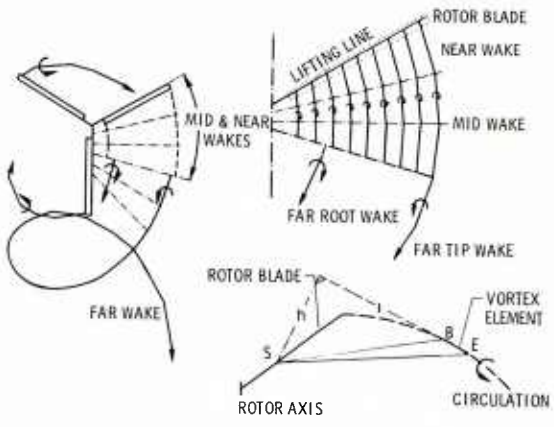

FIG. 321-11

WAKE STRUCTURE OF THE PRESCRIBED-CONTRACTED-WAKE MODEL

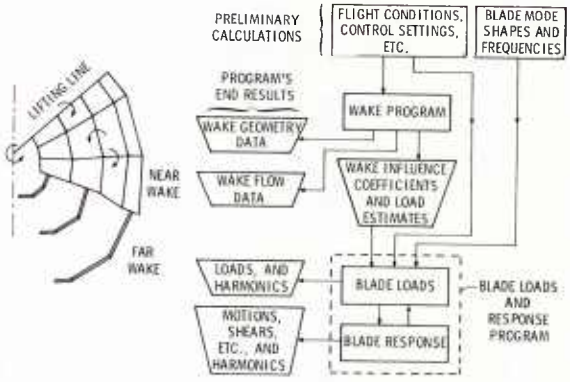

FIG. 321-12

WAKE STRUCTURE AND FLOW DIAGRAM OF THE FREE-WAKE MODEL (SADLER)

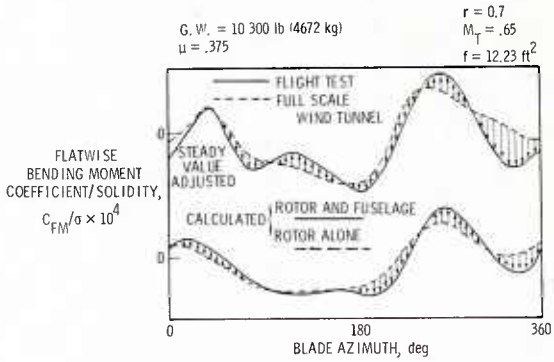

FIG. 321-13

EFFECT OF FUSELAGE ON BLADE FLATWISE BENDING MOMENT TIME HISTORY. TEST AND CALCULATED RESULTS.

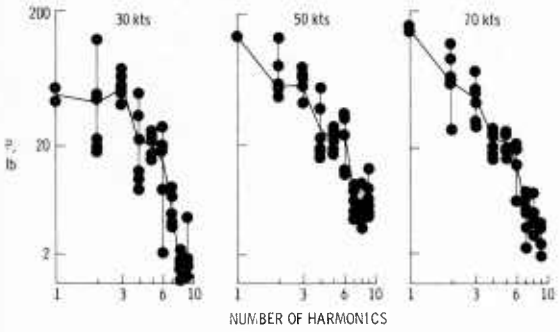

FIG. 321-14

HARMONIC AIRLOADS FOR DIFFERENT HORIZONTAL FLIGHT SPEEDS (FROM BLADE BENDING MEASUREMENT)

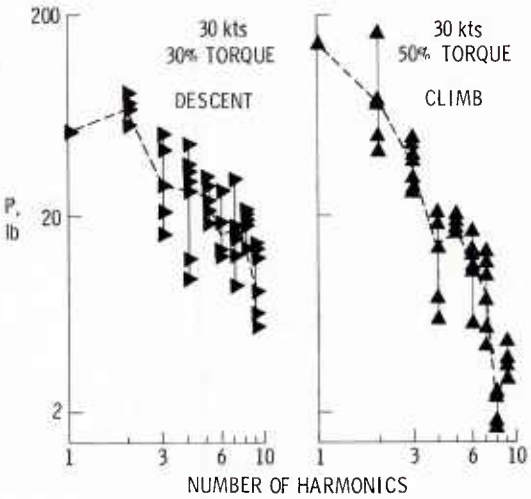

FIG. 321-15

HARMONIC AIRLOADS DURING CLIMB AND DESCENT CONDITIONS AT 30 KTS

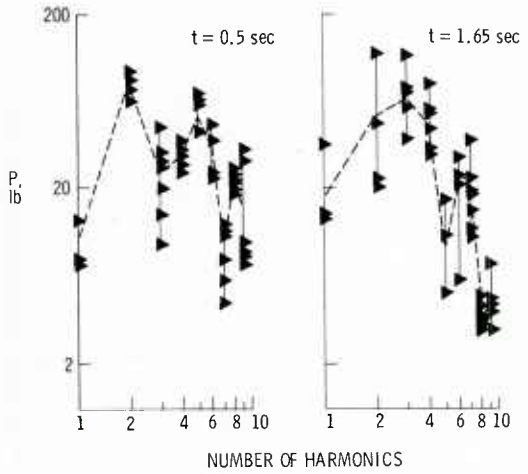

FIG. 321-16

HARMONIC AIRLOADS DURING LANDING FLARE, TRANSIENT CONDITION (FROM BLADE BENDING MEASUREMENTS)

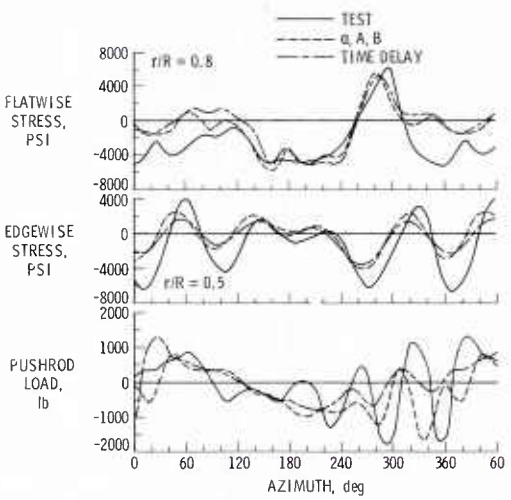

FIG. 321-17

CORRELATION OF CH-53A BLADE STRESSES AND PUSHROD LOADS

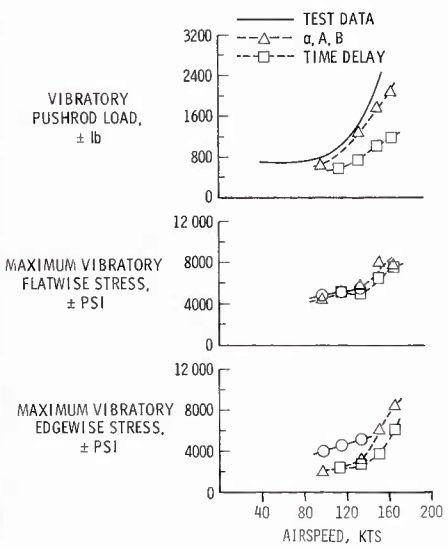

FIG. 321-18

CORRELATION OF CH-53A PUSHROD LOADS, BLADE STRESSES AND REQUIRED POWER

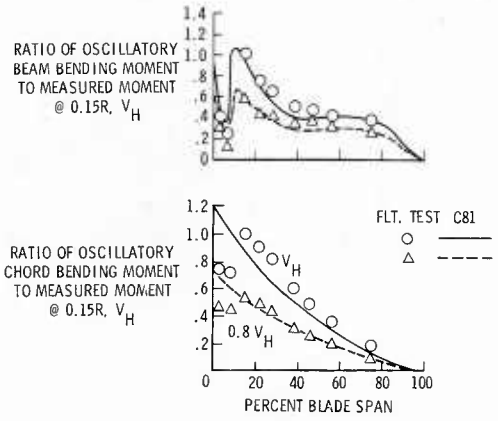

FIG. 321-19

BLADE LOADS CORRELATION AT TWO DIFFERENT AIRSPEEDS FOR A TWO-BLADED TEETERING ROTOR AT DESIGN GROSS WEIGHT, FORWARD CG

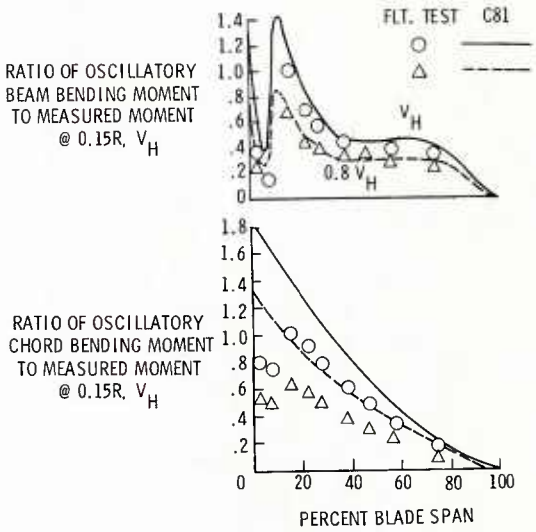

FIG. 321-20

BLADE LOADS CORRELATION AT TWO DIFFERENT AIRSPEEDS FOR A TWO-BLADED TEETERING ROTOR AT DESIGN GROSS WEIGHT, AFT CG

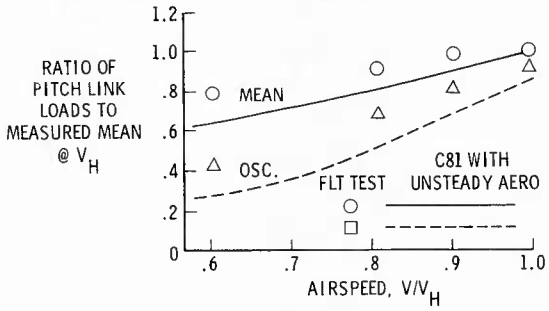

FIG. 321-21

CORRELATION OF PITCH LINK LOADS FOR A TWO-BLADED TEETERING ROTOR AT DESIGN GROSS WEIGHT AND FORWARD CG

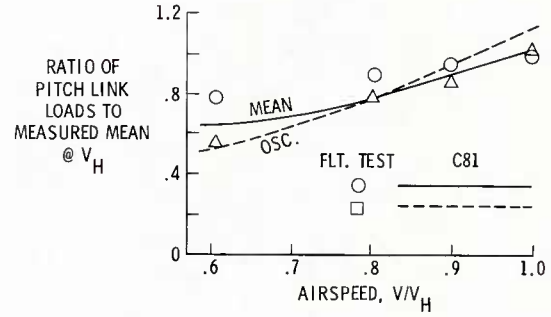

FIG. 321-22

CORRELATION OF PITCH LINK LOADS FOR A TWO-BLADED TEETERING ROTOR AT DESIGN GROSS WEIGHT AND AFT CG

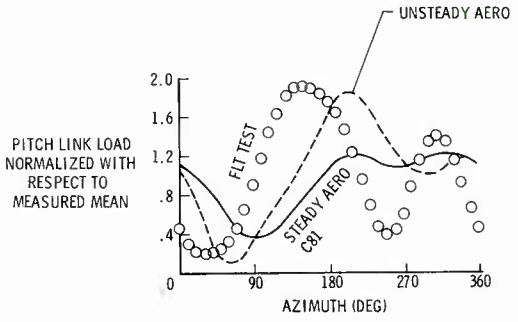

FIG. 321-23

CORRELATION OF PITCH-LINK-LOAD WAVEFORM FOR A TWO-BLADED TEETERING ROTOR AT DESIGN GROSS WEIGHT, V_H AND FORWARD CG

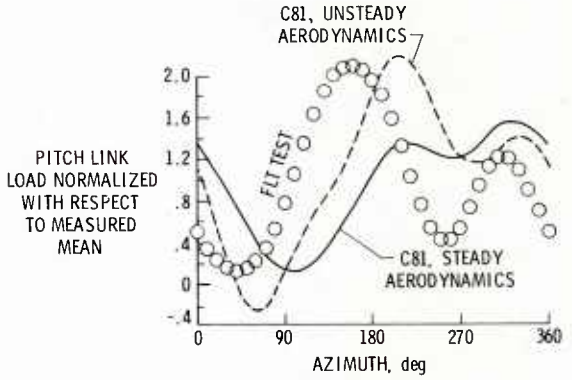

FIG. 321-24

CORRELATION OF PITCH-LINK-LOAD WAVEFORM FOR A TWO-BLADED TEETERING ROTOR AT DESIGN GROSS WEIGHT, V_H AND AFT CT

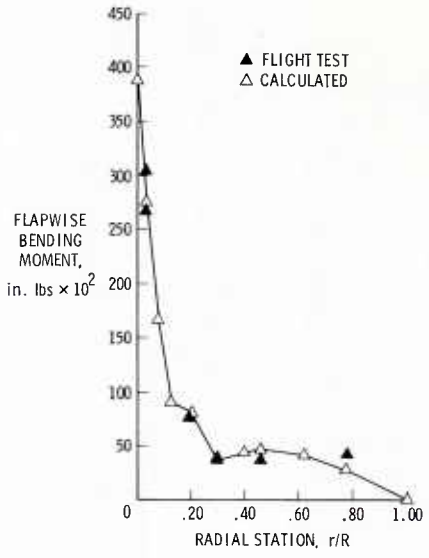

FIG. 321-25

CORRELATION OF WG 30 MAIN ROTOR FLAPWISE BENDING MOMENT WITH R150 ANALYSIS RESULTS

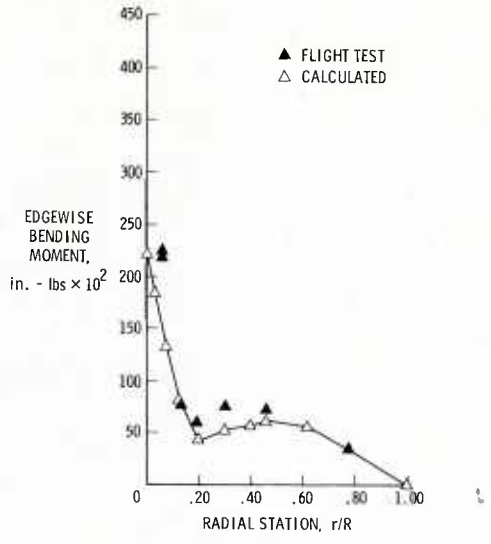

FIG. 321-26

CORRELATION OF WG 30 MAIN ROTOR EDGEWISE BENDING MOMENT WITH R150 ANALYSIS RESULTS

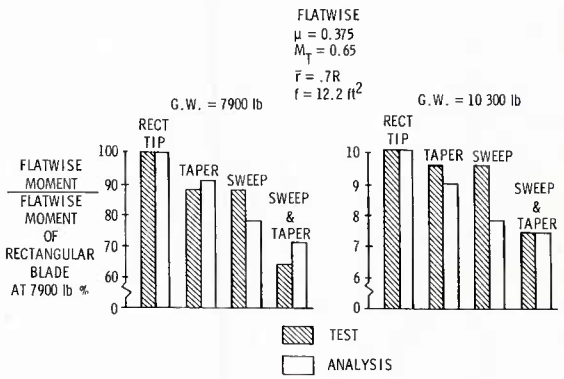

FIG. 321-27

COMPARISON OF PREDICTED AND MEASURED TRENDS OF FLATWISE MOMENT WITH TIP SHAPE CHANGES

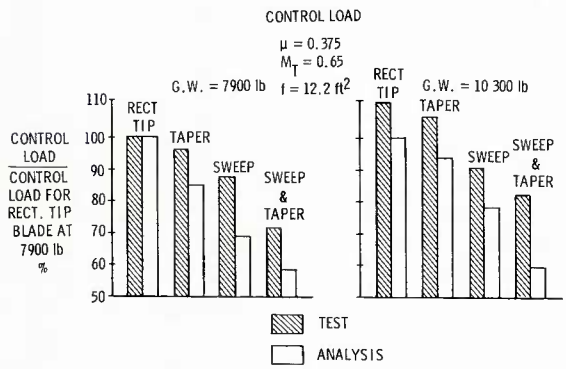

FIG. 321-28

COMPARISON OF PREDICTED AND MEASURED TRENDS OF FLATWISE MOMENT WITH TIP SHAPE CHANGES

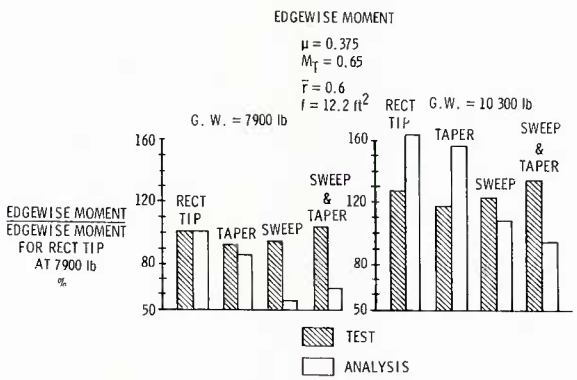

FIG. 321-29

COMPARISON OF PREDICTED AND MEASURED TRENDS OF EDGEWISE MOMENT WITH TIP SHAPE CHANGES

3.2.2 TRANSMISSION SYSTEM

by
René GARCIN

Société Nationale Industrielle Aérospatiale
B.P. 1 – 13725 MARIGNANE CEDEX
FRANCE

CONTENTS

3.2.2 Transmission system

The rotor is a receiver for :

- torque
- data (collective pitch and cyclic pitch).

The transmission system is thus to be broken down into :

- the torsion system which transmits the engine torque to the main and tail rotors
- the control system which transmits the pilot's orders to the rotor.

3.2.2.1 Torsion system

The load to take into account is torque essentially (the shaft bending moment is also to be considered in the particular case of the MGB housing and the shaft itself).

The dimensioning of the torsion system, as well as of all transmission components, must be determined from :

- static strength,
- low cycle fatigue,
- vibration endurance fatigue.

As regards static strength, the point is to substantiate the resistance to limit loads (as well as to ultimate loads equal to limit loads x 1.5) which are the maximum possible accidental loads.

With one engine operating, the limit torque is estimated to 1.25 times the maximum contingency torque (which covers possible transients).

With two engines operating, the limit torque is either 1.25 times the maximum continuous torque or equal to the maximum take-off torque.

The shaft maximum bending moment will be associated with the spectrum maximum load factor.

As regards low cycle fatigue (number of cycles lower than 100 000 : starting/shutdown cycles for instance) only the maximum flight torque is taken into account.

As regards vibration endurance fatigue, it is necessary to know the full spectrum of torque values used during the flight, that is to associate the time percentages defined in paragraph 3.1. with the corresponding torque value.

This will be determined from the power outputs and rotor speeds. The following flight phases can be distinguished :

- **Stabilized flight phases** :
  Hovering, sidewards flight, level flight with and without side-slip, stabilized turns, climb, descent . . . .

- **Transient flight phases** :
  Accelerated transition to forward flight, sidewards flight with gust, stopped turns . . .

Power prediction is conducted differently according to whether a stabilized or a transient flight phase is considered :

- **Stabilized flight phases** :

  The performance computation programmes taking into account the different characteristics of the aircraft used for these flight phases :

  - main rotor : diameter, chord, aerodynamic profile, blade twist, speed
  - fuselage : characterized by its C_x S which can be measured through wind tunnel testing.

  It is thus possible to plot polar curves giving the required power for the flight case considered (hovering, level flight, climb, descent . . .) according to weight, speed and flight conditions (altitude, temperature).

  These polar curves are usually calculated from known polars of existing aircraft, all differences between the two aircraft being carefully taken into consideration (differences as to rotor characteristics, C_x S, etc ...).

  These polars are then refined as flight tests proceed.

  The power taken by the tail rotor is generally obtained from its «Thrust-Power» polar curve.

  In hovering the thrust is calculated as being the tail rotor thrust. In forward flight, the fin must be taken into account (especially for aircraft provided with a fenestron since at a certain speed the fin provides almost all counter torque ; the power taken by the fenestron is then very low, less than 2 % of the total power.

  The power lost in the control linkage equals a certain percentage of the total power. The power required to drive a certain number of ancillaries must be added to this percentage. To take an example, on a 2-ton aircraft 20 kW are necessary to drive the ancillary equipment wilst 3 % of the total power is lost through friction.

The power supplied to the main rotor can be deduced from these data.

– **Transient flight phases**

The theoretical approach to these phases is particularly difficult. For this reason, the results of measurements taken in flight on existing helicopters are used (mainly stress assessment flights where all these transients phases are carried out).

Since maximum torque is not taken during the whole duration of a transient phase, these phases can be broken down in a finer way. This is the case for flight phases such as the sidewards flight or stopped turn.

For instance, as regards the stopped turn, it is assumed that to stop the ship sudden actions on the rudder pedals, sometimes pedal fully down depending on flight conditions, are necessary. The torque taken by the tail rotor is then maximum and could reach 30 % of the main rotor power.

For other phases such as the take-off phase the procedure recommended in the flight manuals is adopted.

Finally, since the spectrum is calculated for different weights or altitudes, the limitations imposed on the aircraft must be taken into account :

- torque mechanical limitation
- thermal power limitation of engine(s)
- pitch limitation (main rotor or tail rotor).

Input power prediction concerns three levels :

- main gearbox input
- main rotor shaft : with a power level less than that at the MGB input because of power losses in the transmission components and various power take-offs (ancillary systems and possibly tail rotor power)
- tail rotor drive.

Example of power spectrum

EXAMPLE 1 MAIN GEARBOX POWER SPECTRUM

Configuration	%	Power in kW		
		MGB input	Main rotor	Tail rotor
Hovering IGE	7	654	524	111
Hovering OGE	3	731	581	129
Backward flight at max. permissible speed	.4	530	425	88
Transition from backward flight to forward flight	.1	700	557	123
RH sidewards flight at maximum speed	1	487	425	45
LH sidewards flight at maximum speed	.9	562	425	120
LH sidewards flight with gust	.1	662	425	220
etc . . .				

Concurrently with the strength analysis, a study of the system dynamic response to torsional loads is necessary in order to ensure that the natural torsional frequencies are correctly situated. This being done, the torque dynamic value is chosen ; from experience, this value is equal to ± 8 % modulation of the static value ; this value can be corrected once the first actual values are recorded.

Taking into account the very high operating frequencies of the reduction gears, dimensioning is generally not intended for a limited service life but rather for unlimited service life, the maximum flight load being covered.

We shall see hereunder that the dimensioning principle is different for the control system or rotor shaft components. As far as the rotor shaft is concerned, it is the bending moment that constitutes the essential load. The moments at the rotor head as well as the blade control loads are covered in paragraph 3.2.1.

The same principle applies to the gear boxes casings submitted to the rotor loads and the reactions at the attachment points to the airframe.

From looking at the example of spectrum given below it is clear that the use of the max. flight load would entail component oversizing.

EXAMPLE 2 SPECTRUM OF MAIN ROTOR SHAFT BENDING MOMENTS

Configuration	Time %	Moment mN
Hovering IGE	3.5 fwd C.G. position	3300
	1.75 neutral position	2300
	1.75 aft position	3200
Hovering OGE	2.75	2700
	1.375	2100
	1.375	6500
Backward flight	.2	7750
	.1	5300
	.1	4000
Etc . . .		

An estimated service life is calculated taking into account the flight spectrum on the one hand and the fatigue curve of material used on the other hand. This exercise makes it possible to plot the service life evolution as a function of the fatigue limit expressed in bending moment. This approach permits the dimensioning load corresponding to the chosen target service life to be considered.

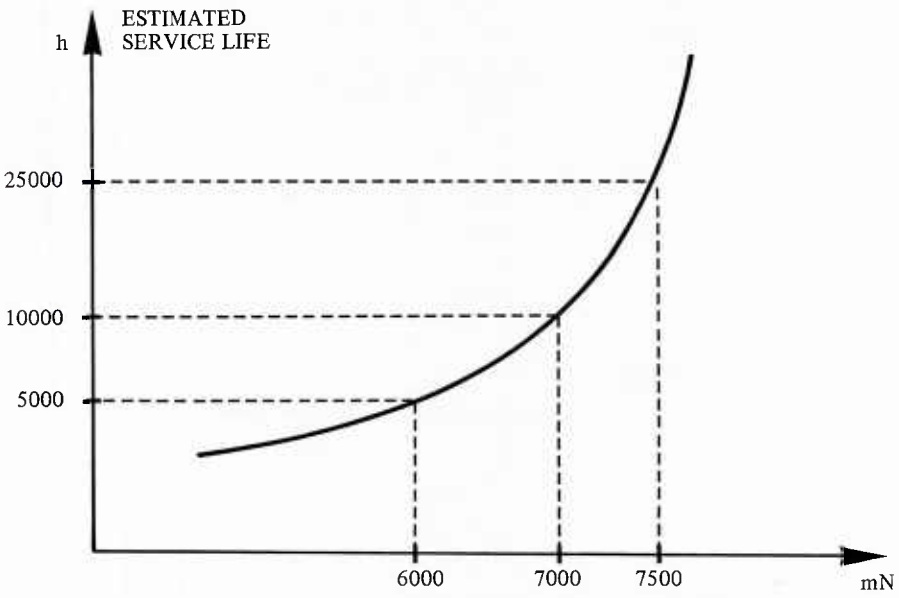

Safe fatigue limit rotor shaft bending

3.2.2.2 Control system

This control system consists of :

- a mobile system (pitch horn, pitch change link, rotating swashplate),
- stationary system (non-rotating star,, servo-unit, servo-unit attachment to structure).

The stresses introduced in the stationary and rotating rods are due to the torsion loads exerted around the blade pitch axis. These stresses are defined in paragraph 3.2.1.

These torsion loads can be generated from :

- loads introduced due to C.G. offsets in blade cross-sections,

- aerodynamic moments induced by Cz and Cm_0 at blade aerodynamic centre. Prediction of these loads is certainly not accurate because of the complexity of the blade airfoil aerodynamic environment,
- bending couplings (flapping and drag),
- torsion (it is most important to know the blade bending moments and its static deflection).

As concerns the stationary control system, a harmonic analysis : $F = F_0 + F_1 \cos(\Omega t + \varphi)$ shows that the static loads in the servo-units vary as static loads (F_0) and dynamic loads in 1 Ω (F_1) in the rotating rods.

On the other hand, dynamic loads are assessed through comparison with aircraft of same weight, or different weight using formulae taking into account the scale factor.

EXAMPLE 3 SPECTRUM OF DYNAMIC LOADS ON A PITCH LINK

Configuration	Time %	Calculated load N
Min. hourly consumption speed	8	1650
Best range cruising speed	25	3450
0.7 max. cruise	9	2230
Max. cruising speed	19	4030
VNE	.8	4720
Turns at :		
Minimum consumption speed n = 2	.0135	9110
Minimum consumption speed n = 1.8	.092	6445
0.7 maximum speed n = 1.6	.112	5230
0.7 maximum speed n = 1.4	1.287	4425
Best range cruising speed n = 1.15	4.404	3790
Load factor		
Max. cruising speed n = 1.8	.004	9110
Max. cruising speed n = 1.6	.061	6450
Max. cruising speed n = 1.4	.585	5300
Max. cruising speed n = 1.15	2	4430
VNE at n = 1.4	.015	9110
VNE at n = 1.15	.085	5410
Other configurations	29.5415	< 1650

3.2.3 AIRFRAMES

by

Ph. PETARD

Société Nationale Industrielle Aérospatiale
B.P. 1 – 13725 MARIGNANE CEDEX
FRANCE

CONTENTS

3.2.3 Structures

Structural fatigue develops as the result of the isolated or simultaneous effect of dynamic loads and of variations to the equilibrium of forces which are necessary for the manoeuvering and stability of helicopters.

Dynamic fatigue and low cycles fatigue, lead to different approaches for predicting loads.

3.2.3.1 Dynamic fatigue loads

They are primarily due to the action of the main and of the auxiliary rotors. Their frequencies are linked to the rotor and transmission r.p.m. and also to the number of blades ; they are consequently known.

On the other hand, the prediction of dynamic loads on a structure remains uncertain and even impossible. This is all the more disturbing as dynamic damage appears from a relatively low stress level.

The main reasons for these difficulties are, on the one hand, the lack of precision concerning knowledge of rotor loading and, on the other hand, ignorance of the response of structures to dynamic loads due to poor knowledge of damping effects.

Some practical or empirical methods enable correct selection of dimensions.

a) Design programs by finite elements in the dynamic range provide the natural modes and natural frequencies associated with a whole structure or with structural components.

   It is therefore advisable to dimension the structure or the structural component so as to move the natural frequency away from the excitation frequencies obtained by analysis.

b) Statistical analysis of measurements taken on known aircraft of the same type as the aircraft under investigation together with sensible extrapolation supplies an order of magnitude for the dynamic loads induced by the rotors or by the stabilizers.

   Comparison of rotor or transmission loads deduced from testing with calculated loads (cf. paragraph 3.2.1. and 3.2.2.). eliminates any risk of significant errors.

   From this, it is possible to determine the dynamic loads concentrated in the components linking these assemblies to the structure. At this stage, it is still possible to neglect damping while it rapidly becomes very important when moving away from the point of application of loads and damping also affects the order of magnitude of the transmitted loads.

c) As soon as the first prototype is complete, it becomes immediately indispensable to check by laboratory measurements and flight testing accuracy of the loads predicted by the above procedures.

   On the ground, dynamic loads resulting from taxying can only be evaluated by measurement on the aircraft. These loads are in fact dependant on the combined effect of the nature of the ground and the response of the landing gear and they are virtually unpredictable.

3.2.3.2 Lowcycles fatigue loads

It is possible to forecast these loads. In fact, they are the result of flight manoeuvres of the aircraft about its three axis and originate at the rotors and stabilizers. On the ground, they are due to the wheel loads during landing.

In both cases and according to the type of aircraft (heavy, medium, light, military or civil) and to the type of mission (liaison, search, sling operation, off shore work, ASW, ground attack, etc ..) the utilization spectrum can be perfectly determined.

In figures 3.2.3 - 1 and - 2 an example is given of the landing spectrum defined by standard MIL-A-8866 B and a deck landing spectrum used for ship-borne aircraft.

Cumulative Occurences of Sinking Speed / 1000 Landings

Sinking Speed FPS	Trainer	All Other Classes
0.5	1000	1000
1.5	870	820
2.5	680	530
3.5	460	270
4.5	270	115
5.5	145	37
6.5	68	11
7.5	31	3.0
8.5	14	1.5
9.5	6.0	0.5
10.5	3.0	0
11.5	1.5	
12.5	0.5	
13.5	0	

Fig. 3.2.3 - 1 LANDING SPECTRUM FROM MIL-A-8866 B

Fatigue loading spectrum			
Sink speed FPS	Pitch	Roll angle degrees	Landings 100 flight hours
6	Three point	5	38
6	Max. tail down	5	38
8	Three point	4	30
8	Max. tail down	4	30
10	Three point	1	7
10	Max. tail down	1	7

Fig. 3.2.3 - 2 EXAMPLE OF DECK LANDING SPECTRUM

a) Determination of flight loads

Once the general characteristics of an aircraft have been defined (weights, inertiae, C.G. locations, rotor characteristics), the prediction of flight loads on the structure may be obtained using a computer simulation programme :

– in straight and level flight, the programme computes the equilibrium of the aircraft for any desired configuration

– during flight manoeuvres, the same programme details the behaviour of the aircraft at any instant of the manoeuvre.

Straight and level flight

The equilibrium is computed about the centre of gravity under the action of loads originating from the main and tail rotors, the horizontal stabilizer and the fin.

The solution of the 6 force and moment equations and of both flapping equations of the main rotor permits to determine the 8 parameters of equilibrium :

i.e. the collective pitch, both cyclic pitches, the tail rotor pitch, both attitudes of the aircraft and both flappings.

These 8 parameters enable the computation of the loads on each component. This is an iterative procedure.

Flight manoeuvres

The flight manoeuvres are obtained by starting with an equilibrium condition, then varying one or several of the 4 pitch controls in accordance with time related functions, and by varying the loads on various parts of the structure and on the rotors until the wanted criteria such as the desired load factor are obtained.

The results obtained are correct in stabilized flight and in gentle flight manoeuvres. In the case of extreme flight manoeuvres, cross checks with experimental results are useful : cf. figure 3.2.3 - 3 : comparison between the computed flight envelope and the values measured during manoeuvres producing load factors.

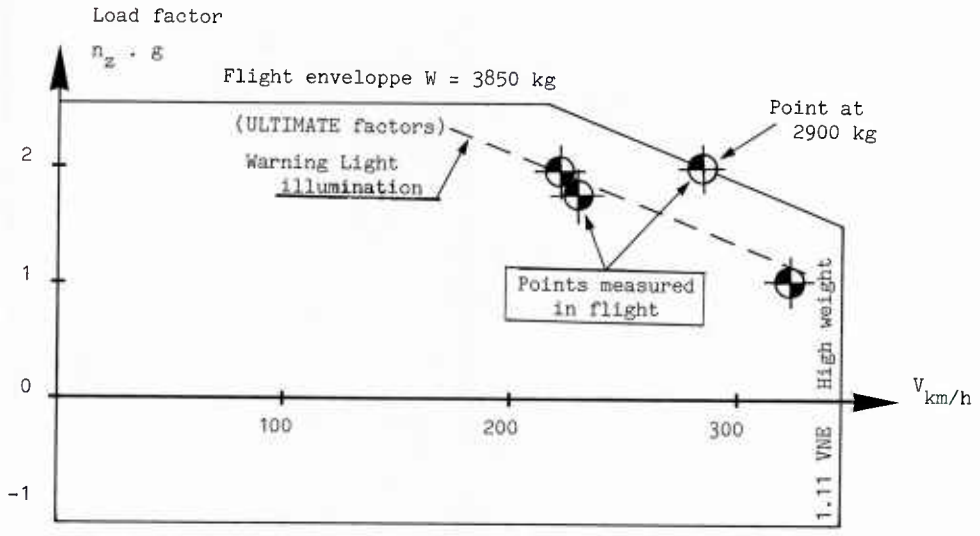

Fig. 3.2.3 - 3 EXAMPLE OF FLIGHT ENVELOPE

b) Determination of loads on the ground

Sinking speeds, low weights, the stiffness and the damping characteristics are basic data for computation of loads. However, it is necessary to differentiate between conventional wheel undercarriage fitted with dampers and skid type undercarriage.

In the first case, the landing gear manufacturers are able to determine accurately the loads involved at various sinking speeds.

For skid type undercarriage, the extension of stress analysis by finite elements for large displacements strains and beyond the elastic limit enables landing loads into the plastic range of the material with reasonable accuracy.
E.g. figure 3.2.3 - 4.

Skid type landing gear Aircraft weight 1900 kg

Comparison of load factors

	Computation	Tests	
Landing - Limit value			Δ
Fwd. C.G. location	$n_z = 2.81$	2.98	+6 %
Rwd. C.G. location	$n_z = 2.91$	3.04	+4 %
Landing reserve factor			Δ
Fwd. C.G. location	$n_z = 2.87$	3.03	+5 %
Rwd. C.G. location	$n_z = 2.98$	3.03	+2 %

Fig. 3.2.3 - 4 EXAMPLE OF GROUND LOAD FACTORS

In both cases, the drop tests required by regulations verify the data obtained by calculation and current experience shows a good correlation between computed data and test results.

SUB-CHAPTER 3.3
LOAD SPECTRA

CONTENTS

3.3.1 MEASUREMENT TECHNIQUES

by

Aldo Jorio
Costruzioni Aeronautiche
Giovanni Agusto
Cascina Costa (Varese)
Italy

3.3.1. MEASUREMENT TECHNIQUES

To define flight loads existing on the helicopter it is necessary to provide measurement of the appropriate physical quantities to obtain information in numerical form capable of describing the situation of the system on test.
This target can be achieved by means of data acquisition systems that can be summarized on fig. 331.1.
Following this process the physical parameters are transferred in a discrete form and organized in a "data base" which is available for any type of computation necessary to produce synthetic information and fatigue life evaluation.
This process realises the following function:
- TRANSDUCER: transfer information from the system on test to the measurement system.
- SIGNAL CONDITIONING AND ENCODING: makes the transducer's signal compatible with the acquisition system.
- DATA COLLECTION: allows storage of information in the format amplitude vs. time.
- DATA HANDLING : transforms the information in a usable form, generally converting raw data into engineering units. So the acquired values are organized on a data base allowing easy access to the users for specific computations.

While the choice of the transducers is generally driven by optimization criteria of its characteristics related to the quantity to be measured, other phases are subject to personalization that, using well known techniques, can configure the system at various complex levels; the signal conditioning can be based on analog or digital multiplexing techniques, the recording can take place on board, on the ground or directly into the computer, the data base organization and the data handling are generally influenced by the methods and facilities available.

3.3.1.1 TRANSDUCERS

The transducer is the first element of the measurement system that transforms the physical entity (acceleration, load, etc.) into a form suitable for recording.
Typical energy forms measured by means of transducers are:

- LOADS
- DISPLACEMENTS OR VELOCITY OF DISPLACEMENT
- ACCELERATIONS
- PRESSURES
- TEMPERATURES

etc.
Those parameters are of course useful for defining the whole helicopter's system.
Therefore, in this chapter we will consider only those that are strictly related to the

fatigue life of the components such as stress and vibration. The engineer will be able to select the most useful transducer for the specific application from among those available. This selection should include weight, dimension, electrical characteristics, environmental conditions and constraints that could arise from the expected measurement system. The characteristics of the component to be examined and the estimated loads envelope are fundamental to decide what kind of transducer (displacement, acceleration, velocity, strain gages) should be used.

In general terms we can assume that:

- Measurement of displacement is applicable in the low frequency vibration analysis where velocity and acceleration do not produce sufficient output level.
- Measurement of velocity is preferred at medium frequency where the displacement is too small for a correct evaluation.
- Measurement of acceleration is generally applied at high frequencies because high output can be produced on those bands.
- Use of strain gages is applicable in all cases in which the component has sufficient strain generated by the stress.

Taking the above into consideration, it can be noticed that, where applicable, use of the strain gages is generally preferred to the measurements related to the load survey for the following reasons:

- The signal obtained is proportional to the strain and so the ratio electrical signal vs load is directly achieved without complex changes involving mass, stiffness etc.
- Dimensions and weight are so small that they can be used without relevant modification to the mass and eventually the aerodynamics of the component on test.
- Mounting (bonding) does not require special supports or holes that are not practical on critical components.

3.3.1.1.1 TRANSDUCER CHARACTERISTICS

Transducer characteristics can be divided as input, transfer and output.

- Input characteristics are the measuring range, the sensitivity and the transverse sensitivity. As in the major part of the transducers the error is proportional to the full scale, better precision can be achieved by measuring entities at not quite full scale and by minimizing the induced effects. When strain gages are used, great care must be taken in defining correct installation in aligning the sensible axis with the direction of strain.
- Transfer characteristics define the relationship between input and output quantities. They are defined by the static level and by the dynamic response in amplitude and phase. A correct choice of the sensor when accelerometers are used, and the suppression of mount induced effects are necessary to eliminate from the measurement all the spurious effects that can alter or complicate measurement interpretation.
- Although output characteristics are less important having the capability of being adapted by means of the signal conditioning, they are fundamental in defining the connections with the measurement system, in designing correct conditioning and in minimizing electrical noise and interference. Parts of this family are the band width, output level and power, output impedance and ground connections.

3.3.1.1.2. TRANSDUCER TYPES

The most commonly used transducers for sensing vibrations and stresses are summarized in table 331.2 which should give an idea of their characteristics and their applicability for different needs. However the following descriptions will cover only the aspects of strain gages and piezoelectric accelerometers which are mainly adaptable for performing measurements related to load survey.

- STRAIN GAGES (see fig. 331.3) are based on the principle that a resistance changes in a constant mode if it is varied within the elastic limit. The relationship between the resistance and the strain can be expressed as:

$$\frac{\Delta L}{L} = \frac{1}{K} \frac{\Delta R}{R}$$

where : L = original length of wire or foil

ΔL = lenght change

R = original resistance value

ΔR = resistance value change

K = gage factor

Considering that the sensitive element (wire or film) is very delicate to handle it is used in conjunction with a support usually made of epoxy or phenolic material. Strain gages are applied to the component by means of cement with high mechanic characteristics. The composition of strain gages following the Wheatstone bridge principle can produce a "sensor" sensible to the different type of stresses (see fig. 331.4).
When strain gages are installed and used for measurement purposes each resistance change is detected as a stress. Therefore the variation caused by the temperature appears as "apparent stress". These values, if negligible for dynamic loads, are a big source of error on the static values. Temperature compensation can easily be obtained with the wheatstone bridge in its simplest form or with the application of further passive components on the bridge arms.

- PIEZOELECTRIC ACCELEROMETERS operate on the principle that an electric charge is generated in some crystals when they are submitted to a mechanical force in a specific direction.

Fig. 331.5 shows a transducer section where the acceleration produces shear or compression forces. Piezoelectric transducers generate an electric charge with output impedance of several hundreds of Mohm. They must be connected with short cables and high impedance amplifiers to obtain voltage outputs.
Piezoelectric accelerometers must satisfy the following criteria:

1. Operate on a wide dynamic range from 2 Hz (long duration vibration) to 10,000 Hz (short duration shocks).
2. Be insensitive to non-vibration environment such as temperature.
3. Be insensitive to unwanted vibration signals such as cross-axis vibrations.
4. Reproduce the desired information without distortion due to damping, filtering or internal resonance.
5. Produce a minimal change in the natural vibration of the object being measured.

3.3.1.2. SIGNAL CONDITIONS

The signal generated from a transducer is usually modified several times before assuming its final form that will be subject to computation. Typical examples of these modifications are amplification, filtering, sampling, digitalization, "data compression", modulation etc.
Basically these functions do not modify the information contained in the signal but match the input requirements of the following unit of the measurement system.
In a general form all the operations that occur between the transducer and the computer used for final computation can be assumed as "conditioning"; however it seems to be simpler to divide those activities in linear operation and signal conversion.
Linear operations can be considered as all those functions of amplification, filtering, zero shift and compensation that are needed to adapt the signal to the measurement system.
Main reasons for performing such operations are:

a) The transducer is defined considering its availability even if the output characteristics are not ideal.

b) The frequency range of the transducer is too wide to be correctly utilized by the recording or telemetry system; therefore the conditioning will reduce the signal band width by eliminating the unwanted frequencies.

Signal conversion operations are those functions which imply modulation, A/D conversion and multiplexing; they are necessary to record or transmit a wide number of parameters as generally required during flight testing.

3.3.1.2.1. AMPLIFICATION

The aim of this operation is to make the output level of the transducer compatible with the measurement system. Since the transducers based on the piezoelectric principle are self-generating devices, we cannot get more energy out than we put in.

For this reason a very low electrical energy will be presented to the conditioner and will be essentially purely capacitive.
Today there are two basic techniques employed to condition piezoelectric transducers:

1. High impedance voltage amplifier.
2. Charge amplifier.

In utilizing voltage amplifier we attempt to keep the amplifier input impedance very high compared with the source impedance.
Fig. 331.6 shows the equivalent circuit where the cable has been represented by C_C to underline that a significant portion of the load is through the interconnecting cable.
In order to avoid the cable capacitance effects "charge amplifiers" are used. They are essentially operational amplifiers with integrating feedback.
A representation is shown in fig. 331.7. With operational type feedback, the amplifier input is maintained at essentially 0 volt; the amplifier output is then a function of input current. With the integrating operational feedback the output is the integral of output current, hence the name "charge amplifier".
For the strain gages the amplification is made by means of operational amplifiers or preferably instrumentation amplifiers. Their use must however be consistent with the isolation level required within the transducer and the subsequent input.
In fact, the use of the amplifiers can create problems in the measurement system in the form of common mode or capacitive noise.
Fig. 331.8 shows two applications using differential or single ended amplifiers.

3.3.1.2.2. FILTERING

Filtering is performed when the signal contains components that do not relate to the measurement. There are three main reasons for use of filters:

1. To attenuate the amplitude of those signal components that are not relevant and that could saturate some parts of the measurement system.
2. To filter the output noise and the high frequency components so that the "aliasing" error can be reduced when sampling is expected.
3. To present and easily understand signal.

Active and passive filters can be used, higher performances and better impedance matching can be obtained however with universal active filters. These modular units can be configured on type hi/band/low pass and cut-off frequencies can be selected by external resistors change.
An example of a universal active filter is shown in fig. 331.9.

3.3.1.2.3. ZERO SHIFT AND COMPENSATION

In the same measurement the dynamic range required is only obtained by a portion of a true full scale of the transducer. Moreover, when strain gages are used it is possible to have an initial offset caused by bonding which could be recovered.
The Wheatstone bridge used in strain gages application is still a good example of compensation: both active and passive arms, if subject to the same environmental conditions, will compensate possible temperature drift or, when this condition is not achieved, it is possible to make eight-component bridges in which the compensation function is committed to the passive strain gages.
Figure 331.10 shows a scheme where balancing and compensation are applied.

3.3.1.3. SIGNAL CONVERSION

When the homogeneity of the signals is obtained or at least when a useful form is acquired, it is necessary to provide data collection on some physical support which should be able to retain them until required. If we thing of rejecting any consideration of graphic recording that implies heavy manual handling, there are two available alternatives: in-flight recording or data transmission to the ground (telemetry). In both cases, it appears obvious, especially in helicopter tests dedicated to load survey, that the quantity of information to be surveyed is not consistent with the number of channels available on a magnetic recorder or with the number of radio frequencies that can be allocated; moreover increasing the number of magnetic recorders or transmitters is not acceptable in terms of weight, cost, synchronization and for management aspects.
For this reason multiplexing techniques are used; they make it possible to build up a single complex signal in which information of several sensors are contained.
The method used is based on the Frequency Division Multiplexing Technique (FDM) or Time

Division Multiplexing Techniques (TDM).

3.3.1.3.1. FREQUENCY DIVISION MULTIPLEXING

The Frequency Division Multiplexing Technique, also known as FM/FM (Frequency Multiplexing/Frequency Modulate) consists of frequency sharing of one R.F. carrier dividing the available bandwidth into up to 25 channels, the center frequency of which ranges from 400 Hz to 560 Hz. Each center frequency is modulated (FM) by the input signal so that a complex carrier can be obtained.
Essentially, in frequency modulation, the amplitude of the modulation carrier is held constant, while the instantaneuos frequency of the carrier is varied in accordance with the modulating signal.
The variation of the instantaneous frequency with respect to the center frequency is called frequency deviation and is proportional to the input signal.
In the general form the FM wave may be expressed by the following equation:

$$V = A \sin (\omega t + m \sin \Omega t)$$

where:

V = amplitude

A = peak amplitude of the wave

ω = angular velocity of the carrier

Ω = 2 times the modulating frequency

m = modulation index or frequency deviation/modulating frequency

The frequency domain presentation of the FM/FM carrier, without modulation, will assume the general form of figure 331.11, where f_1 to f_5 are the center frequencies of the subcarrier .
As mentioned above, this technique allows up to 25 signals to mix in a complex wave that can be easily recorded on a magnetic tape channel or transmitted via data link. Should a 14-track magnetic recorder be adopted, up to 350 parameters can be stored. This number is purely theoretical and does not consider the needs for control signals such as time or voice, but it givesa figure on the total quantity of information that could be stored also taking in consideration today's availability of 28-track recorders on 1 Inch tapes.
Consideration can also be taken on transducers' signal bandwidth that normally drives a selection of a number and type of subcarriers.
To comply with the signals bandwidth requirement, different center frequency deviations can be chosen consistently with IRIG standards.
The two basic families are the Proportioanl Bandwidth modulation (PBW) and the Constant Bandwidth modulation (CBW).
The PROPORTIONAL BANDWIDTH modulation technique, following the general principle of FDM, implies the use of a frequency deviation proportional to the center frequency of the carrier.
The applied standard deviation are $\pm$ 7,5%, $\pm$ 15% and $\pm$ 30%. The PBW, with the minimum channel deviation ($\pm$ 7,5%) allows the greatest signal mixing (25 parameters) but in this case the nominal frequency response of each signal is very different and varies from the 6 Hz of channel 1 (C_f= 400 Hz, deviation = 7,5%) to the 33.6 Hz of the channel LL (C_f= 560 KHz, deviation = 30%).
This spread type of bandwidths could represent an advantage allowing signal-to-channel optimization and therefore a reduction in "anti-aliasing" filtering needs. However, if the load survey application is considered, it may generate the following difficulties:

1. Typical helicopter loads include harmonic frequencies up to 200 Hz for the greater part of the parameters. This makes the channels up to 10 typically not useful, and consequently it implies a limitation on the total availability of channels.
2. Due to the different frequency response each channel has different output filters that cause different time delays. That can represent a great disadvantage when time synchronization between parameters is required.

The CONSTANT BANDWIDTH modulation, in opposition to the PBW technique, uses a constant frequency deviation for each channel, independent from the center frequency value. The standard deviations applied are $\pm$ 2 KHz, $\pm$ 4 KHz and $\pm$ 8 KHz.
With the minimal channel deviation ($\pm$ 2 KHz) the CBW allows the mixing of 21 parameters with a nominal frequency response of 400 Hz; this is normally sufficient for the stress

analysis in the dynamic components of the helicopter.
Moreover, due to the equal frequency content of each channel, equal output filters can be applied with the possibility of good synchronization between channels. However the main disadvantage of this method is that at the higher center frequencies the nominal deviation is not more than 1% and especially considering the noise induced by recorder flutter, an unacceptable S/N ratio can be present.
This limitation can be overcome by the use of "frequency group translation" techniques. The frequency translation implies the use of the lower channels with higher percentual deviation (typical up to channel 6A). The upper channels are obtained by addition of a reference frequency (i.e. 120 KHz, 240 KHz). As an example channel 12A (104 KHz) can be obtained using channel 1A (16 KHz) in the following mode:

120 KHz (ref.) - 16 KHz (1A) = 104 KHz (12A)

HYBRID CONFIGURATIONS can also be made. The use of CBW and PBW channels in the same carriers can increase the total number of channels available and optimise the configuration, sharing the advantages typical of each method.
When this solution is expected, great care should be applied in definition of the configuration in order to avoid frequency overlay in adjacent channels when not properly spaced.
Some consideration must be taken on **practical aspects of the FDM method.** Both CBW and PBW are realized by means of subcarrier oscillators. Wide choice of components is available today including discrete technology components of dual-in-line chips developed for space application.
The general configuration of a subcarriers "block" includes VCOs, a Mixer Amplifier and a Reference Oscillator that is normally used for "flutter compensation" when the carrier is recorded on magnetic tapes. This fixed frequency is detected during the playback and can compensate both static and dynamic errors arising from speed variation of the tape transport. The above mentioned modules are normally installed on special mounts that allow ease of channels configuration plus pre-emphasis resistors installation to avoid amplitude losses caused by non-linearity in the recorder or transmitter bandwidth.
Dynamic range of the input signals must be carefully analysed to avoid overmodulation in the VCOs, applying the appropriate premodulation filtering if convenient. The block diagram of a typical FDM system is shown in fig. 331.12.

3.3.1.3.2. TIME DIVISION MULTIPLEXING

In the time division multiplexing technique the encoding is obtained with periodic interval sampling; it allows the mixing in a single channel of several inputs by means of a mechanical or electronic commutation. The simplest form is represented by a rotating switch, running at constant speed, that can select each channel during predefined time intervals.
This principle is shown in fig. 331.13. The signal presented as multiplexing output will assume the format of an amplitude modulated signal that is commonly defined as PAM (Pulse Amplitude Modulation) and is shown in fig. 331.14.
Referring to the previous chapter it appears that, while the FDM technique has a limited channel capability, the TDM method can handle a greater number of parameters, only limited by the frequency contents of each channel and by the maximum sampling rate available in the scanner.
Different sampling rates for different channels can be achieved by means of surcommutation or subcommutation , by which the frequency contents achievable for each parameter can be reduced or increased (in power of 2). Surcommutation and subcommutation's examples are shown in fig. 331.15.
In past years the PAM was used to handle large quantities of low frequency signals using electromechanical commutators.
Nowadays, the availablity of high-speed electronic switchin has widely increased the system overall capability allowing the handling of signals with greater contents.
The intrinsic limitation of the PAM system is that the information content is strictly related to the amplitude so that it is easily affected by noise and static level changes caused by shielding or grounding problems.
To overcome this problem noise reducing techniques were realized as PDM (Pulse Duration Modulation) or PPM (Pulse Position Modulation) in which the information is related to the time domain instead of the amplitude. Real improvement in the TDM was therefore obtained by the introduction of digital electronics which generated PCM (Pulse Coding Modulation).
PULSE CODE MODULATION is in practical terms a subset of PAM in which the sampled signal is transformed into digital words, in serial format. The relationship between the two methods is shown in fig. 331.16. The digital format of the message makes the PCM relatively free from noise and perturbations that generally occur during transmission or

recording and it allows the great resolution typical of the binary words.
A modern PCM encoder can handle up to 100 K samples per second (1.2 M bits) which in theoretical terms means 100 parameters sampled at 1 KHz rate. This figure does not reach the information density available in a 28-track - 21-channel CBW configuration of a FDM system but, for a medium size load survey, it has the advantage of the availability of all this information in one channel, then the capability to transfer this information to the ground via data link.
The signal availability on the ground will permit a check by means of real time visualization system. This capability to transmit large amount of data directly to the ground can be considered the major advantage of the PCM in the load survey application considering that the improved accuracy intrinsic in digital encoding (8, 10 or 12 bits) is not generally required for such purpose. Therefore it is also necessary to underline that the real time capability is normally used both to verify the quality of data during the flight and for safety reasons. The calculations required to perform load spectra analysis are normally performed off-line on mainframe computers; the advantages of this method are obviously less compared ot the FDM, which is generally more flexible and less expensive.
Today's PCM encoders can practically be considered one-box systems in which several functions are performed. The basic scheme, shown in fig. 331.17 realizes the function of:

a) Multiplexing: a PAM signal is generated from analog signals.

b) Encoding: a serial digital message is generated by means to A/D-parallel-to-serial conversions.

c) Programming: switching gates are activated to define the sampling sequencies using a predefined programme stored on PROM or hardwired.

d) Synchronization: synch words are generated to identify frames, subframes and sequences in the PCM message to allow a correct decommmutation on the ground.

e) Signal mixing: encoded signals, time words, synch words and external digital words are mixed to make up the final message.

The information contained in the output message, as implicit in the TDM technique, is not related to the same instant for each basic cycle, but is delayed at constant time intervals. When necessary, this aspect can be overcome by means of computer correction performed during data reduction or by using hardware devices that allow instantaneous sampling, storage in buffer memories and the subsequent transfer on the PCM message at the appropriate time.
The serial binary output generated by the PCM is not necessarly in the form:
binary 0 = logic level 0, binary 1 = logic level 1.
This type of code is designated NRZ - L (non return to zero level) and other sort of codes are expected by the standard; they imply representation of 1 and 0 using change/no change of level, midbit level changes etc.
These different code waveforms can be selected to optimize the spectral density of the message in order to satisfy the requirements of the recording or transmission media.
An example of spectral densities for different codes is shown in fig. 331.18.
When required to transmit the message via a PM emitter that does not accept frequencies below 400 Hz, a BIØ code could be chosen because it has no significant spectrum contents in the low frequency band.
In a solution using FM emitters, NRZ codes can be easily adopted, reducing the required bandwidth to equal density of information.

3.3.1.3.3 PCM AND FDM MIXING

Both PCM and FDM could each have in optimum performances for different parameters to be transmitted or recorded together.
In this situation composite configurations can be realized using both techniques. A typical example could be the need to mix a slow rate PCM code with the pilot's voice and some vibration information . A possible technique is to modulate PCM in a FDM channel with the sufficient frequency deviation, using the low side channels for analog data transmission (PCM - FM/FM).
Another possibility is to consider the PCM wave like an analog signal and add the unmodulated PCM with the FM/FM subcarriers in the mixer amplifier (Hybrid PCM). Both methods allow an increase in the number of transmitted parameters and the only limitation is to pay careful attention to deviation of the subcarriers to avoid overlays and consequent signal loss. These overlays can be caused essentially by the spread spectrum generated by the PCM. Fig. 331.19 shows some typical frequency distribution in hybrid PCM and PCM - FM/FM applications.

3.3.1.4. DATA RECORDING

Data obtained from multiplexing may be recorded at one or more remote stations or in the helicopter. In this way the test data can be stored indefinitely and replayed in a demodulation station to perform data reduction.
The main advantage of magnetic recorders is the capability of storing signals in the electrical form; this characteristic allows the recorder to transfer information directly into the computers, spectrum analyzers etc., for subsequent handling. When DC response is needed, data is recorded in the FM mode; when DC response is not needed the Direct Record mode is used. FDM signals are recorded in Direct mode as well as PCM waveforms. PCM can also be recorded on high-density, that is a digital encoding compatible with binary codes as NRZ, Miller etc.
Instrumentation recorders are generally used for telemetry work. They normally have 7, 14 or 28 tracks with separate record and reproduction heads for each track.
Each track may be allocated to a single data channel or may carry a multiplex.

3.3.1.4.1. RECORDER'S CHARACTERISTIC

The fundamental elements of a magnetic recorder are:

a) The record and reproduce electronics: this performs the transformation needed to apply or reproduce signals to/from the heads.

b) The record and reproduce heads: these transform the above mentioned electric signal on magnetization states on tape and again reconvert those states into electrical signals.

c) The transport: it drives the magnetic support at constant speed over the heads. The quality achieved in this function is strictly related to the repetition, accuracy and S/N ratio in the output signal, being the transport able to induce speed-dependent amplitude errors as "flutter" or "wow".

d) The magnetic tape: it is composed of a plastic material base on which a thin film of magnetic material is deployed.

A block diagram of the system is shown in fig. 331.20.

3.3.1.4.2. DIRECT RECORDING

The magnetic head is based on a ring-type coil with an air gap. The input signal creates a magnetic field on the tape that correponds to the gap in one instant. When the magnetized tape leaves the gap, the signal remains on the tape because of the remanence characteristic. Taking into account that the remanence diagram is linear only in its central part, the input signal is linearly mixed with a high frequency polarization voltage (BIAS).
The main advantage of direct recording is the capability of allowing a very high frequency response. Moreover, the disadvantages are the practical impossibility of recording signals close to DC and the sensitivity to the amplitude variations.
Another typical source of noise is generated by "signal drop-outs" caused by the imperfections existing on the magnetic tape surface. As a typical application, Direct recording is used to store FM/FM subcarriers. When FM/FM subcarriers are recorded the flutter generated by the transport can induce very high noise in the original signal: this is caused by the limited frequency deviation of each subcarrier. For this reason "flutter compensation" should be applied to minimize the errors (see para 3.3.1.3.1.).

3.3.1.4.3. FM RECORDING

The FM recording is used when it is necessary to overcome the typical disadvantages of Direct recording: the low frequency band limitation and the amplitude instability.
In practical terms FM recording is obtained by applying a frequency modulation to the signal before adding it to the bias. This modulation, however, limits the frequency response of the system. Therefore it is not normally used for multiplexed carriers and application is limited to recording signals at relatively high frequency. Of course, this solution requires the use of a recorder track for each parameter.

3.3.1.4.4. HIGH DENSITY DIGITAL RECORDING (HDDR)

The data acquisition systems have reached a high degree of sophistication in some case. This fact has generated the demand for storing greater quantities of digital data.
A new technique forced by the diffusion of the PCM and other digital methods was therefore developed in order to allow high density digital recording on analog tapes.

This possibility is achieved by means of "scrambling" that signifies to store on the magnetic tape digital messages plus the associated clock.
HDDR makes it possible to record typically 33 K bpi for a total density up to 4 Mbit/sec. The data stream is divided into blocks called frames and the segments into a specific number of data bits. The message is mixed with synch words at a predefined clock rate to allow data recovery. The term "divided" does not imply physical separation as the data is processed as a continuous bit stream.

3.3.1.4.5. RECORDERS' CONFIGURATION

The embedded flexibility of a multi track recorder allows configuration with different electronics (HDDR, Direct, FM) as required for specific needs. In this event the transport speed will be the common parameter that will define the nominal bandwidth of each track. This possibility of diversification allows PCM data streams, FM/FM subcarriers, stand alone vibration parameters, voice, etc. to mix in a single data media, building up a complete measurement system.
All the above described characteristics are valid for both airborne and ground recorders which can be configured in the same way. Of course, weight and environmental constraints make these units different and, for the same reasons, the reliability of the airborne units will be reduced. The reliability reduction is caused by the mechanical parts of the transport that are easily affected by shock and vibration problems.
These points and frequent weight and space limitations existing on small size helicopters make the ground recording (which implies telemetry) very interesting for several reasons.

3.3.1.5. RADIO TELEMETRY

The multiplex baseband signal may be carried over long distances by the radio link. The link consists of a transmitter, a transmitting antenna, the propagation path, a receiving antenna and a receiver.
The modulation used in the transmitter is normally AM, FM and PM. The frequencies used are commonly in the bands 1435 - 1535 MHz and 2200 - 2300 MHz. The adoption of FM (PM can be pratically assumed as a subset of FM) gives a natural protection to the link against undesired electrical perturbations.

3.3.1.5.1. TRANSMITTERS

With a typical L band transmitter, emitted power up to 25 w can be available with less than 2 Kg. of weight. This figure, compared with the 30 - 40 Kg. of an airborne recorder, demonstrates the undoubted advantage of the telemetry solution. Moreover it must also be considered that the absence of moving mechanical parts and the solid state technology gives to the transmitter a very high reliability;however, to maintain this high reliability, great care should be taken in applying the appropriate cooling to the system.
Radio links up to 100 Km. can be easily established without the use of special sensitivity devices (receivers plus antennas) on the ground.
Up $\pm$ 500 KHz being the normal available bandwidth, the multiplex signal is tied directly to the transmitter input.
When non-modulated PCM signals are transmitted, the use of Bessel filters before modulation is suggested to reduce the spread spectrum generated by the square wave that makes up the binary signal.

3.3.1.5.2. ANTENNAS

Antennas are used in order to radiate the signal power output from the transmitter and capture a portion of this radiated power at another point. Significant characteristic of the antennas are the directivity and gain related to it. For flight test telemetry application, omnidirectional antennas are normally used on board, assuring with the 360° propagation characteristic the necessary coverage in all flight condition.
Sufficient propagation during manouvers (typically at high bank angles) must be established with the appropriate antenna siting. To avoid black-outs caused by line of sight loss arising from attitude changes, more than one antenna can be installed.
Antenna coupling can be effected by means of multicouplers and if necessary also with different polarization.
As far as possible this technique is not employed to avoid loss of power caused by the multicoupler and the expected beat between antennas.
On the ground, when long range is not required, omni antenna can also be used, allowing a typical gain of 1 dB. If the receiver cannot be installed close to the receiving antenna, cable loss can be recovered using antenna amplifiers which normally gains up

to 20 dB. Additional gain can be achieved by means of directional antennas (20-30 dB for 15° beam angle) which, however, require quite sophisticated tracking devices. Polarization losses, caused by the above mentioned high attitude angle manouvers, can be minimized using circular polarization in the receiving antenna. Loss of signal caused by tracking errors can be eliminated by combining omni and directional antennas.

3.3.1.5.3. RECEIVERS

As indicated for transmitters, there is a wide variety of available receivers. Important characteristics are the carrier frequency, the frequency stability, the input noise level, the IF bandwidth. Receivers designated for voice communication may be used for telemetry, but they should be carefully checked with respect to distortion.
A general purpose telemetry receiver generally has plus-in modules for the RF tuning, IF and demodulator. The receiver takes the incoming signal from Rx antennas (or antenna amplifiers) and after demodulation, sends it to the appropriate decommutation or recording system.
Some receivers have predection recording feature and predetection playback capability. In this way the received signal is down-translated from IF to a band which can be handled by a tape recorder.
When a receiving system is based on both omni and tracking antennas, the receiver can be connected to the aerial by means of antenna switching or by using a "diversity combiner". Adopting this technique implies that each antenna should be connected to a separate receiver and send both signals to the diversity combiner.
This unit will provide on the output the best available signal defined in term of best S/N ratio or lower AGC (Automatic Gain Control). The system is generally locked to the tracking antenna which performs better than the omni, but in case of tracking loss the system automatically switches on the omni side without loss of signal.
A possible configuration using a diversity combiner is shown in fig. 331.21.

3.3.1.6. DATA HANDLING

In the previous chapters it was shown how it is possible to recover information on the ground. Following the encoding or multiplexing performed on board we now have available complex signals that must be reconverted to the original form.
This is done by means of decommutation stations in which what was done on the aircraft is reversed (see fig. 331.22).
At this point the real target is not to obtain the original signal shape but to make it acceptable to the computer in order to be able to store such data in memory for processing. This function is obviously performed in a different way depending on the methods adopted on board as PCM, FM/FM, PAM encoding etc., however two typical situations of analog (FM/FM) or digital (PCM) demultiplexing are described below:

3.3.1.6.1 ANALOG DEMULTIPLEXING

As a consequence of the FM/FM multiplexing, a complex wave which contains subcarriers with the original signals is made available. To obtain the desired original information, the follwoing steps must be performed:

a) Playback: the signal is reproduced by means of a laboratory recorder/reproducer, configured in the same way as the original recording.
This unit should be a high quality instrumentation type to avoid errors caused by transport deficiencies and it must be elctrically aligned to the recording unit to avoid degradation of signals. System output gain should be adjusted to comply with input specifications of the successive system. Obviously step a) is not applicable in case of real-time operation via radio link.

b) Demodulation: the original signals are obtained by means of "discriminators". The latter are composed of input filters which select the appropriate subcarrier, demodulators, and output filters so that any noise and unwanted frequencies are eliminated. Output filtering is also necessary to make the output frequency spectrum consistent with the digitalization sampling rate if digitalization is required.
Noise generated by recorders transport errors is corrected with a "flutter compensation" device. This kind of device is another discriminator that demodulates a reference signal generated on board by a stable source (typ. 120 KHz, 240 KHz). The result is in effect an error signal that will be substracted from each subcarrier output. If CBW multiplexing is used the detranslation technique can be applied (see para 3.3.1.3.1). The block diagram of a discriminators section is shown in fig. 331.23.

c) A/D conversion: digital transformation of analog signals is obtained through an A/D converter that will present parallel digital words to the computer. This unit performs a sequential scanning of all channels at predefined time intervals, as speed is a function of the highest frequency that is required to be detected. Time delay between channels is very short (few μsec) and, when necessary, it can be eliminated by A/D converters that use simultaneous sample-and-hold.
HIgh transfer rate between the A/D and the computer can be achieved by means of internal buffers (FIFO) in which one or more complete scannings can be stored before the DMA transfer. 8 to 16 bits accuracies and speeds up to 500 Kwords/sec are normally available.

The above mentioned process can be performed both in real-time or in off-line playback mode. The real time involves handling all the parameters at he same time. If the off--line playback is used, this total capability should have the availability of hundreds of discriminators and A/D converters with hundreds of channels and very high transfer rates. For this reason the off-line playback is normally performed track-by-track and using common synchronization signals as IRIG time or rotor azimuth pulses.

3.3.1.6.2. DIGITAL DEMULTIPLEXING

With the PCM encoding a digital serial data stream is generated, in which all the discrete values of the signal related to time intervals are contained (typical of TDM). During the various phases that occured before the decommutation (e.g. filtering, recording, transmission etc.) this digital signal was altered. For this reason the signal should be:

a) Reconstructed in its original binary serial form by means of a "bit synchronizer".

b) Transformed in parallel words that will be sent to the computer at the correct clock rate.

This process is shown in fig. 331.24.
As a major difference to the analog multiplexing, the PCM encoding does not expect a sample rate common to all the channels and function of the maximum bandwidth required. The use of subcommutation and surcommutation allows different sampling rates related to the expected frequencies. However, as the PCM is a synchronous system, the transmission of data to the computer occurs at the basic rate and the relationship of words-parameters-time will be established in the computer. Another relevant aspect of the PCM playback is that the basic recording can be processed at multiple speed, considerably reducing the time devoted to the data formatting.
To allow data synchronization time, data is also transferred separately to the computer or included in the PCM message.

3.3.1.6.3 DATA PROCESSING

Data transferred to the ground station computer is not normally processed in this unit. The computers used on ground station activity are usually "mini" with limited resources devoted to the management of the station and to the data formatting activity. The main target of these units is to store data on physical supports (e.g. discs, magnetic tapes) capable of being transferred to the mainframe computer dedicated to the scientific activity.
In theseapplications where "midi" computers are available, CPU spare time is used to transform raw data in engineering units through the use of "calibraiton files" previously generated, or to perform computations capable of showing preliminary results. This information can be used to verify the quality of the data or to assure the safety of the flight test activity (Quick-look functions).
Following space activity, in recent years a system has been developed devoted to reducing the quantity of data to be handled. This technique, called "Data Compression", consists of the elimination of the redundant data by means of a particular algorythm. It must be noticed that this method is not normally applied in the flight test activity because the normal quantity of data handled is not so great.
However, if we consider that the algorythms normally used for this function are very similar to those used for the fatigue life calculations (rainflow, level-crossing, etc.), we can foresee the application of these data compressor devices as computer front end.

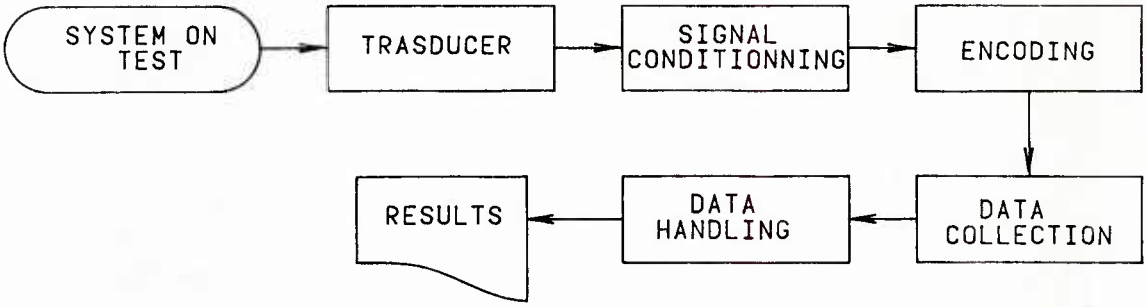

FIG.331.1

TABLE 331.2

MEASURE	TRASDUCER NAME	PRINCIPLE OF OPERATION	MAXIMUM RANGE	DYNAMIC RESPONSE (HZ)
DISPLACEMENT	POTENTIOMETER	POTENTIOMETER	600 MM	20
	LVDT	DIFFERENTIAL TRASFORMER	250 MM	20
VELOCITY	VELOCITY PICK UP	SELF INDUCTION	50 IPS	2000
ACCELERATION	ACCELEROMETER	STRAIN GAGES	+/-100 G	200
		PIEZOELECTRIC	+/-10000 G	10000
LOADS	STRAIN GAGES	RESISTIVE	5 INCH/INCH	10000

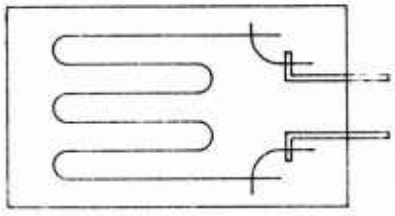

WIRE STRAIN GAGES

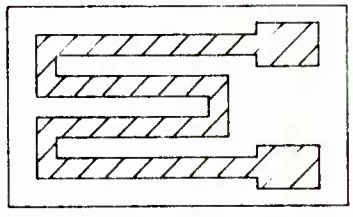

FOIL STRAIN GAGES

FIG 331.3

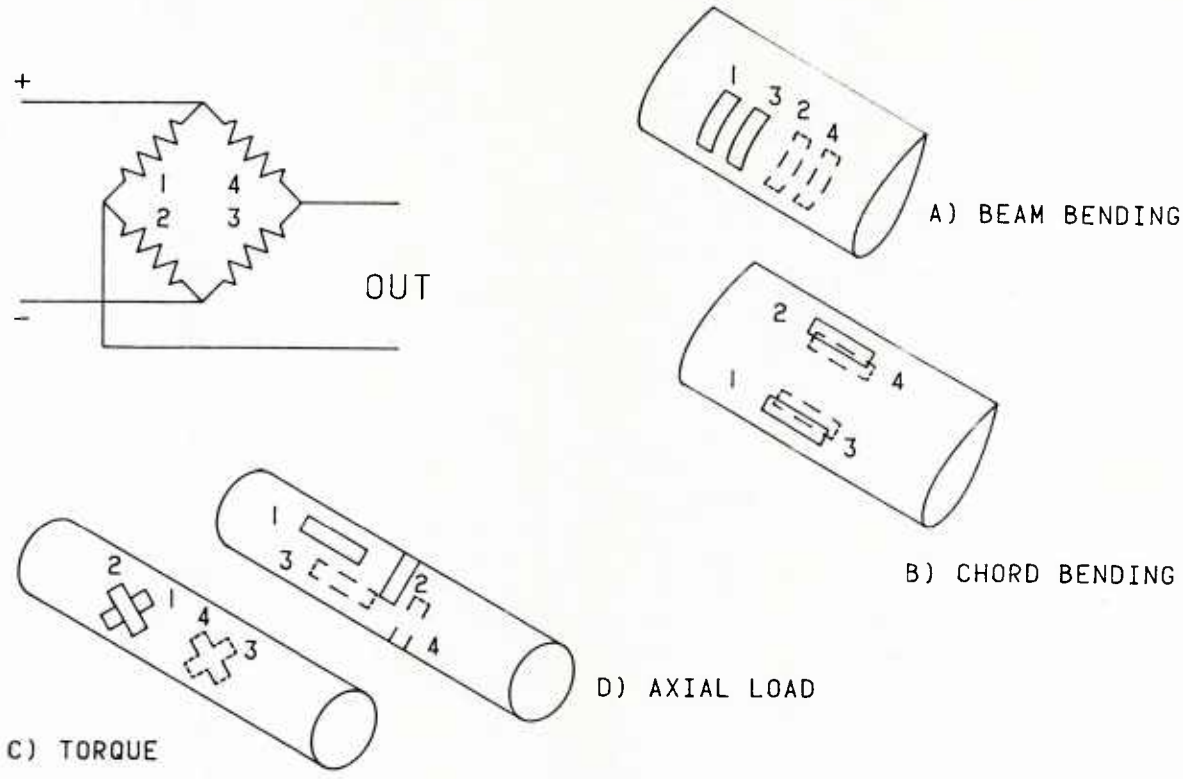

FIG 331.4

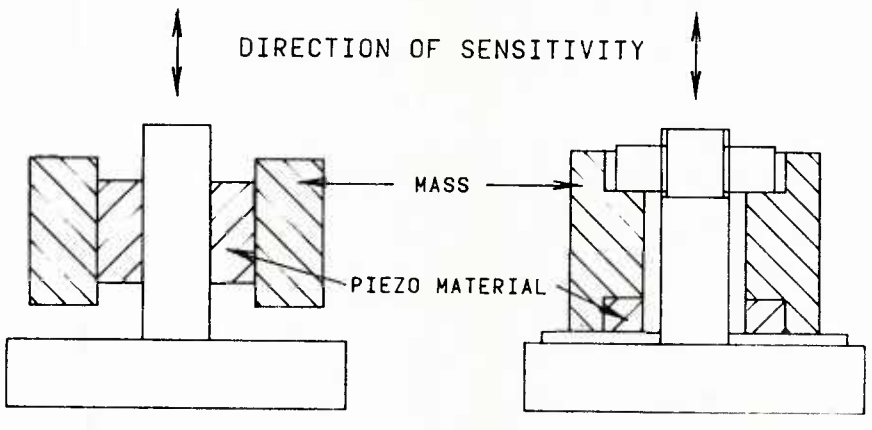

FIG 331.5

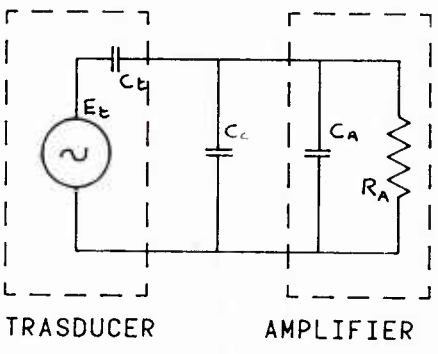

FIG 331.6

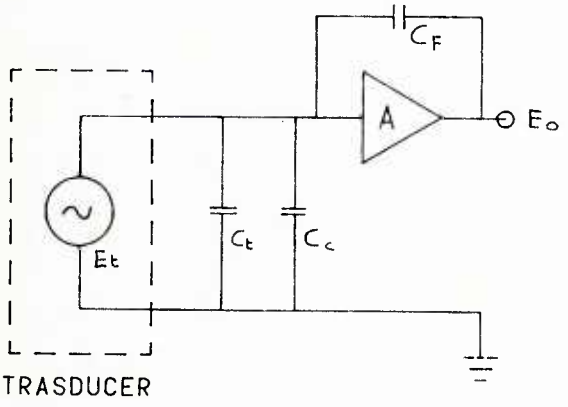

FIG 331.7

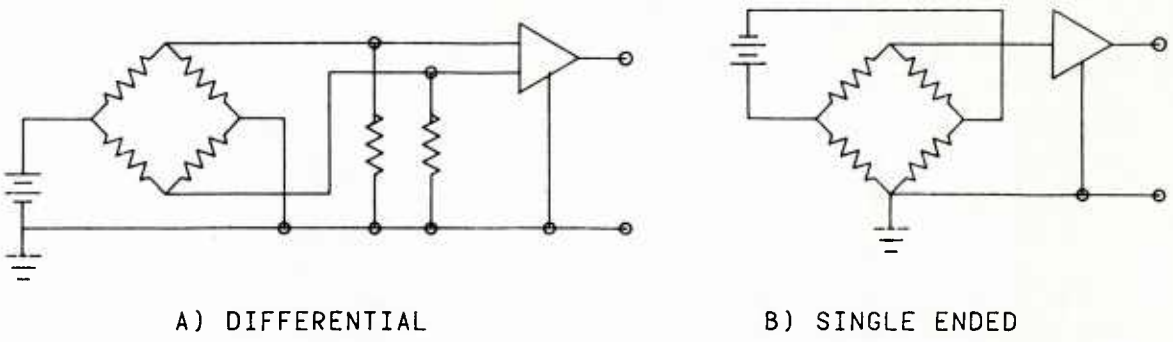

FIG 331.8

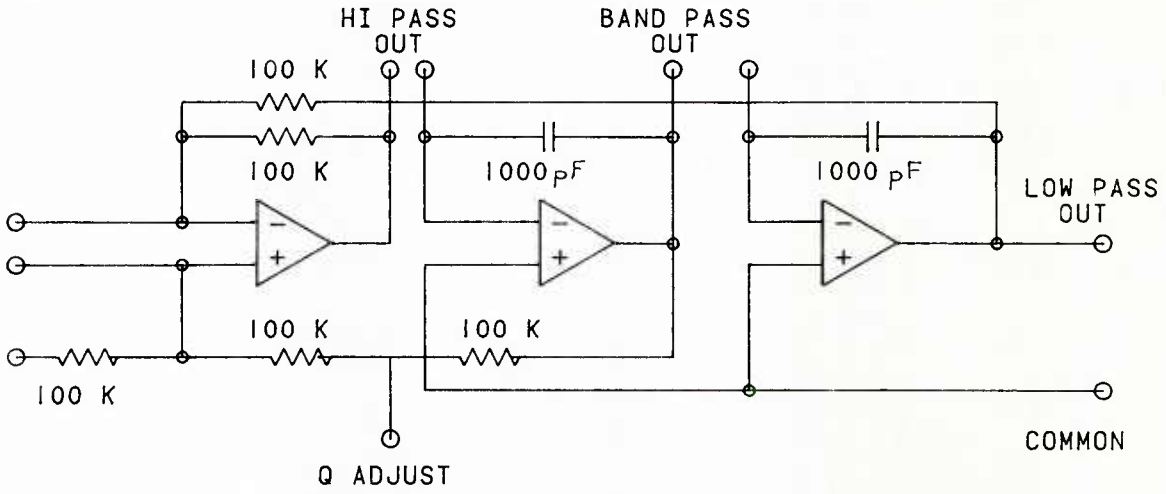

FIG 331.9

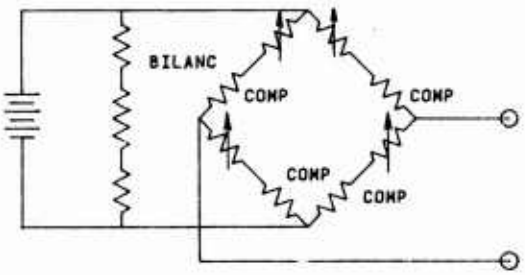

FIG 331.10

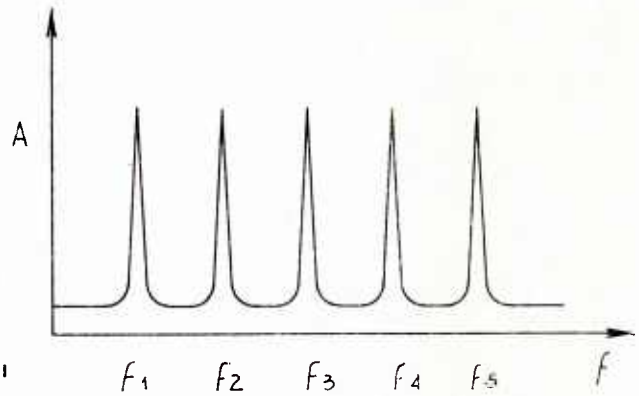

FIG 331.11

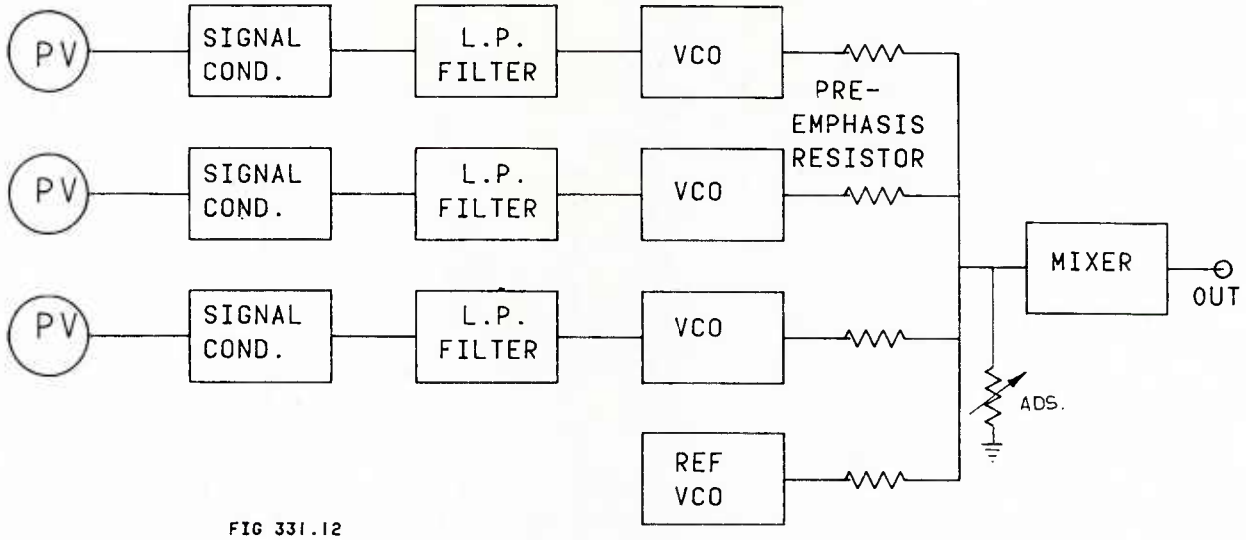

FIG 331.12

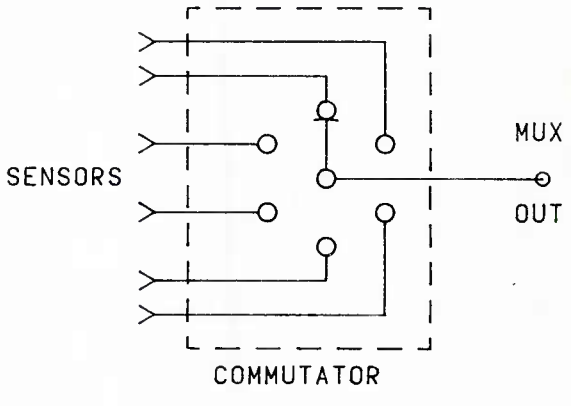

FIG 331.13

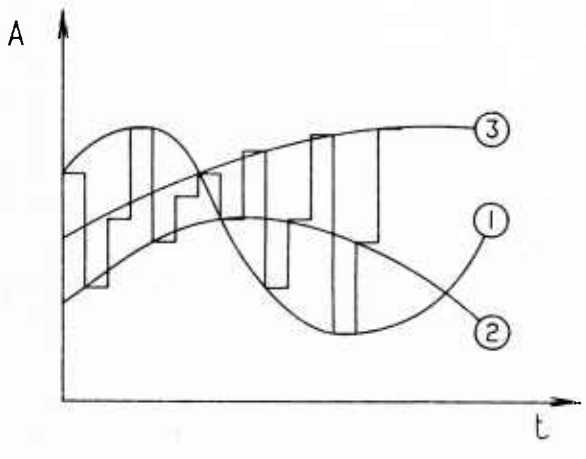

FIG 331.14

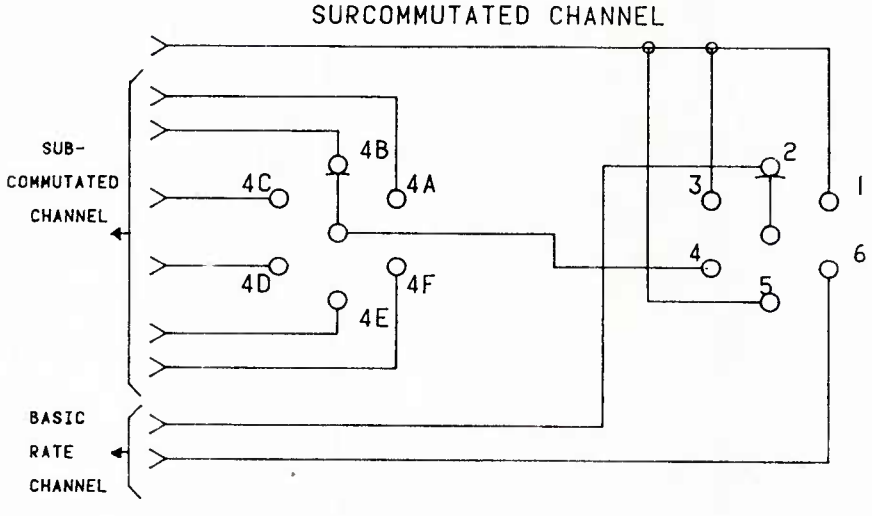

FIG 331.15

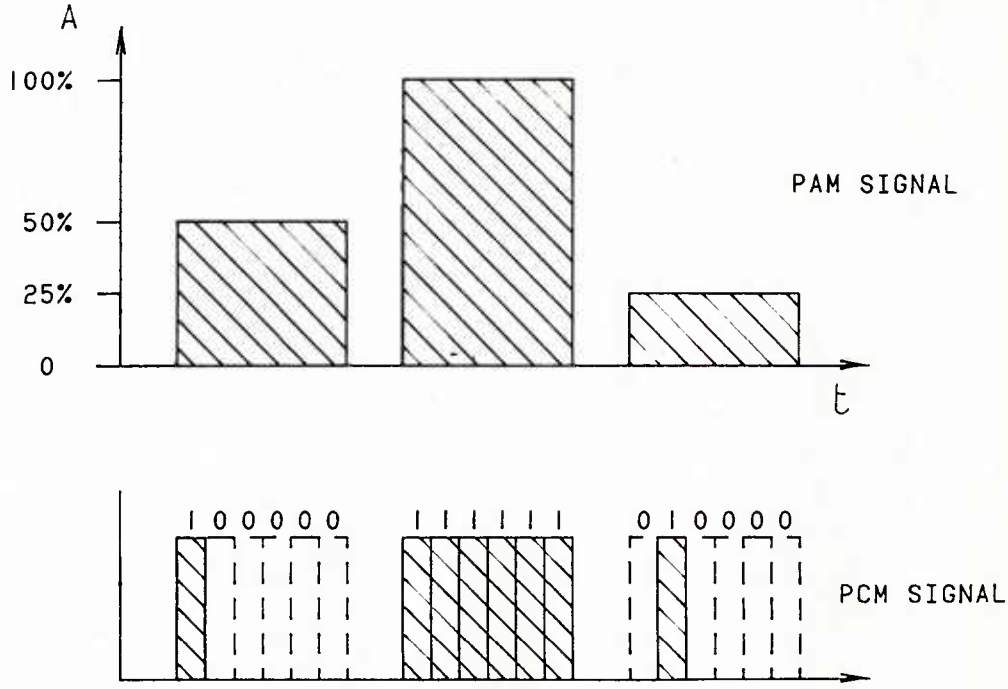

FIG 331.16

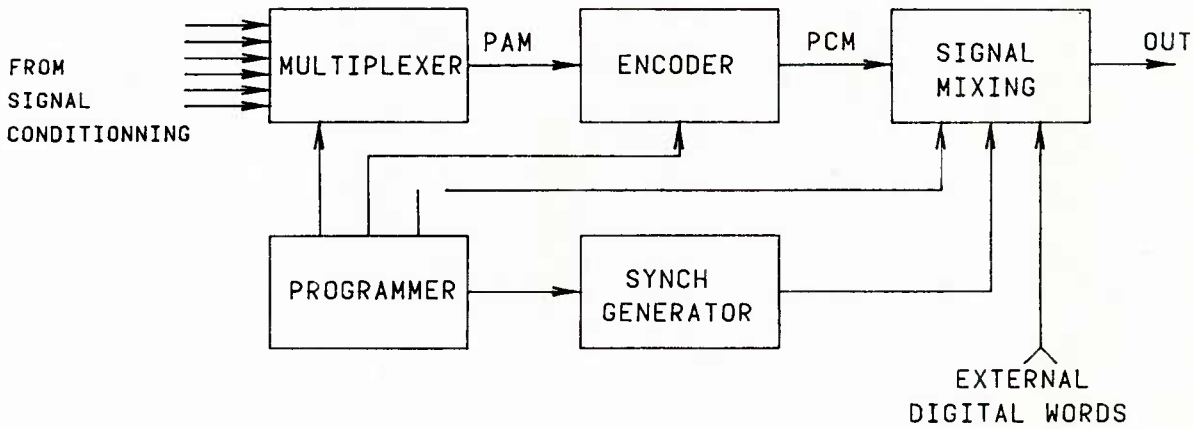

FIG 331.17

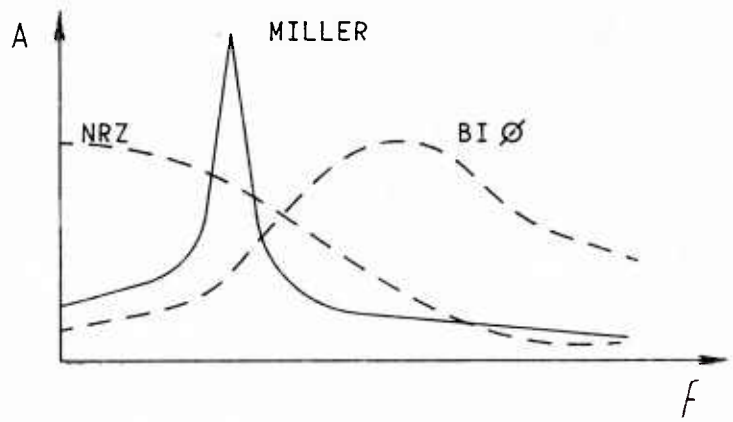

FIG 331.18

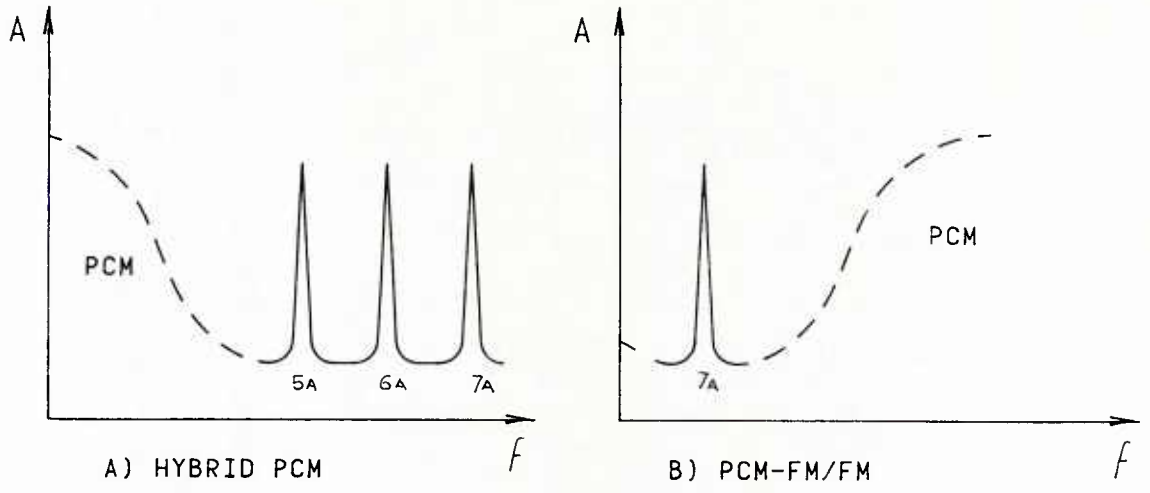

FIG 331.19

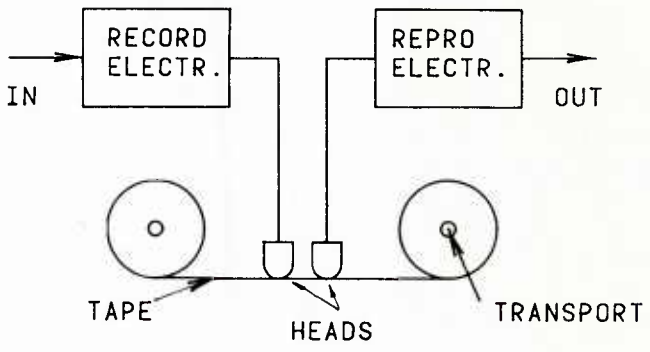

FIG 331.20

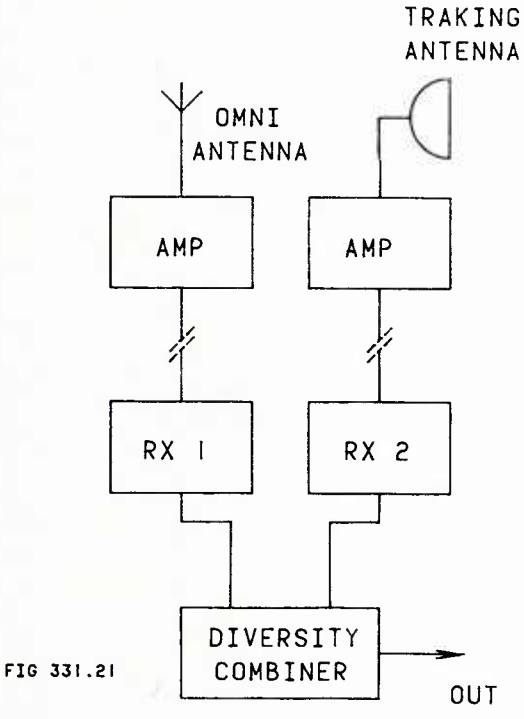

FIG 331.21

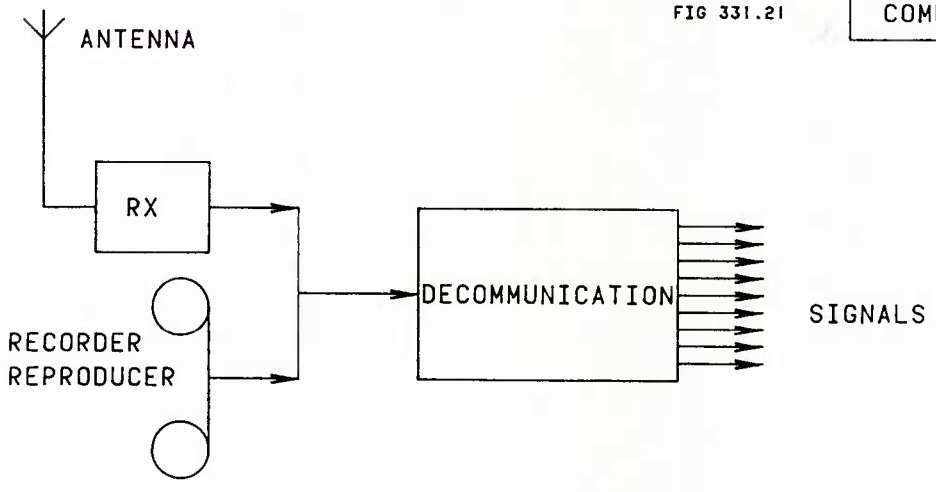

FIG 331.22

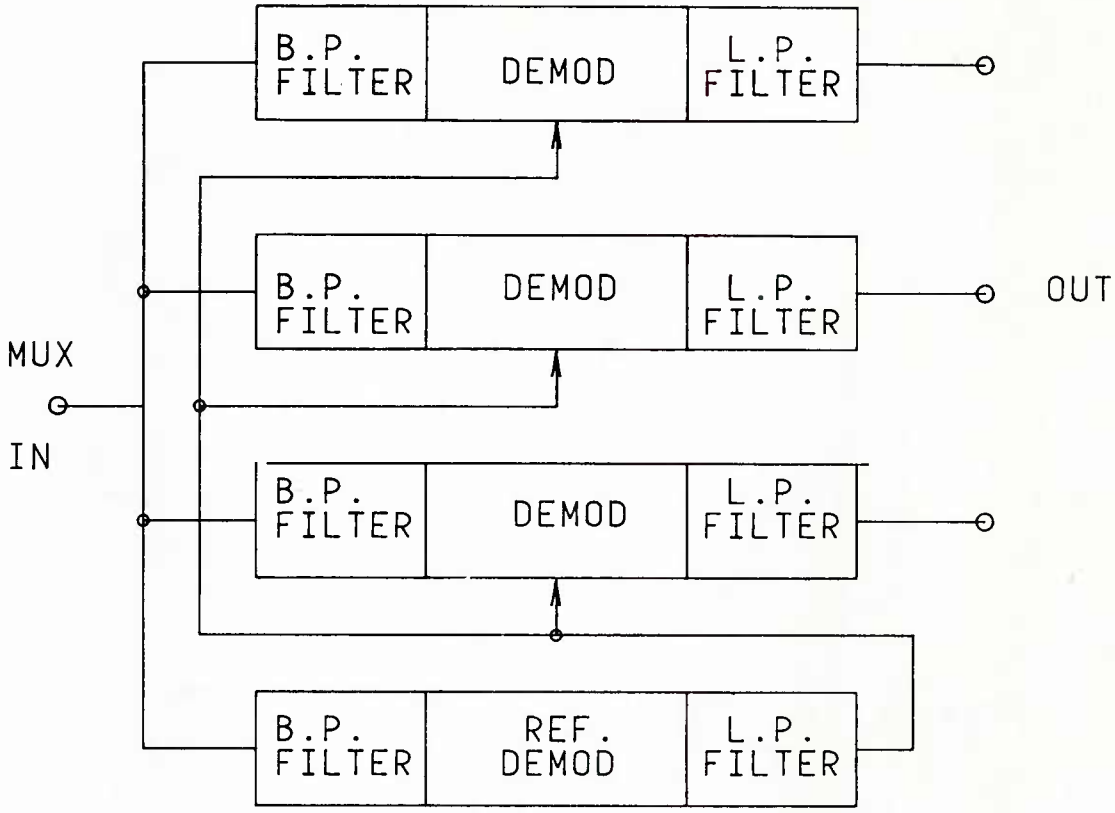

FIG 331.24

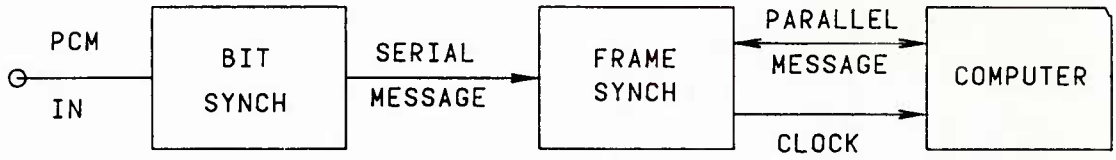

FIG 331.24

SUB CHAPTER 3.3.2

WORKING LOAD SPECTRA

by

F.Och

Messerschmitt-Bölkow-Blohm GmbH
Postfach 801140
8000 München 80, Germany

CONTENTS

3.3.2.0 Introduction

The measurements or predictions of load are analysed to give magnitude and frequency of occurrence of loads associated with various flight conditions. This information is combined with the percent occurrence of the flight conditions from the mission spectrum to produce the working load spectrum for the helicopter. These spectra of loads are devised for each fatigue critical component to cover conservatively all the envisaged role usages of the helicopter or the specific mission of a particular operator, e.g. military.

There is some concern over the variation in loads from pilot to pilot and frome one helicopter to another. The individual pilot's technique and the severity of the manoeuvres which he performs can affect the resulting loads, therefore manoeuvres of different severity are frequently flown to investigate this effect. Also the effects of normal atmospheric turbulence on the oscillatory rotor loads is another complicating factor. Therefore, some manner of accounting for the scatter in loads should be employed.

One of the following methods is practiced in the helicopter industry:

- a stress factor is applied to the typical loads in each flight condition,
- for a given manoeuvre the highest load recorded in a test flight condition is used in the subsequent analysis for substantiation,
- an "upper edge of data scatter" approach is used when enough data are available.

When no measurements are available, as it is the case in the design phase, average load spectra can be estimated, using both generalised design data and information from records taken on other existing helicopters in similar roles.

3.3.2.1 Uncycle-counted flight loads

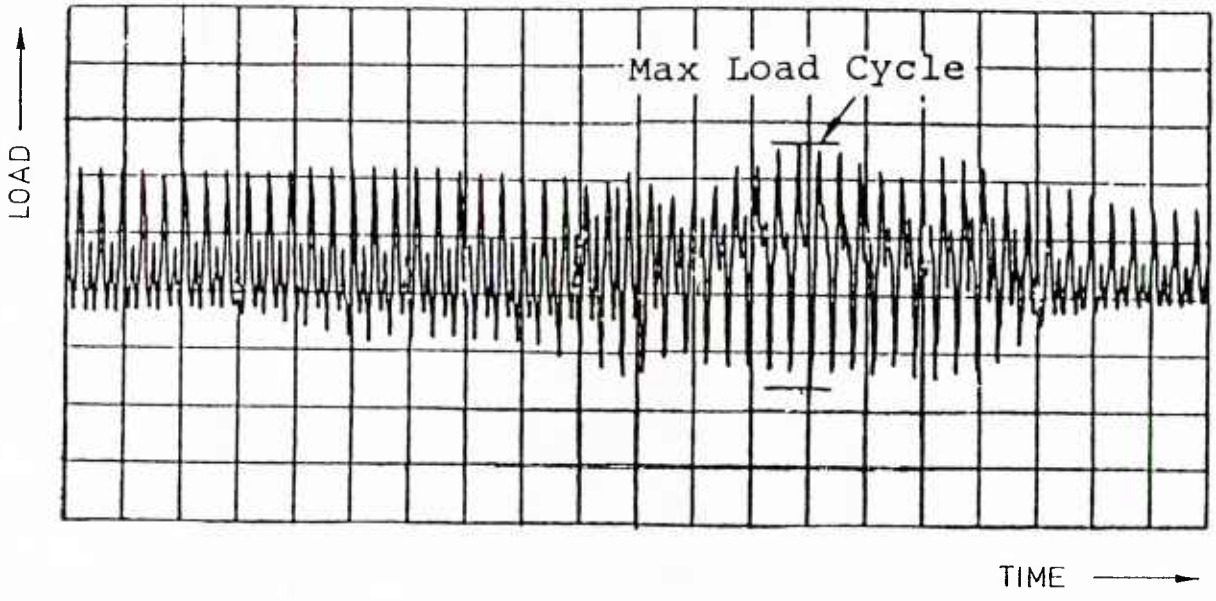

Fig. 332.1 Steady state flight load history

In the most simple form loads are assumed to be equal to the maximum loads during a flight condition or mission element.

The normal treatment of the data is to read the maximum (s_{max}) and minimum (s_{min}) values to give the maximum oscillatory (s_A) value within a mission element. The associated steady (s_S) value is also listed.

$$S_A = \frac{s_{max} - s_{min}}{2} \; ; \quad s_S = \frac{s_{max} + s_{min}}{2}$$

This maximum oscillatory value is assumed to represent all of the load cycles for the duration of that flight condition.

With the known repeating frequency (f_i), mostly the rotor frequency or a whole multiple of the rotor frequency, the total load cycles per hour of that flight condition can be found. The number of load cycles per hour of flight (n_i) is determined by multiplying the total load cycles per hour of that flight condition by the occurrence factor (F_i), which is the ratio of the time period in this condition to the total recording time. This will be done for each condition in the mission spectrum leading to the working load spectrum as shown in Table 332.1.

Flight Condition (i)	Alternating Load (s_A)	Steady Load (s_s)	Repeating Frequency (f_i)	Occurrence Factor (F_i)	Load Cycles per Flight Hour (n_i)

Table 332.1 Working load spectrum without cycle counting

This using of peak value flight loads without cycle counting is conservative because it considers the maximum peak-to-peak load of the flight condition to be applied during all load cycles, but it can cause high maintenance costs, if the conservative life requires frequent replacement of parts. However, never should conservatism in cycle counting be used to compensate for unconservatism elsewhere.

3.3.2.2 Cycle-counted flight loads

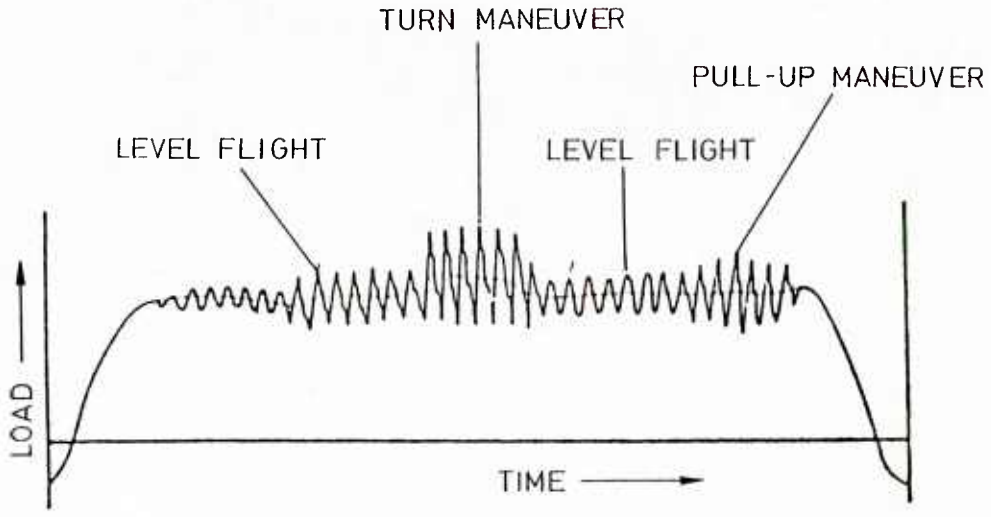

Fig. 332.2 Transient flight load history

In some flight conditions loads on a component may build up from relatively low undamaging levels to a damaging peak and the subside to low levels again, that is to say the loads vary significantly from cycle to cycle. To treat these loads data more realistically, the concept of cycle counting is employed.

The mechanization of processing and analysis techniques enabled replacing the previously used peak values of each flight condition by a load histogram based upon the analysis of the signal recorded over the entire duration of the flight condition considered. As regards manoeuvres with low repetitivity, this operation should be carried out as many

times as necessary to correctly illustrate an average flight.

To employ cycle counting, all load reversals over a lower limit are considered, in addition to the maximum peak-to-peak load of the flight condition. The details of how cycle counting will be conducted is described in Chapter 3.4 of this handbook.

The number of cycles per hour (n_{ij}) at different load classes is determined by multiplying the number of cycles (c_{ij}) at each load class times the occurrence factor (F_i), taking into account the length of time (t_i) for the data record.

It should be noted that in determining load cycles, not only each load reversal but once per manoeuvre or start-stop load cycles, caused by mean load shifts, must be considered as well.

If the steady load is the same for all flight conditions, or if the mean load is not considered by the counting method, a working load spectrum as shown in Table 332.2 will be found.

Flight Condition (i)	Load Cycles per Flight Hour (n_{ij})			
	Load Class 1 $s_1 \div s_2$	Load Class 2 $s_2 \div s_3$	Load Class 3 $s_3 \div s_4$	Load Class j $s_j \div s_{j+1}$

Table 332.2 Working load spectrum without mean load

By accumulating the number of cycles found for each load class, a working load spectrum is obtained as shown in Figure 332.3.

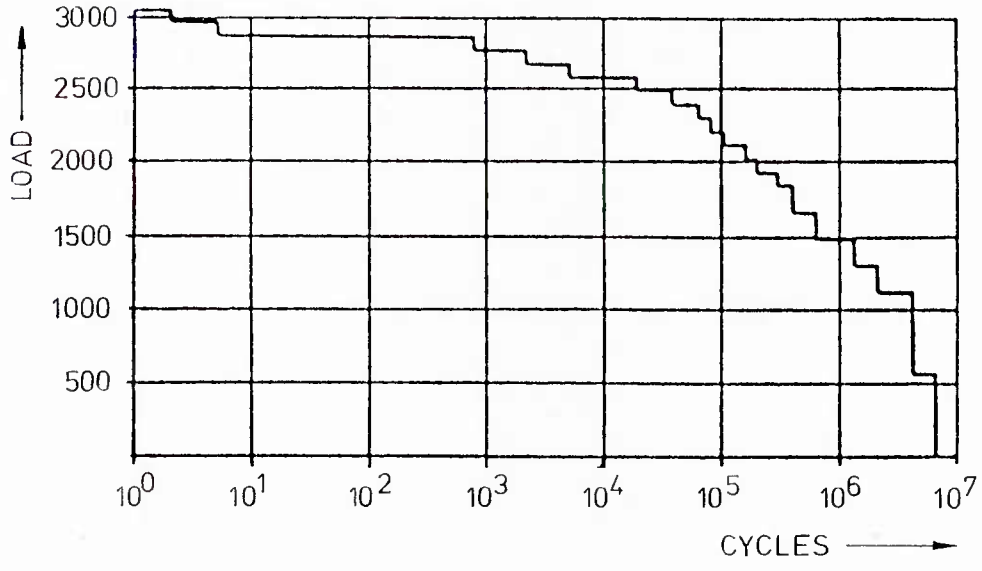

Fig. 332.3 Cumulative frequency working load spectrum

If the effect of steady loads on helicopter components must be taken into consideration, the "Rainflow" counting method can be used, leading to a matrix of load cycles at each class of steady and alternating load for each flight condition as shown in Table 332.3.

Alternating Load \ Steady Load	S_{S_1}	S_{S_2}	S_{S_3}	S_{S_4}
S_{A_1}				
S_{A_2}				
S_{A_3}				
S_{A_4}				

Table 332.3 Load matrix from Rainflow cycle counting for one flight condition

Aside from the counts in the lowest alternating load classes, which very seldom are damaging, the majority of the cycles mostly occur at a small range of mean loads, allowing the alternating load to be taken to be at one mean load. In this case a working load spectrum as shown in Table 332.4 will be found.

ALTERNATING STRESS			20	24	28	32	36	40
No	MANOEUVRE	MEAN STRESS	NUMBER OF CYCLES					
1	Take-off	44	2	-	-	-	-	-
2	Forward flight 20 kn	72	13	-	-	-	-	-
3	Forward flight 30 kn	68	-	12	2	-	-	-
4	Forward flight 40 kn	60	4	9	1	-	-	-
5	Forward flight 60 kn	60	11	2	-	-	-	-
6	Forward flight 103 kn	64	2	4	12	-	-	-
7	Max power climb 70 kn	68	1	-	-	-	-	-
8	Shallow approach to hover	56	12	5	6	8	4	-
9	Normal approach to hover	60	11	2	4	3	5	1

Table 332.4 Working load spectrum with one mean load

3.3.2.3 Statistical based working load spectra

One area which is still a source of concern is the repeatability of manoeuvres of given test points. Such things as pilot technique and reaction times can produce a wide variation in the data obtained. One way of smoothing out such data is to perform each test point a given number of times and to use a statistical approach on the results. The drawback to this is, of course, time and money since flight testing is a costly and time consuming operation and the approach outlined above would extend the time taken by a considerable amount and result in higher costs.

As seen in the previous chapters, cycle-counted flight loads are specified in the form of a series of flight conditions with the number of load cycles counted in each, along with the corresponding steady and alternating load level in each condition. By accumulating the number of load cycles counted for each mean load and at each alternating load level, an overall distribution is obtained as shown in Figure 332.4. This histogram presents the number of load cycles counted at each load level, versus the alternating load level.

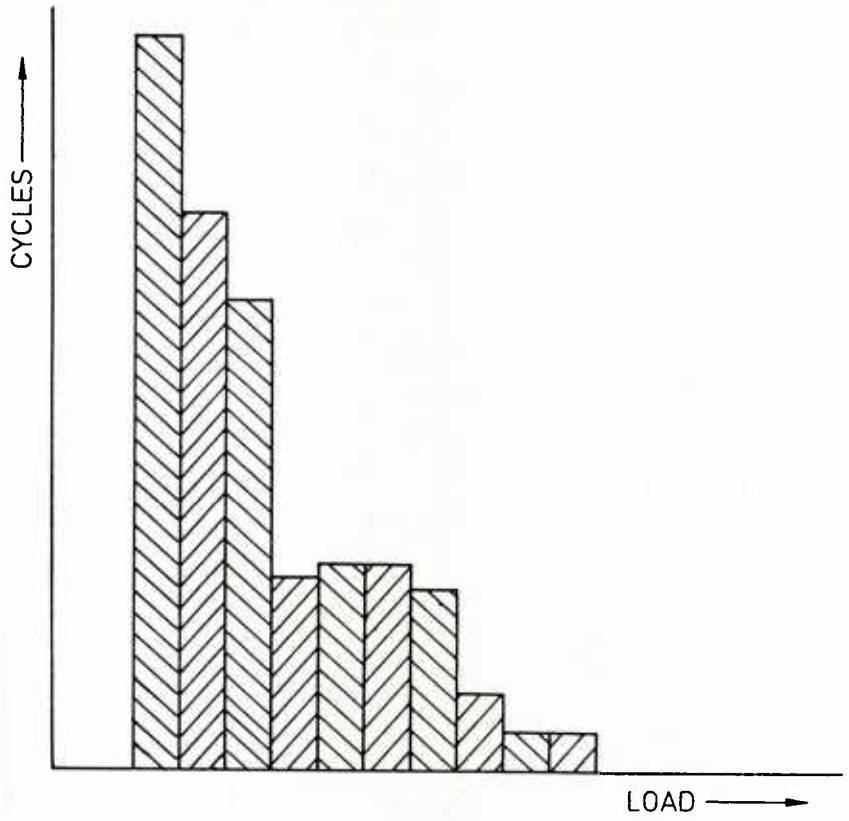

Fig. 332.4 Cycle-counted load spectrum

Experience has shown that a good curve-fit for the histogram can be obtained by using a log-normal distribution, characterized by its median $\tilde{M}$ and standard deviation s.

According to the linear cumulative damage hypothesis (Miner's rule), only loads higher than the component's endurance limit M_∞ must be considered. The cycle counted load spectrum in the region higher than M_∞ will be approximated by the following log-normal distribution:

$$n = \frac{K}{\sqrt{2\pi} \cdot s \cdot \ln 10} \cdot \frac{1}{M} \cdot \exp\left[-(\log M/\tilde{M})^2/(2 \cdot s^2)\right]$$

where:

n = number of load cycles at a load level M
K = arbitrary constant
s = standard deviation
M = alternating load level
$\tilde{M}$ = median

The standard deviation s may be selected from past experience.

The curve of this distribution contacts the histogram of the cycle-counted load spectrum in at least two points (M_1, n_1) and (M_2, n_2) by using the following values for $\tilde{M}$ and K:

$$\tilde{M} = \text{antilog}\left\{\frac{1}{2}\log(M_1 M_2) + s^2 \cdot \frac{1}{\log e} \cdot \left[1 + \frac{\log \frac{n_1}{n_2}}{\log \frac{M_1}{M_2}}\right]\right\}$$

$$K = n_1 \cdot \sqrt{2\pi} \cdot s \cdot M_1 \cdot \ln 10 \cdot \exp\left[(\log M_1/\tilde{M})^2/(2 \cdot s^2)\right]$$

The working load spectrum is found by adding load cycles and load classes to the cycle-counted load spectrum as shown in Figure 332.5.

Maximum load applied for representing a probability of occurrence P_o of all possible loads will be

$$M_{max} = \tilde{M} \cdot 10^{a \cdot s}$$

and is to guard against the unexpected and abnormal load situations.

Values of a can be obtained from any statistics handbooks; e.g. to include 99.9% of all possible loads, a = 3.09 must be used.

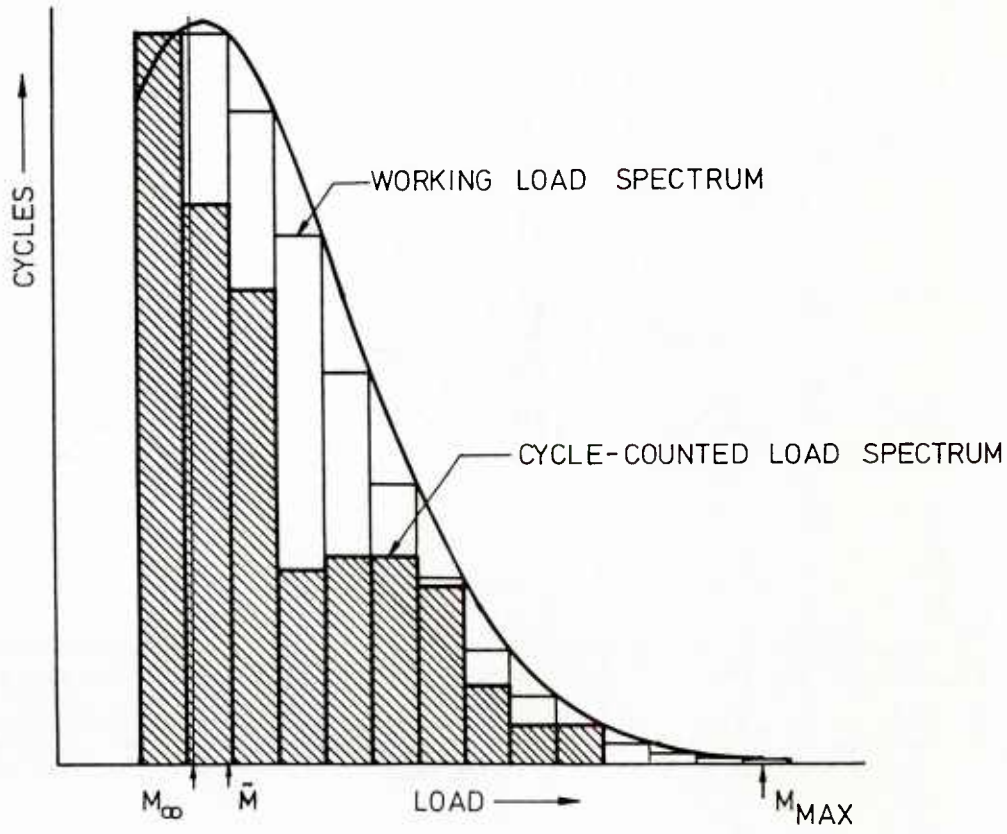

Fig. 332.5 Statistical based working load spectrum

SUB CHAPTER 3.4

THE ANALYSIS OF LOAD-TIME HISTORIES BY MEANS OF COUNTING METHODS

by

J.B. de Jonge
National Aerospace Laboratory NLR
THE NETHERLANDS

CONTENTS

3.4.1 INTRODUCTION

The loads occurring in actual service in helicopters are difficult to predict with high accuracy. As part of the certification process, the assumed design load spectra must be verified on the basis of actual flight load measurements. These measurements will have to be analysed and in some way quantified. Various methods exist to quantitatively asess recorded load time histories.

An important category in this context are the so called harmonic analysis methods. These methods determine the "frequency-content" of the signal, that means they determine the frequencies or, inversely, wavelengths of which the signal is built up.

Loads measured on the rotating parts of a helicopter usually show a periodic character, with the rotor frequency as basic frequency. Harmonic analysis shows that the signal is built up of a discrete numbers of sinusoidal components with frequencies being a whole multiple of the rotor frequency.

Such an analysis is highly relevant to determine the vibrational characteristics of the rotor, but is not very descriptive for the "fatigue damage" of the loading.

This may be illustrated by the simple example given in figure 34.1.

Two signals are considered both having the same frequency content, namely a basic component with frequency ω and amplitude A and one higher harmonic with amplitude $\frac{1}{2}A$ and frequency 2ω.

In the first case the phase difference between the two components is zero, in the second one $\pi/2$.

Figure 34.1 shows that these different phase shifts result in a completely different signal-appearance.

The first one varies between appr. + 1.3A and - 1.3A, hence the "range" is 2.6A.

The second one appears as a "main" load variation between + 0.7A and - 1.5A, hence with a range of 2.2A and a means of - 0.4A, plus a small additional load cycle with a range of appr. 0.2A and a mean of 0.65A.

It will be clear that the fatigue damage associated with these two signals is very different, although their frequency content is the same!

The present sub chapter will pay no further attention to harmonic analysis but will deal with an other category of analysis methods, namely methods which look for the occurrence of specific "events" in a load-time trace.

After a general discussion on counting principles, special attention will be paid to one particular method, known as range pair-range or rainflow-method.

This method will be described in full detail. A numerical example will be used to illustrate the method.

The complete algorithm, laid down in flow diagrams, is contained in two annexes.

The sub chapter ends with a discussion, a summary and conclusions.

3.4.2 GENERAL DEFINITIONS OF COUNTING PRINCIPLES

Typical "events" that can be observed in a load-time trace are

i the occurrance of load "peaks" at specific levels,
ii the exceedance or "crossing" of specific levels and
iii the occurrance of load changes or "ranges" of a specific size.

Accordingly, the following "groups" of counting methods can be distinghuished.

a Peak count methods

The turning points in a load-time trace are indicated as "peaks" and "troughs" successively.

The number of times that peaks and troughs occur at various levels is counted.

b Level cross count methods

The number of times that the load signal crosses various levels is counted. Distinction can be made between a crossing in an "upward" or positive sense and a "downward" or negative crossing. Obviously, the number of upward crossings of a specific level must be equal to the number of downward crossings.

Peak counts and level cross counts are closely related: the number of positive crossings of a certain level is equal to the number of peaks above that level minus the number of troughs above that level. This implies that the result of a level cross count can be derived from a peak/trough count result. As the opposite is not true, level cross counting may be considered as being of a "lower order" than peak/trough counting.

c Range count methods

It is known that the fatigue-damage of a varying load depends primarily on the amplitude, the variation in load rather than the absolute load level reached.
Hence, in order to quantify a load-time history in terms of fatigue-damage, it appears logical to observe the load variations or "ranges" occurring in the load history. This is the background of so-called range count methods.
In the counting of variations or ranges two principles can be distinguished, indicated as

i counting of single ranges
ii counting of range-pairs.

The counting of single ranges, usually indicated as range-count, is illustrated in figure 34.2. In this load history the following ranges are successively counted:
an upward Range $r_1 = S_2 - S_1$
a downward Range $r_2 = S_3 - S_2$
an upward Range $r_3 = S_4 - S_3$ etc.

The counting method is simple and straightforward but figure 34.3 indicates its sensitivity to small load variations. Analysis of the signal on the left would have resulted in counting of a large number of relatively small ranges. If the signal would have gone through a filter suppressing the small load variations, as on the right side, only one very range would have been counted.

The range-pair counting principle avoids this sensitivity. This principle is explained in figure 34.4: Rather than splitting upt the load trace shown in three successive ranges, the load trace is interpreted as one "main" load variation or range with super-imposed on it a small load cycle or range-pair.

The counting methods described sofar considered the occurrance of single events.
On the other hand, it is also possible to look for the simultaneous or subsequent occurrance of two different events. Such counting methods are indicated as two-dimensional.

For example, such a "combined event" can be the occurrance of a peak at level j followed by a trough at level i.
The result of such counting can be presented in a so-called Markov-Matrix A[i,j]; the element a_{ij} gives the number of load variations "from" level j "to" level i.
The load variation from j to i can also be expressed as a "load range" r = (i - j) with an

associated "mean" $m = \frac{i + j}{2}$

Obviously, the counting result can also be expressed in a "Range-mean" matrix M, in which the element M[r,m] gives the number of counted ranges of size r with a "mean" m.

The next section gives a detailed description of a two-dimensional counting method of special interest namely the range pair-range counting method. In this section the properties of the Markov-Matrix will be studied in more detail.

3.4.3 THE "RANGE PAIR-RANGE" OR RAINFLOW COUNTING METHOD

Some 12 years ago, the NLR developed a two-dimensional counting procedure (Ref. 1,2) which was later baptized Range pair-Range method (Ref. 3). At the same time and independently in Japan a method which became known as Rainflow-method (Ref. 4) was defined, described e.g. in reference 5.
Both methods yield exactly the same result, i.e. they extract exactly the same range pairs and single ranges from the sequence, thus combining the range pair counting principle and the single range counting principle in one counting method.
However, the descriptions of the methods are very different.
The present author prefers the range pair-range algorithm because it is easier to understand and to explain and can very easily be programmed for computations.
In the following, a detail description of the range pair-range method will be presented.

3.4.3.1 Conversion of a load-time history into a peak/trough sequence

As the counting procedure only considers the values of succesive peaks and troughs, the complete load-time history may firstly be reduced to a peak/trough sequence.

In the classification of peaks and troughs it is usual to apply a specific "range filter size" R as show in figure 34.5.
A peak at a certain level is only recognized as such if the signal has dropped to a level which is "R" lower than the peak level. In the same way a trough is counted if the signal has risen "R" above the trough-level.

A complete algorithm for this peak/trough search has been presented in annex A.
It will be assumed that the result is a series of n integer values S_p[p = 1,2...n] ranging from 0 to k.
These values represent the successive peaks and troughs in the load sequence.

3.4.3.2 Description of the counting procedure

The counting procedure consists of two phases. In Phase I, the peak/trough sequence is searched for range-pairs. At the end of this phase a "residu" is left which is analysed according to the single range principle. The counting result will be stored in a Markov-Matrix A of size (k + 1) x (k + 1).
The element a_{ij} presents the number of counted ranges "from" level j "to" level i. Obviously, the elements for which i < j (elements "above" the main diagonal) contain "downward" load changes, and vica versa.

Phase I: Starting with the first recorded peaks/troughs, groups of four successive extremes S_{p-3},S_{p-2},S_{p-1} and S_p are considered.
In this group a range-pair is counted if the values of the two "inner" extremes S_{p-2} and S_{p-1} fall within the range bound by S_p and S_p-3: (see Fig. 34.6).
Counting a pair implies that the value of the appropriate element a_{ij} in the "upper" triangle" and the opposite element a_{ji} in the lower triangle of the Markov-Matrix are increased by one.
Next, the "counted" extremes S_{p-2} and S_{p-1} are deleted from the record and the procedure is repeated "moving backward", by considering the four extremes S_{p-5},S_{p-4},S_{p-3} and S_p.
If the counting criterion is not met, one moves one step forward, hence the extremes S_{p-2},S_{p-1},S_p and S_{p+1} are considered and so on.

It can easily be shown that if the whole sequence has been searched for pairs in this way, eventually a "residu" remains which has the shape indicated in figure 34.7, namely a "diverging" part followed by a converging part.

Phase II: The "residu" S_1,S_2,S_3 etc. is simply counted as successive single ranges S_1 - S_2,S_2 -S_3, etc.
It can easily be shown that the maximum length of the residu is 2k + 1 extremes, containing 2k ranges.

Figure 34.8 gives as an example the complete range pair-range counting of a sequence of 8 extremes.
First the extremes S_1,S_2,S_3 and S_4 are considered, next S_2,S_3,S_4 and S_5, next S_3,S_4,S_5 and S_6. This is the first time that a range pair is counted. S_4 and S_5 are deleted. Next, stepping "backward" S_1,S_2,S_3 and S_6 are considered. Again a "pair" S_2 - S_3 is found. From the remaining four extremes no pairs can be subtracted. This residu is further counted as single ranges.

A complete algorithm for the range pair-range counting method is presented in annex B.

As a further example the load traces presented in figures 34.9 and 34.10 have been analysed. The counting results are given in figure 34.11.

3.4.3.3 Further analysis of the counting result

The final counting result is contained in a matrix A of size (k + 1) x (k + 1), in which the element a_{ij} gives the number of counted variations "from" level j "to" level i:
as mentioned before, the "upward" or positive" load variations will be contained below the main diagonal and downward variations in the triangle above the diagonal. Obviously, the elements on the diagonal (i = j) must be zero.

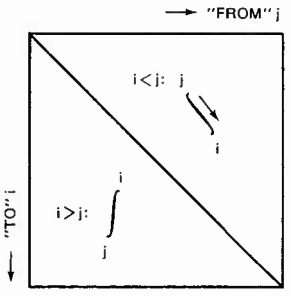

Looking at the example counting result given in figure 34.11, some interesting features of range pair-range counting should be noted:

i The maximum load variations counted must be equal to the distance between the highest peak and the lowest trough in the record. In our example the lowest trough is 0 and the highest peak 9; as the peak at 9 occurred earlier than the trough at 0, the associated variation of size 9 is a "downward" one and an entry is found in element $a_{0,9}$.

An important consequence of this property is that the result of the range pair-range counting depends on the length of the record analysed at one time. If a record is split in two halves, counting each half separately and adding these results together, the result can be different from the one obtained if the whole record is counted in one batch.

ii The size of the range-filter has only an effect on the counts of ranges smaller than that filter.

Figure 34.11 shows that the only effect of increasing the range filter size from R = 1 to R = 3 is that all elements a_{ij} for which $|i - j| < 3$ become zero.
In other words, the choice of the Range filter size R is not critical. The counting result pertaining to a certain filter size can easily be converted to larger filter sizes.

Derivation of peak count result

The number of peaks at level x must be equal to the number of "upward" ranges ending at level x:

$$N_p(x) = \sum_{j=0}^{x-1} a_{xj}$$

or the number of downward ranges coming from level x

$$N_p(x) = \sum_{i=0}^{x-1} a_{ix}$$

Both expressions give essentially the same result with one exception, associated with the first and last extreme of the load sequence: if the last extreme is a peak, this will be included in the sum of upward ranges but not in the sum of downward ranges.

Thus, in our example the number of upward ranges ending at level 6 is equal to 7, and the number of downward ranges starting at level 6 is equal 6, see figure 34.11 a.

To avoid ambiguity, it is useful to define the first and last extremes in the record as "halve extremes"; the peak count result can then be obtained from:

$$N_p(x) = \tfrac{1}{2}\left[\sum_{j=0}^{x-1} a_{xj} + \sum_{i=0}^{x-1} a_{ix}\right] \qquad (3.4.1)$$

In the same way, the number of troughs at level x is given by:

$$N_t(x) = \tfrac{1}{2}\left[\sum_{j=x+1}^{k} a_{xj} + \sum_{i=x+1}^{k} a_{ix}\right] \qquad (3.4.2)$$

The number of peaks at or above x is equal to:

$$N_p^c(x) = \sum_{d=x}^{k} N_p(d) \qquad (3.4.3)$$

The number of troughs at or below x is equal to:

$$N_t^c(x) = \sum_{d=0}^{x} N_t(d) \qquad (3.4.4)$$

The peak/trough count results for our example are presented in table 34.1 and figure 34.12. It may be noted that the result depends very heavily on the size of the range filter R.

Derivation of level cross count result

The number of positive crossings of a certain level x is equal to the number of upward ranges starting at a level lower than or equal to x and ending at a level higher than x:

$$N_{\ell}^{+}(x) = \sum_{i=x+1}^{k} \sum_{j=0}^{x} a_{ij} \qquad (3.4.5)$$

The level cross count results for our example are presented in table 34.1 and figure 34.13. It may be noted that also the level cross count result is very sensitive for the size of the range filter used.

Reduced Range pair Range count result

Because of its two-dimensional character the counting result, as presented in the Markov-matrix, is not very well suited for pictorial presentation. For this purpose, the complete two-dimensional counting result may be reduced to a simplified format yielding

a The number of load changes N (r) with range r

b The average mean $\bar{m}$ (r) pertaining to the load changes with range r.

c Additionally, to give an information about the variability of the mean, the variance σ_m (r) is sometimes presented.

The range r can take all integer values from 1 to k inctusive.
These quantities can be deduced from the complete natrix using the following expressions:

N(r) = number of "downward" and "upward" load changes with range r = $N(r^-) + N(r^+)$

$$N(r) = \sum_{i=0}^{k-r} a_{i,i+r} + \sum_{i=r}^{k} a_{i,i-r} \qquad (3.4.6)$$

$$\overline{m}(r) = \left[\sum_{i=0}^{k-r} \left(a_{i,i+r} \times \frac{2i+r}{2}\right) + \sum_{i=r}^{k} \left(a_{i,i-r} \times \frac{2i-r}{2}\right)\right] / N(r) \qquad (3.4.7)$$

$$\sigma_m(r) = \overline{m^2}(r) - [\overline{m}(r)]^2 \qquad (3.4.8)$$

$$\overline{m^2}(r) = \left[\sum_{i=0}^{k-r} a_{i,i+r} \times \left(\frac{2i+r}{2}\right)^2 + \sum_{i=r}^{k} a_{i,i-r} \times \left(\frac{2i-r}{2}\right)^2\right] / N(r) \qquad (3.4.9)$$

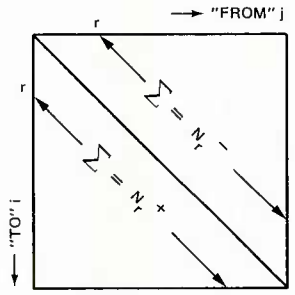

The number of load changes with range equal to or larger than r, $N_{cum}(r)$ is calculated from:

$$N_{cum}(r) = \sum_{r^*=r}^{k} N(r^*) \qquad (3.4.10)$$

The reduced counting results for the example-trace have been presented in table 34.2 and figure 34.14. So far, it was assumed that the counting result was actually stored in a complete Markov Matrix and that the reduced range pair-range result was derived from that matrix.

If a high resolution (meaning a large value of k) is required, the necessary memory capacity to store the matrix, namely (k + 1) x (k + 1), may become very large. For example, if k = 255, the matrix consists of 65.536 elements!

If it is intended to eventually use only the reduced range pair-range result, it becomes advisable to calculate the "reduced" quantities N(r), $\Sigma m(r)$ and $\Sigma m^2(r)$ directly during counting rather than filling up a matrix. As k values for r are possible, the required memory-capacity will be 3 x k or, for e.g k = 255, 765 only. Counting a "range pair" with range r and mean m than means that the "reduced" quantities are updated:

$$\left[N(r)\right]_{"new"} = \left[N(r)\right]_{"old"} + 2$$

$$\left[\Sigma m(r)\right]_{new} = \left[\Sigma m(r)\right]_{old} + 2m \qquad (3.4.11)$$

$$\left[\Sigma m^2(r)\right]_{new} = \left[\Sigma m^2(r)\right]_{old} + 2m^2$$

Obviously, for counting single ranges in plase II, the figure 2 in equations 3.4.11 must be replaced by 1. When the counting is completed, $\bar{m}$ (r) and σ_m (r) are computed:

$$\bar{m}(r) = \Sigma m(r) / N(r)$$

$$\sigma_m(r) = \{\Sigma m^2(r) / N(r) - [\bar{m}(r)]^2\}^{\frac{1}{2}} \qquad (3.4.12)$$

It will be clear that if the reduced quantities are counted directly, the peak count result and the level cross count result can no longer be obtained.

3.4.4 DISCUSSION

In the previous sub-chapter, the Range pair-Range counting method came out as a very powerful counting method.

Essentially, the method splits up a load-time history into separate loadcycles, having a specific amplitude or "range" and a specific mean. The counting result can be directly applied in cumulative fatigue damage calculations according to Miner's rule and in simple crack growth calculations. Methods exist to generate from the "matrix" load sequences to be applied in fatigue tests or for application in more complex crack growth calculation methods. It may be recalled that the counting method is insensitive for the size of "range filter" applied to the signal. In summary, the range pair-range method appears to be the most appropriate one to define the "fatigue content" of a loading sequence.

One aspect of the counting method needs some further consideration. It may be recalled that the counting method will always yield as largest range counted the load variation between the lowest trough and the highest peak. This variation is interpreted as a "half load cycle". Suppose that this lowest trough occurs very early in the load sequence and the highest peak at the end. If the load sequence in question is a very long one, one may ask whether it makes physically sense to combine these "timely remote" occurrances into one cycle. Specifically in the case of a growing crack, one can imagine that the peak at the end will be seen by a crack which is very different in size and cracktip condition from the one prevailing at occurrance of the lowest trough.

In other words, from a physical point of view it is advisable to restrict the size of the load history on which the range pair-range method is applied at one time. Very long load histories should be split up, and each part counted separately.

For the analysis of helicopter rotor loads, "one flight" seems to be a reasonable choice as a maximum length.

Finally, a few things will be said about the use of other counting methods. It may be useful to apply peak count- or level cross counting to a loading history in order to allow comparison with other load data which have been presented as peak/trough spectra or load level exceedance spectra. In this context, it should be kept in mind that a vast amount of load data have been and are being obtained from counting accelerometers. These instruments actually apply a level cross counting technique. These methods, however, must be considered as less relevant for describing the fatigue damage of a load history than range countings.

3.4.5 SUMMARY AND CONCLUSION

In the present chapter methods to analyse load time histories by means of counting methods were discussed. Specific attention was paid to the range pair-range method or rainflow method, which was discribed in full detail. The following conclusions can be made:

- The rangepair-range or rainflow method is a very powerful method to describe the "fatigue-content" of a load time history.
- Peak count results and level cross counts can easily be obtained from the complete range pair-range matrix.
- Use of a "reduced" range pair-range count result may be practical, specifically if computer memory limitations are important.

3.4.6 REFERENCES

1. de Jonge, J.B., Fatigue load monitoring of tactical aircraft. Paper, presented at the 29th Meeting of the AGARD SMP, Istanbul, Sept. 1969, NLR Report TR 69063 U, August 1969.
2. de Jonge, J.B., The monitoring of fatigue loads. Paper, presented at the ICAS-Congress, Rome, Sept. 1970, NLR MP 70010.
3. v. Dijk, C.M., Statistical load data processing. Paper, presented at the 6th ICAF Symposium Miami, Florida, USA, May 1971.
4. Matsuiski, M., Endo, T., Fatigue of Metals subjected to Varying Stress. Paper, presented at the Kyushu district meeting of the Japan Society of Mechanical Engineers, March 1968.
5. Watson, P., Cycle counting and fatigue damage. Paper, presented at SEE Symposium, 12 February 1975, published in Journal of the Society of environmental engineers, September 1976.

TABLE 1

Results of peak counting and level cross counting

level	Range filter = 1					level	Range filter = 3				
	peaks		troughs		pos. level cross		peaks		troughs		pos. level cross
	N_p	N_p^c	N_t	N_t^c	N_ℓ		N_p	N_p^c	N_t	N_t^c	N_ℓ
9	2	2	0	30.5	0	9	2	2	0	12	0
8	5	7	0	30.5	2	8	3	5	0	12	2
7	5	12	0	30.5	7	7	2	7	10	12	5
6	6.5	18.5	3	30.5	12	6	1	8	0	12	7
5	6	24.5	5	27.5	16	5	4	12	1	12	8
4	5	29.5	4	22.5	17	4	0	12	0.5	11	11
3	1	30.5	5.5	18.5	18	3	0	12	1	10.5	11
2	0	30.5	7	13	13	2	0	12	4.5	9.5	10
1	0	30.5	5	6	6	1	0	12	4	5	5
0	0	30.5	1	1	1	0	0	12	1	1	1

TABLE 34.2

Reduced range pair-range counting result

Range r	Filter R = 1				Filter R = 3			
	N(r)	$N_{cum}(r)$	$\bar{m}$ (r)	σ_m (r)	N(r)	$N_{cum}(r)$	$\bar{m}$ (r)	σ_m (r)
1	11	61	4.6	1.3	0	24		
2	26	50	4.7	1.5	0	24		
3	12	24	4.2	1.2	12	24	4.2	1.2
4	1	12	6.0	0.0	1	12	6.0	0.0
5	1	11	4.5	0.0	1	11	4.5	0.0
6	3	10	4.0	0.0	3	10	4.0	0.0
7	2	7	4.5	0.0	2	7	4.5	0.0
8	4	5	4.8	0.5	4	5	4.8	0.5
9	1	1	4.5	0.0	1	1	4.5	0.0

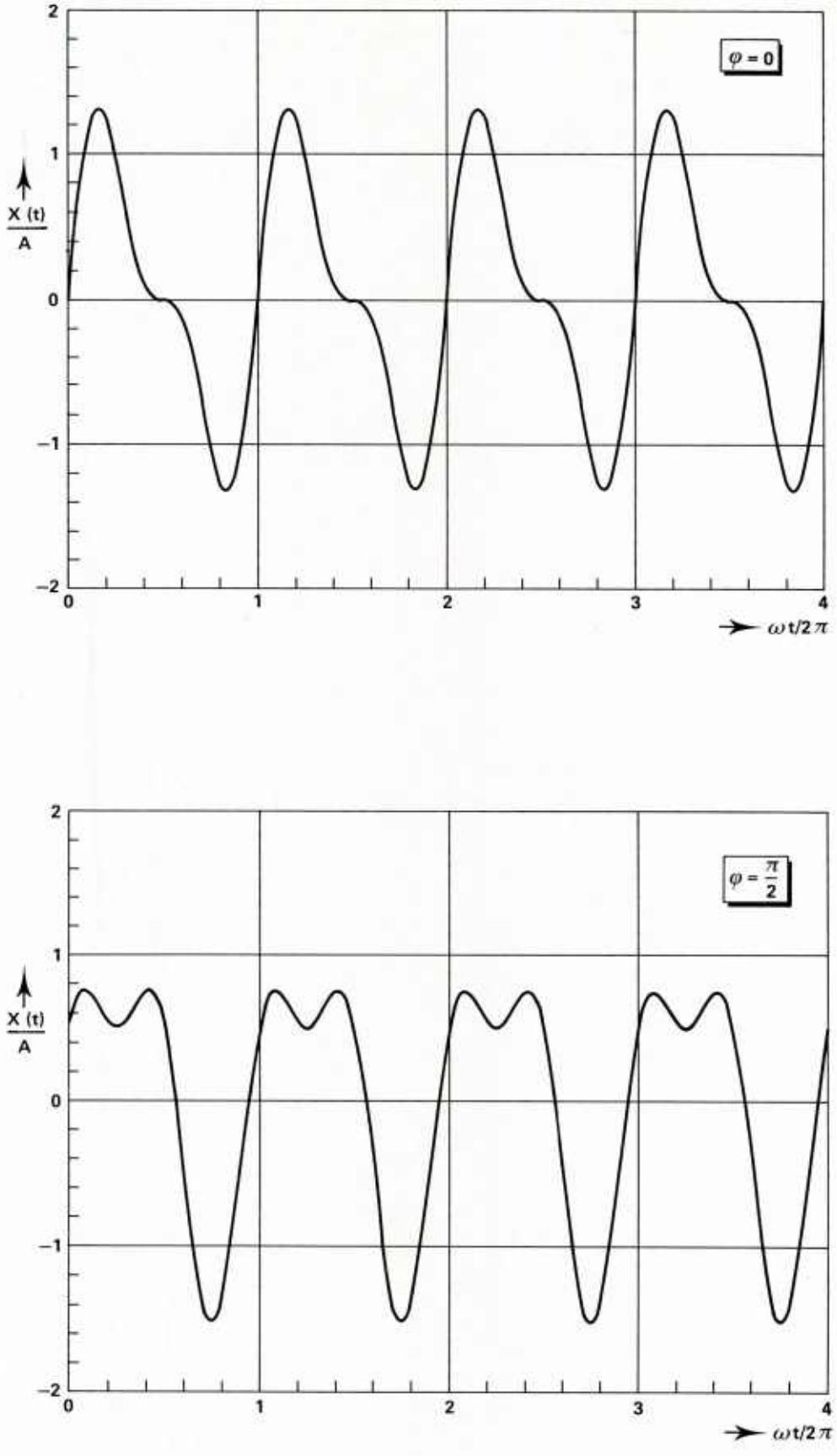

$$X(t) = A \sin(\omega t) + 1/2\, A \sin(2\omega t + \varphi)$$

Fig. 34.1 The effect of phasedifference φ on the shape of the periodic signal considered

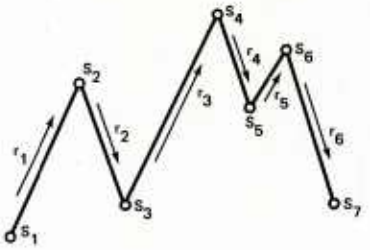

Fig. 34.2 Principle of the range count method

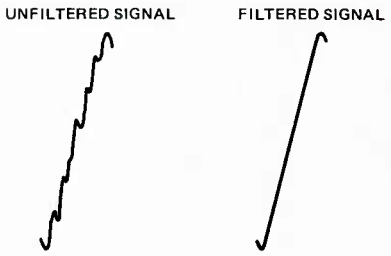

Fig. 34.3 Sensitivity for small load variations

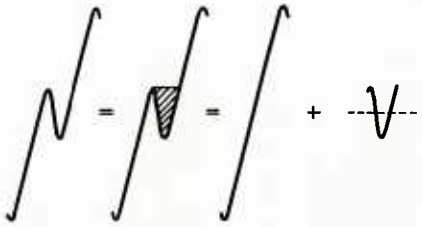

Fig. 34.4 Range pair counting principle

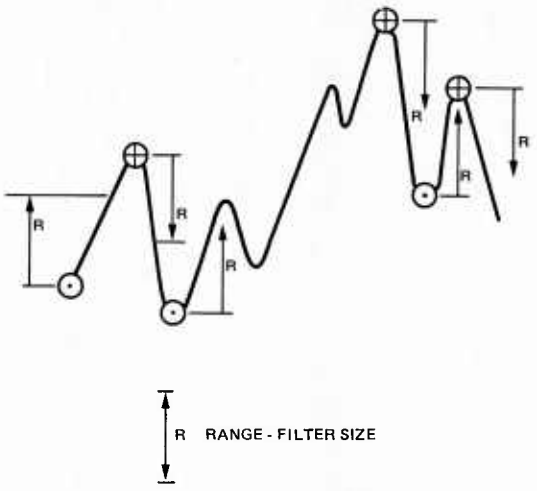

Fig. 34.5 Classification of peaks and troughs using a range-filter R

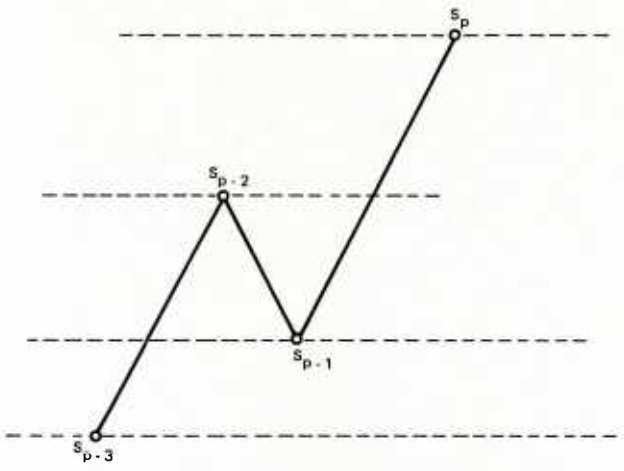

THE RANGE PAIR $S_{p-2} - S_{p-1}$ AND $S_{p-1} - S_{p-2}$ IS COUNTED IF

$S_{p-1} > S_{p-3}$ AND $S_{p-1} \geqslant S_{p-3}$ AND $S_p \geqslant S_{p-2}$

OR

$S_{p-2} < S_{p-3}$ AND $S_{p-1} \leqslant S_{p-3}$ AND $S_p \leqslant S_{p-2}$

Fig. 34.6 Range pair counting criterion

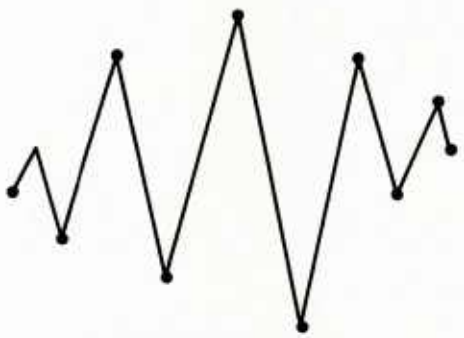

Fig. 34.7 Shape of the residu after counting phase I

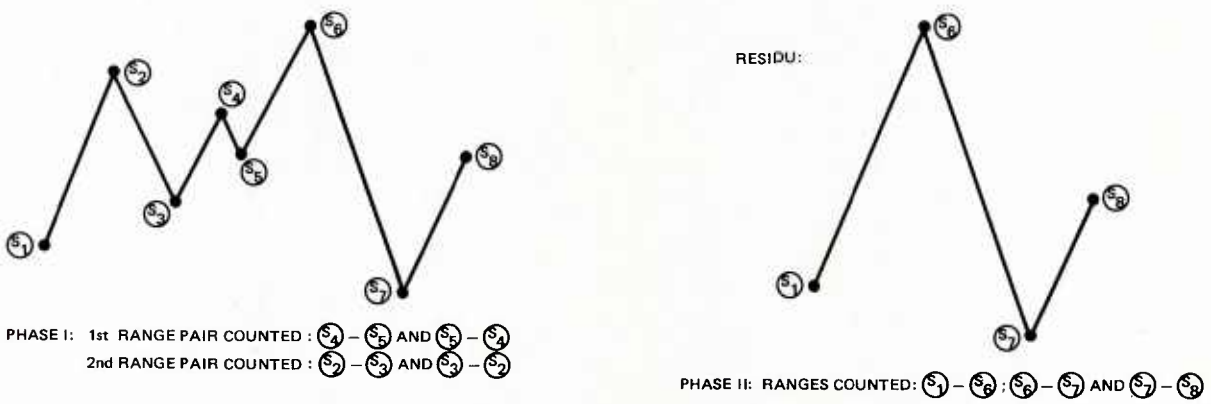

Fig. 34.8 Simple example of range pair-range counting

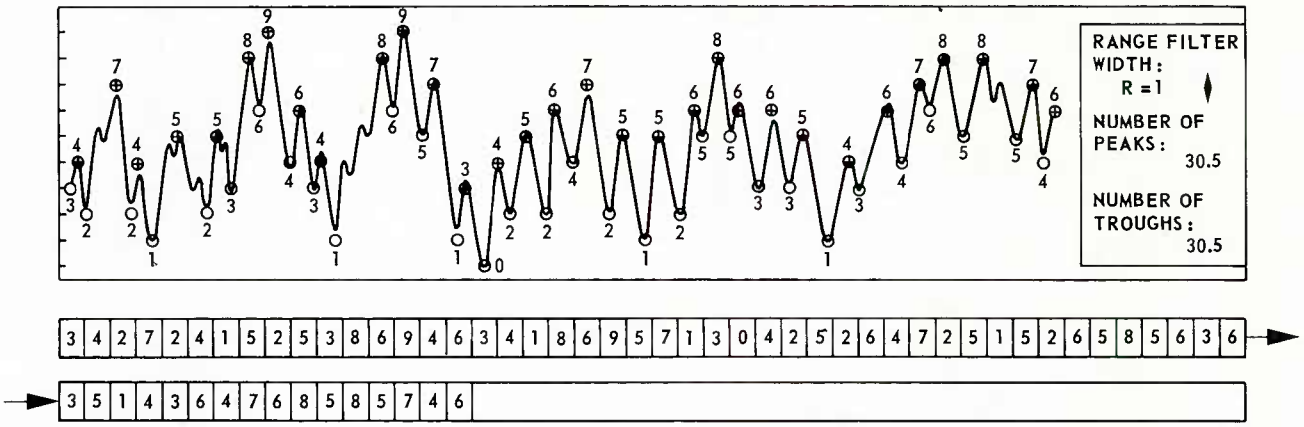

Fig. 34.9 Analysis of a load-time history for peaks and troughs

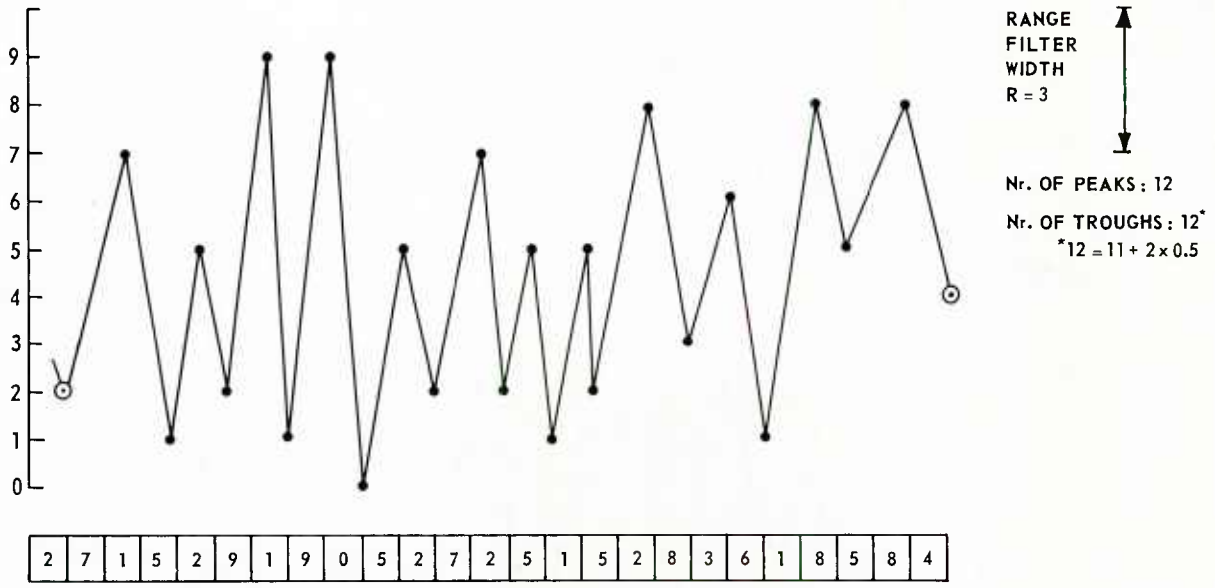

Fig. 34.10 Peak/trough sequence of figure 34.9 after filtering with bigger range filter

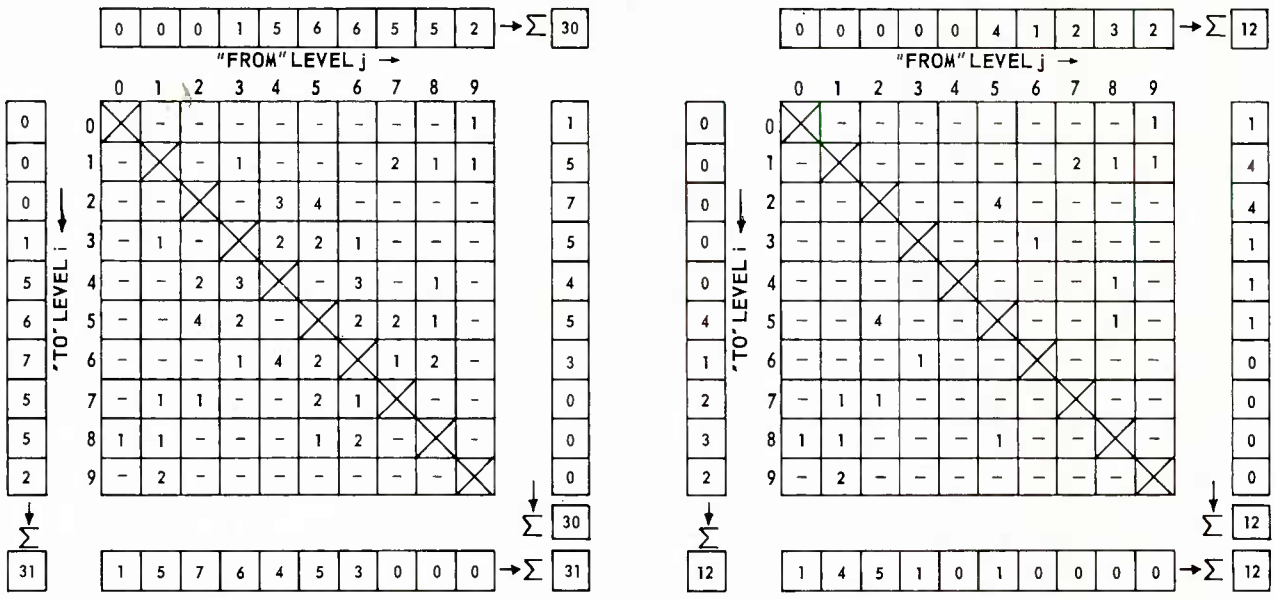

a) Range filter value R = 1

b) Range filter value R = 3

Fig. 34.11 Range pair-range count results for the load trace of fig. 34.9

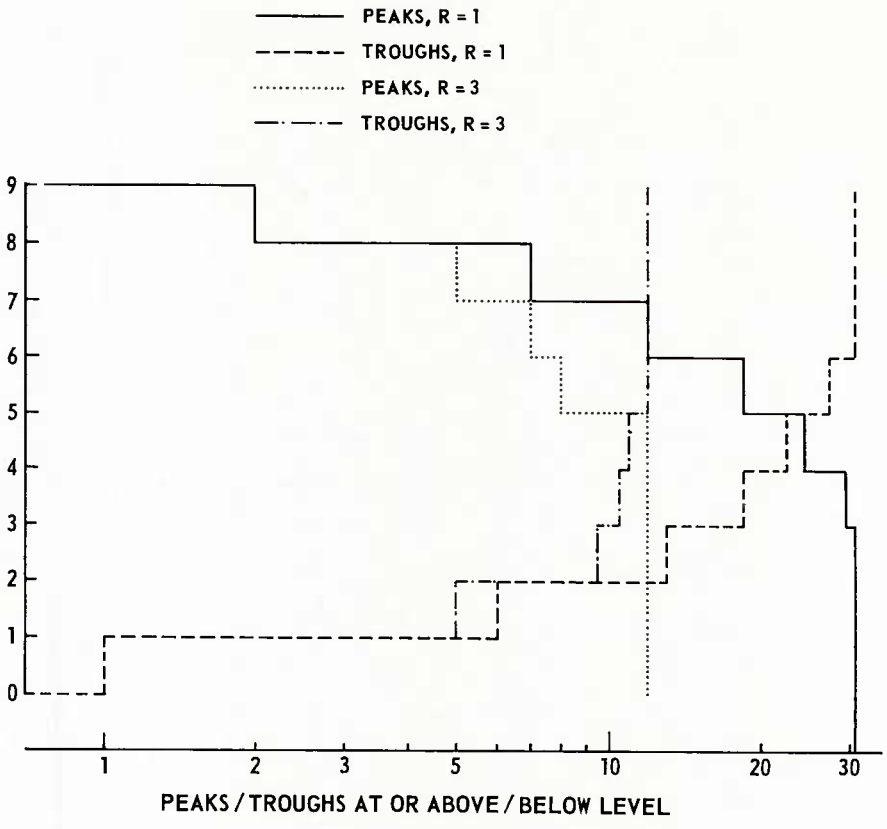

Fig. 34.12 Peak/trough exceedance curves

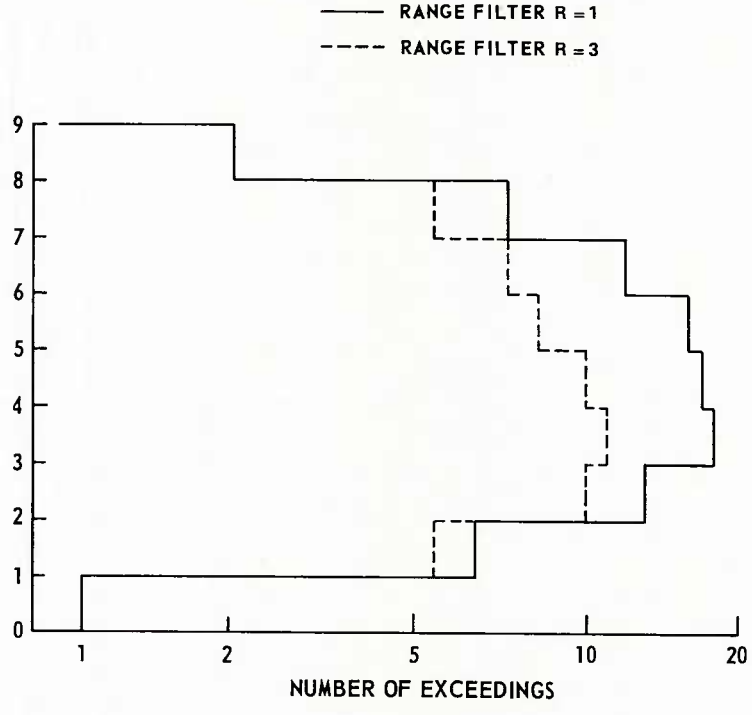

Fig. 34.13 Result of level cross counting

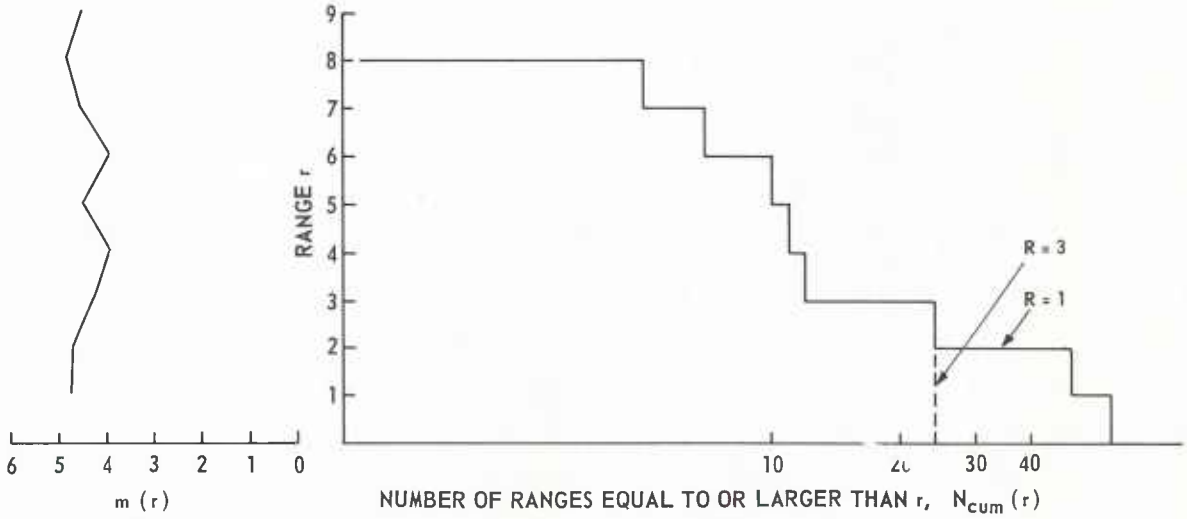

Fig. 34.14 Counted ranges with range pair-range method for two range filter values

ANNEX 3.4 A

Peak/trough search algorithm

A load history x(t), 0 < t < T, may be either recorded in an analog format and converted into a digital form or recorded directly in a digital format as a series of integer values $x_i [i = 1 \ldots \ell]$. The values x_i are numbers ranging from 0 to k. This sequence is searched for peak/through values. The successive extremes found are called S_1, S_2 and so on. The last extreme found is S_n. A range-filter with size R is used. This means that successive peaks and troughs differ at least a value R The algorithm is defined in the following flow diagram, which consists of the parts 'BEGIN', 'MINZO', 'MAXZO' and 'ENDZO'.

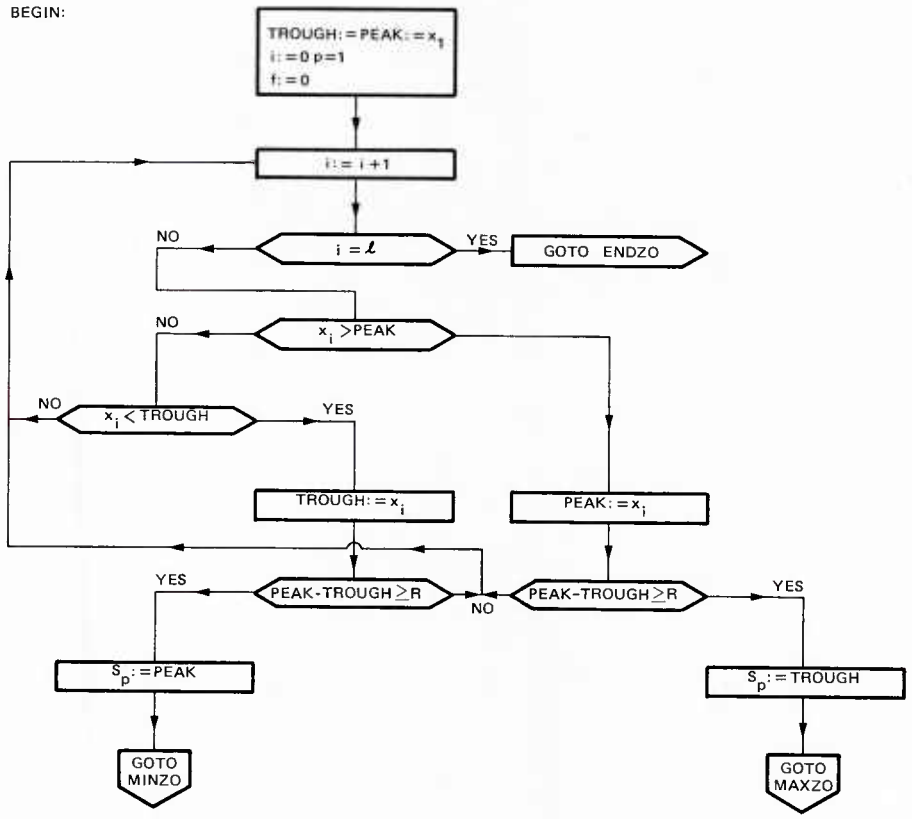

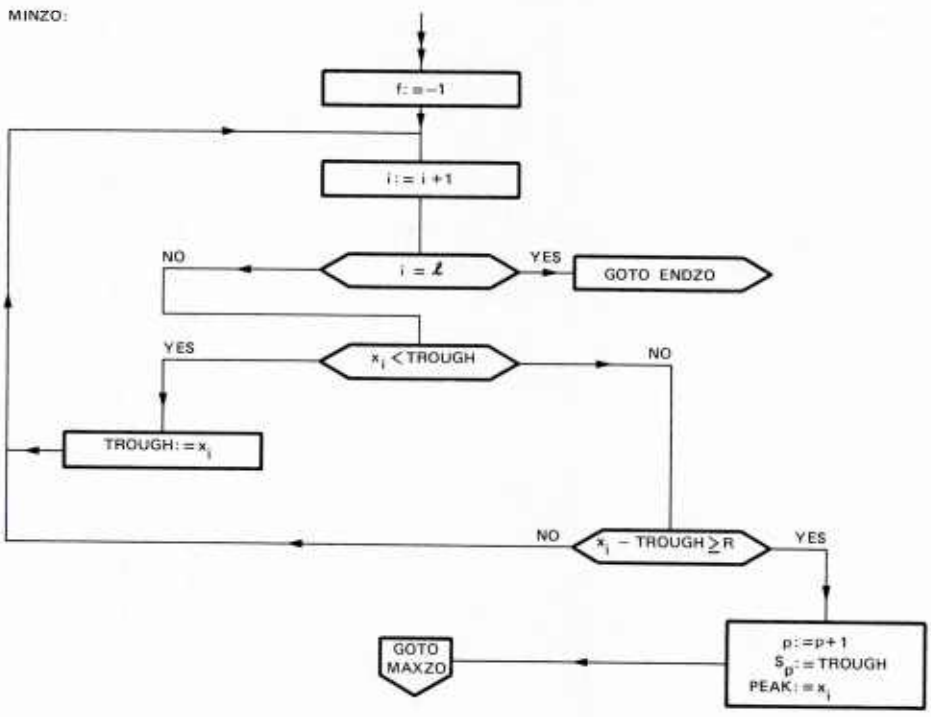

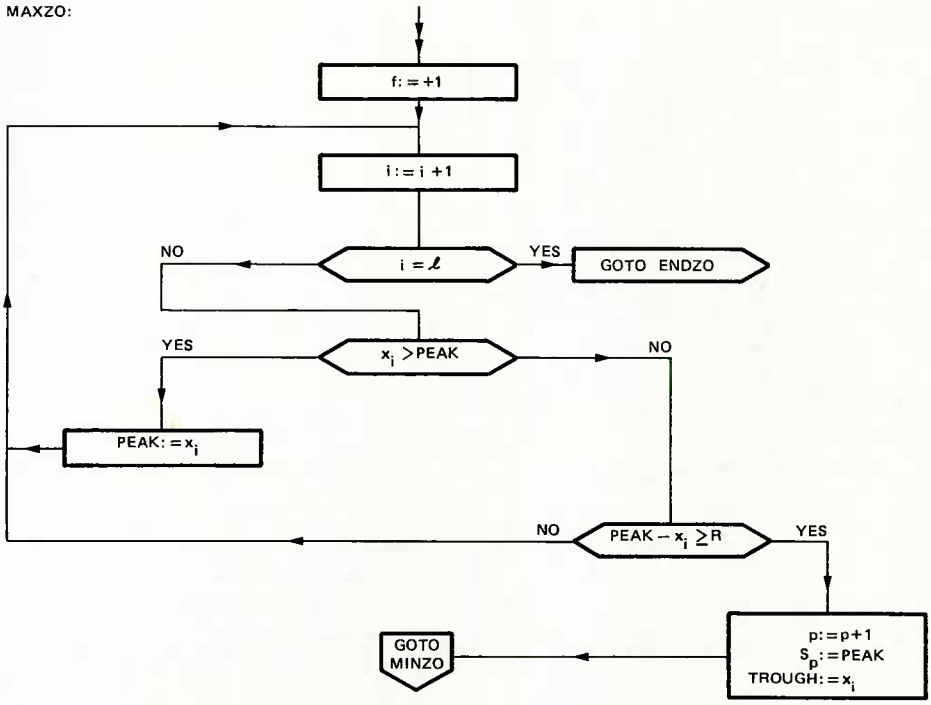
MAXZO:
f: = +1
i: = i +1
NO
i = ℓ
YES
GOTO ENDZO
YES
x_i > PEAK
NO
PEAK: = x_i
NO
PEAK − x_i ≥ R
YES
GOTO MINZO
p: = p+1
S_p: = PEAK
TROUGH: = x_i

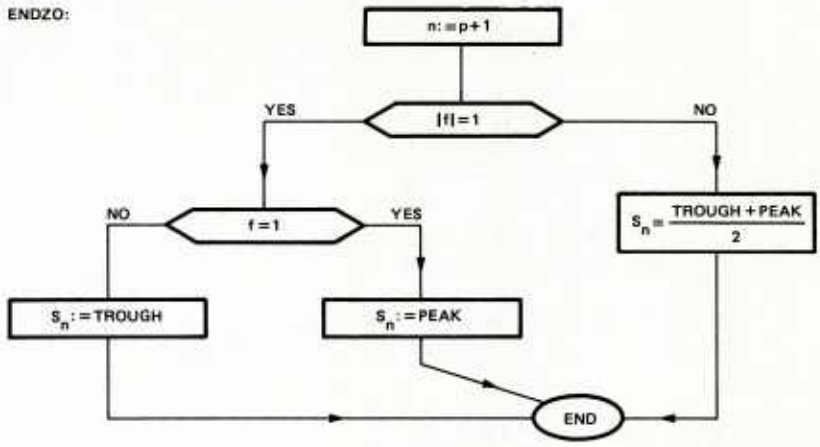
ENDZO:
n: = p+1
YES
|f| = 1
NO
NO
f = 1
YES
S_n = TROUGH + PEAK / 2
S_n: = TROUGH
S_n: = PEAK
END

ANNEX 3.4 B

Range Pair-Range Algorithm

General:

The input consists of a stream of n integer values ranging from 0 to k, which represent successive peaks and troughs in a load-time history. Counting ends when last input data has been read, and counting results are put out. Output consists of matrix A of size (k + 1) x (k + 1).
a_{ij} is number of counted load changes starting at level j and ending at level i.
The algorithm is presented in the following flow diagram.

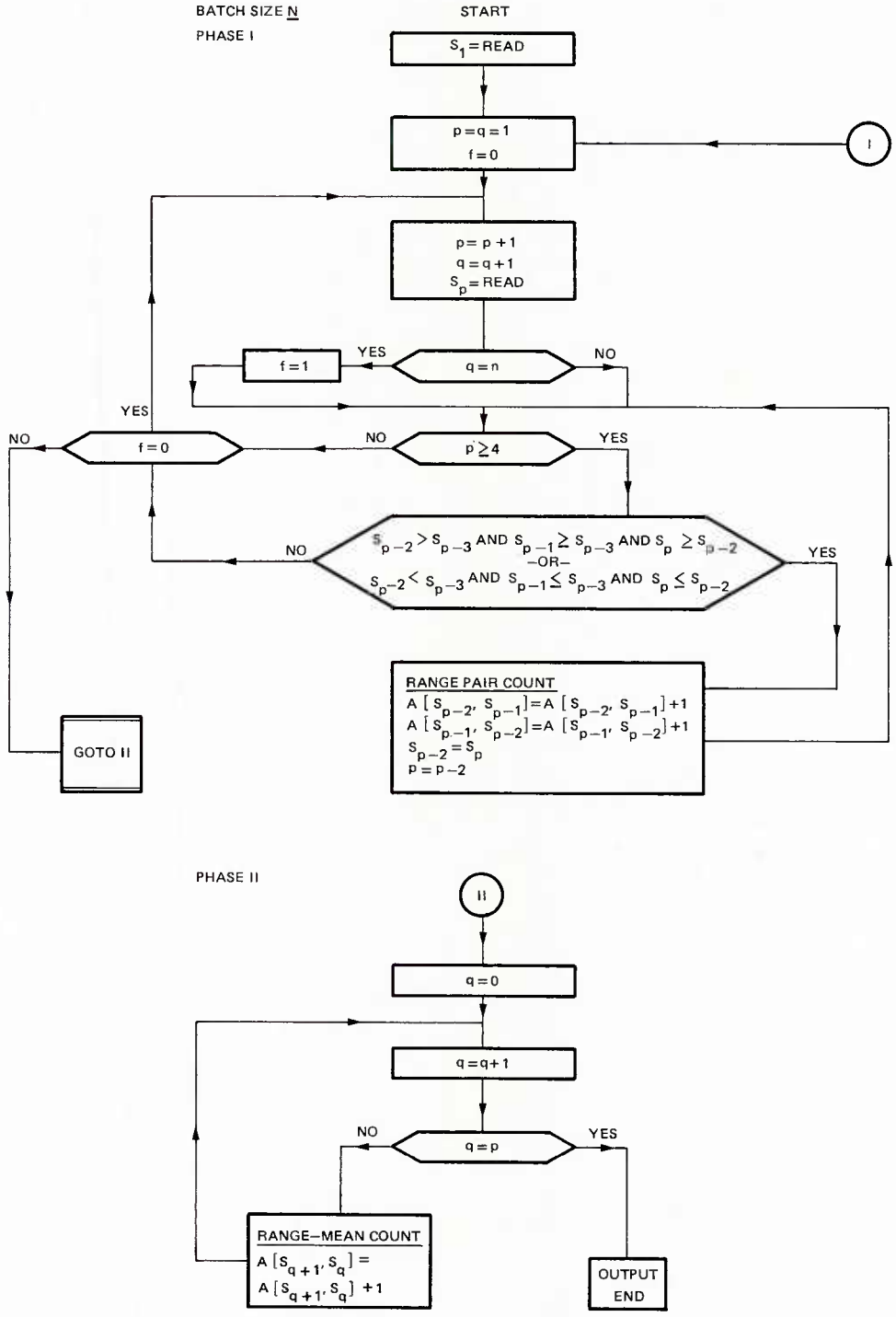

CHAPTER 4
FATIGUE DESIGN DATA

CONTENTS

SUB CHAPTER 4.1

FATIGUE STRENGTH

by

F.Och

Messerschmitt-Bölkow-Blohm GmbH
Postfach 801140
8000 München 80, Germany

CONTENTS

4.1.0 INTRODUCTION

Fatigue strength should be based on past full-scale fatigue tests and/or materials fatigue data under consideration of size, shape, surface finish, and environment of the structure. There is a large quantity of information available on the fatigue strength characteristics of material specimens, built-up specimens and parts. However, in many cases the differences between past test specimens and the actual part cannot be accounted for with a reasonable degree of accuracy (Ref. 41.1).

In the helicopter industry the fatigue strength of critical structural components, defined as components subjected to significant fatigue loading, the failure of which would be catastrophic in terms of flight safety, is usually determined by full-scale fatigue tests.

An analytical determination of fatigue strength of structural components through use of coupon tests on specific materials with subsequent application of factors concerning stress concentration, fretting, size effect, and so on, will be regarded as sufficient only in those cases, for which the fatigue margin of safety is extremely high or when the service loads are clearly defined and the primary mode of failure is evident, and if the precise stress distribution is known.

Fatigue is a failure mechanism that occurs as a consequence of repeated stressing. Fatigue properties are reported and used in terms of fatigue strength, i.e. the stress required to produce failure in a designated life-time. These properties, however, are determined in terms of fatigue life, i.e. the number of stress applications required to produce failure under designated conditions of loading and environment (Ref. 41.2).

4.1.1 FATIGUE TESTING

The objective of a fatigue test is to determine the fatigue life and the location of failure of a test piece subjected to a prescribed sequence of load amplitudes. If the test piece is a structural component and the applied load is to simulate the service load conditions, this may be the sole purpose of the test.

In most cases, however, it is required that the test be designed in such a way that it will allow a generalization of the result obtained, to provide the entire load versus number of loadings curve from static strength up to the endurance limit. For this purpose it is indispensable that the test conditions be simplified, be it with regard to the sequence of load amplitudes or to the test piece or to both, to establish the factors which influence the fatigue life.

Since fatigue strength is of a statistical nature, a relatively large number of tests has to be carried out even if one only considers average values of such parameters as e.g. standard deviation. This requirement has some influence on the choice of the testing procedure.

The type of tests varies depending on how the component is loaded in service and on the complexity of the component and can be characterized by

- the sequence of load amplitudes and
- the types of test pieces.

4.1.1.1 Types of load sequences

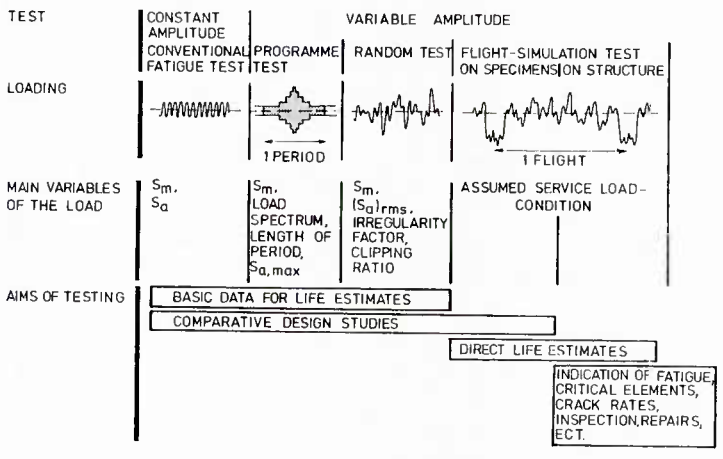

Fig. 41.1 Survey of different types of load sequences (Ref. 41.3)

Constant amplitude

A constant amplitude test is performed by applying reversals of load of a constant amplitude to the test piece until failure occurs or for a preassigned number of cycles. Different specimens of the test series may be subjected to different load amplitudes, but for each individual item the amplitude will be helt constant.

This type of fatigue testing is used mainly to define an S-N curve, i.e. the relation between load and life, keeping constant the mean load S_m or the stress ratio R, which is the ratio of the minimum to the maximum stress during a loading cycle. The result and its usefulness depend upon the total number of specimens, the choice of load levels, and the allocation of specimens to the load levels.

If the total mumber of specimens is small, the only information obtainable is an estimate of the average S-N curve corresponding to a probability of survival of fifty per cent. It is common practice in the helicopter industry to use some twenty to thirty specimens to establish each S-N curve, because of material and fabrication variations. The number of specimens tested has a self-evident influence on the accuracy of the parameters computed from the observations. Other factors viz. the choice of the load levels, the inherent scatter of the specimens and of the testing machine, may be of equal importance. A small number of specimens therefore can to some extent be compensated for by a more efficient design of the test conditions.

The choice of load levels depends upon the purpose for which the data are required. If the main interest is e.g. in the endurance limit range of the S-N curve, low load levels will be chosen. If the complete S-N diagram is wanted, the load levels may be more evenly distributed. It is strongly recommended that static tests should also be included. It may be said that the greater the difference between the highest and the lowest load levels, the greater the accuracy of computed parameters. An often used test approach is the "two level" test, with emphasis on the high level. The "high" test level is usually selected at or slightly above load levels which produce an average performance of 10^5 cycles. The first specimen will usually quickly indicate the life potential and influence any further load level adjustments. The "low" level is usually sought to yield about 10^6 cycles per specimen. The objective of this approach is to supply depth of testing to the high load region where failures occur at low numbers of cycles and where there is more potential for competing failure modes to appear and also to allow for the possible emergence of a different mode of failure at lower loads (Ref. 41.4).

The allocation of specimens to the load levels is not very crucial under the condition that a proper transformation of the test results has been performed, as shown later in this design guide. All the observations can then be pooled and used to determine the average curve and the distribution of the deviations from it.

In the helicopter industry simple fatigue tests are usually carried out, i.e. each single test piece will be subjected to a different alternating load of constant amplitude. The normal method of carrying out this test is to establish the static strength and then to place a second specimen in the machine and to apply reversals of load of a magnitude somewhat lower than the static strength. If the specimen fails after a certain number of reversals, a third specimen is placed in the machine and subjected to a range of load less than that used for the first fatigue experiment. Again failure results after a certain endurance and the process is repeated, the applied range of load being reduced with each succeeding specimen until a load is reached which does not cause failure within a preassigned number of cycles. The result of such a test is represented for each specimen by a paired number (S,N) which may be plotted to appropriate co-ordinates and used for establishing an average S-N curve as well as the variability in fatigue strength (Ref. 41.5).

In some cases multiple fatigue tests will be carried out, i.e. a simple fatigue test is repeated a number of times under identical conditions. The result of such a test is represented by a number of (S,N) pairs which will provide an average value and, in addition, will indicate the scatter of this average, usually measured by the statistical distribution of fatigue life.

Variable amplitude

A variable amplitude test is required in order to simulate an extremely complicated pattern of load cycles of varying amplitude and mean load to which a component is subjected in actual service. These load cycles appear in a random order, and must therefore be described in statistical terms. When these loads are simulated in a fatigue testing machine, considerable simplifications are usually introduced, depending upon the test purpose and the available fatigue testing machine.

In the programme test the load amplitude varies periodically, either continuously or stepwise, depending on the fatigue testing machine. The relative frequency of a load cycle of a certain amplitude has been determined by a counting method as shown earlier in this design guide. A limited number of load cycles with constant amplitude is selected to constitute a step. Naturally, the fewer the cycles within each step, the more realistic the simulation will be. A limit is imposed, however, by the condition that the largest amplitude must have at least one or preferably a few cycles in the step. The steps are grouped together in blocks which are applied to the test piece and repeated until failure

occurs without changing the shape of the block, i.e. the pattern in which the steps are arranged within the block. Failure may occur in any one of the steps, and consequently the load level at which this happens cannot be anticipated. For comparative design studies programme tests may give useful information.

The spectrum test represents the most realistic simulation of an extremely complicated pattern of load cycles by either randomizing the individual load cycles (random test) or by directly applying the load sequences occurring in flight (flight-simulation test). Spectrum tests require sophisticated fatigue testing machines employing electro-hydraulic servo valves with a closed-loop system. In general, actual components are used in the flight-simulation tests to directly establish replacement times. If realistic but different load sequences are applied by different investigators the test results cannot be compared. Therefore a demand grew for standardisation of load sequences that could be considered as representative for a specific type of loading. For detailed information see later in this design guide.

4.1.1.2 Types of test pieces

Test pieces used in fatigue testing may be divided into two categories, which will be designated coupons and components.

Coupon

The coupon is a test piece of simple shape, frequently standardised, of small size, and prepared carefully and with good surface finish. The coupon may be unnotched or notched. The purpose of the simplification is to make it less expensive, but moreover to reduce the variability of the product and to keep different influential factors under control. Test pieces of this type are usually intended for testing the material under varying conditions and to study the effect of various factors on its fatigue life.

The unnotched coupon should be designed in such a way that its test portion is subjected to a uniform or smoothly varying stress over the test length, of such a magnitude that premature failure does not develop at unintentional stress raisers in the grip or transition portion.

The notched coupons are used for studying the notch sensitivity of materials and for simulating stress raisers appearing in actual components. Maximum stresses within a notched specimen are determined by calculating nominal stresses in the same way as for unnotched specimens and correcting these values by means of a stress concentration factor K_t. This theoretical stress concentration factor K_t is defined as the ratio of the local peak stress to the nominal stress at the cross-section.

Due to economic and time constraints it must be recognized that only a limited amount of testing can be tolerated in a helicopter development programme, therefore, coupon test results on the same material to that on the helicopter are used to assist in defining the S-N curve shape through the actual helicopter component test results.

Component

The component signifies any machine part, actual structure, machine and assembly, including scale models and elements simulating actual components. The latter two are designed and tested in order to reduce the cost of testing large and complicated structures and include bolted, riveted, welded and bonded joints, screw connections, loaded holes and lugs.

It is common practice in the helicopter industry to group components of the helicopter with respect to types of fatigue loading and the following is suggested:

- dynamic components,
- gear-boxes,
- airframe.

Dynamic components comprise the rotor blades, hubs, shafts and controls of both the main and tail rotor systems as well as the supporting structure for rotors, transmissions and engines, and the drive shafts.

For development purposes, prototype components are subjected to a searching series of fatigue tests. The aim is to establish the potential fatigue lives of the parts. In these early stages of testing, it is normal to define a loading programme in terms of the primary dynamic load, which may be: control load, main rotor shaft bending moment or any other primary parameter which is easily measured in flight and in the laboratory or which may even result from calculations assuming simplified structures and using basic mechanical knowledge.

The mode of testing may vary, dependent upon type of loading and complexity of the component. A realistic fatigue strength would come from a simple multi-level, repetitive load programme, which should take mean load variation into account. If the load pattern is sufficiently simple, a constant amplitude type of loading may be used. During this phase, alternative design studies are often tested for comparison.

In the fatigue substantiation phase, the component must be an exact replica of the part that is flown on the helicopter. Usually it is selected from the production lines at random and must have suitable attaching parts to simulate its installation on the helicopter. The test must be designed to achieve representative stress distribution in the components, with load applied and reacted through actual mating parts to verify that boundary conditions such as fixity and clamping stiffness are representative. The information required from these tests is an estimate of the average fatigue strength, usually stated in the form of an S-N curve, and also some confirmation of the degree of scatter of strength about the average value.

As much as possible, or practical, loads are applied to the full-scale part to represent the load application experienced by the part on the helicopter. Due to high load frequencies experienced by the dynamic components of a helicopter, fatigue tests at higher load levels are carried out in order to reveal modes of failure within a reasonable testing time. Obviously, the failure mode is significant in the selection of the S-N curve and therefore it is a considerable advantage to aim for failure of the part rather than a run-out.

Simulation of oscillatory flight test loads in fatigue test machines is often not an easy task. For instance, simulation of rotor forces presents problems which may cause overloading in one area of the rotor blade and loads that are too low in another place. For this reason full-scale fatigue tests are conducted with the root end and the aerofoil section separately. Phasing and frequency simulation of loads must be carefully considered.

If an assembly of components is tested, it may be necessary, in some cases, to replace the weakest components by dummy members in order to test the stronger ones and to collect test data on each component.

Fatigue tests on a component with different materials, e.g. elastomerics in metal parts, may present unusual situations. Difficulties may also arise in applying environmental factors, such as temperature and moisture in composite parts. In other cases, accelerated tests may not be practical because of overheating, but the general principles in establishing fatigue strength for these materials are similar to those of conventional materials.

It is common practice in the helicopter industry to test from four to six specimens, and choose one load level estimated to yield the magnitude of 10^7 cycles. The other specimens are tested to failure at various load levels.

If the measured loads are very low in comparison with the endurance limit, then very few specimens are required.

For economic reasons it is usually not possible to test a sufficient number of components to obtain a high level of confidence in these results, therefore the full-scale data are used essentially to establish only the mean location of the S-N curve and information about S-N curve shape and scatter are obtained from tests on a large number of coupons.

Gear-boxes comprise gear trains, gear teeth, bearings, freewheels, and the gear-box casing itself. Usually two basic types of fatigue tests are performed:

- component tests in standard testing machines,
- bench tests in special purpose rigs.

The component fatigue tests can be seen as being equivalent to those previously described for general dynamic components, and they will be carried out, e.g. on parts which are not adequately covered by the bench tests or on parts for comparative tests of gear material. However portions of the gear-box casing, where the supporting structure and the control jacks are attached, may also be fatigue evaluated in component tests.

The bench test of a gear-box is centred on the testing of a complete gear-box rotating under a spectrum of torque in transmission closed-loop or power-absorption test stands, which have the capability of applying the correct power-torque-speed relationships. Fatigue loading on gear teeth is in the form of a pulsed load acting once per gear wheel rotation. The magnitude of this load is dependent on the torque being transmitted. The test will usually take the form of an overload or factored torque test with the gear-box running at normal speeds. The test requirements can be up to 140% of the maximum expected input power for 10 million cycles on the slowest operating component.

In order to obtain representative casing deflections, full representation of external loadings should be applied during the test.

As direct fatigue design data will not be established during this bench testing, it is not intended to describe it in any more detail.

The airframe of a modern helicopter is built on the principles in current use on fixed wing aircraft. This construction has a certain amount of inherent failsafe characteristics and may be subject to damage tolerant methods of assessment.

As it is necessary to establish that the airframe will have a satisfactory economic life without major repair and an extremely remote probability of a catastrophic fatigue

failure, fatigue tests on a full-scale airframe are conducted mainly for fail-safe strength evaluation. In general, however, it is most difficult to apply a realistic loading to the helicopter, composed of low frequency manoeuvre loadings with superimposed high frequency vibrations.

Major parts of the airframe, e.g. tail plane, are usually subject to a realistic programme of manoeuvre loads to establish the lives at which cracking occurs, the locations of such cracks, their detectability and the rates of crack propagation. There are other parts of the airframe which have single load paths and must therefore be treated as critical dynamic components. These parts are the attaching points of main and tail rotor, of engines, of hydraulic systems and of control jacks.

Concluding the information on fatigue testing, the following statements can be made:

- Without doubt, the best life predictions would result from tests with actual components and true service loads under realistic environmental conditions. On the other hand, realistic loadings for helcopter parts generally contain a high number of cycles with low and medium loads and only a few reversals with high loads. So, in substantiating requested lifetimes of some thousand hours, intolerably long testing time would be necessary. Therefore constant amplitude testing is mostly used to evaluate fatigue strength.

- To extract the maximum knowledge from the component, all failed specimens should be studied by design and structures supervision and subjected to an evaluation by the materials laboratory.

4.1.2 FATIGUE RESULTS

The main purpose of fatigue testing is the experimental establishment of the relation between the magnitude of the applied load, stress or strain, and the fatigue life for the coupon or component under test. The fatigue results can be condensed into a graph or an analytical expression for engineering purposes.

A number of other significant factors, e.g. mean stress or notch factor, are always involved in fatigue testing and must be recorded on the graphs so that they can be interpreted correctly.

Fatigue tests are conducted under a variety of loading conditions that include a tensile or compressive mean stress with a superimposed sinusoidal and the like alternating stress. The load may be applied in several ways, including axial loading, rotating bending, plate bending, torsional loading, and in various combinations of the above.

Fatigue failures usually originate from the surface of the specimen. Surface condition and geometry; as for example smoothness or residual stresses, are influenced, e.g. by manufacturing processes, surface treatment, and service usage.

An inherent property of the fatigue tested specimens is that the results show variability, which is always observed when a number of identical tests are performed. This scatter is much too large to be neglected. In order to keep the probability of catastrophic failure extremely remote, it is necessary to apply a reduction factor. In the helicopter industry it is general practice to use a reduction on load, so that with reasonable confidence it can be stated that a large portion of components will fail only above the reduced or working S-N curve.

4.1.2.1 S-N curve shapes

While the stress-strain diagram is used to interpret static properties of a material, the S-N curve, where S is related to the applied load and N is the number of cycles, is used to interpret fatigue properties.

The fatigue test data obtained on a group of identically prepared specimens, all tested in the same environment at one stress ratio R, with one or more specimens tested at each of several stress levels, can be presented in an S-N diagram as shown in Fig. 41.2. The graph upon which the data are plotted has the maximum stress S_{max} or alternating stress S_a as ordinate on any standard scale and the number of cycles to failure N as abscissa on a logarithmic scale, and is therefore called semi-logarithmic.

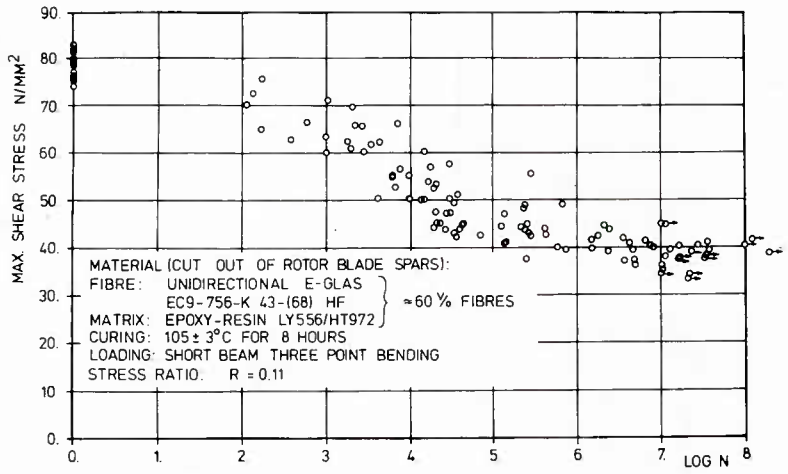

Fig. 41.2 Shear fatigue S-N diagram of glass fibre composites

Run-out points are typically considered part of the population and are displayed at the number of cycles endured with an arrow attached. If a run-out was tested at a reasonable load level, e.g. within the scatter-band or just below the bottom of scatter of failure points, the nonfailure point would normally be treated as a failure in deriving the S-N curve.

From numerous fatigue test results, presented in S-N diagrams as shown in Fig. 41.2, it can be seen that an S-N curve which is practically horizontal for small and large values of N and which has a point of inflexion at some thousands of load cycles would represent the relation between load and life as found in fatigue tests.

To overcome the well known limitations of the graphical methods for determining S-N curves, several attempts have been made to find general mathematical laws for the relation between load and life, or at least to propose analytical expressions which may be fitted to the S-N data with sufficient accuracy.

The requirements of such an equation depend on the fact that it is not intended to reveal any physical laws regarding the properties of the specimen tested but that it is wanted for design purpose. Consequently, it must be as simple to use as it is consistent with its practical purpose. Any accuracy can be obtained by using an equation containing a sufficient number of parameters. But every increase in this number makes the calculations more tedious and it is therefore a fair demand that the number of parameters should be as small as is consistent with the requirements. The parameters of the S-N curve may be arbitrarily chosen, but it must be regarded as an advantage if the parameters have some physical meaning, particularly if they can be determined by more rapid methods than the fatigue test, e.g. the static strength S_u.

For a representation of the whole field from N = 1 (static strength S_u) to N = ∞ (endurance limit S_∞) at least four parameters are needed and the following formula, proposed by WEIBULL (Ref. 41.5), is used:

$$S = S_\infty + (S_u - S_\infty) \cdot e^{-\alpha (\log N)^{\beta}} \qquad (41.1)$$

Best estimates of the unknown constants S_u, S_∞, α and β are obtained in fitting the Equation 41.1 of the S-N curve to the fatigue life data by applying the method of least squares. As Equation 41.1 is nonlinear, a nonlinear regression algorithm must be used.

Due to the fact that the S-N curve is practically horizontal for small and large values of N, the regression of S on log N is performed, i.e. the sum of squared deviations in the vertical direction between the test data points and the best fitting curve is least.

The principle of least squares fit is shown in Figure 41.3.

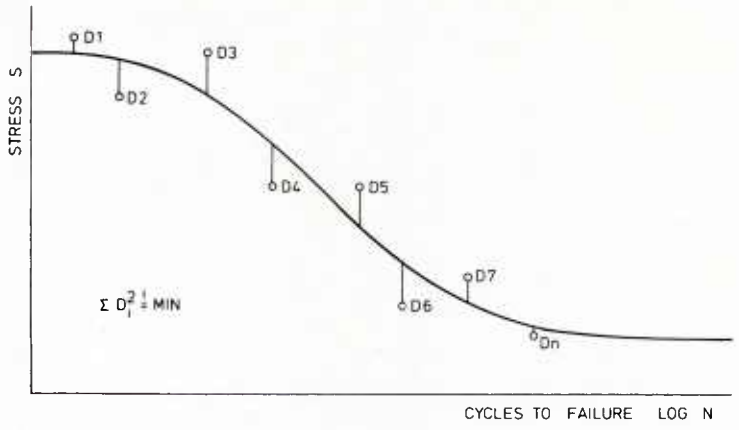

Fig. 41.3 Least squares fit

Applying the nonlinear regression analysis on the fatigue life data shown in Figure 41.2 leads to the following mean S-N curve:

$$S = 39 + 40 \cdot e^{-0.022\ (\log N)^{2.75}} \quad N/mm^2 \qquad (41.2)$$

For engineering judgment the S-N curve according to Equation 41.2 is plotted together with the corresponding fatigue test data in Figure 41.4.

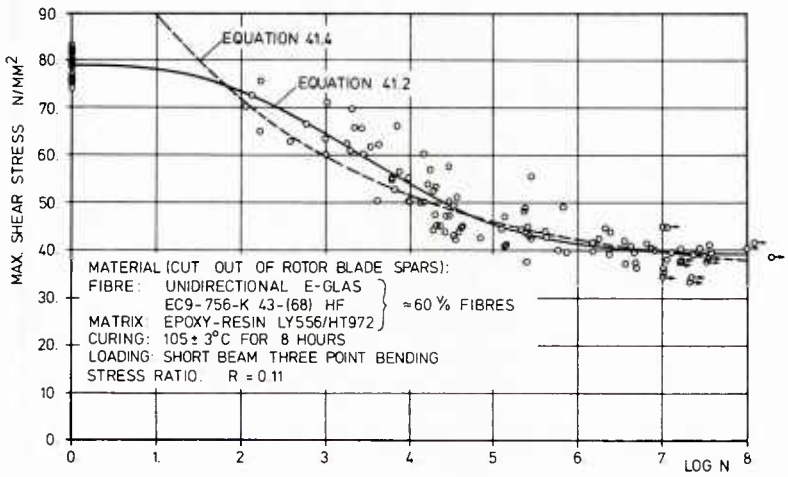

Fig. 41.4 Shear fatigue S-N curves of glass fibre composite

The minimum required fatigue life for all dynamic components of modern helicopters is at least 5000 hours, leading to minimum load cycles of some 10^4 even for such components which are loaded by start-stop cycles mainly. For representing the S-N curve in the range $N \geq 10^5$, a simplified formula can be drawn from Equation 41.1 by setting $\beta = 1$ which leaves:

$$S = S_\infty + B/N^x \qquad (41.3)$$

Due to the simplicity of Equation 41.3 this formula can be found in all companies of the helicopter community.

For comparison, the three parameter S-N curve from Equation 41.3 is also plotted in Figure 41.4. Here a material constant of $x = 1/6$ for fibre composites was used and the parameters S_∞ and B were found by regression analysis, using the fatigue data with $N \geq 10^5$ cycles, leading to the following equation:

$$S = 34 + 116 / N^{1/6} \quad N/mm^2 \qquad (41.4)$$

High cycle fatigue data ($N \geq 10^5$) can generally be represented with sufficient accuracy by using the following material constants for x in Equation 41.3:

Material	x
Steel	1/2
Light alloys	1/3
Fibre composites	1/6

Table 41.1 S-N curve parameter x

If sufficient fatigue test data are available, i.e. at least six to ten specimens evenly distributed between N = 1 and some 10^6 cycles, a best fit curve based on Equation 41.1 can be drawn through the test points, paying no attention to predetermined material curve shapes. The advantage of this approach is that it treats the test data from a purely statistical aspect and hence results in a mean curve with the lowest data scatter. Since the number of full scale component specimens, necessary to establish this S-N relationship, generally cannot be tested within the constraints of time and cost, characteristic curve shapes or curve shape parameters, as e.g. shown in Table 41.1, for different materials have been developed from small specimen data. This information can be used to establish the complete S-N curve from limited full scale test data.

This methodology is shown for the pitch link, used in the hypothetical fatigue life problem of the American Helicopter Society (Ref. 41.6), with the fatigue data as shown in Table 41.2.

Id-No.	Peak to Peak osc.load (lb)	Mean load (lb)	Max. load (lb)	Stress Ratio R	Cycles to Failure N	Remarks
1	5800	450	3350	- 0.731	1.32×10^5	All failures occurred in the threaded section of the steel end fitting!
2	5000	450	2950	- 0.695	1.73×10^5	
3	4500	450	2700	- 0.667	7.49×10^5	
4	4400	450	2650	- 0.660	2.48×10^6	
5	4100	450	2500	- 0.640	3.34×10^6	
6	3800	450	2350	- 0.617	7.31×10^6	

Table 41.2 Fatigue test results on pitch link

Although the tests have been conducted with different stress ratios, this variation is small and will therefore be neglected here.

As all specimens failed at numbers of cycles $N > 10^5$ and no test data between N = 1 and 10^5 are available, the simplified S-N curve shape according to Equation 41.3 is used. Failures occurred in the steel end fitting, therefore the parameter x = 1/2 is chosen and a regression analysis must be carried out to establish the parameters S_∞ and B.

The sum of the squared deviations then is

$$f = \sum_{i=1}^{n} (S_i - S_\infty - B/N_i^{1/2})^2 \quad , \tag{41.5}$$

where the summation is taken over all the tested specimens n.

The values of S_∞ and B which minimise f have to satisfy the following normal equations

$$\partial f/\partial S_\infty = 0 = \sum_{i=1}^{n} S_i - n \cdot S_\infty - B \sum_{i=1}^{n} 1/N_i^{1/2} \tag{41.6}$$

$$\partial f/\partial B = 0 = \sum_{i=1}^{n} S_i/N_i^{1/2} - S_\infty \sum_{i=1}^{n} 1/N_i^{1/2} - B \sum_{i=1}^{n} 1/N_i \tag{41.7}$$

Using the fatigue test results from Table 41.2 the following S-N curve shape is found

$$F_{max} = 2317 + 330530/N^{1/2} \text{ lb} \tag{41.8}$$

which is plotted together with the fatigue test data in Figure 41.5 on an F_{max} -logN basis.

It is recognized that the curve shape according to Equation 41.8 becomes quite steep at low cycles and is not generally adequate for estimating damage in this region. Often, encountered failures in this range fall below the steeply rising curve. The high- and low-cycle range can be sufficiently represented by the four parameter S-N curve according to Equation 41.1. If one or two low-cycle fracture points are additionally available, the low-cycle portion of the mean curve will be established by a regression analysis completely based on fatigue test results. If there are no additional data points, as in the hypothetical pitch link example, and the static strength can be deduced from component description, a complete S-N curve between N = 1 and N = ∞ can be found by using the static strength and the high-cycle data points and matching the complete S-N curve as close as possible to the simplified S-N curve.

For the hypothetical pitch link the information was given that the critical area is the threaded section of the end fitting with a 0.5 inch diameter rod of 4340 steel, heat treated to 150 000 psi, and with 20 threads per inch. From MIL-S-8879 A a stress area of 0.151 in^2 is found, leading to an ultimate strength of 22650 lb.

Applying the nonlinear regression analysis the following mean S-N curve is found

$$F_{max}' = 2600 + (22650 - 2600) \cdot e^{-0.02\ (\log N)^{3.24}}\ lb \qquad (41.9)$$

which is also plotted in Figure 41.5.

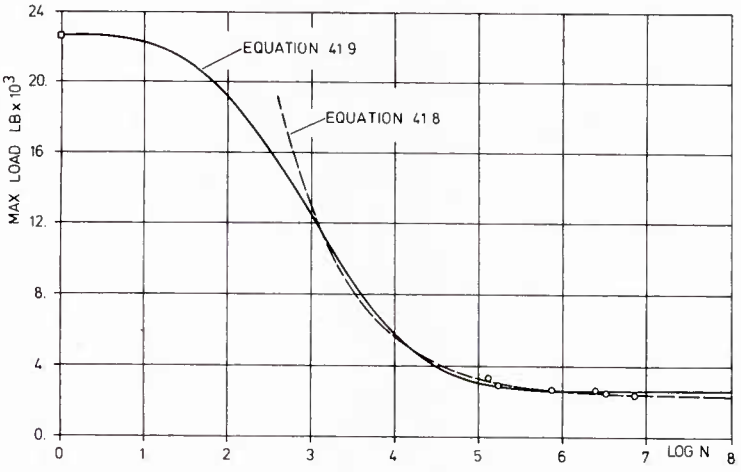

Fig. 41.5 Fatigue test data and S-N curves of a hypothetical pitch link

Test levels in terms of load rather than stress should be used for full-scale component specimens. However, it is important to bear in mind that the characteristic curve shapes or the curve shape parameters generally are derived from relevant small specimen data in terms of stress versus cycles to fracture. Fitting these shapes to load versus cycles data is only valid when stress is directly proportional to load and when similar failure modes occur. In many designs this is in fact the case, but in a number of cases, nonlinearity between stress and load affects the accuracy of this simplified load/cycles approach.

Nonlinear stress/load relationships may be found, e.g. when alternative load paths come into play, or when load is transferred due to distortion, or when load levels in excess of assembly preloads are applied (Ref. 41.7).

When more than one failure mode is involved, it will be necessary to take a good look at the physical factors. It is common practice to include all test data, but one has to be careful if fretting is involved in some of the test failures. There is a possibility that one mode of fracture especially exposed during accelerated fatigue testing may "mask" the existence of a second, more critical mode of fracture. The hidden mode will not be exposed, if tests at a low enough load level will not be conducted. Therefore test load levels must be selected which cause fracture of the specimens over a wide range of cycles.

Since only six full-scale specimens typify the usual fatigue test program, it will always be necessary to use S-N curve data from some other sources and to use actual data to define the ordinate position only.

4.1.2.2 Factors affecting fatigue strength

The S-N curve shape is known to be affected considerably by a number of factors such as material composition and heat treatment, type of loading as well as size, shape, surface condition and environment of the test specimen. These factors must be kept constant if large variations in results are to be avoided or at least they must be known and specified if the observed results are to be interpreted properly.

Material

Generally a material is sufficiently well defined by its chemical composition and heat treatment. The composition directly affects the fatigue properties of a material, since the nature and strength of the chemical bonds between the atoms govern the potential range over which the strength and ductility can be varied. Many attempts have been made to correlate tensile strength, hardness and ductility with fatigue properties but any such relationships must be considered quite approximate and applicable to only a very limited range of conditions. In Reference 41.8 the following correlation formulae between the ultimate tensile strength S_u of steel and the endurance limit in rotating-bending $S_{\infty rb}$ was found, not taking into account effects as, e.g. corrosion and notches:

For normalised carbon steels (S_u = 340 - 700 N/mm^2)

$$S_{\infty rb} = 0.454\ S_u + 8 \quad \text{N/mm}^2 \tag{41.10}$$

For heat-treated carbon steels (S_u = 400 - 1300 N/mm^2)

$$S_{\infty rb} = 0.515\ S_u - 24 \quad \text{N/mm}^2 \tag{41.11}$$

For heat-treated alloy steels (S_u = 800 - 1300 N/mm^2)

$$S_{\infty rb} = 0.383\ S_u + 94 \quad \text{N/mm}^2 \tag{41.12}$$

For stainless steels (S_u = 500 - 1300 N/mm^2)

$$S_{\infty rb} = 0.484\ S_u \tag{41.13}$$

A less definite correlation between $S_{\infty rb}$ and S_u is given for aluminium-alloys:

For low and middle strength Al-alloys ($S_u \leq 350$ N/mm^2)

$$S_{\infty rb} = 0.4\ S_u \tag{41.14}$$

For high strength Al-alloys ($S_u \geq 350$ N/mm^2)

$$S_{\infty rb} = 140 \quad \text{N/mm}^2$$

For magnesium-alloy the following correlation is given:

$$S_{\infty rb} = (0.30 - 0.50)\ S_u \leq 150 \quad \text{N/mm}^2 \tag{41.15}$$

For titanium-alloy TiAl6V4, annealed, the following value can be found in handbooks:

$$S_{\infty rb} = 550 \quad \text{N/mm}^2$$

For unidirectional fibre composites with 60% fibre volume content the following endurance limits have been established at MBB:

Bending fatigue of glass fibre composite (E-glass):

$$S_{\infty b} = 250 \pm 250 \quad \text{N/mm}^2$$

Shear fatigue of glass fibre composite (interlaminar shear):

$$S_{\infty ILS} = 22 \pm 17 \quad \text{N/mm}^2$$

Bending fatigue of carbon fibre composite (T300):

$$S_b = 250 \pm 250 \text{ N/mm}^2$$

Shear fatigue of carbon fibre composite (interlaminar shear):

$$S_{ILS} = 15 \pm 15 \text{ N/mm}^2$$

There are features of a material, not reflected by the ultimate tensile strength, that may have a large influence on its fatigue resistance.

Most difficulties in relating fatigue properties to the usual mechanical properties are encountered in the long life region with metals that have low ductilities. This happens because fatigue is governed by the "weakest link" in the material, where crack-initiation starts. Local zones of weakness can be flaws between grains, inclusions, and inhomogeneities. It is impractical to completely eliminate such defects or to completely describe their quantitative influence when they govern fatigue resistance. The state of the art is such that it is necessary to determine this quantitative influence by fatigue tests involving the materials, processes, and shapes in question (Ref. 41.9).

Loading

The simplest type of stressing is obtained by subjecting the specimen to a reversed, tension-compression load. The stress within a smooth, unnotched specimen, is then uni-axial and uniformly distributed over the volume.

A very easy and therefore widely used test for determining the fatigue properties at completely reversed stress cycles is the rotating-bending test. The state of stress (normal stress) is the same as in reversed tension-compression but the stress distribution is different. Since most fatigue failures originate at the surface or slightly below, little difference between rotating-bending and axial tests generally should be expected and may be taken as the reference to which the other types may be compared.

In alternating bending the state of stress is the same as that obtained by axial load but the stress distribution is different. If these two types of stressing are compared on the basis of the maximum stress in the specimens, it is generally found that the fatigue strength is higher in bending than under axial load.

The torsion test provides the easiest way of producing a biaxial state of stress. The stress distribution is identical with that obtained in a rotating-bending test, and for this reason the comparison between the results from these two types of test offers an excellent way of studying the influence of the normal complementary stress.

Based on the maximum-distortion-energy theory the following relationship is found between the endurance limits of alternating torsion and rotating-bending:

$$S_{\infty at} = S_{\infty rb}/\sqrt{3} \qquad (41.16)$$

Components of circular cross section often are subjected to combined bending and torsion. In Reference 41.10 the following equation for design of parts subject to combined stresses can be found:

$$\left(\frac{S_t}{S_{\infty at}}\right)^2 + \left(\frac{S_b}{S_{\infty rb}}\right)^2 \cdot \left(\frac{S_{\infty rb}}{S_{\infty at}} - 1\right) + \left(\frac{S_b}{S_{\infty rb}}\right) \cdot \left(2 - \frac{S_{\infty rb}}{S_{\infty at}}\right) = 1 \qquad (41.17)$$

Equation 41.17 is an empirically derived equation of an elliptical arc which best fits test data.

In the above equation, the alternating stresses S_b and S_t are nominal values of stress; they do not include the stress concentration factor. To establish the endurance limit in bending, divide the endurance limit for $K_t = 1$ by the appropriate stress concentration factor for the particular type of concentration. Having thus determined the bending endurance limit, the torsional endurance limit is determined by Equation 41.16. Thus, with both bending and torsional endurance limits established, the elliptical arc equation can be applied and the margin of safety determined graphically as shown in Figure 41.6.

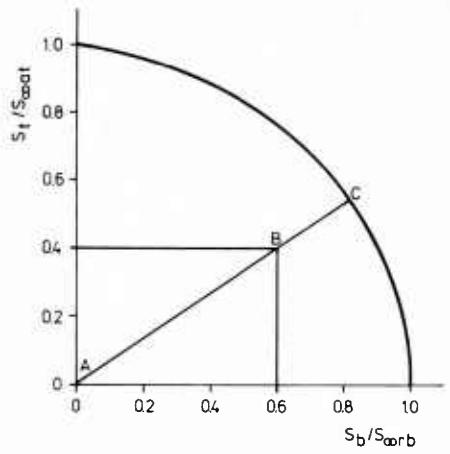

EXAMPLE:

$\frac{S_t}{S_{\infty at}} = 0.4\,; \quad \frac{S_b}{S_{\infty rb}} = 0.6$

$M.S. = \frac{AC}{AB} - 1 = \frac{9.8}{7.2} - 1 = 0.36$

Figure 41.6 Fatigue failure of a circular cross section under combined bending and torsion

If the part to be analyzed is not circular, then the following procedure is recommended in Reference 41.10.

Fatigue under combined normal (bending or tension) and torsional stresses:

$$M.S. = S_{\infty rb}/\sqrt{S_b^2 + 3\,S_t^2} - 1 \qquad (41.18)$$

Geometry

Geometry factors which influence fatigue resistance include the overall size and shape as well as the size and shape of notches.

The size effect has several causes, one being the corresponding change of the stress gradient with the specimen diameter. In larger shafts the stresses-decrease from maximum on the surface to zero at the neutral line is slower and the material layer subjected to high stresses is thicker. This results in a decrease of the endurance limit with increasing specimen diameter, but should not exceed 20%.

The endurance limit of specimens with square or rectangular cross-section is reported to be somewhat smaller than in the case of a standard circular cross-section, because of the stronger effect of the surface at the corners.

The endurance limit of a specimen cut transversely to the rolling or forging direction is smaller than for a longitudinal specimen. The anisotropy of the fatigue properties is connected with the longitudinal orientation of inclusions and other microstructure defects and is more evident for high strength and brittle materials.

As fatigue fractures initiate at some location where the peak stress exceeds the fatigue strength of the material for the stress ratio and number of cycles under consideration, the peak stresses govern the life of the assembly. When the peak stress is within the elastic range and when for the geometry of the part the theoretical stress concentration factor has been established by analytical or experimental methods, it is relatively easy to calculate the peak stress. Stress concentration is always present in cases of cross-sectional changes such as notches, grooves, fillets, holes, corners, undercuts, cut outs, etc., but it is also found in unsymmetrical and eccentrically loaded parts that must necessarily bend with each application of load. In some cases two or more stress concentration features are superimposed, for example, when fabrication marks are superimposed on holes or re-entrant corners; punched rivet holes with rough surface on the inside and lubrication holes in highly stressed areas are other examples.

In many cases the computed peak stresses are above the elastic range and some plastic action takes place on the first cycle, influencing the actual fatigue strength. For this reason the fatigue notch factor K_f has been introduced, which is usually less than, but never greater than K_t. K_f is defined as the ratio of the fatigue strength of a smooth specimen to the fatigue strength of the notched specimen, both strengths taken at the same number of cycles. If K_f is not known, K_t may be used for analysis, but this may be considerably conservative. On components not subject to fretting, K_f is rarely greater than 3, whereas fretting may create a higher K_f factor. Notch sensitivity is not a unique property of a particular material but varies principally with type and severity of notch, state of stress, size of specimen, and grain size in the region of the notch. Notch sensitivity is defined as

$$q = \frac{K_f - 1}{K_t - 1} \qquad (41.19)$$

q = 0 indicates a material unaffected by a notch, while q = 1 indicates an actual fatigue strength reduction equal to the calculated theoretical factor K_t.

From Equation 41.19 follows for the fatigue notch factor K_f

$$K_f = 1 + (K_t - 1) \cdot q \ , \qquad (41.20)$$

where the notch sensitivity factor q may be estimated from the following equation (Ref. 41.8):

$$q = 1/(1 + \sqrt{A/R}) \qquad (41.21)$$

with A = Material constant having the dimension of length and depending upon strength and ductility (NEUBER constant)
R = Radius of the notch root.

Surface finish has a marked influence on fatigue strength of smooth specimens; the smoother the surface, the higher the endurance limit of the specimen. In the presence of all the usual stress raisers such as rivet holes, welds, and re-entrant corners, any beneficial effects from extreme care in surface finish and freedom from minor blemishes are completely overshadowed. In many cases, with different finishes intersecting S-N curves have been observed.

Residual Stresses

Residual stresses have a similar effect on the fatigue behaviour of materials as do mechanically imposed mean stresses of the same magnitude. Thus, the significant residual stresses are beneficial if compressive and detrimental if tensile particularly in materials that have been hardened by working or by heat treatment.

Near the endurance limit the residual stresses remain practically unchanged by the fatigue loading. At stresses above the endurance limit, residual stresses may relax as an accompaniment of the fatigue process, this effect being greater in materials that have been annealed or softened and at stresses well above the endurance limit.

A very effective method of generating compressive residual stresses in the surface layers is cold working, by means of shot peening, localized cold rolling, hammering, hole calibration etc. In all these cases, cold working generates in the surface layers high compressive residual stresses, which are in equilibrium with low tensile residual stresses distributed in the large cross-section below the cold worked layer. There is no question of the beneficial effects of such treatments when properly carried out, but care should always be taken to avoid an excessive amount of such localized cold working. If the operation had been carried too far, incipient fractures may result. Another commonly used technological means, which increases surface hardness and generates strong compressive residual stresses in the steel surface layer, is carburizing or nitriding.

Chromium or nickel plating results in reduced fatigue strength of quenched steel parts, because of detrimental residual tensile stresses in the surface layer. Similarly aircraft Alclad sheets have inferior fatigue properties than similar unclad sheets.

Heat treated steel parts with nonmachined surfaces after thermal treatment contain a layer decarburized during the heat treatment, which has lower microhardness than the core and is subjected to detrimental tensile residual stresses. A very effective means of overcoming the effect of decarburizing are all methods of cold working.

Welding also generates detrimental tensile residual stresses, and this is one of the reasons why welded joints have a low fatigue strength. However, it is known that machining of the welds improves the fatigue strength of the joint.

It must not be forgotten that most metal products have some degree of residual stresses over which the designer has no control. These initial residual stresses come about by virtue of operations performed by the material producer. Each subsequent operation merely modifies the residual stresses already present so that without a special investigation it is impossible to evaluate accurately the final residual stress resulting after any specific operation performed on a given piece of metal.

Environment

The environment is defined by the temperature and the surrounding medium, which may consist of inert or chemically aggressive gases or liquids.

A particular type of environmental effects is obtained by fretting corrosion. Radiation may in some cases be of influence; for example, plastics and rubber may be affected by sunlight or heat radiation.

The tendency for practically all materials at room temperature is that the fatigue strength declines with increasing temperature. The slope of the curve relating fatigue strength to temperature is exceptionally large for titanium and aluminium up to 400°C.

In general, fatigue acting jointly with corrosion behaves as an intensified form of fatigue.

Fretting corrosion is a frequent occurrence in engineering practice, when two surfaces touch and there is relative motion. A simple example of fretting is the case of a cyclically loaded bolt in a hole. The part will fret at the hole and its allowable stress is reduced. If the hole is opened up and a bushing pressed in, it might seem that the fretting should only occur between the bolt and the bushing. This is not the case. Small elastic deflections will still permit relative motion between the bushing and the part, hence, fretting will occur. It can be stated that the degree of fretting is less and the fatigue strength is usually higher with the bushing. The degree of improvement, if any, depends upon the material, size, interference fit, and load conditions.

4.1.2.3 The effect of mean load on fatigue strength

Many helicopter components are subjected to mean loads with alternating loads superimposed upon them. Thus the mean stress-alternating stress relation is important. Fatigue test data are usually plotted with alternating stress as ordinate and mean stress as abscissa.

Such diagrams indicate that the allowable alternating stress decreases with increasing tensile mean stress.

Owing to the infinity of combinations of mean and alternating stress and the enormous amount of experimental work required to obtain fatigue behaviour over a comprehensive range of alternating and mean stress values, various equations have been proposed to predict generalized $S_a - S_m$ behaviour. The well known expressions devised by GOODMAN , GERBER, and SODERBERG were intended to represent the endurance limit as a function of mean stress; of these the GERBER parabola and the modified GOODMAN straight - line relationships are probably the most widely used and may be summarised by the following equation:

$$S_{a\infty m} = S_{a\infty o} \left[1 - \left(\frac{S_m}{S_u} \right)^c \right] \qquad (41.22)$$

where:

$S_{a\infty m}$ = stress amplitude of the endurance limit at mean stress $S_m \neq 0$

$S_{a\infty o}$ = stress amplitude of the endurance limit at mean stress $S_m = 0$

$c = 1$ for the modified GOODMAN line

$c = 2$ for the GERBER parabola

Other degrees of convexity may be obtained by using other values of c.

The modified GOODMAN diagram, as shown in Figure 41.7, is commonly used in industry and is constructed from laboratory test data for a particular part. The straight line is conservative for most materials and surface conditions because it is drawn between the ultimate stress for the material and the alternating stress endurance limit for a zero mean stress.

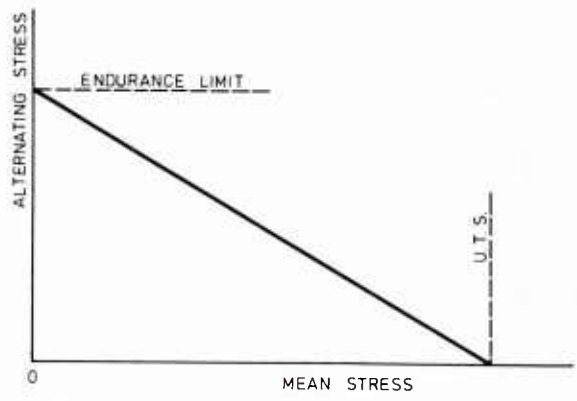

Fig. 41.7 Modified GOODMAN diagram

With Equation 41.22 it is possible to compute a value of the endurance limit at any mean stress if at least one endurance limit is available and the value c is known. However, any inherent errors in the endurance limit at a given mean stress result in proportionately larger errors when used to compute endurance limits at lower values of mean stress; conversely, proportionately smaller errors are obtained when used to compute values at higher mean stresses.

Thus, in order not to introduce additional errors in the predictions obtained by using Equation 41.22 requires that a value of the endurance limit be available at the lowest value of mean stress of the range of mean stresses in which predictions are to be made.

Since there are generally more data on fatigue at various mean stresses for unnotched than notched specimens, it is very useful to have a method for predicting the effect of mean stress for notched specimens from unnotched data. The simplest approach, when considering Equation 41.22, is to divide the ordinate and abscissa by the theoretical stress concentration factor K_t, which leads to the following equation (Ref. 41.11)

$$S_{a\infty mK_t} = \frac{S_{a\infty o}}{K_t} \left[1 - \left(\frac{K_t \cdot S_m}{S_u}\right)^c\right] \qquad (41.23)$$

$$\text{with } K_t \cdot S_m \leq S_u$$

In order to analytically evaluate the effects of mean load or stress ratio on fatigue, based on Equation 41.22 but without a predetermined value of c, it is necessary that data for a particular material and notch condition be available for at least three stress ratios.

In many cases the GOODMAN straight-line relationship can be regarded as sufficient for the mean stress correction. If the fatigue data are based on constant stress ratios instead of constant mean stress, the GOODMAN straight-line can be written as

$$S_{a\infty m} = S_{a\infty o} / \left[1 + \frac{S_{a\infty o}}{S_u} \cdot \frac{1 + R}{1 - R}\right] \qquad (41.24)$$

To compute a value of the endurance limit at any stress ratio R_2, if the endurance limit at a stress ratio R_1 is available, the following equation can be derived from Equation 41.24:

$$S_{a\infty R_2} = S_{a\infty R_1} / \left[1 + \frac{S_{a\infty R_1}}{S_u} \left(\frac{1 + R_2}{1 - R_2} - \frac{1 + R_1}{1 - R_1}\right)\right] \qquad (41.25)$$

4.1.2.4 Reduction factors

To obtain representative results from fatigue testing, a large number of test specimens is desirable in establishing each S-N curve.

While the more the better is the obvious desire of the fatigue evaluation engineer, in practice the number of specimens is always limited, as most manufacturers cannot afford the cost and time necessary to obtain such accuracy. Therefore the mean fatigue strength of the component is defined with a relatively small number of specimens by fitting an established S-N curve shape to the data or by conducting a regression analysis as shown in Section 4.1.2.1.

In order to account for normal scatter in fatigue, the mean curve should be reduced by an appropriate reduction factor to define a working S-N curve or to establish an S-N-P diagram. This factor should be based on the type of material being tested, past service experience with the material, and type of design (Ref. 41.12). It should include consideration of the number of specimens tested, the variability of the fatigue results and should be selected to assure that the probability of failure is extremely remote. Where new materials or designs are being evaluated, it is recommended that a larger reduction factor be used until additional test data justifying a change are available.

In helicopter industry, the reduction factor normally is applied to the stress axis, but in the region $N < 10^5$ cycles life reduction factors sometimes are used by the companies. These factors are based on the number of specimens, similar to the method used in the fixed wing industry.

Although significant differences in the application of reduction factors exist between the helicopter manufacturers, the following common procedure can be found:

- It is assumed that the distribution of deviations in fatigue strength from the average S-N curve is independent of the number of cycles, which is the assumption of homoscedasticity (Ref. 41.13).

- All failure points, used to derive the mean S-N curve, are projected to a given number of cycles through the use of the appropriately shaped S-N curve, as shown in Figure 41.8.

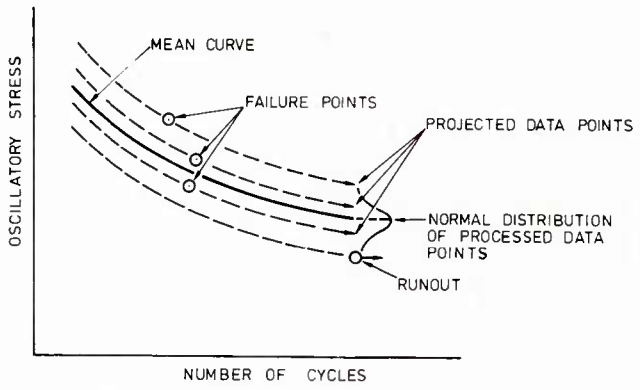

Fig. 41.8 Extrapolation of data for statistical analysis

- The extrapolation is usually carried out to 10 million cycles for ferrous materials and 50 million cycles for nonferrous materials. In some cases extrapolation to 100 million cycles can be found. Due to the above assumption, the extrapolation can be made to any number of cycles convenient, without changing the results. When a four parameter S-N curve according to Equation 41.1 is used, the failure points may well be projected to N = 1.

- From the extrapolated data points the mean and standard deviation are calculated for the log normal probability distribution function according to the following equations:

$$\log \bar{S} = \frac{\Sigma(\log S_i)}{n} \tag{41.26}$$

$$\sigma = \sqrt{\frac{\Sigma(\log S_i - \log \bar{S})^2}{n-1}} \tag{41.27}$$

where:

$\bar{S}$ = mean fatigue strength at extrapolated number of cycles

S_i = fatigue strength of individual specimen at extrapolated number of cycles

n = number of specimens

σ = standard deviation

Some manufacturers assume a normal distribution of the fatigue strength with the following equations for $\bar{S}$ and σ:

$$\bar{S} = \frac{\Sigma S_i}{n} \tag{41.28}$$

$$\sigma = \sqrt{\frac{\Sigma(S_i - \bar{S})^2}{n-1}} \tag{41.29}$$

and the coefficient of variation

$$V = \sigma/\bar{S} \tag{41.30}$$

- As the sample size of most component fatigue tests is totally inadequate to provide a meaningful measure of population variability, some companies use reduction factors based on coupon data.
  Coefficients of variation of .05 for steels and .07 for aluminium are reported in Reference 41.14 for coupon data. According to the approximate relationship of Equation 41.45 these coefficients of variation correspond to standard deviations of .022 for steels and .032 for aluminium. At MBB a minimum standard deviation of .025 has been assessed for all materials.
  Sometimes the coupon variability is increased to account for variations in stress concentration factors, steady stress and other variables that are expected to influence the full-scale population variation.
  In Reference 41.15 a standard deviation on rotor blades has been assessed to approximately .045 for steels and .06 for light alloys, and these values have been extended to all the aircraft parts.

- Once the proper standard deviation or coefficient of variation is selected for the type of specimen under consideration, the variation of the mean fatigue strength can be determined.

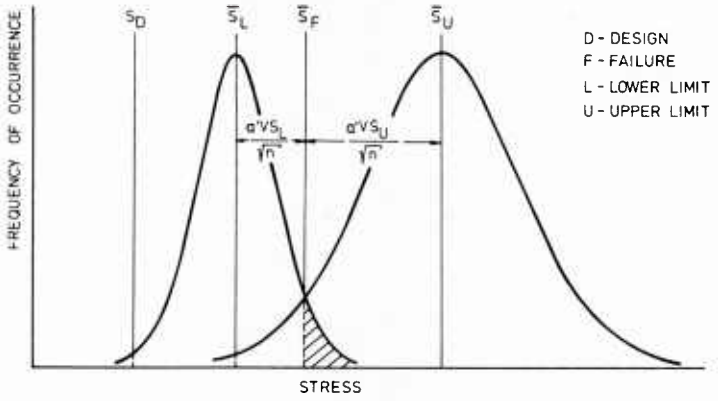

Fig. 41.9 Variation of the mean (Ref. 41.16)

Figure 41.9 depicts the variation that can exist for the mean fatigue strength $\bar{S}_F$, when only limited tests are available. A frequency distribution curve can be drawn so that P_C per cent of all specimens tested would fall below the mean fatigue strength. The actual mean corresponding to this distribution would lie at $\bar{S}_L$. A similar distribution can be drawn representing the upper limit conditions at $\bar{S}_u$. Analytical expressions representing these conditions are as follows:

For a log-normal distribution:

$$\log \bar{S}_L = \log \bar{S}_F - \frac{a'}{\sqrt{n}} \cdot \sigma_{Ln} \tag{41.31}$$

or

$$\log \frac{\bar{S}_F}{\bar{S}_L} = \frac{a'}{\sqrt{n}} \cdot \sigma_{Ln} \tag{41.32}$$

thus

$$\bar{S}_L/\bar{S}_F = \varepsilon^{-a'/\sqrt{n}} \tag{41.33}$$

where

$$\varepsilon = \text{antilog } \sigma_{Ln}$$

For a normal distribution:

$$\bar{S}_L = \bar{S}_F - \frac{a'}{\sqrt{n}} \cdot \sigma_n = \bar{S}_F - \frac{a'}{\sqrt{n}} \cdot V \cdot \bar{S}_L \tag{41.34}$$

thus

$$\bar{S}_L/\bar{S}_F = 1/(1 + \frac{a'}{\sqrt{n}} \cdot V) \tag{41.35}$$

The next item under consideration is the determination of the design fatigue limit S_D, which characterizes the working S-N curve for a given survival rate P_s.

For a log-normal distribution:

$$\log S_D = \log \bar{S}_L - a \cdot \sigma_{Ln} \tag{41.36}$$

or

$$\log \frac{\bar{S}_L}{S_D} = a \cdot \sigma_{Ln} \tag{41.37}$$

thus

$$S_D/\bar{S}_L = \varepsilon^{-a} \tag{41.38}$$

By substitution of $\bar{S}_L$ from Equation 41.33

$$S_D = \bar{S}_F \cdot \varepsilon^{-(a + a'/\sqrt{n})} \tag{41.39}$$

For a normal distribution:

$$S_D = \bar{S}_L - a \cdot \sigma_n \tag{41.40}$$

where $\sigma_n = V \cdot \bar{S}_L$

then $$S_D = \bar{S}_L \, (1 - aV) \tag{41.41}$$

By substitution of $\bar{S}_L$ from Equation 41.35

$$S_D = \bar{S}_F \cdot \frac{1 - aV}{1 + a'V/\sqrt{n}} \tag{41.42}$$

Statistical based reduction factors thus are defined as follows:

For log-normal distribution:

$$r_{Ln} = \varepsilon^{-(a + a'/\sqrt{n})} \tag{41.43}$$

For normal distribution:

$$r_n = \frac{1 - aV}{1 + a'V/\sqrt{n}} \tag{41.44}$$

Values of a' and a can be obtained from any statistics handbooks. Between the standard deviation σ_{Ln} and the coefficient of variation V the following approximate relationship can be used (Ref. 41.16):

$$\sigma_{Ln} = \log \left(\frac{1}{1 - V}\right) \tag{41.45}$$

- Reduction factors are mostly based on a survival rate of P_s = 99.9% and a confidence level of P_c = 95%, but a reduction of three standard deviations also can be found very often. However, a minimum reduction of 25% for aluminium and magnesium parts and 20% for steel and titanium parts often is used when these values exceed the three standard deviation values.
- When the number of test specimens is less than four, the following reduction factors are proposed similar to the method in Reference 41.17, if this results in a lower working curve:

number of test specimens	1	2	3
reduction factor	1/2	2/3	3/4

where the reduction factor is to be applied to the lowest test result.

Example

Using the results of the hypothetical pitch link, shown in Section 4.1.2.1, and projecting the failure points to N = 1, leads to the following equation to determine the strength of the individual specimens at N = 1:

$$S_{i\,(N=1)} = S_u \cdot S_i / [S_\infty + (S_u - S_\infty) \cdot e^{-\alpha (\log N_i)^{\beta}}] \qquad (41.46)$$

From Equation 41.9 the following values are found:

S_u = 22 650 lbs
S_∞ = 2 600 lbs
α = 0.02
β = 3.24

Using the individual fatigue test results from Table 41.2, the processed data shown in Table 41.3 are derived.

Id.-No.	Max. load (lb)	Cycles to Failure	Processed Load (lb)
1	3 350	1.32×10^5	25 791
2	2 950	1.73×10^5	23 439
3	2 700	7.49×10^5	23 209
4	2 650	2.48×10^6	23 044
5	2 500	3.34×10^6	21 757
6	2 350	7.31×10^6	20 468

Table 41.3 Processed data points on pitch link

According to Equations 41.26 and 41.27 the following standard deviation is calculated from the processed data:

$$\sigma_{Ln} = 0.034$$

which leads to a scatter factor of

$$\varepsilon = \text{antilog } \sigma_{Ln} = 1.08.$$

From this a statistical based reduction factor of $r_{Ln} = 0.75$ is calculated from Equation 41.43 with a = 3.09, according to a onesided distribution for a survival rate of 99.9%, and a' = 1.645, according to a onesided distribution for a confidence level of 95% (Ref. 41.18).

With this reduction factor the working S-N curve is found from Equation 41.9 to be:

$$F_{max} = 1950 + (16988 - 1950) \cdot e^{-0.02(\log N)^{3.24}} \text{ lb} \qquad (41.47)$$

In Figure 41.10 this working curve is plotted together with the fatigue test data and the mean S-N curve.

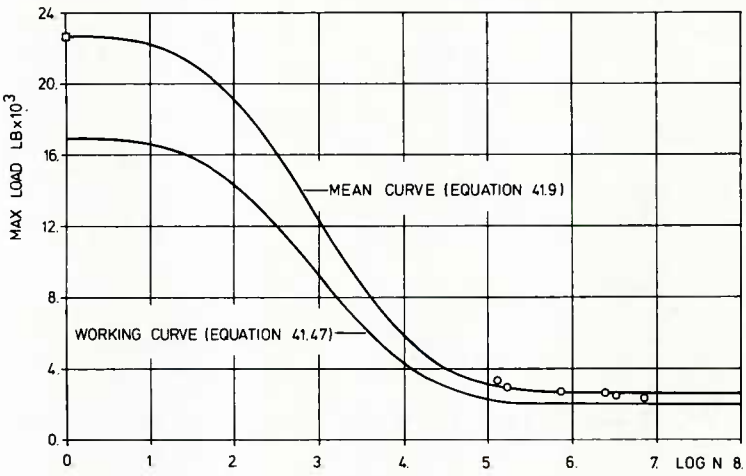

Fig. 41.10 Mean and working S-N curves of a hypothetical pitch link

4.1.3 REFERENCES

41.1 Fatigue Evaluation of Rotorcraft Structure, Advisory Circular, AC No: 20-95, Federal Aviation Administration, 5/18/76

41.2 Metallic Materials and Elements for Aerospace Vehicle Structures, MIL-HDBK-5C, September 1976

41.3 Schijve, J., Fatigue in aircraft structures, Luchtvaarttechniek 2, Oktober 1969

41.4 Hardersen, Ch.P., Fatigue Life Prediction of Helicopter Pitch Link Using KAMAN Life Calculation Methods, Proceedings of the AHS Midwest Region Helicopter Fatigue Methodology Specialists' Meeting, March 1980, St. Louis, Missouri

41.5 Weibull, W., Fatigue Testing and Analysis of Results, Pergamon Press, New York, 1961

41.6 Arden, R.W., Hypothetical Fatigue Life Problem, Proceedings of the AHS Midwest Region Helicopter Fatigue Methodology Specialists' Meeting, March 1980, St. Louis, Missouri

41.7 Stocker, B.P.W., Fatigue Substantiation of Non-Linear Structures, Proceedings of the AHS Midwest Region Helicopter Fatigue Methodology Specialists' Meeting, March 1980, St. Louis, Missouri

41.8 Buch, A., Fatigue Strength Calculation Methods, TAE No. 314, Technion-Israel Institute of Technology, Haifa, Israel, September 1977

41.9 Graham, J.A., Fatigue Design Handbook, Society of Automotive Engineers, New York, 1968

41.10 Structural Design Manual, Section 2.10 Fatigue, The Boeing Co., Vertol Division

41.11 The effect of mean stress on fatigue strength, Engineering Sciences Data Unit, Fatigue-Endurance data, London

41.12 Handbook on Vibration Substantiation and Fatigue Evaluation of Helicopter and Other Power Transmission Systems, Order 8110.9, Federal Aviation Administration, January 1975

41.13 Little, R.E., Jebe, E.H., Statistical Design of Fatigue Experiments, Applied Science Publishers, London, 1975

41.14 Altman, B., Pratt, J., The Challenge of Standardizing Fatigue Methodology, Proceedings of the AHS Midwest Region Helicopter Fatigue Methodology Specialists' Meeting, March 1980, St. Louis, Missouri

41.15 Liard, F., Fatigue of Helicopters-Service Life Evaluation Method, AGARD Report No. 674, Published February 1979

41.16 Albrecht, C.O., Statistical Evaluation of a Limited Number of Fatigue Test Specimens Including a Factor of Safety Approach, ASTM Special Technical Publication No. 338, Philadelphia, 1963

41.17 Dougherty, J.E., Spicer, H.C., Helicopter Fatigue Substantiation Procedures for Civil Aircraft, ASTM Special Technical Publication No. 338, Philadelphia, 1963

41.18 Sachs, L., Statistische Auswertungsmethoden, Springer-Verlag, Berlin, 1968

SUB CHAPTER 4.2

FRACTURE MECHANICS

by

A.Salvetti - G.Cavallini - A.Frediani

Department of Aerospace Engineering-University of Pisa
Via Diotisalvi, 2 - 56100 Pisa
ITALY

CONTENTS

4.2.1 CRACK PROPAGATION

4.2.1.1 Introduction

The process of failure due to fatigue damage generally evolves through the following phases, namely: - the nucleation of numerous microcracks; - the coalescence of microcracks to one or more dominant macrocrack; - the stable propagation of the dominant macrocracks by fatigue loading; - unstable propagation and immediate final failure.

Each fatigue process always evolves through the steps indicated above and depicted in Fig. 4.2-1, even if certain phases might not even be present or so clearly defined. Moreover, the boundaries between these phases are difficult to establish and some kind of engineering judgment is necessary in order to make the proper distinction. Nevertheless, the failure process depicted in Fig. 4.2-1 is a suitable reference frame for the purpose of the present chapter, aimed at presenting the crack propagation phase.

To be more detailed, the chapter contains a general analysis of the stable crack growth phenomenon due to fatigue loading from the initial to the final dimension, and cases of constant and variable amplitude loading are considered.

The question of initial dimension of the crack, which may be nucleated or may be present in the structures as a consequence of the manufacturing process, is beyond the scope of this presentation and can be established in the general context of the particular design, namely on the basis of the accuracy of the N.D.I. methods used; the methodologies by means of which the initial dimension is established are discussed in another chapter of this manual.

The final dimension of the crack is generally a fixed fraction of the critical dimension at which unstable propagation occurs.

This problem is examined in sec. 4.2.3, where the methodologies for assessing the critical crack dimension are also discussed.

4.2.1.2 Crack propagation under constant amplitude loading

The growth of a crack under constant amplitude loading may be characterized by a suitable relationship between the crack growth rate, (da/dn), and the stress intensity factor, K.

Consider, first, a through crack in a plate. Fig. 4.2-2 shows the stress state in the neighbourhood of the crack tip in the idealized case of small deformations and pure elastic behaviour. The stress intensity factor, K, completely defines such a state of stress in a region which is small in relation to the half-crack length, ($r/a \ll 1$). K depends on the crack length and the boundary conditions; it varies linearly with the applied load. The stress intensity factor can, therefore, be evaluated within the framework of the theory of linear elasticity. The general methods for computing K are well known and are discussed in several books, of which Ref. 1,2 can be quoted. A useful collection of K solutions is presented in Ref. 3.

Fig. 4.2-3 shows a typical relationship between (da/dn) and ΔK, namely the variation of K associated with the load excursion ΔP between the maximum and the minimum value, P being a reference load proportional to any other applied load. Results such as those shown in Fig. 4.2-3 are obtained following the sketches in Fig. 4.2-4, by calculating (da/dn) by numerical derivation from the test data, (a-n), by computing K by a suitable theoretical approach, and by obtaining ΔK on the basis of the load excursion ΔP.

The existence of a functional relationship between (da/dn), ΔK and R, the so-called K-rate relationship, namely $(da/dn)=F(\Delta K,R)$, is the key point in any approach for analyzing the phenomenon of crack growth under constant amplitude loading. Knowledge of function F allows engineers to compute (da/dn) and, by integration, the crack length reached after a given number of cycles, once the stress intensity factor relevant to the structure under investigation has been obtained.

Function F must be selected to fit the typical sigmoidal shape displayed by the K-rate relationship on a log-log plot, as in the curve in Fig. 4.2-3. In this curve, the lower asymptote is associated with a threshold in crack growth, namely $(da/dn)\neq 0$ only if ΔK is higher than a threshold value ΔK_{th}. The upper asymptote allows for the rapid increase in (da/dn) for crack length near to the critical one (*). The central part of the plot, which is linear in a log-log plot, indicates a power relation between (da/dn) and ΔK.

The process of defining F is essentially empirical and is based on the selection of analytical expressions that suitably comply with part or all the sigmoidal shape. Several analytical expressions are currently available for function F. The one proposed by Paris, when he and his coauthors first pointed out the existence of a functional relationship between (da/dn) and ΔK, is of the type:

$$da/dn = C_p \, \Delta K^m \qquad (4.2\text{-}1)$$

(*) For details on critical crack length see sec. 4.2.3.

where C_p and m are constants. This relationship, known as the Paris law, complies only with the linear part of the sigmoidal shape. As a consequence, the rate predicted near the threshold is higher that the actual one, the opposite being true at the higher crack lengths. Another limitation of this law arises from disregarding the dependence of the crack rate on the stress ratio R. To overcome the abovementioned limitations other analytical expressions have been utilized. In particular, Forman proposed:

$$da/dn = C_F \, \Delta K^n \left[(1-R) \, K_c - \Delta K\right]^{-1} \qquad (4.2\text{-}2)$$

in order to take into account the effect of the R parameter and the rapid increase in the rate for K_{max} near the critical value of the stress intensity factor, K_c.

Collipriest proposed:

$$\log (da/dn) = C_1 + C_2 \, \text{tangh}^{-1} \frac{\log \left[K_c \, K_{th}/K_{max}^2 \, (1-R)^s\right]}{\log(K_{th}/K_c)} \qquad (4.2\text{-}3)$$

The empirical constants in (4.2-1,2,3) namely C_p, m, C_F, n, C_1, C_2, s, depend on the material and environment, and must be assessed by means of crack growth test data and numerical procedures of best-fit, as explained in a later section. K_c and K_{th} are two important parameters which define the behaviour of a growing crack in the high rate region and in the very low rate region, respectively. K_c represents "fracture toughness" and is, within the limits explained in sec. 4.2.3, a material constant. Knowledge of this allows engineers to calculate the critical crack length in a structure within the frame of Linear Elastic Fracture Mechanics as explained in sec. 4.2.3. K_{th} is the threshold value of the stress intensity factor, the knowledge of which is very important for predicting the growth of small cracks. App. 4.2.A provides further remarks on this quantity.

Finally, another significant law is based on Elber's model of fatigue crack growth. This limits itself to the linear range of the log-log plot, but is nevertheless important for its basic idea, which provides a convincing explanation of the R effect under constant as well as under variable amplitude loading. Elber (Ref. 5,6), observed that, as a consequence of the residual compressive stresses due to the plastic wake behind the crack, a crack is closed not only in the case of compressive loads but also in that of low tensile loads. The crack opens only when the average tensile stress in the uncracked region reaches a particular value called opening stress, σ_{op}.

Elber supposes a crack grows only when the average tensile stress is greater than σ_{op}; therefore the crack grows under the action of an effective $\Delta K_{eff} = K_{max} - K_{op}$. Then Elber utilizes the Paris law but with the effective ΔK_{eff}, so that:

$$da/dn = C_E \, (\Delta K_{eff})^r \qquad (4.2\text{-}4)$$

By adopting this hypothesis the Elber approach explains the R effect; in fact for the same nominal value of ΔK, the greater the value of R, the greater the value ΔK_{eff}.

Relationship (4.2-4) can be modified in order to make the dependence of (da/dn) on R explicit in the form:

$$da/dn = C_E \left[U(R) \cdot \Delta K\right]^r \qquad (4.2\text{-}4')$$

which implies $K_{op} = f(R) \, \Delta K$. In this case, also U(R) and the constants C_E and r must be assessed from experimental results.

From the point of view of application, Elber's law is not unlike the previous semiempirical laws, but, because of the principles on which it is based, this approach is useful for the interpretation and prediction of the crack growth phenomena under variable amplitude loading.

So far, the effect of the structure thickness has not been taken into account and the phenomenon has been considered as a two-dimensional problem. There is a difference, however, between the free surface, where a state of plane stress exists, and the inside where there is a state of plain strain. The two states produce plastic zones of different sizes, the larger of these being the one relevant to plain stress. According to Elber's model, therefore, the plastic deformations in the crack wake are greater in the case of plain stress with the result that the crack growth rate is reduced. This explains why the crack growth rate increases as the thickness increases, since the plane stress zone decreases in relation to the full thickness, Fig. 4.2-5.

Finally, the constants of the semiempirical laws must be regarded as being dependent on the type of materials, environment (*) (including temperature and load frequency) and thickness. It must be pointed out again that the expression "type of material" means the specification of a number of characteristics, i.e. type of product, heat treatment, fiber orientation, manufacturer and also batch. If these characteristics are sufficiently specified, the scatter of experimental data is reduced to a certain extent. If, instead, all the data relevant to the same nominal material is grouped irrespectively of other specifications, the scatter band may be very wide (Ref. 7).

(*) A detailed assessment of environment effects and some relevant design data are given in Ref. 44, 45, 46.

So far the problem of crack propagation has been restricted to the case of through cracks. The same empirical laws can be utilized to predict the growth of a three-dimensional crack, often referred to as flaw. Several types of the flaws of technical interest are shown in the Fig. 4.2-6. With these types of cracks, the stress intensity factor varies along the crack border. In the case of semicircular crack or circular embedded cracks (often called penny shaped cracks) the application of the crack propagation laws is straight-forward, because it is sufficient to calculate how the radius increases with the number of load cycles. In the case of semielliptical or embedded elliptical cracks, the stress intensity factor varies along the border, so that a change of shape can take place during the propagation. The problem of the evaluation of the stress intensity factor in flaw with elliptical shape is discussed in sec. 4.2.3. The results presented in that section together with the laws presented in this section allow us to calculate the growth of a flaw under constant amplitude loading in several cases of practical interest.

4.2.1.3 Crack propagation under variable amplitude loading

Analysis and prediction of crack growth under variable amplitude loading is a complex and difficult problem. The new factor, in comparison with the constant amplitude case, is the interaction effect arising from the subsequent loading cycles of different amplitudes.

An early, but significant, description of the interaction effects was given by J. Schijve (Ref. 8). If a peak load is introduced in a constant amplitude loading, Fig. 4.2-7, the result is a delay effect, i.e. the crack growth rate greatly decreases in comparison with what happens in the case of constant amplitude loading without a peak load. The delay effect is much less noticeable when the peak is followed by a valley of the same value. A crack growth can also be stopped by an appropriate overload and, on the contrary, a crack growth can be increased by an underload.

The interaction effects are even more intricate in the case of more complex load sequences where rapid peak and valley variations are present. Comparative tests carried out with the same load cumulative distribution but with different load sequences, clarify the importance of these effects.

The explanation of the interaction effects that are responsible for the different endurances shown in Fig. 4.2-8, has been identified in certain characteristics phenomena, or rather, in a combination of these.

- Residual stresses. At the crack tip, a plastic zone is formed under load, the extent of which depends on the K_{max} value. Upon load release, the elastic part of material presses on the plastic zone and compressive residual stresses build-up at the crack tip. In the case of variable amplitude loading residual stresses modify the stress ratio and, if sufficiently high, also the stress amplitude at the crack tip.
- Crack closure. As far as Elber's model of crack growth is concerned, test data shows that σ_{op} depends on the applied load in a non linear manner. As a result of such non-linearity, in the case of variable amplitude loading the effective ΔK_{eff} follows a different pattern in comparison with the applied load. Fig. 4.2-9 showing a typical variation of ΔK and ΔK_{eff} in the case of two load levels, clarifies the role of crack opening in the interaction effects.
- Incompatibility of crack front orientation. Shijve, (Ref. 10), suggested that the interaction effect between two cycles of different amplitude may also be ascribed to the incompatibility of the crack front orientation; one orientation is perpendicular to load direction for low K values, while the other forms a 45° angle with the load direction for high K values.
- Blunting and sharpening of the crack tip. It is conceivable, and also demonstratable, that high ΔK cycles blunt the crack tip whereas low ΔK cycles sharpen it. Therefore the damage produced by a load cycle depends upon the geometry of the blunted or sharpened crack tip and then on the amplitude level of previous cycles. Other possible explanations of the interaction effects have been proposed, e.g. strain hardening history at crack tip, but none of them seems to be able to take completely into account each interaction effect. Probably, a lot of these elements contribute to a certain degree to the interaction effects. Nevertheless, Elber's model and the model which takes residual stresses at crack tip into account seem to be more effective and to be grounded on a more solid basis. Indeed, they have been used as a basis for developing computational models for the evaluation of crack growth in variable amplitude loading.

4.2.1.4 Models for crack growth evaluation in variable amplitude loading

Several models have been proposed for the evaluation of crack growth in structures subjected to variable amplitude loading. The models are generally based on simple assumptions deduced from the observations discussed previously. As the phenomena produced by interaction effects are very complicated, the models cannot give accurate results in all situations. Each of them is satisfactorily accurate for the cases where the particular aspect of the interaction phenomenon contemplated in the model is dominant, but no general application is possible.

The most important models and their range of application are dealt with in the following paragraphs.

. The non interactive model. The model is based on the hypothesis that each load cycle extends the crack of the same degree as that produced by the load cycle in the case of constant amplitude loading. The necessary information is provided by the K-rate relationship and crack growth is calculated by a cycle-by-cycle procedure. The method is simple to apply, as it does not take interaction effects into account. It predicts the crack growth with acceptable accuracy only in the case of loading sequences characterized by smooth variation in the subsequent load cycles. The method is generally conservative as the retardation effects predominate over the acceleration effects in aircraft spectra. In certain cases, as for fighter aircraft, where the load sequence contains several high tensile peaks, the results are by far conservative; in other cases, as for narrow band Gaussian sequences, the results are fairly accurate.

. The Wheeler model. To take into account the interaction effect due to overloads, Wheeler, (Ref. 11), suggested the application of a corrective factor to the crack growth rate, which is obtained by a K-rate relationship (Paris, Forman, or other). The corrective factor is given as:

$$C_w = (r_{pi}/(a_o + r_{po} - a_i))^m \qquad r_{pi} < r_{po}$$
$$C_w = 1 \qquad r_{pi} \geq r_{po} \qquad (4.2\text{-}5)$$

where, in Fig. 4.2-10, a_i is the crack dimension when the load cycle i-th is applied, r_{pi} is the size of the plastic zone produced by the load in question, r_{po} is that of the plastic zone generated by the overload applied to the crack dimension a_o. The plastic zone dimension is calculated by means of the formula $r_p = 1/C(K^2/\sigma_{ys}^2$ (*) discussed in sec. 4.2.3. m is an empirical constant which is determined by means of the fit between specific experimental data and the results from the model. The basic shortcoming of Wheeler's model is the empirical character of the constant m which is highly dependent on the kind of material, on the loading spectrum and probably on the geometry too. Therefore the application of the Wheeler model is restricted to the material and the loading spectrum which is identical or very similar to the ones for which m was obtained. The procedure for applying the model is very simple and the calculations are to be made cycle-by-cycle.

. The Willenborg model. In the model proposed by Willenborg, (Ref. 12), the delay effects in crack growth are ascribed to the influence of the compressive residual stresses. These stresses are computed by following the highly simplified approach outlined in Fig. 4.2-11 which is still based on the utilization of an idealized plastic zone. The residual stresses are utilized to compute the stress intensity factor by means of an effective stress equal to the difference between the nominal and the residual stress. The method does not rely on any empirical coefficient. The model, at least in its original formulation, does not allow for the acceleration effects due to negative peak loads and consequently produces unconservative results when dealing with those spectra with significant compressive peak loads. On the contrary it is likely to work accurately with a flight-by-flight type of loading with a randomized distribution of loads and only few not significant compressive loads.

. Models based on the crack opening concept. The application of Elber's model to variable amplitude loading relies on the evaluation of the crack opening stress which is obviously variable throughout the stress history.
Bell and Eidinoff, (Ref. 13), proposed to evaluate the ΔK_{eff} by means of certain empirical functions which described the acceleration and retardation behaviour of the material under representative, very short, variable amplitude spectra. The model does, indeed, give accurate results in comparison with experimental data, but this data is not sufficient for a reliable evaluation of its accuracy. In any case, the model is difficult to apply because of the large number of empirical constants involved.
Führing and Seeger (Ref. 14,15), on the other hand, devised a method which does not require the determination of any other empirical data besides the usual semiempirical law of crack growth and mechanical constants. The σ_{op} is calculated analytically by an improved Dugdale model at the crack tip. The calculation is quite quick and the first comparisons have already been encouraging. Further extensive checks have to be carried out, however, before it is possible to draw general conclusions.
Newman (Ref. 16) also proposed a very general, solely analytical procedure for calculating σ_{op} by using the finite-element method. A satisfactory level of agreement exists

---

(*) C is taken equal to (2π) for plain stress condition and $(4\sqrt{2\pi})$ for plain strain condition.

between the theoretical and experimental data, but, since it is very time-consuming, the method is impracticable for application and its use must be restricted to checking the results obtained by more simple methods.
De Koning and van der Linden, (Ref. 17), propose a model for the prediction of growth rates of fatigue cracks in aluminium alloys subjected to spectrum loading, which is based on an approximate and simple description of the crack opening behaviour. The predictions obtained with this model match fairly well the experimental data and so the model seems to be very promising, though further development is still required.

4.2.1.5 Utilization of crack growth prediction methods for design purpose

One of the main problems in designing structural components within the framework of damage tolerance requirements is the evaluation of the flight-time a crack takes to grow to a certain dimension.

In the case of constant amplitude loading the task can be fulfilled by an integration of the K-rate relationship $da/dn = f(\Delta K)$ to obtain the number of cycles N necessary to grow a crack from a_i, the initial crack length, to a_f the final crack length, namely:

$$N = \int_{a_i}^{a_f} da/f(\Delta K) \qquad (4.2\text{-}6)$$

To carry out the integration, it is at first necessary to select an appropriate analytical expression for $f(\Delta K)$. The choice can be made on the basis of the initial and final crack length, a_i and a_f respectively. If the interval of integration (a_i, a_f) belongs to the linear portion of the K-rate relationship in the log-log plot, see Fig. 4.2-3, a power law, that proposed by Paris for example, is the best choice, since the analytical expression is simple to handle and only two empirical constants may be introduced. On the contrary, if the initial crack length is in the threshold range and/or the final crack length is near the critical one, it is necessary to resort to more complicate expressions which better describe the sigmoidal shape of the K-rate relationship in the log-log plot.

A comment needs to be made as far as the selection of the empirical constants is concerned. Crack propagation is typically a random phenomenon and therefore the empirical constants can be selected only on a statistical basis. The procedure by which this choice can be performed is discussed in section 4.2.2. Here attention is focused on the consequences of the different choices in the prediction of crack growth time. The scatter in da/dn deduced from a-n experimental data stems from two main causes: the scatter around the (da/dn)-ΔK best fit for each test and the differences among the best-fit curves pertaining to various tests. The width of the scatter band is greatly reduced if the material comes from the same batch, while it may become very large if data relevant to different batches, manufacturers, test laboratories and so on are grouped together. The nature of the scatter of a single test needs some specification. The crack propagation phenomenon is not continuous but is jerky, and this trend may be magnified by the process of derivation applied to (a-n) experimental data to obtain (da/dn)-ΔK data. Besides, the measurements are subject to typical errors which are normally distributed around the (da/dn)-ΔK best-fit curve. These causes produce a significant scatter which is greater than that relevant to many specimens from the same batch. But, in fact, this can be considered to be an "apparent" scatter because it does not affect the number of cycles which elapse in order to propagate the crack to a given length. During the propagation phenomenon in fact these fluctuations of the rate around the (da/dn)-ΔK best-fit curve cancel each other out and so do not affect significantly the final result.

Coming back to the problem of selecting the empirical constants, the procedure generally adopted is to calculate them not from the relationship obtained by the best-fit of experimental data which refers to 50% probability, but from the curve which includes 95% or 99% of the data. This approach is essentially accurate if the data is taken from many specimens, and also from different sources; in this case, the apparent scatter around each individual relationship is negligible in comparison with the scatter produced by the specimen population. The opposite occurs when specific tests are carried out on a batch of material which is the same as that used to build the component under investigation. Here the use of 95% or 99% probability curves produces too conservative an estimate of the life in the crack propagation phase. In this case, the empirical constants must be based on the best-fit curve and a safety level, based on the scatter relevant to experimental a-n curves, must be used.

The next step before performing the integration is to find the expression of K relevant to the component under examination. As pointed out before, this step can be often accomplished utilizing existing solutions, published in the relevant literature. The stress intensity factor can be put in the form:

$$K = \sigma \sqrt{\pi a}\, C(g,a) \qquad (4.2\text{-}7)$$

where a is the half crack length or the whole length, whichever is appropriate, σ a reference stress and C a function of the geometry and crack length. In the case of an infin

ite plate loaded in tension, the function C is equal to one and σ is the stress on the boundary parallel to the crack line. References 3 and 18 give a rather complete collection of existing solutions. In the case where no solution can be found in the literature or it cannot be constructed in approximate way by comparison to existing solutions, it is necessary to solve the specific problem of the theory of elasticity by following one of the methods analyzed in Ref. 2. In most cases the finite element method approach offers the most effective way to solve the problem. In these cases general purpose computer programs with subroutines particularly devoted to fracture mechanics are available, see Ref. 19 for instance.

At this point all the elements are available to carry out the integration.

Usually this task can be fulfilled by numerical integration. This operation can be carried out cycle-by-cycle, but this proves to be very time consuming. A more efficient procedure is the integration with constant Δa or Δn steps and so obtaining Δn or Δa, respectively, from the semiempirical law. The procedure and step value must be chosen for each specific case. A reference value of Δa equal to 2% of half the crack length allows a good agreement to be reached between the calculation time and a fairly accurate estimate of ΔK in the step. If the procedure with constant Δn steps is selected, the subsequent values of Δn must be properly varied by reducing its value in order to take into account the typical a-n relationship during propagation, (Ref. 20).

In the case of damages of a single dimension, namely through cracks in thin sheets, the problem is obviously simple, provided that the stress intensity factor can be assessed. There are difficulties in the case of damages which are described by a line or a surface, for instance flaws or embedded defects. In such a case each point of the crack front has a different crack growth rate and the shape of the crack front line changes during growth. From a strictly logical point of view, this requires the calculation of the stress intensity factor and crack growth rate at each point of the crack front. It must be observed that the K value at any point is generally dependent on the shape of the crack front. As this approach leads to an impracticable procedure, the calculation is performed by assuming that the shape of the crack front remains the same (hence, we are faced by a one-dimensional problem) or by assuming the crack is elliptical in shape and so calculating the K value in two points only, corresponding to the maximum and minimum axes. The latter way is more accurate and the time required for the calculations is certainly acceptable.

In the case of variable amplitude loading no general procedure is presently available to predict the crack growth time. As explained in sec. 4.2.1.3, this stems from the fact that the interaction phenomena, namely the influences of the load sequence on the crack growth, are not yet fully understood in their physical bases. Moreover, each of the proposed models takes only partial aspects of the interaction causes into account by means of simplified idealizations. As a consequence, it is likely that a method may be successful with certain load spectra and sequences, but inaccurate with other types of load conditions.

Nevertheless, there are several cases, significant from an engineering point of view, that can be faced with a satisfactory accuracy as far as the prediction of crack growth time is concerned.

A first case concerns load sequences characterized by smooth variation in the amplitude of successive loads. In these conditions the influence of interaction phenomena is negligible and an integration of the K-rate relationship appropriate to the material and K range is usually successful. Load conditions that can be treated in this way are Gaussian narrow band sequences. In this case, a formula can be developed (Ref. 21), to calculate the number of cycles which elapse during the growth of a crack from a_1 to a_2.

Other cases that received attention are spectra and sequences of loads representative of fixed wing aircraft operations. The Wheeler model can be used successfully with an appropriate selection of the plastic zone empirical constant. In these cases standardized load sequences have been developed - FALSTAFF for fighters (Ref. 22), and TWIST for transport airplanes (Ref. 23). Such load sequences can be used to check the accuracy of the models and to obtain the relevant values of the empirical constant. Fig. 4.2-12 shows the result of crack propagation tests with the above said load sequences together with the prediction carried out with the Wheeler, Willenborg and non interactive models. It is noteworthy that the non interactive model yields always conservative predictions.

In the case of helicopters, there is at present a lack of experience as far as crack propagation tests with realistic load sequences are concerned. The recent development of standardized spectra (HELIX and FELIX, see Appendix A of this manual) might offer a valuable reference frame to investigate the crack growth phenomenon in dynamic components. In the case of airframe structural components, the load spectrum is prevailingly dependent on mission and pay-load configuration, even if vibratory levels due to dynamic component operation may have a not negligible influence. In the case of airframes, no reference load spectrum is currently available and, therefore, only tests pertaining simple aircraft are likely to be conducted in the near future.

In conclusion it can be observed that the crack growth under variable amplitude loading can be predicted with an acceptable accuracy in the case of fixed wing aircraft. This is due especially to the experience accumulated with load sequences representative of the

relevant operational conditions. In the case of helicopters, as there is a lack of this type of experience, no precise recommendation can be given as far as the "a priori" choice of a model is concerned. However the non interactive model and the Wheeler's models seem to be promising for the helicopter field. The first might be used for nearly constant amplitude sequences, the other for spectra that depart from such a condition. Obviously crack growth tests with the relevant spectra have to be carried out to substantiate such choices.

4.2.2 CRACK PROPAGATION TESTS

4.2.2.1 Test articles and test equipment

Crack propagation tests can be carried out on standard specimens, test articles representing airframe components as well as on complete airframe components where, as will be shown later, some initial damages related to design specifications are introduced. The last two categories are so much peculiar test articles that they cannot be dealt with from a general point of view. Obviously, one needs to pay attention to the accurate reproduction of the real operative conditions, principally of stress field in the critical area.

The present paragraph, consequently, is devoted to a brief description of the standardized or generally used specimens and test equipments. The general design data relevant to fatigue crack growth is carried out usually using plain sheet specimens, centrally precracked by saw cut to obtain a through crack. A typical layout of these specimens is shown in Fig. 4.2-13, but also wider specimens can be used with the aim of producing a larger amount of experimental data. To achieve this, the specimen length must be increased by the same ratio. In any case, the specimen aspect ratio must be high enough for the stress distribution in the middle of the uncracked specimen -that is along the line where the crack will propagate- to remain constant. The calculation of the stress intensity factor values corresponding to the crack length values can be carried out, therefore, easily and accurately in the processing of experimental data.

Particular care must be taken to avoid the unrealistic buckling of crack lips which may occur in the thin specimens in the range of the high values of the crack length. In actual structures this situation generally is prevented by the stiffeners; in the test, antibuckling guides can be used to this aim.

In some particular cases, other configurations of specimens are used. Where the attention of the designer is focused on medium or large thickness components, crack propagation tests on part-through cracked specimens are also carried out. The initial damage is manufactured by means of a very thin milling cutter or by means of the E.D.M.

Finally, if one is concerned with very thick components, such as forgings, standardized C.T.S. (Compact Test Specimens), see Fig. 4.2-14, are used. These are directly made out of the component; the criteria for this operation and some examples are discussed in Ref. 26.

As previously stated, the introduction of the initial damage (one or more cracks) is made at a first stage, by means of a saw, a milling cutter, an E.D.M. or other mechanical system and then the correct dimension is obtained by applying a fatigue loading. Hence the crack tips are sharpened and the machining process does not influence the crack propagation data.

As far as the testing machine is concerned, a discussion on the selection of the more suitable apparatus is beyond the aim of this paragraph; an analysis of the problem is carried out in Ref. 27. Anyway, the selection of the testing machine is often conditional on laboratory availability and on the crack dimensions monitoring system. Servo-hydraulic machines are felt to be the optimal solution, in relation to their present reliability and their wide possibility of use as well as for many other types of tests, in particular for the variable amplitude loading tests. The greatest attention must be payed to avoid unexpected overloads which can lead to unrealistic and unconservative delays in the crack growth. However modern machines have load limits to prevent these setbacks.

The principal element of the apparatus for these tests is the crack dimensions monitoring method. A very effective presentation of the principal methods is made in Ref. 28, where such methods as optical, compliance, replicas, potential difference, eddy current, ultrasonic, fractographic, acoustic emission, breaking-wire are carefully reviewed. Among all these methods, the optical method is the simplest system and very easy to use. The crack dimensions are measured by an operator by means of a travelling microscope; otherwise they may be measured automatically by means of a video camera and tape recorder(*). The optical method allows us to carry out measurements with an accuracy of .1 mm, a figure adequate for technical evaluations. The drawback of this method is its inability to measure the depth of surface cracks. An assessment of the crack depth in correlation to

---

(*) The use of a stroboscopic light matched to test frequency makes easier the observation of crack tips.

crack length (and so the shape of the crack during its growth is plotted) can be made by replicas technique or by observing the "marking" lines on the surface of the crack by means of an electronic microscope after the final failure of the specimen. But this last technique can be used only for some materials and where the spectrum loading has characteristics particularly suitable in producing the phenomenon. The evaluation of this fact cannot be made a priori and the use of this technique requires some care; in particular, the introduction into the actual spectrum of "extra" blocks to bring out the phenomenon must be made with great caution to avoid unrealistic crack growing. All the other methods are more sophisticated and require some operations of calibration. They are more complex to use and are generally restricted to special applications.

4.2.2.2 Constant amplitude tests

The crack propagation tests with constant amplitude loading are carried out principally with the purpose of determining the laws of crack growth rate relevant to a particular material.

To this end, the following procedure may be applied. The crack growth laws have the general form:

$$(da/dn) = f(\Delta K, R, m_1, m_2, \ldots\ldots, b_1, b_2 \ldots) \qquad (4.2.8)$$

where the constants m_i must be determined by means of test data and b_i are the constants known relevant to material, for instance the K_c or K_{th} value. Each law can be also put in the form of a straight line equation by means of a suitable coordinate change. For instance the Paris law $\{(da/dn)=C_p(\Delta K)^{n_p}\}$ can be converted into $\{\log(da/dn) = \log C_p + n_p \log \Delta K = m_1 + m_2 \log(\Delta K)\}$ and then $\{y=m_1+m_2 x\}$; and the Forman's law $\{(da/dn)=C_F\Delta K^{n_F}/((1-R)K_c-\Delta K)\}$ as $\{\log((da/dn)((1-R)K_c-\Delta K))=\log C_F+n_F\cdot\log\Delta K=m_1+m_2 \log\Delta K\}$ and then $y=m_1+m_2x$; and the Collipriest-Walker's law $\{\log(da/dn)=C_1+C_2\tanh^{-1}(\log(K_cK_{th}/((1-R)^r K_{max})^2)/\log(K_{th}/K_c))\} = = m_1+m_2\tanh^{-1}(\log(b_1b_2/((1-R)^{m_3}K_{max})^2)/\log(b_2/b_1)\}$ and then $\{y=m_1+m_2x\}$.

Now the experimental data and the known constants b_i allow us to obtain a set of pairs of corresponding values $\{x_i,y_i\}$. Then the specific constants m_1 and m_2 are easily determined by means of a linear regression analysis of the $\{x_i,y_i\}$ data. In some cases (Collipriest law and others), more than two m_i constants, but generally not more than three, have to be evaluated.

The linear regression analysis procedure can, therefore, be applied for some fixed values of the constant m_3; the final solution of m_1,m_2,m_3 is the one for which the scatter of $\{x_i,y_i\}$ experimental data around the best-fit line is lower.

It is worth discussing further some aspects of this procedure. The first aspect is the process to obtain the values $\{x_i,y_i\}$ or, as it is clear from the previous expressions, the corresponding values $\{(da/dn)_i-\Delta K_i\}$; from the latter the values $\{x_i,y_i\}$ are immediately obtained. In effect, the (da/dn) and ΔK values must be drawn out from the corresponding pairs of the a_i and n_i values, which are the quantities really measured during the test.

If the specimen is in a standard configuration whose expression is well known, the value of ΔK_i is determined easily from the a_i data and the loading conditions ($\Delta\sigma$ and R). In any case, the calculation of K can be carried out by means of general methodologies outlined previously.

The calculation of $(da/dn)_i$ values, which are obtained through a numerical procedure of derivation on the discrete points $\{a_i,n_i\}$ is, however, a complex problem. Crack propagation is, in effect, not a continuous process but the crack dimension grows jerkily; besides, the measurement of crack length is affected by small random errors.

In these conditions, the procedure of derivation may produce unrealistic magnification of the scatter of the (da/dn) data around the best-fit straigth line.

This unwanted fact is likely to occur if a derivation procedure based on a divided difference method is used. A more effective procedure is the use of a 3-th or 5-th degree polynomial fitted to the data point $\{a_i-n_i\}$, where $(da/dn)_i$ is to be determined, and to the two or three data points behind and before. The crack growth rate is then obtained by differentiating the polynomial in the i-th point (Ref. 29). The procedure is repeated for each data point. A more powerful procedure is the use of a spline function technique. In this case, the numerical process does not give rise to an "oscillation" of the function between the data points as does sometimes occur when using the simple polynomial approach. Fig. 4.2-15 shows a typical output of this analysis.

A second aspect of the procedure which is worthwhile examining is the statistical treatment of the results obtained. A first step is the checking of the capability of the crack growth law to represent the phenomenon shown by the experimental data. This is done by supposing that the scatter around the best-fit line is normally distributed, and then by evaluating the correlation coefficient; it allows us to check the significance of the test data and of the "model" assumed to describe the phenomenon. This quantity can be evaluated for each test and, if the test has been carried out carefully, the check is positive; in these cases values of the correlation coefficient higher than 0.9 - a good figure- are generally obtained. The Fisher test also can be used to assess the significance of the semiempirical laws obtained in representing the phenomenon; moreover, this

kind of test allows us to evaluate the correctness of the hypothesis on the significance level (Ref. 30). As mentioned above, the correlation coefficient and the Fisher test are significant if the distribution of the differences between the experimental data and the corresponding points of the best-fit line is normally distributed. Hence, at the same time, the χ^2 test is carried out to check the goodness of this hypothesis with a certain level of significance (Ref. 30). On the basis of the results of the previous statistical analysis, the straight line relevant to a given percentile (95% or 99% for instance), with an established level of confidence (95%, generally), is immediately determined.

Obviously a single test does not allow us to fully assess the variability in the crack propagation data. Indeed, two specimens of the same batch tested under the same conditions show generally two different a-n curves and two different (da/dn-ΔK) relationships. Consequently, several specimens must be tested and generally it is better to carry out tests with various values of R, if a law taking into account this parameter is to be determined. For each test the previous statistical treatment can be applied, but also a further statistical analysis must be carried out to verify whether the data of all the tests may be thought as belonging to the same population. This analysis requires three consecutive steps (Ref. 31): checking to see if the variance about the regression lines can be considered the same (Bartlett's test), checking the parallelism among the regression lines, checking the identity of the regression lines. The fulfilment of all the checks allows us to group all the data into the same population and so to obtain a general regression line. If it is not so, the scrutiny of the results makes it possible to identify a test carried out in an incorrect way or even to realize the inability of the examined law to represent reliably the phenomenon in the ΔK range considered, particularly to take the effect of R into account.

4.2.2.3 Variable amplitude tests

Variable amplitude tests are carried out with load sequences representative of operational conditions of a particular class of aircraft. Tests are usually carried out with plane sheet specimens with the aim of evaluating the crack propagation models for the spectrum involved. In the case of models dependent on one or more constants, these can be adjusted by fitting the model results with the test data.

Another application that is getting increasing interest in the field of fixed wing aircraft is the determination of the crack propagation law in variable amplitude loading, namely da/dF=f(K), in analogy with the case of constant amplitude. F is the number of flights, and K is evaluated with reference to the average crack length in the flight and a characteristic value of the stress in the spectrum. The law so obtained can be used to predict the crack growth behaviour of different structures under the same spectrum. The field of applicability of such a procedure, as far as the type of structure and spectrum is concerned, is still open to investigation. Anyway this procedure, if conveniently improved and substantiated, might become an effective design tool, simple and accurate to use.

Variable amplitude tests are also carried out on specific structures to assess their behaviour as damage tolerant structures. These tests are usual for fixed wing aircraft designed within the framework of damage tolerance requirements.

Irrespective of the kind of test and its objective, the significance of variable amplitude loading tests is tightly connected with the type of spectrum and sequence adopted. Some of the variable amplitude tests are carried out with "standardized" load sequences. The use and the meaning of such tests is well documented in the literature (Ref. 32). In all the other cases the load sequence must be selected in such a way as to make it representative of the operational conditions to which the test refers. The problem of the representativeness of the load sequence, which is of fundamental importance in any fatigue test, is out of the scope of the present section. Reference can be made to specific publications among which Ref. 20 and Ref. 25 can be quoted.

Nevertheless, in the present context some considerations are worthwhile. One of the first considerations concerns the very high loads with very few occurrences. These loads are to be eliminated from the test sequence to avoid unconservative results (clipping of the spectrum). On the other hand it is desirable to eliminate the lower load excursions with a large number of occurrences to reduce the testing time (truncation of the spectrum). This operation is very complex and can easily produce very conservative results. Moreover, the compression loads are sometimes eliminated from the spectrum because they are considered erroneously ineffective in crack propagation; besides, the test set-up can be simplified. Moreover, this action yields unconservative results as the compression loads produce an acceleration effect cancelling partially the retardation effect of peak loads.

Finally, the problem is to establish the clipping and truncation load levels to produce accurate results anyway. The definition of clipping and truncation levels depends also on the experience relevant to a particular spectrum and to a particular structure. For the fixed wing aircraft, for example, it is common practice to truncate the spectrum at the level at which the maximum stress occurs ten times in the course of a single life-

time of an aircraft (Ref. 20). In the case of helicopters, the available experience does not allow us to establish confidently these levels.

4.2.3 RESIDUAL STATIC STRENGTH EVALUATION

4.2.3.1 Introduction

The final collapse of a cracked body loaded in tension generally occurs when a certain combination of applied stress and crack length assumes a well stated value characteristic of a given material. This is expressed by what is known as a "fracture criterion" i.e.:

$$f(\sigma,a) = I \qquad (4.2\text{-}9)$$

where l.h.s. is a function of applied stress, σ, and crack length, a, and I is an invariant characterizing the thoughness of the material with respect to fracture. The "fracture criterion" allows us:

- to classify materials with respect to their fracture toughness because, for a given crack length, we may apply high stress levels for materials having high fracture toughness I and viceversa;
- given a crack of certain dimensions in a structure, to determine the maximum load which can be applied without catastrophic failure of the structure itself.
  On the contrary, it is also possible to determine the maximum crack dimensions which can be tolerated when maximum load is applied.

The application of eqn. (4.2-9) for assessing residual static strength of a given structure built in a given material, is subordinated to the solution of these problems: to calculate the function $f(\sigma,a)$ for any combination of applied stress and crack length (in a given cracked structure) and to assess the Fracture Toughness (I in eqn. (4.2-9)) relevant to the real material.

This section 4.2.3 aims to show how these problems can be solved. The discussion is divided into 3 parts: first, a report on a brief analysis of general results in Fracture Mechanics and, in particular, a discussion of the already mentioned Stress Intensity Factor (S.I.F.) K; second, a report of the most common techniques for evaluating the S.I.F., both in small and large thickness structures; third, a discussion of the assessment of F.T. The concluding comments will consist of a brief discussion on the residual static strength evaluation of small and large thickness structures.

4.2.3.2 An engineering classification of fracture

A preliminary classification of fracture is based on macroscopic considerations of material separation. In this engineering classification the terms "brittle" and "ductile" fracture are used to indicate a situation where, respectively, the fractured surfaces are almost completely flat or inclined relative to the tensile direction, as shown in Fig. 4.2-16. In an ideally brittle fracture no crack propagation occurs until the load applied is smaller than a certain critical value. In this condition, a sudden crack propagation takes place and final failure occurs with a low absorption of energy. When dealing with a ductile fracture, a subcritical (and stable) crack propagation takes place until the final failure occurs in the presence of the large yielded region in front of the crack.

Common experience tells us that low yield strength and high temperature are favourable to the formation of a ductile fracture (the opposite is valid for brittle fracture). Moreover, a remarkable influence is due to the degree of stress axiality. In fact, some of the models which have been proposed for explaining the thickness effect show that an improvement of the axiality order corresponds to a virtual embrittlement of material.

This phenomenon is particularly important, since we have different stress and strain conditions at the crack tip, according to the thickness of the cracked specimen. Two extreme models can be distinguished in this connection: "plane stress" and "plane strain".

In a plane stress state, the stress according to the z-axis, normal to the middle plane of a cracked plate (Fig. 4.2-2) is nil ($\sigma_{zz}=\tau_{xz}=\tau_{yz}=0$); this scheme is satisfactory as far as thin plates are concerned. In the case of plane strain state the deformation according to the z-axis, is also nil ($\varepsilon_{zz}=\varepsilon_{xz}=\varepsilon_{yz}=0$); consequently, the stress state is triaxial because of the presence of the stress $\sigma_z=-\nu(\sigma_x+\sigma_y)$. In thin plates (typical of small thickness aeronautical structures) the stress state is, therefore, virtually biaxial and, when crack borders open, lateral necking zones are formed owing to the lack of lateral tie; the plastic zones are relatively large.

In a thick cracked body, where the condition of plane strain is prevalent, plastic zones at crack tips are, relatively speaking, smaller and a virtual embrittlement of material takes place.

These two situations are idealized cases, of course. More realistically, in all but the very thin plate-like specimens (Fig. 4.2-16, case A) a mixture plane stress-plane strain exists along the z-direction, where plane stress prevails near the plane surfaces and plane strain over the central portion. Now, having brought to mind the main phenome-

na connected to fracture, we will examine a mechanical theory of fracture and, subsequently, discuss about the application of this theory to the two extreme situations of plane strain and plane stress.

4.2.3.3 Elements or linear elastic fracture mechanics

The only and simplest continuum theory of fracture is founded upon the hypothesis that a cracked body loaded in tension experiences small elastic deformations everywhere. This linear theory is known as Linear Elastic Fracture Mechanics (L.E.F.M.). A description of the crack tip is one of the fundamental achievements of L.E.F.M. The stress field at a crack tip of a plate can be considered to be the superposition of the fundamental modes shown in Fig. 4.2-17:

mode I , or opening mode
mode II , or sliding mode
mode III, or tearing mode.

The stress tensor around the crack tip can, then, be expressed as follows:

$$\sigma_{ij} = \frac{1}{\sqrt{2\pi r}} \left[K_I f_{ij}^{I}(\theta) + K_{II} f_{ij}^{II}(\theta) + K_{III} f_{ij}^{III}(\theta) \right] \qquad (4.2\text{-}10)$$

where r,θ are relevant to a polar frame of reference; $f_{ij}^{I,II,III}$ are non dimensional functions which depend only on the parameter θ; and K_I, K_{II} and K_{III} are functions of the applied load and crack length, named Stress Intensity Factors (S.I.F.) relevant to the modes I, II and III.

In the Opening Mode the crack surfaces are moving symmetrically apart with respect to the middle plane of the crack. This is the most interesting situation occuring in engineering applications, since it is a situation typical of through cracks, of embedded cracks in solids, and part-through cracks where the load is of a tensile type, normally to the crack plane.

The other two modes are not interesting as far as engineering applications are concerned and so, given the scope of this manual, we will not mention these modes in the rest of the section.

In correspondence to the Opening Mode conditions outlined above, the stress and displacement fields, in a region near the crack tip, have the following forms (Ref. 33):

$$\sigma_x = \frac{K}{\sqrt{2\pi r}} \cos\frac{\theta}{2} \left[1 - \operatorname{sen}\frac{\theta}{2} \cos\frac{3\theta}{2} \right] + \ldots$$

$$\sigma_y = \frac{K}{\sqrt{2\pi r}} \cos\theta \left[1 + \operatorname{sen}\frac{\theta}{2} \cos\frac{3\theta}{2} \right] + \ldots \qquad (4.2\text{-}11)$$

$$\sigma_{xy} = \frac{K}{\sqrt{2\pi r}} \operatorname{sen}\frac{\theta}{2} \cos\frac{\theta}{2} \cos\frac{3\theta}{2} + \ldots$$

$$\sigma_z = \begin{cases} -\nu(\sigma_x+\sigma_y) & \text{plane strain} \\ 0 & \text{plane stress} \end{cases}$$

$$\sigma_{xz} = \sigma_{yz} = 0$$

$$u_x = K \frac{2(1+\nu)}{E} \sqrt{\frac{r}{2\pi}} \cos\frac{\theta}{2} \left[1 - 2\nu + \operatorname{sen}^2\frac{\theta}{2} \right] + \ldots$$

$$u_y = K \frac{2(1+\nu)}{E} \sqrt{\frac{r}{2\pi}} \operatorname{sen}\frac{\theta}{2} \left[2 - 2\nu - \cos^2\frac{\theta}{2} \right] + \ldots \qquad (4.2\text{-}11')$$

$$u_z = 0 \qquad \text{(plane strain)}$$

The terms omitted in the above series are not important near the crack tip because the first term dominates, especially in the case of the stresses, since these are proportional to $r^{-\frac{1}{2}}$. The expressions (4.2-11) and (4.2-11') specify the tip region elastic stresses and displacement with a sufficient accuracy.

The term K(which corresponds to K_I in (4.2-10)) is independent of r and θ. It is a positive-defined function which can be shown to depend on the geometry of the cracked body and location of the crack. K depends linearly, moreover, on the applied load. The above mentioned expressions (4.2-11) and (4.2-11') are interesting also because of their generality, since they are valid for all stationary plane cracks, regardless of the geometry of the body or the crack location. When going from a given configuration to another the only change necessary in (4.2-11) and (4.2-11') is the functional form of K. It follows that the stress and strain elastic fields around a crack tip are completely characterized by the Stress Intensity Factor K.

The only exact solutions available in the Opening Mode are relevant to infinitely wide bodies. For the plane, infinitely large, sheet shown in Fig. 4.2-18 (Griffith model)

we have:

$$K = \sigma \sqrt{\pi a} \qquad (4.2\text{-}12)$$

For a penny-shaped crack located in the interior of an infinite solid loaded in uniform tension (Fig. 4.2-19), we have:

$$K = 2\sigma \sqrt{\frac{a}{\pi}} \qquad (4.2\text{-}12')$$

The interesting applied engineering problem of assessing K in cracked structures will be discussed later.

Since the previously mentioned expressions (4.2-11) and 4.2-11') are based on linear elastic analysis, the validity of application of this analysis for practical situations is questionable, unless the influence of any crack tip yielded region on the surrounding elastic stresses and displacements is comparatively small.

If the crack tip region over which plastic deformation takes place is relatively small, the elastically calculated K-formulas will be substantially correct.

A method for the correction of small scale plastic region effects was proposed by Irwin. A brief explanation is reported in Appendix 4.2.B.

4.2.3.4 Failure criterion of linear elastic fracture mechanics

The linear elastic model provides a description of the stress and strain states around the crack tip. Our previous discussion has shown the existence of the quantity K characterizing the intensity of the elastic field in this region. Although the mathematical procedure is beyond the scope of the present discussion(*), we have to quote here an interesting energetic interpretation of the S.I.F. In this interpretation K is connected to the rate of potential energy U of a cracked body with respect to the crack length, as follows:

$$G \equiv -\frac{\partial U}{\partial a} = \frac{K^2}{E} \qquad \text{(plane stress)} \qquad (4.2\text{-}13)$$

$$G \equiv -\frac{\partial U}{\partial a} = \frac{1-\nu^2}{E} K^2 \qquad \text{(plane strain)} \qquad (4.2\text{-}13')$$

(U is the strain energy minus the work of external forces).

In particular (but the result has a general validity) when external forces make no work, K is proportional to the square root of the relaxed elastic energy at a crack tip per unit crack length extension.

Apart from other considerations, it seems now reasonable to suppose that the final failure in a cracked body occurs when the quantity $-(\partial U/\partial a) \equiv G$ assumes a well defined value for a given material. It follows from (4.2.13) that K is constant in a critical condition, i.e.:

$$K = K_C \qquad (4.2\text{-}14)$$

The l.h.s. in eqn. (4.2.14) is a function of the applied stress, the crack lenght and the geometry of the cracked body, whereas the constant K_C is invariant for a given material and characterizes its toughness against fracture. K_C is known as Fracture Toughness (F.T.). Eqn. (4.2-14) is, then, a particular case of (4.2-9). The failure criterion (4.2-14) is the main instrument for assessing the residual static strength of a cracked structure. We will now discuss the assessment of both K and K_C.

4.2.3.5 The assessment of stress intensity factor

Very different problems arise when dealing with through the thickness cracks and embedded or part-through cracks. These will be known (in the rest of the section), respectively, as "through cracks" and "part-through cracks". Both the types will be discussed in this section.

A. Through cracks

The assessment of the S.I.F., in the presence of through cracks in thin plates, can be obtained by means of numerical or analytical calculation.

Closed form solutions are provided in certain configurations, including infinitely wide plates and infinitely wide stiffened panels. Some typical results are given in Fig. 4.2-20. Ref. 3 reports a lot of solutions relevant to unstiffened panels, under various loading configurations, stiffened panels, disks, tubes, bars, etc.....

The solution relevant to stiffened panels derives from the principle of superposition

---

(*) The mathematical procedure can be found, for example, in Ref. 1, ch. 5.

of effects and, in particular, on the superposition of the solutions of the problems in Fig. 4.2-21 (given in Ref. 35).

Stiffeners are supposed to be simmetrical strips connected to the cracked plate through points set on the rivet positions. The forces between cracked plate and stiffeners are transmitted through these points alone; certain non linear phenomena, like friction between plate and stiffeners or the presence of possible plastic deformations around the rivet holes, are disregarded. When refined calculation of the S.I.F. is required, it is possible to modify the model in Fig. 4.2-21 to include the presence of a reasonable distribution of the pressure on the rivet holes.

These closed-form results are particularly interesting because:

. they don't require time consuming calculation;
. they can be used as reference points in order to judge the reliability of numerical computation;
. it is possible to reduce easily an effective stringer to a strip having an equivalent area; Fig. 4.2-22 shows an example of this.

A second way to calculate the S.I.F. in a given structure is provided by the Finite Element Method. This procedure is fundamental when closed-form solutions are not available.

A remarkable improvement in the finite element computations applied to Fracture Mechanics was provided by isoparametric elements with 8 nodes, in bidimensional problems, and with 20 nodes, in the tridimensional ones. In particular it is now possible to simulate the presence of a singularity of the type $r^{-\frac{1}{2}}$ in the stress tensor at the crack tip by means of the particular isoparametric elements shown in Fig. 4.2-23. This procedure is known as "Quarter Point Node Technique". These elements are 8 nodes isoparametric elements with a side collapsed into a point on the crack tip while the nodes on the sides converging into the crack tip are set at a quarter of this side from the crack tip itself. An equivalent modification is carried out on a 20 nodes isoparametric element for three-dimensional problems.

These elements are implemented in important well known programs (for example Ref. 19), together with the options to compute the S.I.F.

The methods for assessing the S.I.F. by the finite element technique can be divided into 2 groups:

a) Direct Methods
b) Energy Methods

a) Direct Methods

Direct methods provide the S.I.F. by means of the expression of

a.1 - Stresses
a.2 - Displacements.

a.1 - Assessment of S.I.F. by the stress method.
S.I.F. can be assessed (both in two and in three-dimensional cracks) by using eqn. (4.2-11); the expression of the stresses are valid around the crack tip and then, many Gauss points(*) are necessary there.
As a consequence, two disadvantages are present:
- a remarkable refinement of the mesh is necessary;
- stresses are calculated as the derivatives of the displacements fields and, of course, the errors are larger than those relevant simply to the displacement method.

a.2 - Assessment of S.I.F. by the displacement method.
As shown in (4.2-11'), the displacements of the points around the crack tip are known functions of the S.I.F.
As a rule, the displacements u_x and u_y are assessed along straight line θ = const., in a set of points so as to obtain diagrams such as in Fig. 4.2-24 is obtained as shown in the same figure.
The method allows us to determine K_I, K_{II}, and K_{III} in bi- and, as it is proved in Ref. 16, in three-dimensional problems.

b) Energy Methods

These methods are known as V.C.E. (Virtual Crack Extension) and are based on the calculation of the relaxed energy per unit crack extension, or G, according to two possible procedures:

b.1 - Total Energy Method
b.2 - J-Integral Method.

b.1 - Total Energy Method.
This method is based on the evaluation of the total potential energy per unit crack

---

(*) Gauss points are certain points inside the elements where the stress tensor is given; displacements are given in the nodes.

extension, $G = -(\partial U/\partial a)$; because of the relationship (4.2-13), $G = K^2/E$, which is valid in L.E.F.M. (in plane stress conditions), we can calculate the S.I.F. by means of the estimation of G.
Some remarks are now necessary:
- two runs of the program are necessary for crack lengths "a" and "a+Δa" (Fig. 4.2-25); this is not a big problem in bidimensional conditions even from an economical point of view;
- some problems exist in the choice of the quantity "Δa"; one needs to be careful about one's choice when Δa is very little, to avoid large errors due to numerical instabilities and, on the contrary, when Δa is too large, to avoid having to compute S.I.F. K as the average value in a large crack rate; many authors suggest that a proper choice for Δa is:
  $\Delta a = (0.01 \div 0.02)a$.
- less refined meshes than those relevant to the direct methods are necessary; it depends on the evaluation of the total energy instead of concentrating the analysis on a local and singular stress or displacement field.
- an accurate estimation of K is possible because finite element methods converge in energy.

b.2 - J-Integral Method.
The J-Integral is a line integral along a path Γ around the crack tip, which is define as follows (Fig. 4.2-26):

$$J = \int_{\Gamma} \left(w\,dy - \underset{\sim}{T} \cdot \frac{d\underset{\sim}{u}}{dx}\, ds \right) \qquad (4.2\text{-}15)$$

where:
w is the strain energy density
$\underset{\sim}{u}$ is the displacement vector
$\underset{\sim}{T} = \sigma_{ij} n_j$
ds is an element of the Γ path.
If one adopts the hypothesis that:
- body is homogeneous but, in general, non-isotropic and non-linear;
- body forces are nil;
- Yielding is present, even in large scale,

the following properties are valid:
1. J is invariant for different paths
2. $J = -\frac{dU}{da}$ (4.2-16)
   where U is the total potential energy of the system.

In plane stress state and small scale yielding it follows from (4.2-13) and (4.2-16) that:

$$J = \frac{K^2}{E} \qquad (4.2\text{-}17)$$

Now, from (4.2-16) and (4.2-17), it follows that S.I.F. K can be evaluated by the assessment of the potential energy rate per unit crack length, in the same way as the Total Potential Energy method. This procedure is implemented in important stress analysis programs (e.g. Ref. 19) and the assessment of K is relatively simple.
Another way to calculate J and then, by (4.2-17), the S.I.F. K, is now in progress; it consists of an evaluation of J as a line integral.
The integration function in (4.2-15) can be evaluated along any integration path; in a finite element computation the integration path passes through the Gauss points of the elements. Up till now, this procedure has not been implemented in important stress analysis programs.

B. Part-through cracks

The analysis of part-through cracks is interesting from an engineering point of view because these cracks are quite common in real structures. Unfortunately, however, a closed form solution of the problem is not available.

On the contrary, a well stated mathematical model exists for an elliptical shaped crack (in Fig. 4.2-19); this shows an infinitely wide body subjected to a uniform tensile stress, directed normally to the crack plane.

Given the notations of Fig. 4.2-19, the equation of the border of the ellipse is:

$$\frac{x_1^2}{a^2} + \frac{z_1^2}{c^2} = 1 \qquad (4.2\text{-}18)$$

If η is taken to indicate the crack opening in a point (x,z) inside the contour of the ellipse, the following result is valid:

$$\eta = \eta_o \left(1 - \frac{x^2}{a^2} - \frac{y^2}{c^2}\right)^{\frac{1}{2}} \qquad (4.2\text{-}19)$$

that is "the applied (uniform)stress produces an elliptical shape of the crack opening". The S.I.F. expression can be obtained by using the following procedure:
1) determine the expression of η in the vicinity of the crack tip;
2) relate K to η in the plane strain state.

By operating in accordance with these two steps, we get the expression of the S.I.F. vs. the position in the ellipse border (given by the angle ϕ) - i.e.:

$$K^2 = \frac{1}{4}\left(\frac{E}{1-\nu^2}\right)^2 \frac{\eta_o^2}{ac}\left(a^2\cos\phi + c^2\,\mathrm{sen}^2\phi\right)^{\frac{1}{2}} \qquad (4.2\text{-}20)$$

The unknown quantity η_o is connected to the applied stress σ. To determine the expression of η_o, we use the previously examined procedure used in through cracks, where we calculated the elastic energy variation relevant to a small increment of crack contour.

The final expression of the Released Elastic Energy G, where G is connected to K according to (4.2-13') is, then:

$$G = \frac{\pi(1-\nu^2)}{E\Phi^2}\,\sigma^2\left(\frac{a}{c}\right)\left(a^2\cos^2\phi + c^2\,\mathrm{sen}^2\phi\right)^{\frac{1}{2}} \qquad (4.2\text{-}21)$$

Some remarks are necessary:

i) G (and K) is a function of the position on the ellipse contour; it varies according to ϕ and reaches a maximum where the crack contour intersects the minor axis ($\phi=\pi/2$); here we have $K^2=\sigma^2 a/\Phi$, where Φ is defined in (4.2.22);

ii) it follows that the crack shape in the x-z plane tends to become circular in subcritical static and fatigue propagation;

iii) Φ varies with a/c. In particular:
$\Phi = \pi/2$ for a circular crack shape,
$\Phi = 1$ in the extreme case in which "a" tends to zero.
The complete expression of Φ is:

$$\Phi = \int_o^{\pi/2} \left\{\mathrm{sen}^2\phi + \frac{a^2}{c^2}\cos^2\phi\right\}^{\frac{1}{2}} d\phi \qquad (4.2\text{-}22)$$

The solution of the problem of the part-through crack in Fig. 4.2-27 can be gained by adopting the following steps:

A. solve the previous problem of an elliptical crack embedded in an infinitely large solid;

B. correct this solution by means of factors relevant to the real situation; that is:
   1) the correction relevant to the plane passing through the major axis of the ellipse,
   2) the correction relevant to the presence of small scale yielding around the crack tip,
   3) the correction of the presence of a free α' surface parallel to α in Fig. 4.2-27.

To assess the S.I.F., these three corrections must be evaluated. When "a" is small with respect to "c" and plate thickness B, the coefficient 1.2 takes conventionally into account the presence of the two planes α and α'. The presence of α' has little importance however. This correction can be applied in the range:

$$\frac{a}{c} < 0.1 \qquad \frac{a}{B} < 0.5$$

When a/B > 0.5 the presence of the plane α', opposite to α, becomes important and, in particular, it improves K (and G) in the thickness direction.

This effect can be taken into account by the so-called "Stress Intensity Magnification Factor" (Fig. 4.2-28). The mathematical hypotheses and many results for M_f are given in Ref. 41.

No satisfactory solution exists to carry out some correction relevant to the presence of the plastic zone at the crack border. We can consider the plastic zone effect to be equivalent to a virtual crack extension.

This criterion leads us to obtain the final expression of the maximum S.I.F. as follows:

$$K^2 = \frac{1.2\,\sigma^2 a}{\Phi^2 - 0.212\,(\sigma/\sigma_{ys})^2} \qquad (4.2\text{-}23)$$

where the term depending on σ/σ_{ys} is connected with the plastic zone correction, and the coefficient 1.2 is relevant to the presence of the lateral planes.

In general, linear elastic S.I.F. solutions can be provided by the finite element

method alone. The elements utilized are usually 20 nodes three-dimensional isoparametric elements, the singularity at the crack border being obtained by means of the quarter point node technique. The S.I.F. is assessed by the relationship:

$$K = \frac{u_z E}{2(1-\nu^2)} \frac{\sqrt{\pi}}{r} \qquad (4.2\text{-}24)$$

where u_z is the displacement according to the direction of the load applied, r is the distance of the control point from the crack border, and the projection of the $\underset{\sim}{r}$ vector in the x-z plane is normal to the crack border itself (Fig. 4.2-29).

Fig. 4.2-30 shows a typical mesh in a little substructure containing the crack border; typical results are shown in Fig. 4.2-31.

It must be remarked that these finite element computation are very time consuming if a sufficient accuracy of results is required in every point along the border. A less refined mesh and, consequently, less expensive computation is required to obtain a good agreement only in the positions $\phi=0$ and $\phi=\pi/2$ (Fig. 4.2-31), where K is minimum or maximum.

4.2.3.6 The assessment of fracture toughness

Our previous discussion has shown that the value of F.T. characterizes the strength of a material with respect to fracture, while allowing us to assess its residual static strength on the basis of eqn. (4.2-14).

In principle, to assess the quantity K_c we can choose any cracked specimen for which the expression of the S.I.F. $K(\sigma,a)$ is given. Eqn. (4.2-14) is valid independently of the specimen configuration or crack position. The critical values of applied stress, σ_c, and crack length, a_c, which correspond to the beginning of an unstable propagation, define K_c. But since it has already been stated that a certain amount of brittleness exists in the metallic materials used in engineering, according to the thickness of the cracked plates, one might then expect to find a certain degree of fracture toughness variations with regards to the thickness.

Experiments have shown this to be true. This is illustrated in the qualitative K_c vs thickness diagram (Fig. 4.2-32). These experiments also show that a correlation exists between fracture surface appearance and thickness, which indicates that an embrittlement takes place in large thicknesses.

Beyond a certain thickness, the F.T. K_c approaches a minimum value. This is usually indicated as K_{Ic} i.e. Plain Strain Fracture Toughness. This quantity is independent of thickness and it allows us to operate a preliminary selection of materials with respect to their behaviour against fracture.

Some basic remarks are now necessary:

i) a selection of materials on the basis of K_{Ic} values is certainly valid in plane strain conditions, but these conclusions cannot always be transferred to structures having a thickness in the transition range. The situation shown in Fig. 4.2-33 can, in fact, occur.

ii) because of the dependency on thickness, the assessment of K_c is not less important than K_{Ic} values, especially in the design of aerospace structures. Design based on the Plane Strain Fracture Toughness would give rise to unreasonable thick panels or too many stiffeners.

Another possible influence on K_c is due to temperature.

Experimental observations have indicated that K_c and K_{Ic} can be expected to show a certain temperature dependence and, in particular, both these quantities tend to increase as the temperature is raised.

This is valid especially for steel, where it would be desirable to have information on the toughness over the whole range of possible service temperatures. When dealing with aluminium alloys, experience shows that no particular dependence of K_c on the service temperature exists.

Now, for the sake of clarity, we can divide the discussion into two sections: A) Small thickness F.T. tests, and B) Plain strain F.T. assessment.

A. Small thickness F.T. tests

F.T. was supposed to be invariant for a given material, independently of the geometrical configuration of specimens, crack position and loading condition. The assessment of F.T. in small thickness plates is usually carried out in flat panels centrally cracked and loaded normally to the crack line (as shown in Fig. 4.2-13).

A qualitative trend of the σ-a curve (σ is the average applied stress), is shown in Fig. 4.2-34, where we can distinguish three stages, i.e.:

1) $\sigma<\sigma_i$, without crack propagation;
2) $\sigma_i<\sigma<\sigma_c$: the "subcritical or stable crack propagation", so called because an extension of a crack is possible only by increasing the load applied;

3) $\sigma=\sigma_c$ or "critical condition". The F.T. is assessed by checking this quantity together with the correspondent crack length "a_c".

Transition from stage 1) to 2) is not always clearly detectable because of the presence of slip bands at the crack tip. Moreover the crack grows by steps at the low values of the applied load in stage 2) (especially for high strength materials).

The σ-a curve becomes more and more regular as it reaches the point of transition between stage 2) and 3); the $\Delta a/\Delta\sigma$ velocity grows continuously up to not clearly defined "high values", that are no longer measurable. The consequence is that the critical value of applied stress and, above all, of the crack length can depend on the test rig and the methodology adopted.

Engineers are used to taking shortcomings into account by means of "safety factors", whose values are defined in accordance with the degree of uncertainty of the values of the parameters.

Recently the probabilistic approach has gained acceptance as far as the figures for safety factors are concerned. This approach recognizes that any structure is prone to failure and this probability to failure can be calculated by a proper use of statistics. It is beyond the scope of the present section to go into more detail about these problems. The existence of specialized literature dealing with these (for an e.g. of this see Ref. 37), allows us to elaborate experimental data statistically.

It is easy to assess now the factors by which the average values of the quantities we are dealing with (such as, for example, K_c), must be reduced in order to obtain the required probability of survival.

The values of K_c to be used in a design, relevant to all the materials which are usually utilized here, are given in Ref. 2. It is, nevertheless, common practice to carry out F.M. tests on specimens drawn up from a batch of material used.

No particular problem exists as far as test machines are concerned. Usually very thick plates are used, in order to clamp specimens at the boundaries according to the loading condition.

Many techniques exist for assessing the crack length during the subcritical stage. It is usual practice to record the crack history by means of a television camera or, more simply, by using a camera.

A typical σ_c vs a_c diagram for a plate panel is shown in Fig. 4.2-35, which qualitatively indicates that the invariability of K_c is not possible, when dealing with small or very large cracks in a specimen.

It would mean that when "a" is very short or, theoretically speaking, when it tends to zero, we would obtain an infinite value of σ_c and this is clearly impossible. When "a" becomes very large, or it tends to be as large as the panel width, the failure mode can be no more governed by the laws of fracture mechanics.

Feddersen (Ref. 39) proposed to modify the σ_c vs a_c curves in these two extreme ranges of crack lengths according to the previously figures. It follows from this that a comparison of K_c values relevant to specimens of the same thickness and different materials has got significance only when the critical values of the crack length and applied stress are within the field of valid K_c tests.

B. Plane strain F.T. tests

It has already been stated that plane strain F.T. tests aim at assessing the quantity K_{Ic}, and that very large specimen sizes are necessary in order to maintain the validity of the linear elastic K characterization of the crack tip stress field.

The minimum specimen thickness required, in order to have valid plane strain F.T. tests, is established on the basis of the results of experiments. In fact, it can be observed that, in order to have a flat fracture surface larger than ninety percent, we need a minimum thickness $B \cong 40\ r_y$ - where r_y is the size of the plastic enclave. According to (4.2.C-3) in App. 4.2.C, in other words, for all thickness values $B \geq 2.1(K_I/\sigma_{ys})^2$, F.T. tests carried out on any specimen configuration will yield approximately the same K_{Ic} value.

The requirements for K_{Ic} tests of the American Society for Testing Materials (ASTM) specify an even larger specimen thickness for a given crack length, in order to ensure valid K_{Ic} values. The requirement is:

$$B \geq 2.5 \left(\frac{K_{Ic}}{\sigma_{ys}} \right)^2 \qquad (4.2\text{-}25)$$

Possible specimen geometries are shown in Fig. 4.2-36, but the most usual configurations are those shown in Fig. 4.2-14 -i.e., Compact Tension and Bending specimens.

4.2.3.7 Residual static strength evaluation

As already pointed out, the assessment of residual static strength in small thickness structures and in internal or plane strain conditions require two different kinds of

considerations. We will discuss these two situations separately.

A. Small thickness structures

A.1 The Stress Intensity Factor Approach

Let us consider first the above mentioned Griffith model. If we apply the $K=K_c$ equation, and suppose again that the critical stress in a damage tolerant structure is assigned, for given fracture toughness, it is then possible to assess the critical crack size, a_c, in the form $a_c=K_c^2/(2\pi\sigma_c^2)$. When dealing with flat unstiffened panels the critical crack length can be obtained by means of experimental results, like that shown in Fig. 4.2-35. In this figure we have: $a_c=a_o+\Delta a_c$, where a_o is the initial crack length and Δa_c the total subcritical crack propagation. If a_o is assigned, an estimate of Δa_c is necesary, for any a_o. In other words, the function $\Delta a_c=f(a_o)$ has to be assessed by means of tests. A typical result is shown in Fig. 4.2-37.

Sometimes, this correction Δa_c on crack length, a_o, is disregarded, especially in the case of more brittle materials.

As far as stiffened panels are concerned, Fig. 4.2-38 shows different ways of possible failure in relation to stringer stiffeness and stringer distance. In particular, a crack length range may exist, where crack arrest becomes possible after the critical condition has been reached. In stiffened panels, yielded regions exist not only around the crack tip but also in relation to the rivets connecting the cracked plate to the stiffeners. The influence of this phenomenon produces certain modifications in the final crack length prediction, as Fig. 4.2-39 qualitatively shows.

A.2 R-Curve Approach

In metallic materials, plastic deformation occurs in front of the crack and some energy is expended in the formation of a new plastic zone at the crack tip. Experiments show that plastic energy is the same for every crack increment in plane strain, whereas it varies with the amount of crack length in plane stress state.

Figure 4.2-40, which illustrates thin plates in a plane stress state, shows that the crack starts to propagate at a certain stress level, and a further increase of the applied load is required in order to maintain crack propagation. During this crack propagation phase the rate of energy released is just equal to a "crack resistance" R, which increases as a result; Fig. 4.2.41 schematically shows this.

Suppose a crack is present, a_i, and a stress is applied, σ_1, the available energy release is given by A. This value, however, is too low for a crack extension.

Crack starts to propagate at $\sigma = \sigma_i$, and failure occurs at $\sigma=\sigma_c$, (Point E) where:

$$G = R \quad \text{and} \quad \frac{\partial G}{\partial a} = \frac{\partial R}{\partial a} \ .$$

Krafft et alii (Ref. 39) suggested that the R curve is invariant for a given material; in other words, that R-curve is the same irrespective of initial crack length. (Fig. 4.2-43).

This hypothesis, often accepted without reservations, is satisfactory only in the range of crack length, where K_c is also invariant, as shown in Fig. 4.2-42, which illustrates the experiments on Aluminum alloy 2024-T3.

In stiffened panels the situation is qualitatively modified as shown in Fig. 4.2-43 and different possibilities exist, including the start of a crack (point B') and its stopping (point C').

B. Plane strain conditions

The assessment of residual static strenght in plane strain state is provided suitably by the Fracture Criterion of L.E.F.M. $K=K_{Ic}$, irrespective of the subcritical crack extension.

Let us consider, first, a penny shaped crack (such is the case where an elliptical embedded crack becomes circular) of radius a, in an infinite solid under the action of a tensile uniform stress, σ, normal to the crack plane.

By means of the espression (4.2-12') of the Stress Intensity Factor, we get:

$$a_c = \frac{\pi}{4}\left(\frac{K_{Ic}}{\sigma}\right)^2$$

A structure is assessed to be safe just when these penny-shaped flaws have diameters smaller than $2a_c$.

Other solutions both numerically and, sometimes, experimentally are provided in a lot of configurations such as flaws in corner holes, etc.

In situations different from those, the assessment of a_c is more complicated and only suitable finite element computations of K are possible.

Nevertheless the method for assessing residual static strength is the same.

Finally, a final remark needs to be made as regards the modification of the expres-

sion of K, due to the crack tip plastic front. This modification, which gives rise to a non-linear problem, is generally disregarded because of the high brittleness of fracture in these plane strain conditions.

4.2.4 FRACTURE MECHANICS APPROACHES IN COMPOSITE STRUCTURES

The Fracture Mechanics methods are not profitably extensible to composite materials, because the anisotropy and the inhomogeneity of these materials cause quite different patterns of local stress concentrations and damage developments. The typical pattern of the damage growth usually found in metallic materials, namely nucleation and crack growth in the direction perpendicular to the principal stress up to the critical dimensions does not take place in composite materials. With this type of material, various damage forms can develop; in particular, multidirectional laminates, that are the basic components of a composite structure, show different kinds of damage: transverse matrix cracking, delamination, fibre-matrix debonding, matrix voids growth, local fibre breakage, out-of-plane buckling of deliminated plies. Each one of these damage mechanisms can be present and even interact with the others, according to the type of fibre, matrix, geometry and loading.

Fig. 4.2-44 shows a sketch of a section of a typical carbon fibre reinforced plastic (CFRP) multidirectional laminate. Transverse matrix cracks develop, starting in the 90°-layers, and may initiate cracks in neighbouring 45°-plies, but are restrained by 0°-plies. The stress concentration due to transverse matrix cracks may initiate delaminations, which is a dominant failure mechanism.

The behaviour of a typical boron fibre reinforced plastic (BFRP) laminate usually is slightly different, because the adiacent plies, oriented in different directions, offer a lower resistance to the growth of transverse cracks in the thickness, because of the larger fibre diameter (average 0.15 mm for boron, while carbon fibre diameter is about 0.008 mm). Besides, delamination occurs in BFRP in a slightly minor extent with respect to CFRP, while more frequently fibre breakage is a significant fatigue degradation mode. This is due to local stress concentrations, which are consequence of the irregularities in the fibre surface, unavoidably introduced by the production technique of vapours deposit.

In conclusion, as a consequence of the complexity and variety of the damage forms, whose developments depend also on the nature, geometry and loading conditions, as it has been briefly outlined above, the existing F.M. methodologies do not lead to useful applications, from an engineering point of view, in the field of composite materials. Moreover, no other available criterion seems to be able to predict reliably the fatigue failure and/or the residual strength of a composite structure. A large research activity is required in this field to obtain, analyze and interpret rationally experimental data on damage growth.

4.2.5 REFERENCES

1 Broek D., Elementary Engineering Fracture Mechanics. Noordhoff Int. Publ., Leyden, 1974.
2 Rooke D.P. et alii, Simple Methods of Determining Stress Intensity Factors. AGARDograph 257, Ch. 10, 1980.
3 Rooke D.P., Cartwright D.J., Compendium of Stress Intensity Factors. London, HMSO, 1976.
4 Schijve J., Four Lectures on Fatigue Crack Growth. Delft Univ. of Technology, Report LR-254, 1977.
5 Elber W., Fatigue Crack Closure under Cyclic Tension. Eng. Fracture Mech., Vol. 2, pp. 37-45, 1970.
6 Elber W., Crack Closure and Crack Growth Measurements in Surface-flawed Titanium alloy Ti-6A1-4V. NASA TN-D 8010, 1975.
7 Rice R.C. et alii, Consolidation of Fatigue and Fatigue Crack Propagation Data for Design Use. NASA CR-2586, 1975.
8 Schijve J., The Accumulation of Fatigue Damage in Aircraft Materials and Structures. AGARDograph 157, 1972.
9 Trebules V.W. et alii, Effect of Multiple Overloads on Fatigue Crack Propagation in 2024-T3 Aluminium Alloy. ASTM STP 536, pp. 115-146, 1973.
10 Schijve J., Fatigue Damage Accumulation and Incompatible Crack Front Orientation. Eng. Fracture Mech., Vol. 6, pp. 245-252, 1974.
11 Wheeler O.E., Spectrum Loading and Crack Growth. J. of Basic Eng., Trans. ASME, Series D, pp. 181-186, 1962.
12 Wood H.A., A Summary of Crack Growth Prediction Techniques. AGARD LS-62, 1973.
13 Eidinoff H.L., Bell P.D., Application of the Crack Closure Concept to Aircraft Fatigue Crack Propagation Analysis. 15th I.C.A.F. Conference, 1977, Darmstadt.
14 Führing H., Seeger T., Remarks on Load-interaction Effects Based on Fatigue Fracture Mechanics Calculations. 9th I.C.A.F. Symposium on Aeronautical Fatigue, Darmstadt, 1977.

15 Führing H., Seeger T., Dugdale Crack Closure Analysis of Fatigue Cracks under Constant Amplitude Loading. Engineering Fracture Mechanics, Vol. 11, Number 1, 1979.
16 Newman J.C., A Finite-Element Analysis of Fatigue Crack Closure. ASTM STP 590, pp. 281-301, 1976.
17 de Koning A.U., van der Linden H.H., Prediction of Fatigue Crack Growth Rates under Variable Loading Using a Simple Crack Closure Model. NLR MP 81023 U, 1981.
18 Sih G.C., Handbook of Stress Intensity Factors. Bethlehem, Pa., Lehigh Univ., 1973.
19 MARC Analysis Res. Corp. . MARC User Manual.
20 Wood H., Engle R., USAF Damage Tolerant Design Handbook: Guidelines for the Analysis and Design of Damage Tolerant Aircraft. AFFDL-TR-79-3021, Air Force Flight Dynamics Laboratory, 1979.
21 Osgood C.C., Fatigue Design. Wiley Int., 1970.
22 Description of a Fighter Aircraft Loading Standard for Fatigue Evaluation. I.C.A.F. Doc. 839, 1976.
23 de Jonge J.B. et alii, A Standardized Load Sequence for Flight Simulation Tests on Transport Aircraft Wing Structures. LBF-Bericht FB-106, NLR TR 73029C, ICAF Doc. 665.
24 Salvetti A., Cavallini G., Lazzeri L., The Fatigue Crack Growth under Variable Amplitude Loading in Built-up Structures. Final Technical Report, DA ERO-78-G-107, European Research Office, 1982. ICAF Doc. 1300.
25 Schutz D., Planning and Analysing a Fatigue Test Programme. AGARD LS 118, 1981.
26 Schutz W., Forgings, Including Landing gears. AGARDograph 257, Ch. 6, 1980.
27 Nowack H., Fatigue Test Machine. AGARD LS 118, 1981.
28 Edwards P.R., Methods of Obtaining Crack Growth Data in Metals. AGARD LS 118, 1981.
29 Hudak S.J. and Bucci R.J. Editors, Fatigue Crack Growth Measurements and Data Analysis. ASTM STP 738, 1981, Appendix I and II.
30 Hald A., Statistical Theory with Engineering Applications. J. Wiley Inc., 1952.
31 Little R.E., Jebe E.H., Statistical Design of Fatigue Experiments. Applied Science Publ., 1975.
32 de Jonge J.B., The Use of Standardized Fatigue Load Sequences in Coupon and Component Tests. NLR MP 80001 U, 1980, ICAF Doc. 1202.
33 Paris P.C., The Growth of Fatigue Cracks Due to Variations in Load. Ph. Thesis, Lehigh, Univ., 1962.
34 Poe C.C., Stress Intensity Factor for a Cracked Sheet with Riveted and Uniformly Spaced Stringers. NASA TR R-358, 1971.
35 Newman J.C., Raju I.S., Stress Intensity Factors for a Wide Range of Semi-elliptical Surface Cracks in Finite Thickness Plates. Eng. Fracture Mechanics, Vol. 2, pp. 817-829, 1979.
36 Feddersen C.E. et alii, An Experimental and Theoretical Investigation of Plane Stress Fracture of 2024-T3 Aluminium Alloy. NASA CR-1678.
37 Schutz W., Treatment of Scatter of Toughness Data for Design Purposes. AGARDograph n. 257, Ch. 8A, 1980.
38 Proceedings of "Meeting and Panel Discussion about Industrial Systems for Crack Speed and Propagation Resistance Prediction". Organized by Costruzioni Aeronautiche Giovanni Agusta, Milano, 1979.
39 Krafft J.M. et alii, Effect of Dimensions on Fast Fracture Instability of Notched Effects. Proc. of the Crack Propagation Symp., Vol. I, pag. 8, Cranfield, England, 1961.
40 Vlieger H., Built-up Structures. AGARDograph n. 257, Ch. 3, 1980.
41 Shah R.C., Kobayashi A.S., Elliptical Crack in a Finite-Thickness Plate Subjected to Tensile and Bending Loading. J. of Press. Vessel Technology, pp. 47-54, February 1974.
42 Kullgren T.E., Smith F.W., Part-elliptical Cracks Emanating from Open and Loaded Holes in Plates. J. of Eng. Materials and Technology. Trans. of ASME, Vol. 101, pp. 12-17, January 1979.
43 Schijve J., Hoeymakers A.H.W., Fatigue Crack Growth in Lugs and the Stress Intensity Factor. Delft Univ. of Technology, Report LR-273, 1978.
44 Corrosion Fatigue Technology, ASTM STP 642, 1978.
45 Corrosion Fatigue, AGARD CP n. 316, 1981.
46 Damage Tolerant Handbook. Metals and Ceramics Information Center, Battelle, Columbus, Ohio, 1975.
47 Blom A., The Threshold Stress Intensity Factor in Fatigue. Institute of Technology, Linköping, Sweden, Lith-IKP-S-136, 1980. ICAF Doc. 1180.
48 Frediani A., An Evaluation of the Reliability of Fracture Mechanics Methods. Eng. Fract. Mechanics, Vol. 14, 1981, pp. 289-322.

a) Damaged sites showing nucleation of microcracks and some coalescence (microgrowth)

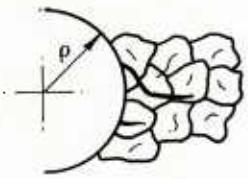

b) Further microgrowth and appearance of dominant crack

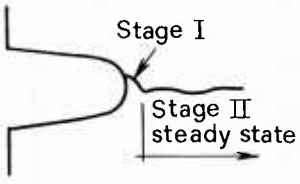

c) Steady state extension of dominant crack

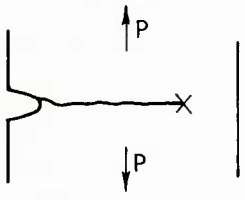

d) Final fracture imminent

Fig. 4.2-1 Sequence of events from microcrack nucleation to final fracture, from AGARDograph 176.

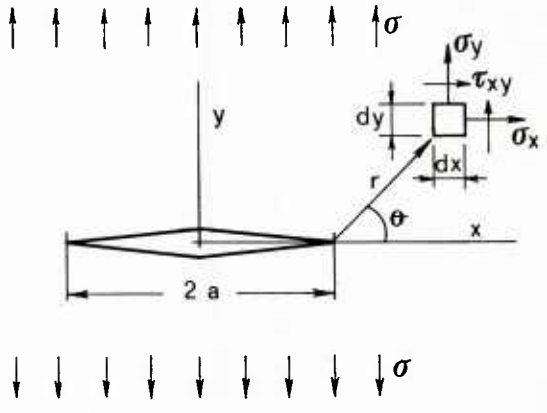

$$\sigma_x = \sigma \sqrt{\frac{a}{2r}} \cos\frac{\theta}{2}\left[1 - \sin\frac{\theta}{2}\sin\frac{3\theta}{2}\right]$$

$$\sigma_y = \sigma \sqrt{\frac{a}{2r}} \cos\frac{\theta}{2}\left[1 + \sin\frac{\theta}{2}\sin\frac{3\theta}{2}\right]$$

$$\tau_{xy} = \sigma\sqrt{\frac{a}{2r}} \sin\frac{\theta}{2}\cos\frac{\theta}{2}\cos\frac{3\theta}{2}$$

$\sigma_z = 0$ (plane stress)

$\sigma_z = \nu(\sigma_x + \sigma_y)$ (plane strain)

Fig. 4.2-2 Stress state at the crack tip.

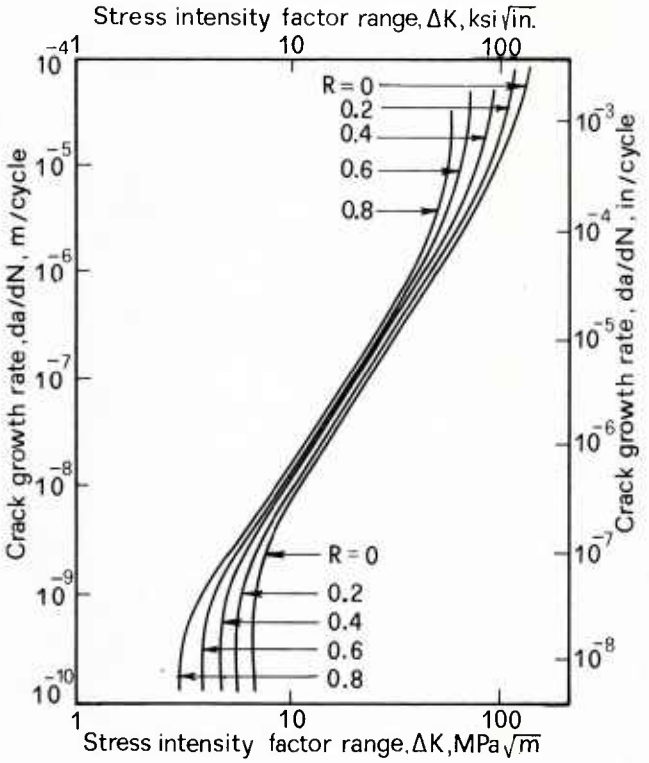

Fig. 4.2-3 Typical (da/dn) vs. ΔK relationship.

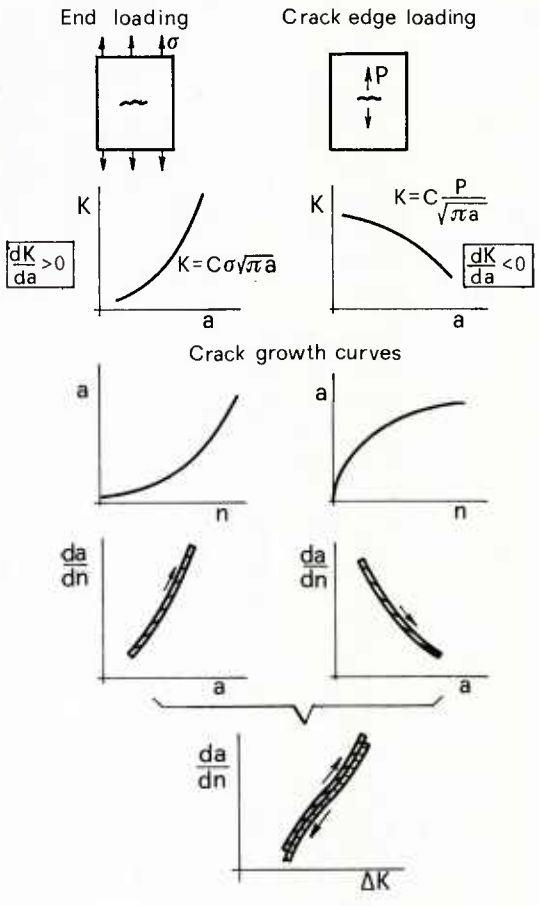

Fig. 4.2-4 Procedure for evaluating the (da/dn)-ΔK relationship in two different cases (Ref. 4).

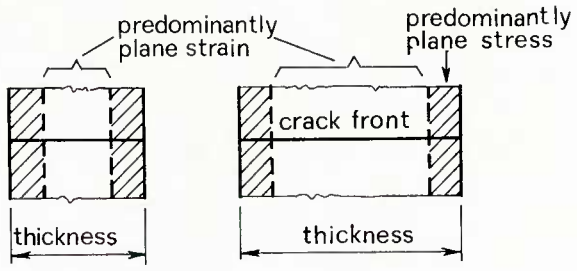

Fig. 4.2-5 Plain strain and plain stress zone in the thickness, (Ref. 4).

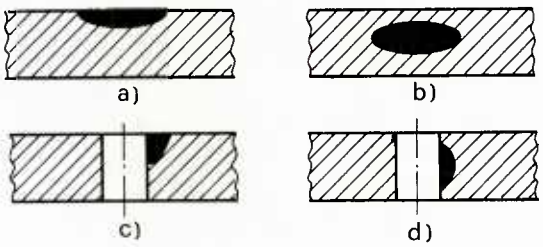

Fig. 4.2-6 Typical flaws of technical interest. A formula for the stress intensity factor can be found in several references among which can be quoted Ref. 3, 41 for the cases a) and b), and Ref. 42, 43 for the cases c) and d).

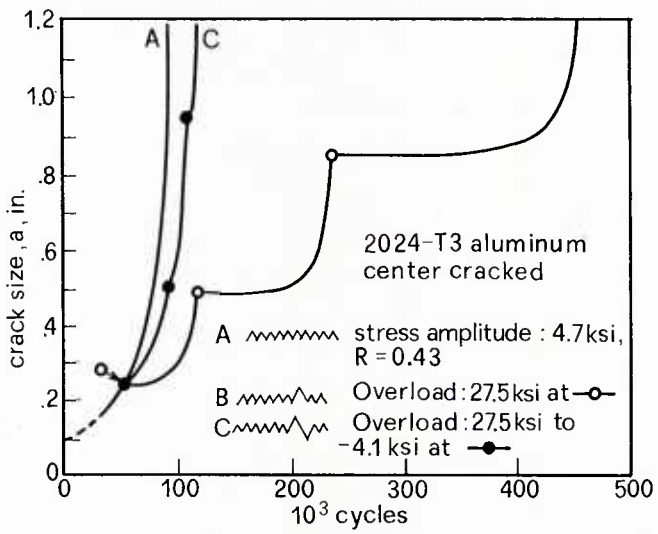

Fig. 4.2-7 Interaction effects due to overload and overload-underload cycles, (Ref. 8).

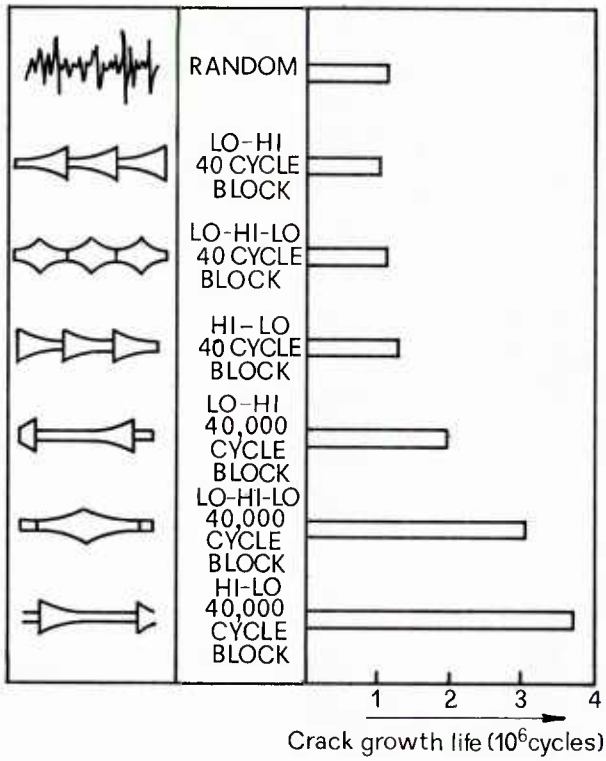

Fig. 4.2-8 Effect of load history on crack growth life, (Ref. 8).

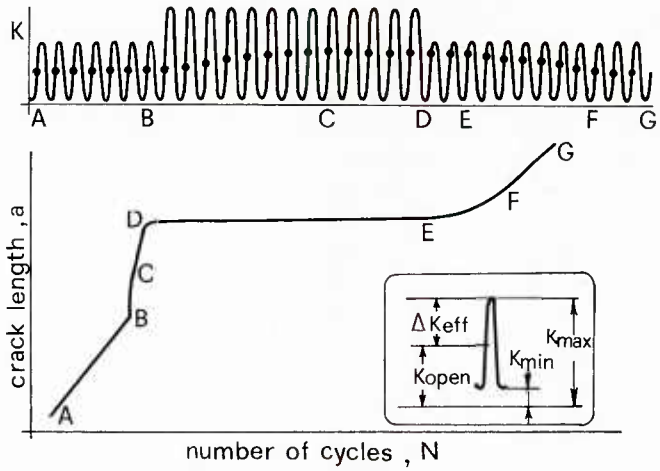

Fig. 4.2-9 Explanation of interaction effects by means of Elber's model, (Ref. 9).

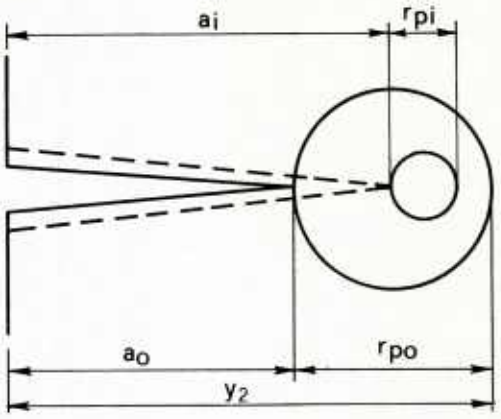

Fig. 4.2-10 Wheeler model.

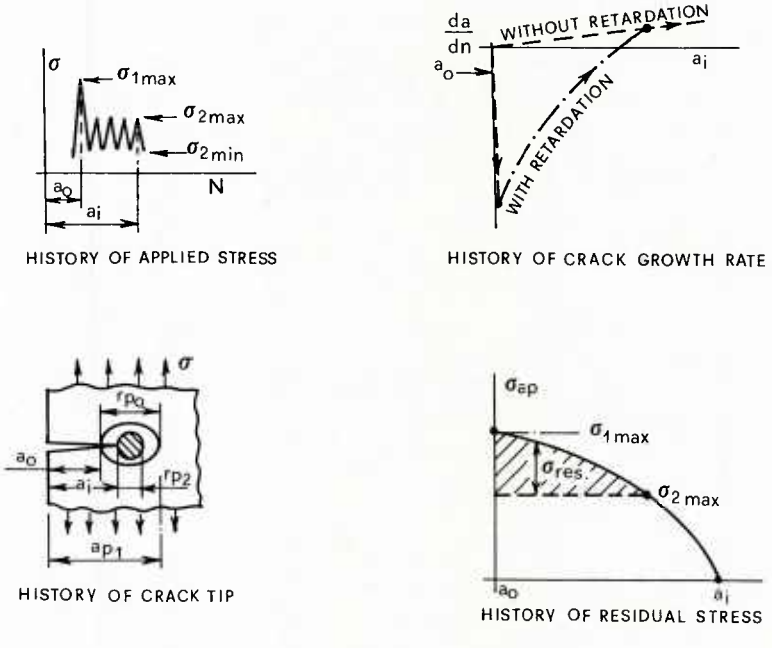

$$a_i + \frac{\sigma_{ap}^2 (\pi a_i)}{\beta \sigma_y^2} = a_{p_1}$$

$\beta = 2\pi$ FOR PLAIN STRESS

$\beta = 4\sqrt{2\pi}$ FOR PLAIN STRAIN

$$\sigma_{ap} = \sigma_y \sqrt{\frac{(a_{p_1} - a_i)}{(\pi a_i / \beta)}}$$

$$\sigma_{res.} = \sigma_{ap} - \sigma_{2max}$$

$$(\sigma_2)_{eff.} = \sigma_2 - \sigma_{res.}$$

Fig. 4.2-11 Willenborg model.

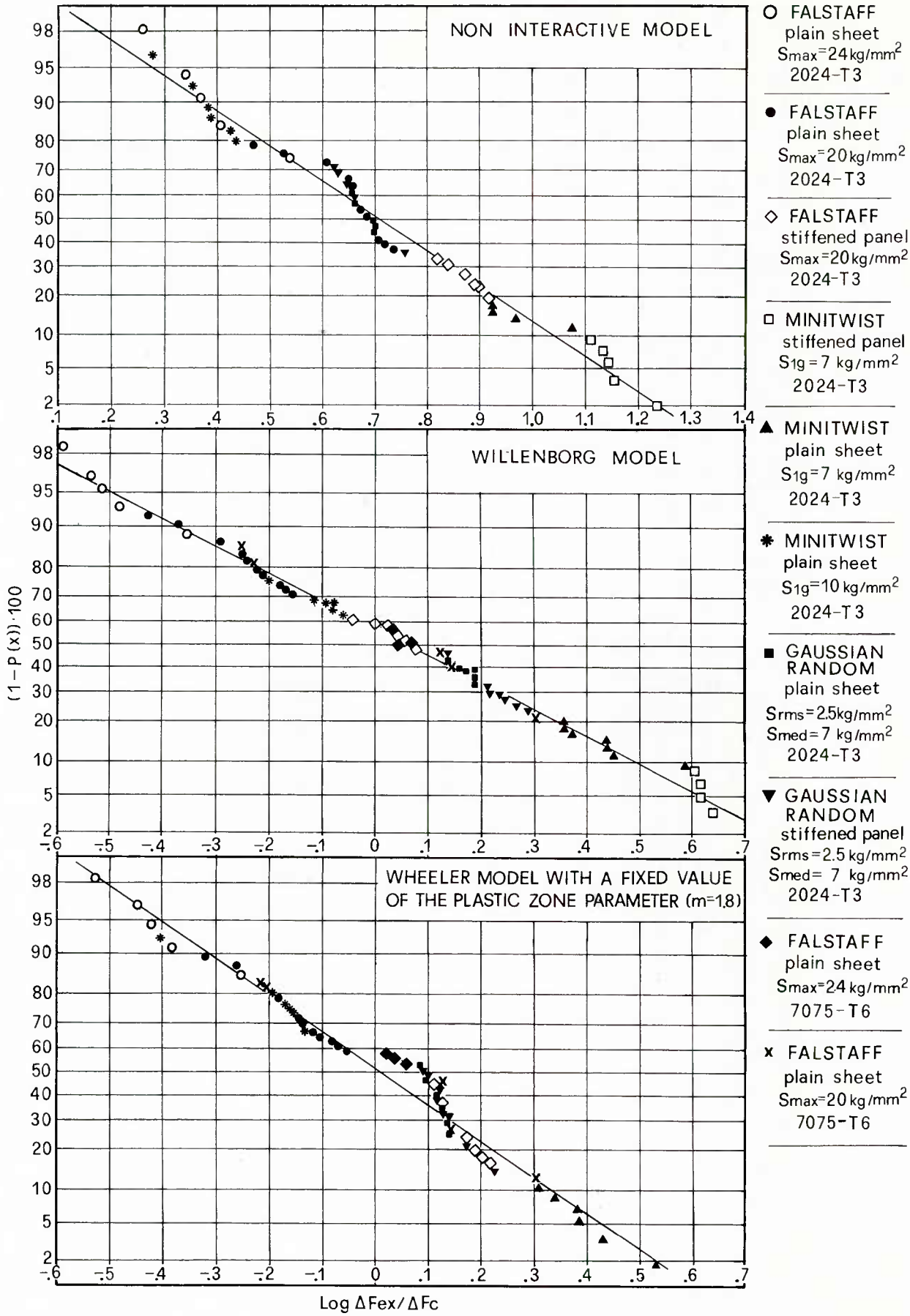

Fig. 4.2-12 Normal distribution of the variate $\text{Log}(\Delta F_{ex}/\Delta F_c)$, where ΔF_{ex} and ΔF_c are the number of flights required, according to experimental results and to predictions, respectively, for a given crack growth interval. From Ref. 24.

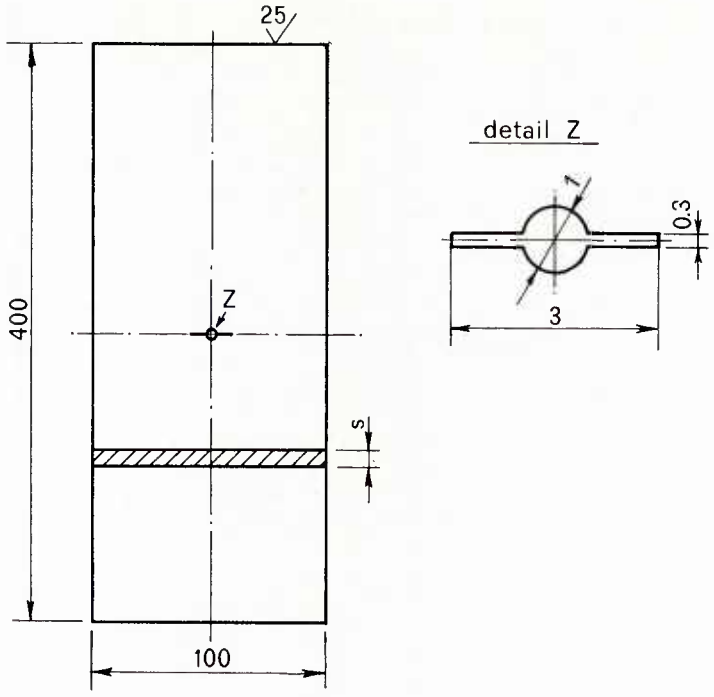

Fig. 4.2-13 Crack propagation specimen, (Ref. 25).

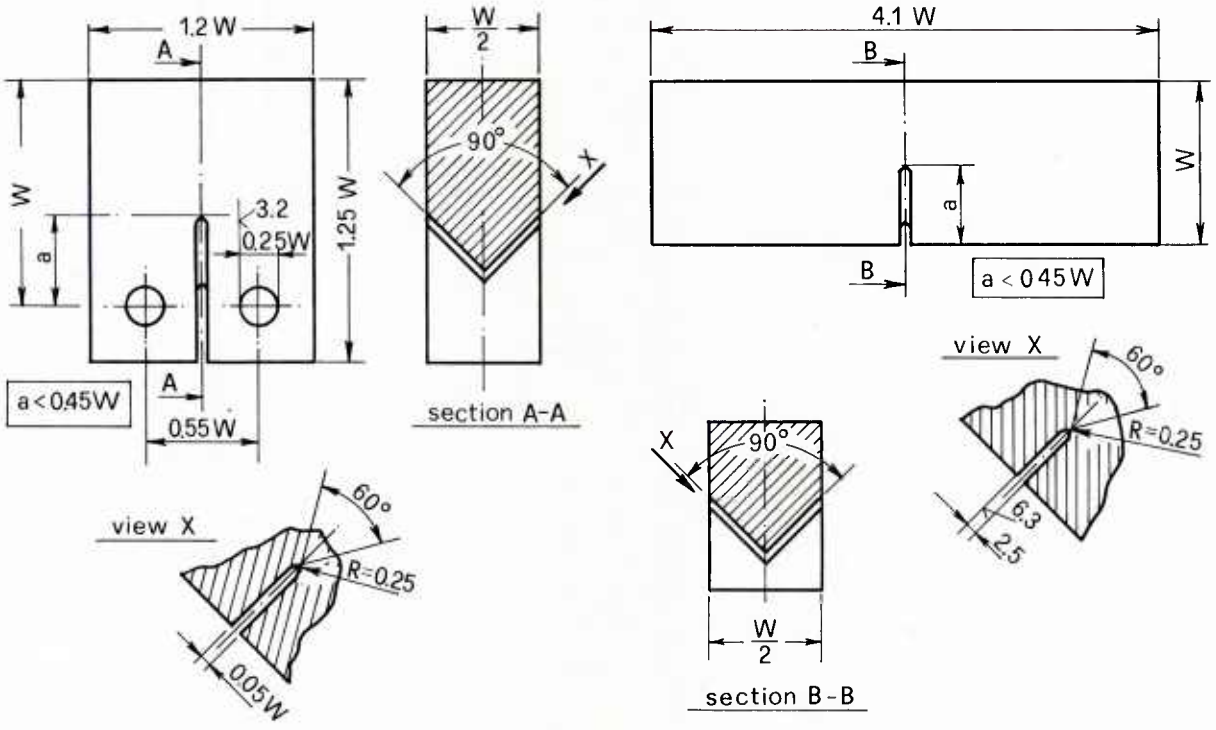

Compact tension specimen
acc. to ASTM

Bending specimen
acc. to ASTM

Fig. 4.2-14 Standardized Fracture Mechanics specimen, (Ref. 25).

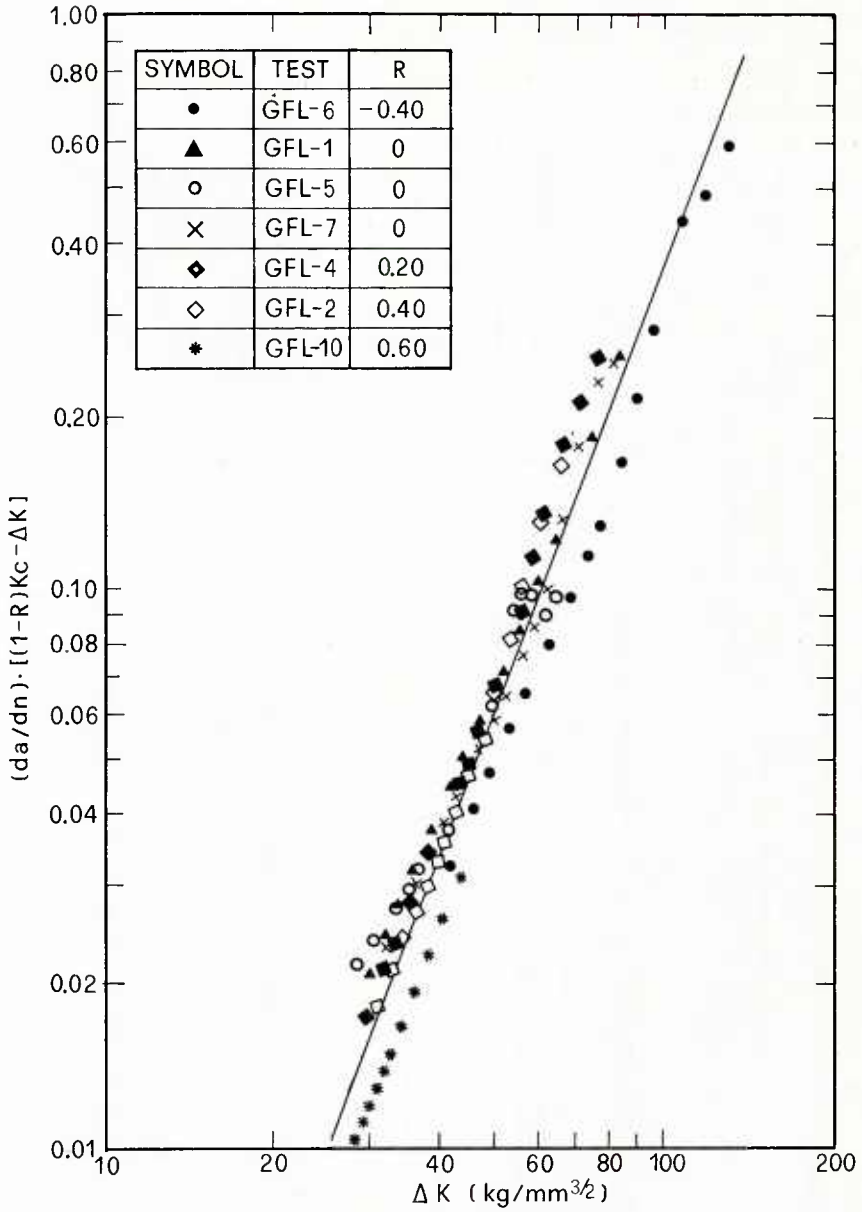

Fig. 4.2-15 Typical output of the procedure to obtain Forman's law. The figure shows the test data and the best-fit line, (Ref. 24).

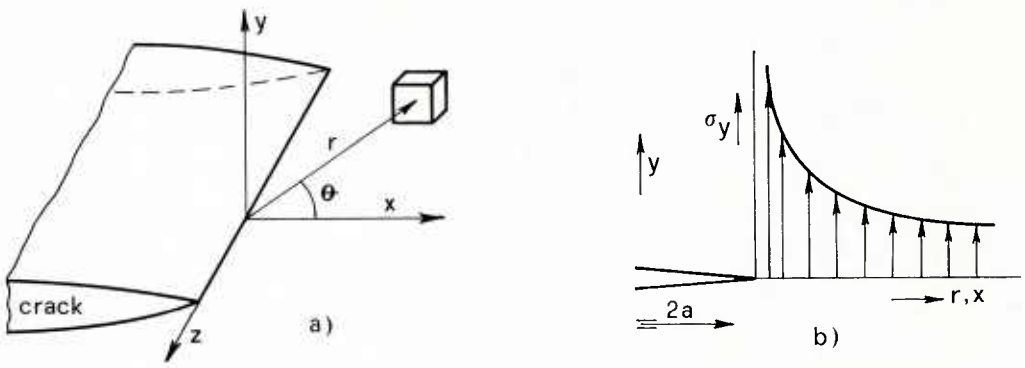

Fig. 4.2-16 Reference system and distribution of the stress σ_y, along the x-axis.

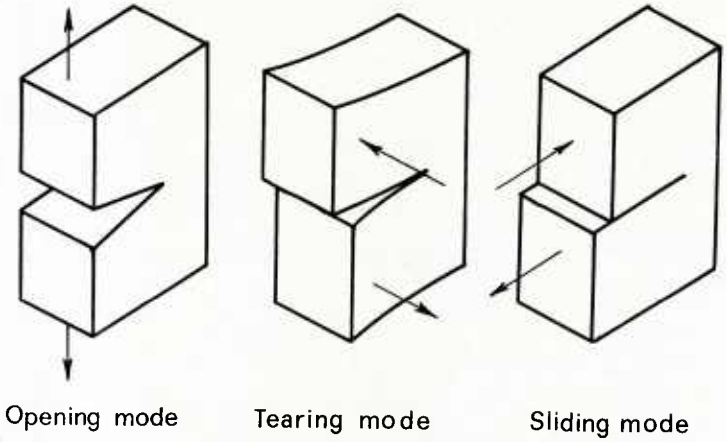

Fig. 4.2-17 Fundamental modes in Fracture Mechanics.

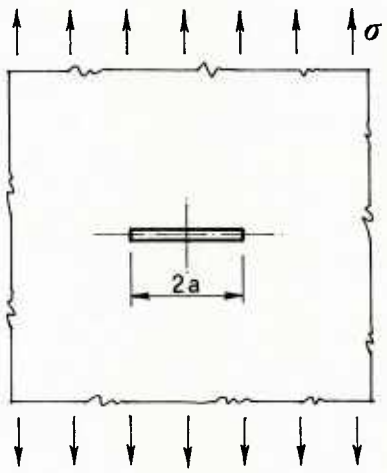

Fig. 4.2-18 Griffith model.

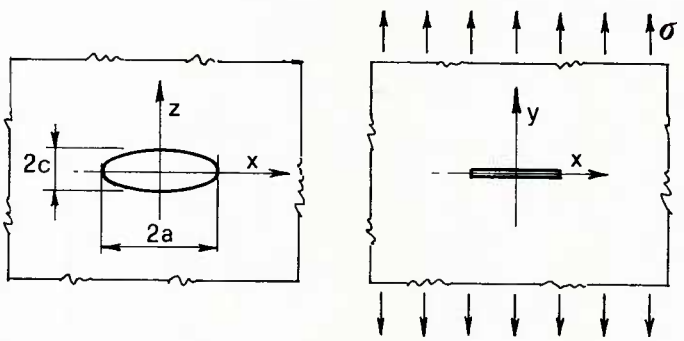

Fig. 4.2-19 Penny-shaped crack model.

Example 1: Griffith's crack in an infinitely large plate under:

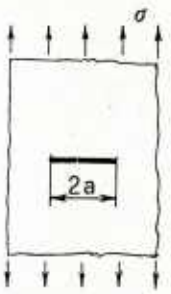

A) monoaxial tension load

$$K_I = \sigma\sqrt{\pi a}$$

$$K_{II} = K_{III} = 0$$

B) crack surface with a constant pressure

$$K_I = p_o\sqrt{\pi a}$$

$$K_{II} = K_{III} = 0$$

C) shear in the plate plane

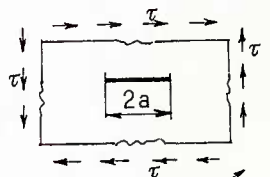

$$K_{II} = \tau\sqrt{\pi a}$$

$$K_I = K_{III} = 0$$

D) superposition of σ and τ

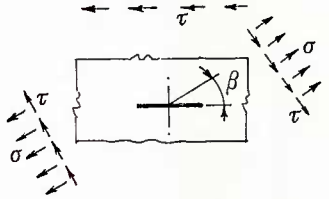

$$K_I = (\sigma\,\mathrm{sen}\beta - \tau\,\mathrm{sen}\beta)\,\mathrm{sen}\beta\sqrt{\pi a}$$

$$K_{II} = (\sigma\cos\beta + \tau\,\mathrm{sen}\beta)\,\mathrm{sen}\beta\sqrt{\pi a}$$

Example 2: infinite half-crack in an infinite large plate with surface cracks under constant pressure p_o:

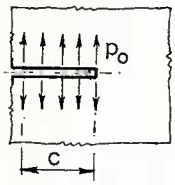

$$K_I = \frac{2p_o}{\pi}\sqrt{2\pi C}$$

Example 3: compact specimen

Thickness B

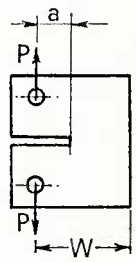

$$K_I = \frac{P}{BW^{\frac{1}{2}}}\left[29.6\left(\frac{a}{W}\right)^{\frac{1}{2}} - 185.5\left(\frac{a}{W}\right)^{\frac{3}{2}} + 655.7\left(\frac{a}{W}\right)^{\frac{5}{2}} - 1017\left(\frac{a}{W}\right)^{\frac{7}{2}} + 63.9\left(\frac{a}{W}\right)^{\frac{9}{2}}\right]$$

Example 4: bending specimen

Thickness B

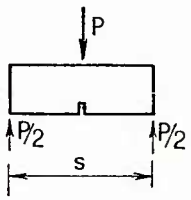

$$K_I = \frac{PS}{BW^{\frac{3}{2}}}\left[2.9\left(\frac{a}{W}\right)^{\frac{1}{2}} - 4.6\left(\frac{a}{W}\right)^{\frac{3}{2}} + 21.8\left(\frac{a}{W}\right)^{\frac{5}{2}} - 37.6\left(\frac{a}{W}\right)^{\frac{7}{2}} + 38.7\left(\frac{a}{W}\right)^{\frac{9}{2}}\right]$$

Fig. 4.2-20 Some examples of closed form solutions of S.I.F.

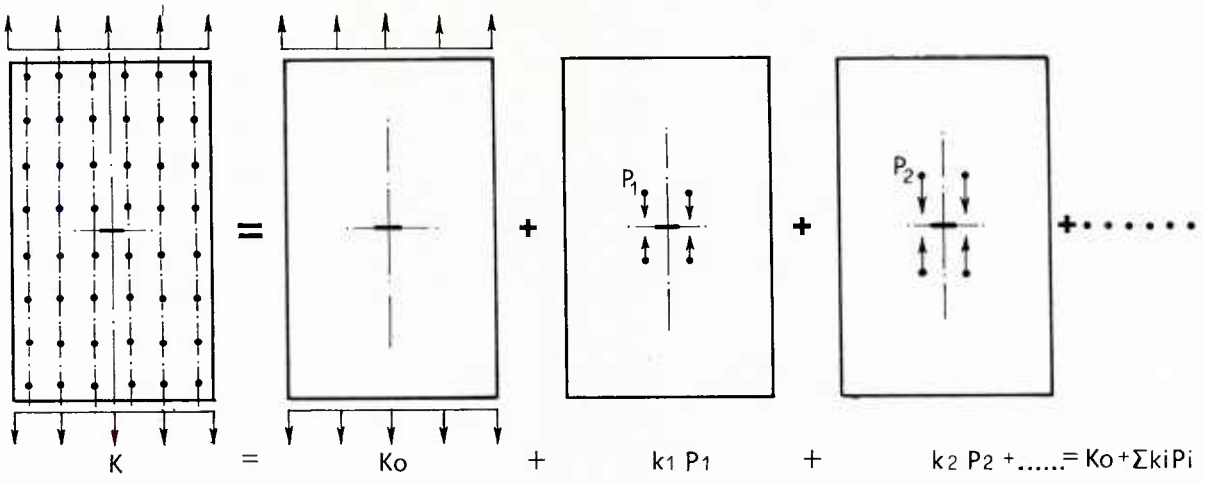

Fig. 4.2-21 Method of superposition of effects to assess S.I.F.K in stiffened panels.

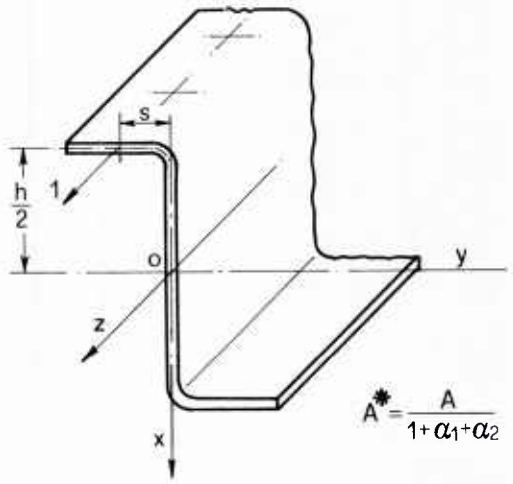

$$\alpha_1 = \frac{\frac{s^2}{\varrho_x^2} + \frac{sh}{2\varrho_x^2} \cdot \frac{Jxy}{Jy}}{1 - \frac{Jxy^2}{Jx\,Jy}} \qquad \alpha_2 = \frac{\left(\frac{h}{2\varrho_y}\right)^2 + \frac{sh}{2\varrho_y^2} \cdot \frac{Jxy}{Jx}}{1 - \frac{Jxy^2}{Jx\,Jy}}$$

Fig. 4.2-22 Equivalent area calcu lation; A is the effective area of the stringer and A* is the area of an equivalent strip-type stringer loaded purely in tension.

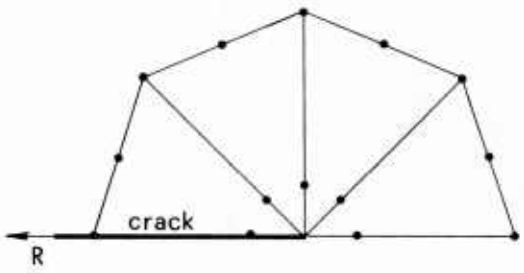

Fig. 4.2-23 Quarter Point Node Technique.

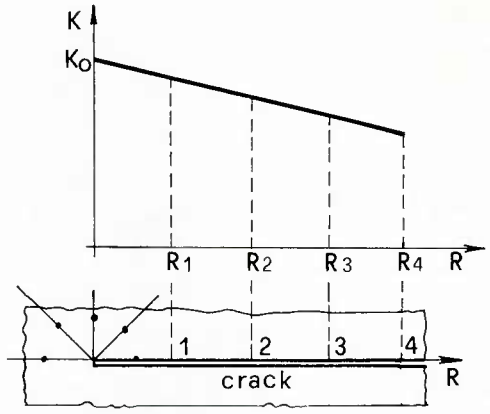

Fig. 4.2-24 Assessment of S.I.F.K by extrapolation along the R direction.

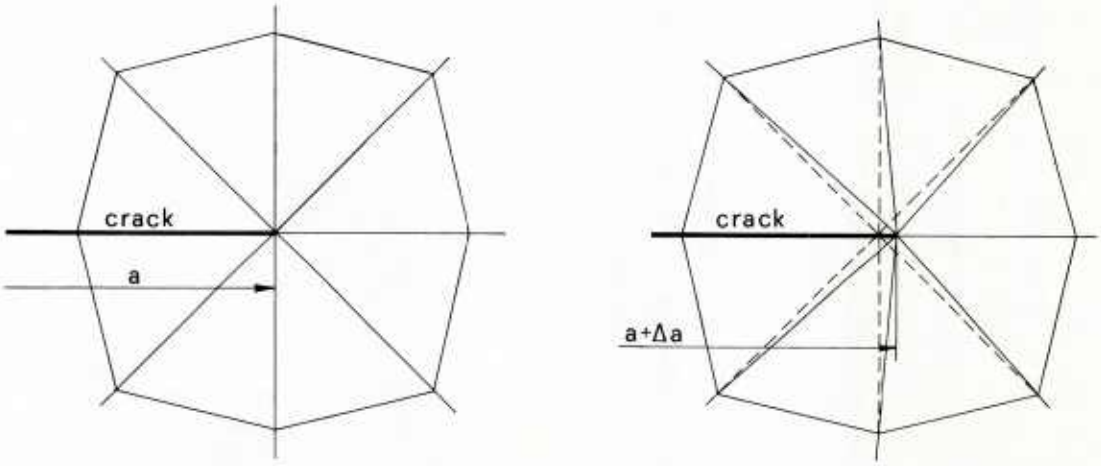

Fig. 4.2-25 Evaluation of energy rate per crack increment, Δa.

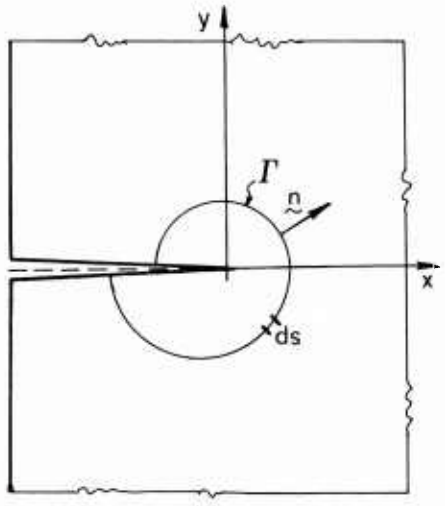

Fig. 4.2-26 J-Integral integration path.

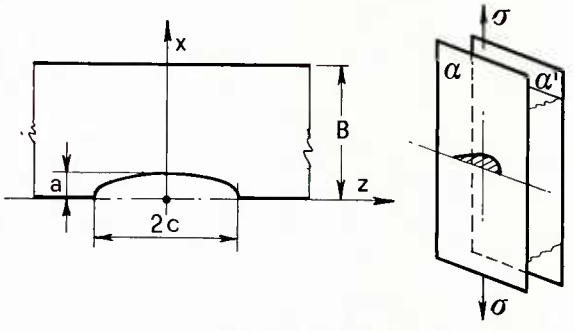

Fig. 4.2-27 Surface elliptical crack.

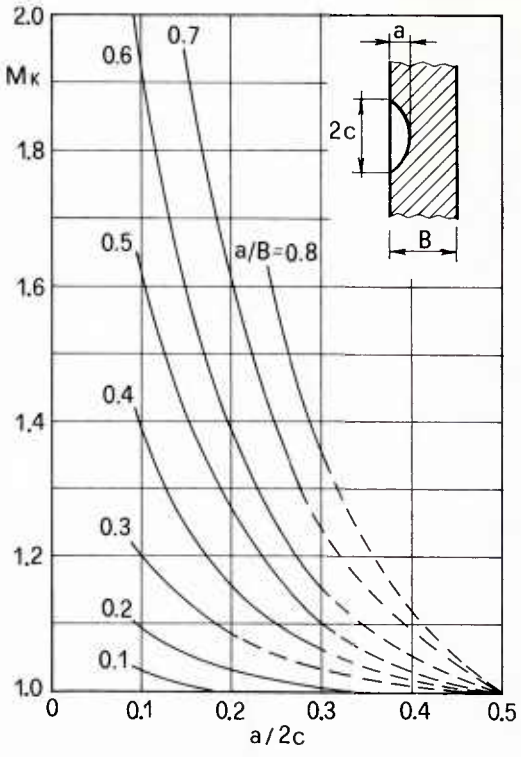

Fig. 4.2-28 An example of Kobayashy stress Intensity Magnification Factor (M_K) for proximity of front free-surface (from Ref. 1).

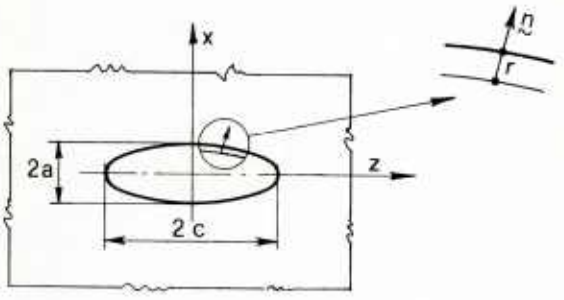

Fig. 4.2-29 Internal elliptical crack.

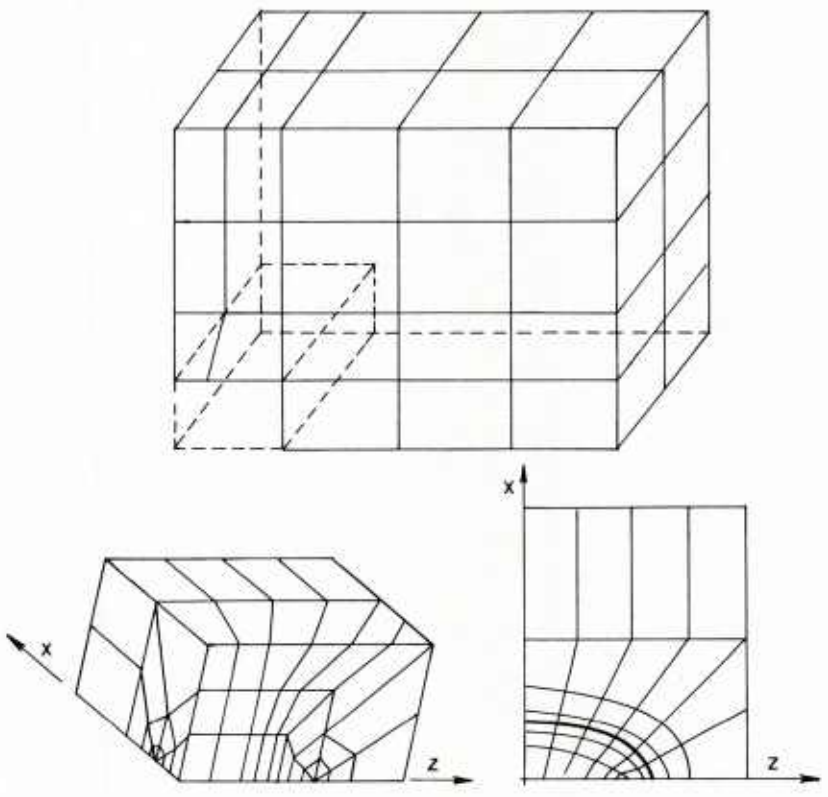

Fig. 4.2-30 An example of finite element mesh in a three-dimensional problem; crack is contained in the brick-type substructure.

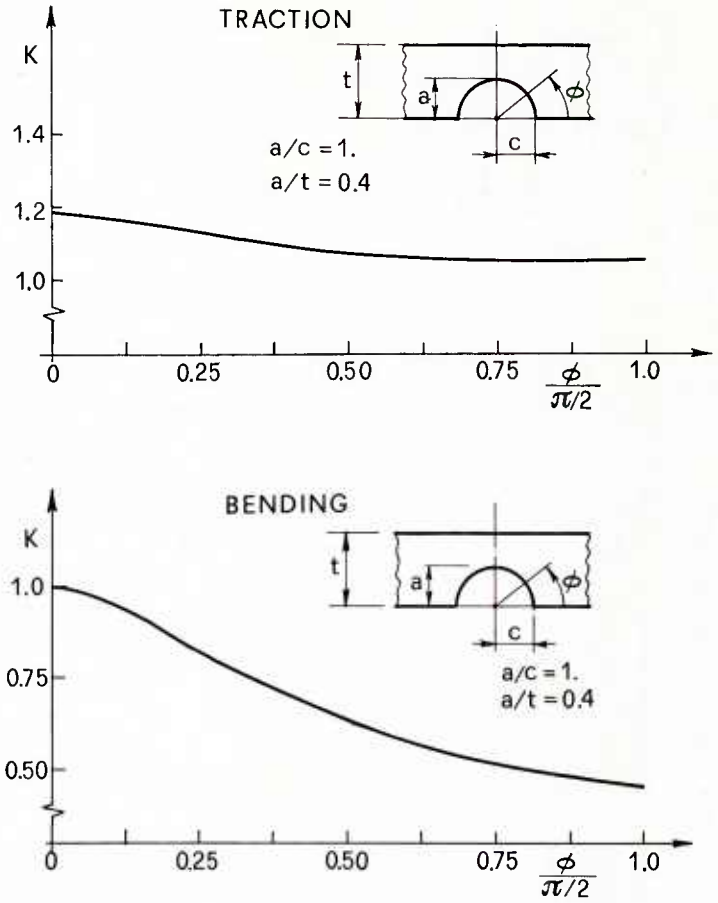

Fig. 4.2-31 Typical Stress Intensity Factor results along the crack border of a surface crack.

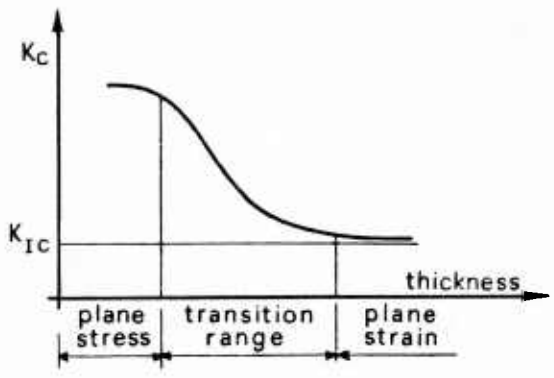

Fig. 4.2-32 a) Fracture Toughness vs. thickness (schematic).

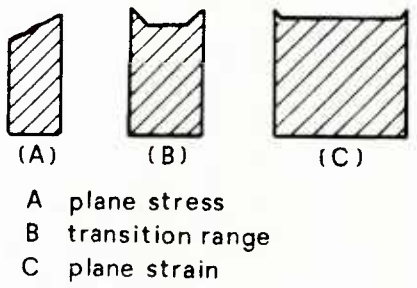

Fig. 4.2-32 b) Failure sections relevant to different thicknesses (schematic).

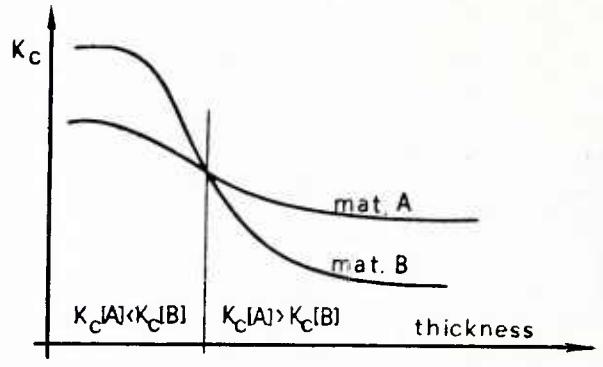

Fig. 4.2-33 Possible K_c vs. thickness conditions for different materials.

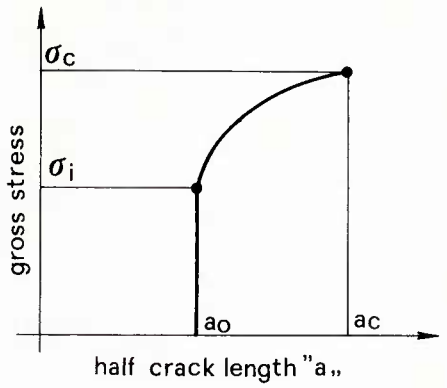

Fig. 4.2-34 Qualitative trend of the "σ" vs "a" curve.

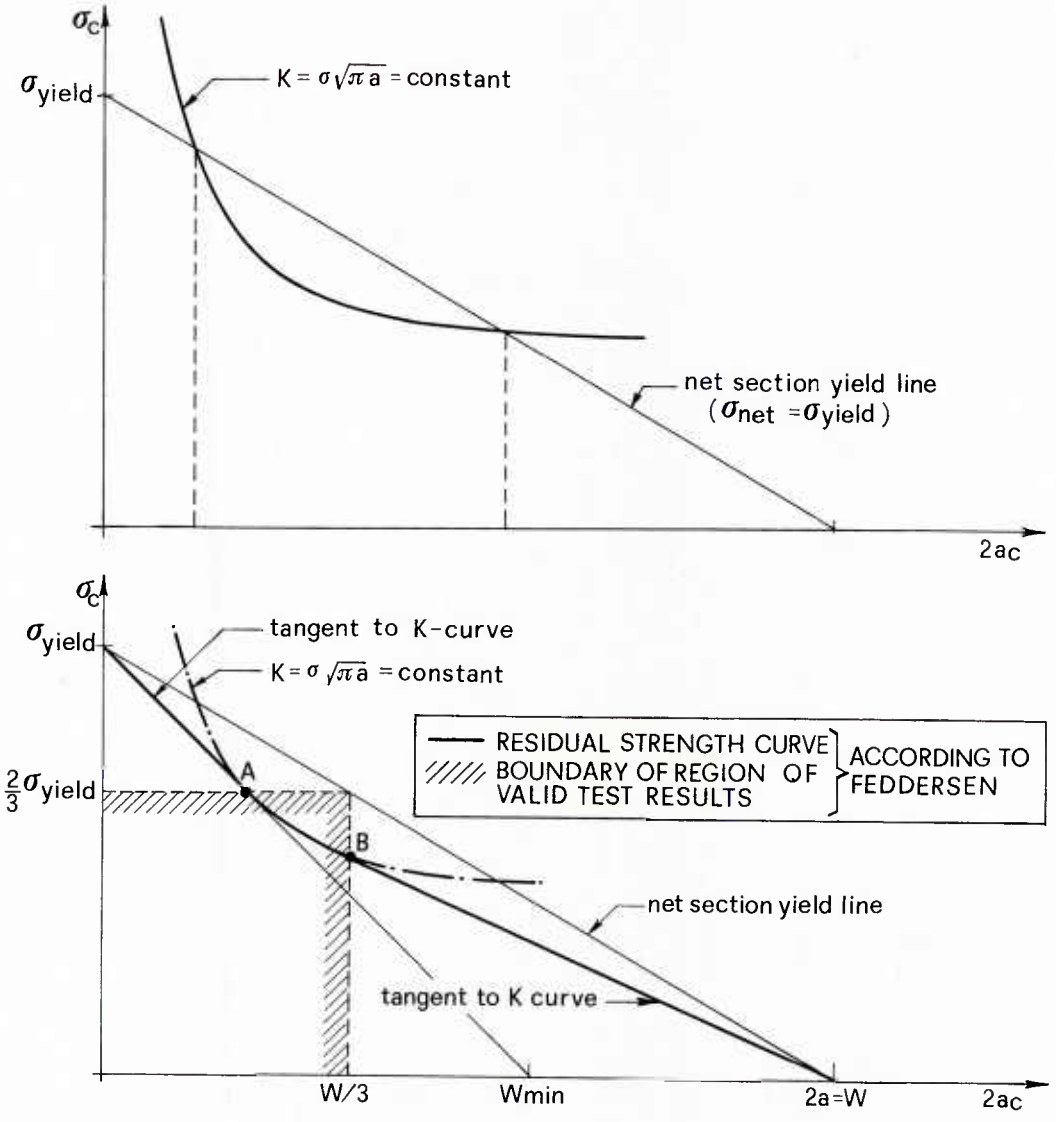

Fig. 4.2-35 Boundaries of "σ" and "a" for valid K_c results according to Feddersen.

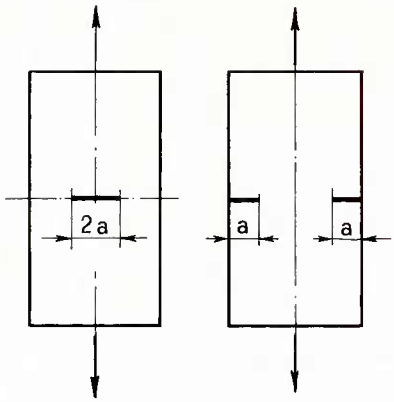

Fig. 4.2-36 Possible specimen configurations to evaluate K_c.

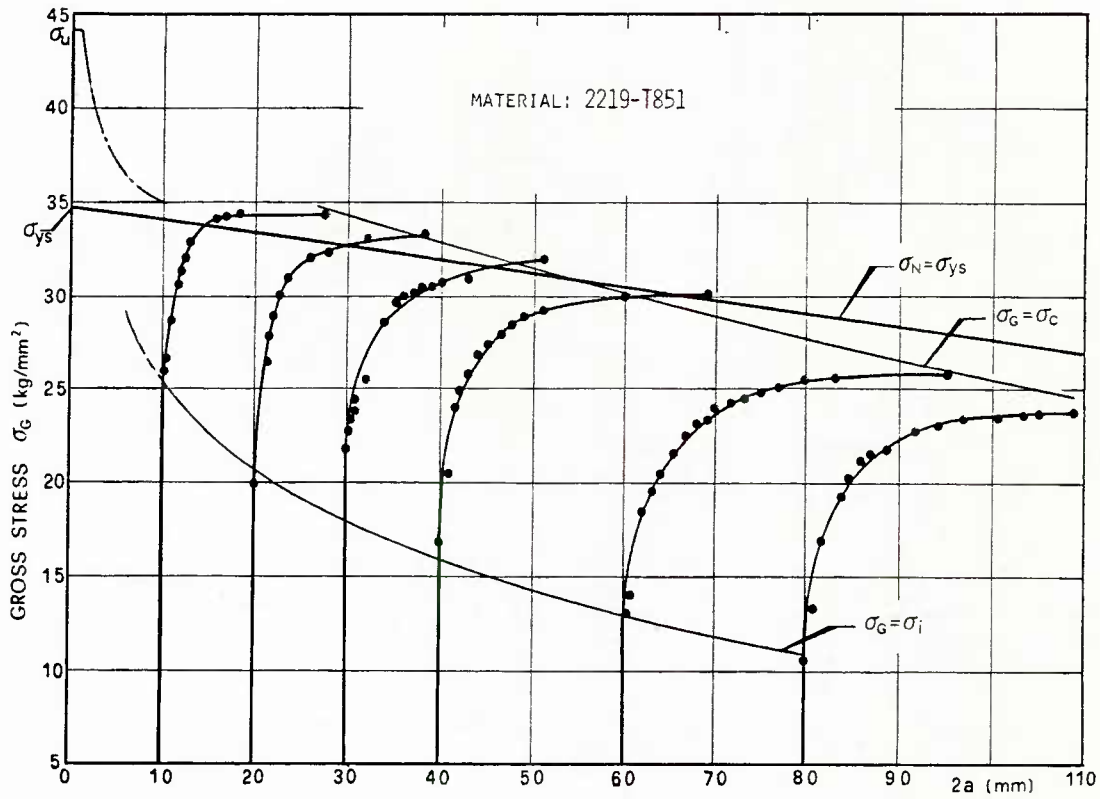

Fig. 4.2-37 Typical function $\Delta a_c = f(a_o)$ for aluminium alloys, (from Ref. 48). (σ_N and σ_G are, respectively, net stress and gross stress).

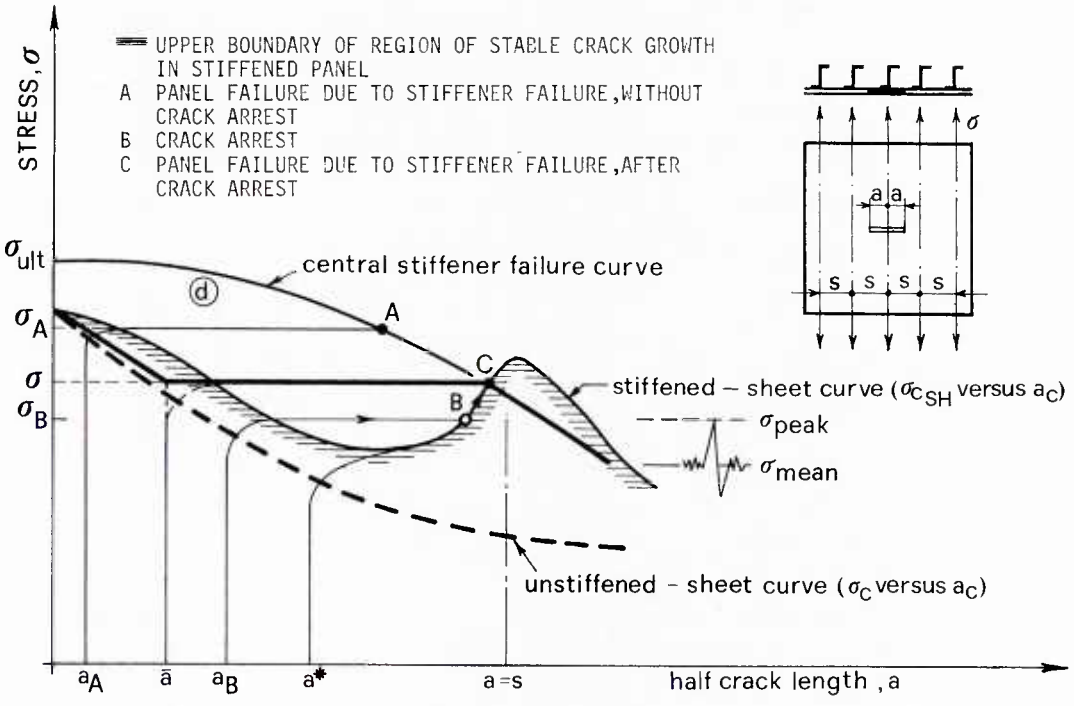

Fig. 4.2-38 Stiffened panel failure due to peak load and shape of residual strength diagram (From Ref. 40).

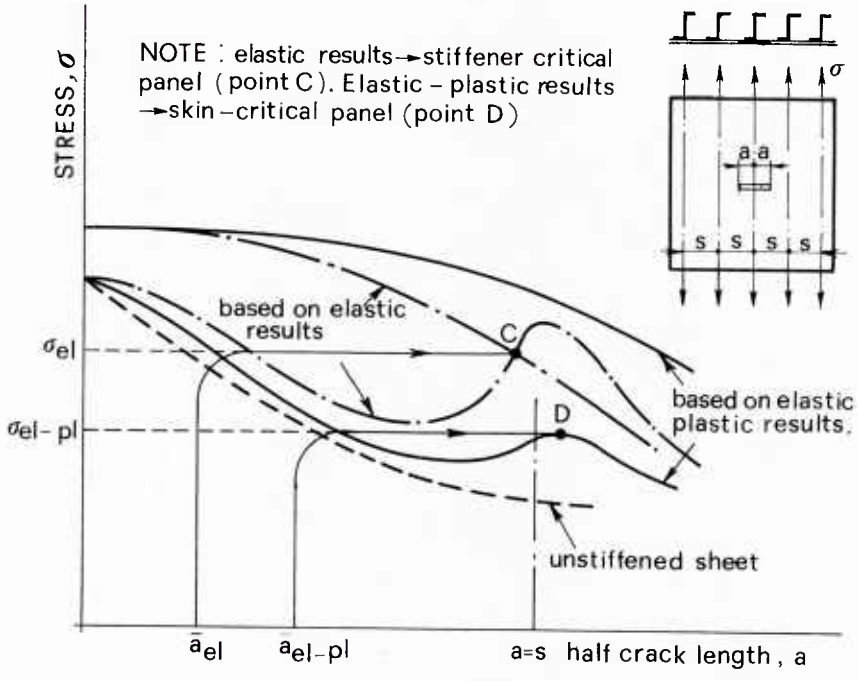

Fig. 4.2-39 Effect of rivet elastic-plastic behaviour on the residual static strength of stiffened panels (schematic); compare with Fig. 4.2-38.

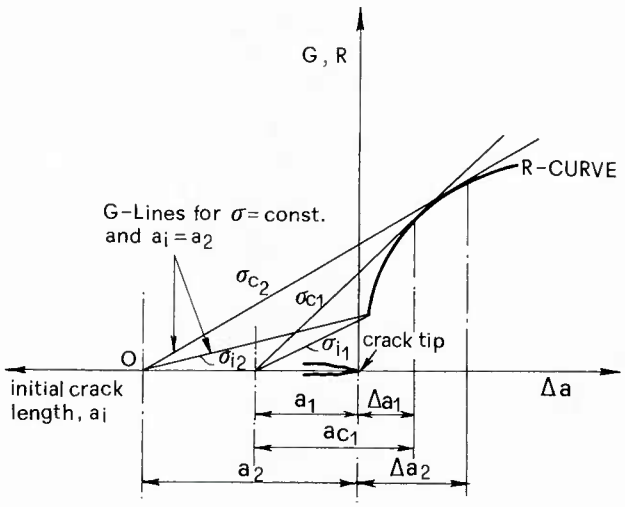

Fig. 4.2-40 R-curve in plane stress (schematic) (From Ref. 40).

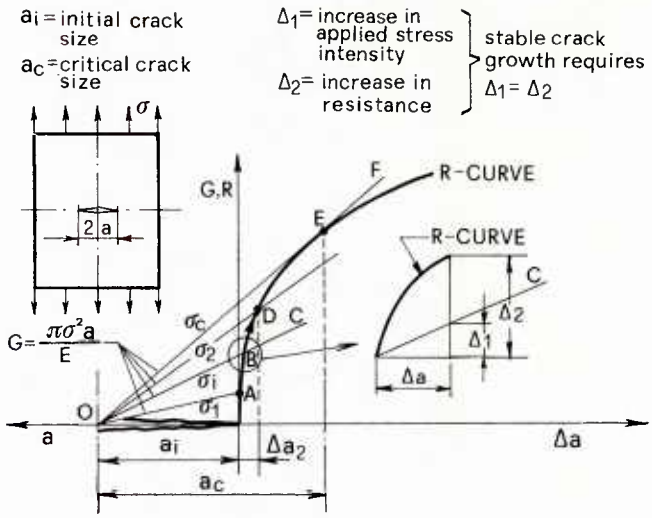

Fig. 4.2-41 R-curve concept in unstiffened panels (From Ref. 40).

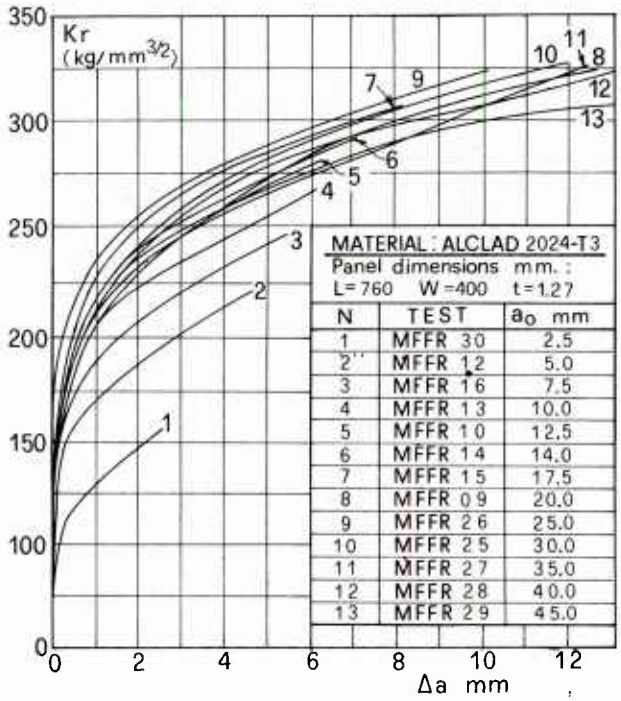

Fig. 4.2-42 Experimental R-curves for aluminum alloy 2024-T3. Kr is defined as $(ER)^{\frac{1}{2}}$. (From Ref. 48).

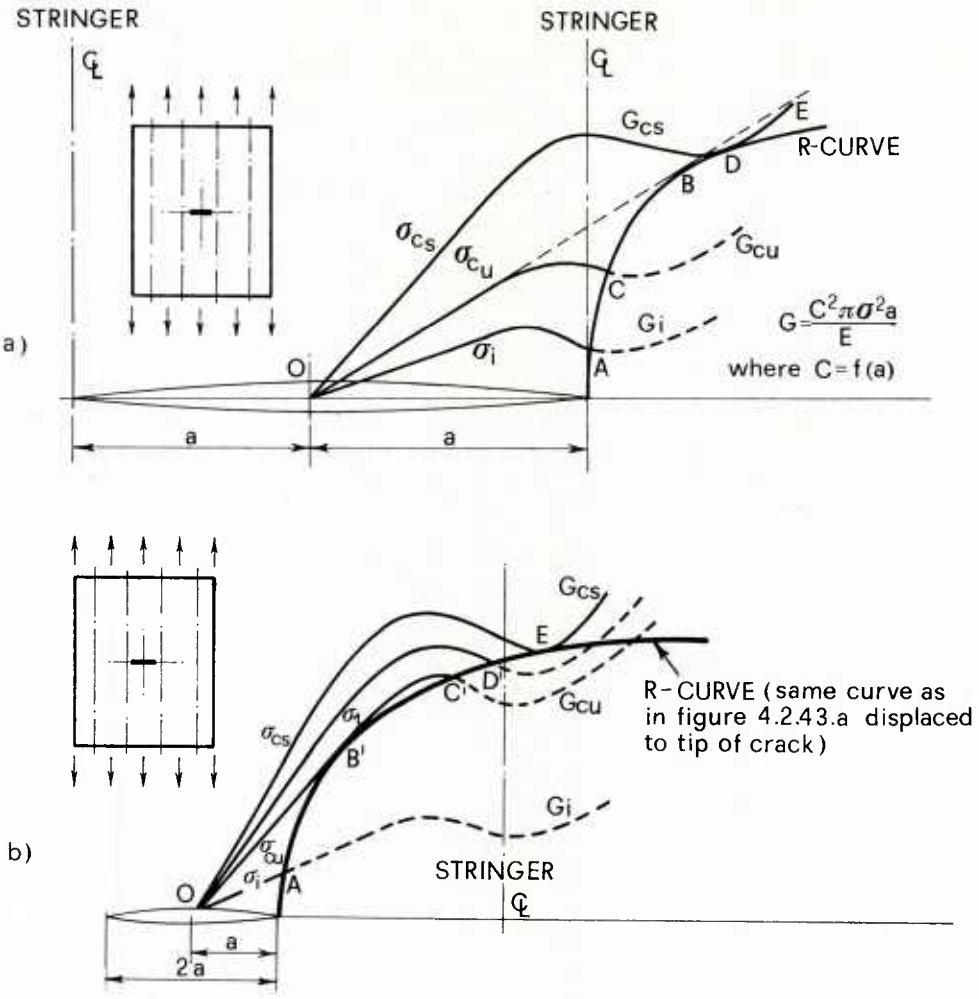

Fig. 4.2-43 R-curve concept in stiffened panels (From Ref. 40).

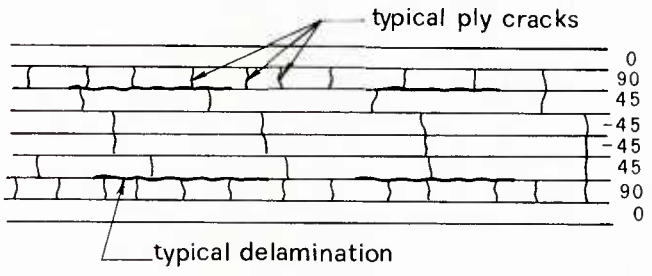

Fig. 4.2-44 A section of a typical multidirectional CFRP laminate, showing ply cracks and delaminations. The numbers on the right indicate the ply orien tation with respect to the loading direction.

APPENDIX 4.2.A

The threshold on fatigue crack propagation

The conditions, namely crack dimension and fatigue stress amplitude, under which the crack does not grow can be expressed by:

$$\Delta K = \Delta\sigma \cdot \sqrt{\pi a} \cdot C \leqq \Delta K_{th} \qquad (4.2.A\text{-}1)$$

where ΔK_{th} is a typical parameter of the material, which depends significantly on the minimum to maximum stress ratio in the cycle, R, and on the environment.

Certain values of ΔK_{th} relevant to some more usual materials are given in Tab. Ia. It is worthwhile pointing out that the values in Tab. Ia are only indicative because the ΔK_{th} value is greatly influenced by the particular chemical composition of the material and by metallurgical treatment. Accordingly, significant differences as far as the threshold value is concerned may be found between two metals of the same nominal composition. Another thing to notice is the particular complexity of the tests for the evaluation of ΔK_{th} and their sensitivity to general test conditions. Very scattered data is obtained on ΔK_{th} as no unifying procedures have so far been established. Caution is needed, therefore, in the use of the ΔK_{th} values found in literature.

The ΔK_{th} is greatly influenced by the stress ratio R. When R parameter increases, the ΔK_{th} value decreases. At present, no satisfactory knowledge or theoretical prediction of this phenomenon is available. The crack closure hypothesis is probably the most appropriate explanation, but does not seem to provide a full understanding of the phenomenon, (Ref. 44). As far as engineering application is concerned, the problem is dealt with by empirical relationships in the form:

$$\Delta K_{th} = \Delta K_{o} \, (1-R)^{\gamma} \qquad (4.2.A\text{-}2)$$

where ΔK_{o} is the threshold stress intensity factor relevant to R=0 and γ is a characteristic parameter of the material shown in Tab. Ib. More sophisticated relationships have been proposed, (Ref. 47), but these do not give more satisfactory results.

The ΔK_{th} value is also influenced by environment, but in this case there are several, different mechanisms. The presence of corrosive agents can reduce the threshold value because of the corrosion phenomenon or it can prevent also the crack from growing as a consequence of crack tip blunting or passive film formation. Since environment influence, as well as practical results, are greatly dependent on the particular situations created by the combination of material and environment, no general trends can be stated.

MATERIAL	ΔK_{th} (MPa$\sqrt{m}$)
Mild steel	6.4
18/8 Austenite steel	6.0
Aluminium	1.0
Copper	2.7
Phosphor bronze	3.7
60/40 brass	3.1
Nickel	5.9
Monel	5.6
Inconel	6.4

Tab. Ia - Threshold value for R=-1 and laboratory environment, Ref. 47.

MATERIAL	γ
Ferritic-pearlitic steel	0.71÷1
Pearlitic steel	0.94
Martensitic steel	0.53
Pressure vessel steel	0.82
High strength steel	0.71

Tab. Ib - γ parameter of ΔK_{th} sensitivity to R changes, Ref. 47.

APPENDIX 4.2.B

Plasticity correction of the stress intensity factor

The contour of the plastic zone may be established through the following steps:
1) by determining the stress state around the crack tip;
2) by using a "plasticity correction", that is a law of the type

$$\phi\ (\sigma_{ij}) = \text{const}$$

where ϕ is the extreme plasticity surface.

In the hypothesis of small scale yielding, the stress field in the neighbourhood of the crack tip may be described fairly accurately by the equations of L.E.F.M.. Let us assume the Von Mises's law as the plasticity criterion; then we get

$$(\sigma_1-\sigma_2)^2 + (\sigma_2-\sigma_3)^2 + (\sigma_3-\sigma_1)^2 = 2\ \sigma_{ys}^2 \qquad (4.2.B\text{-}1)$$

where $\sigma_1,\sigma_2,\sigma_3$ are principal stresses and σ_{ys} is the yielding stress.

In mode I, $\tau_{xy} = 0$ along the crack line and, therefore, σ_x and σ_y are principal stresses; when dealing with other directions, starting from the crack tip, principal stresses are defined by Mohr's circle whose support is the z-axis, normal to the mean plate plane.

By using the notations in Fig. 4.2-2, it follows that

$$\sigma_1 = \frac{K}{\sqrt{2\pi r}} \cos\theta \left(1 + \operatorname{sen}\frac{\theta}{2}\right)$$

$$\sigma_2 = \frac{K}{\sqrt{2\pi r}} \cos\theta \left(1 - \operatorname{sen}\frac{\theta}{2}\right) \qquad (4.2.B\text{-}2)$$

$\sigma_3 = 0$ in plane stress state

$\sigma_3 = \dfrac{2\nu K}{\sqrt{2\pi r}} \cos\dfrac{\theta}{2}$ in plane strain state

The equation of the limit surface in terms of polar coordinates is a function of θ; putting (4.2.B-2) into (4.2.B-1), it follows that:
- in plane strain state:

$$\frac{K^2}{2\pi r_p}\left[\frac{3}{2}\operatorname{sen}^2\theta + (1-2\nu)^2\ (1+\cos\theta)\right] = 2\ \sigma_{ys}^2$$

- in plane stress state:

$$\frac{K^2}{2\pi r_p}\left(1 + \frac{3}{2}\operatorname{sen}^2\theta + \cos\theta\right) = 2\ \sigma_{ys}^2$$

From these equations it is easy to obtain the size of the plastic zone along the θ-direction: $r_p(\theta)$. Fig. 4.2.B-1 shows the function $r_p(\theta)$ in the cases of Von Mises and Tresca criteria.

Irwin proposed a method for correcting the expression of K, to take the presence of the crack tip plastic zone into account: plastic zone shape is shown in Fig. 4.2.B-1. The presence of the plastic zone decreases the stiffness of the specimen in the same way as a larger crack; let us indicate as "a_{eff}" the corrected crack length and "δ" the correction to the crack length "a" due to the plastic zone; we have:

$$a_{eff} = a + \delta \quad ,$$

where "δ" is a crack length increment such that the situation is as shown in Fig. 4.2.B-2. Now, we suppose that, in correspondence with the crack length a_{eff}, the stress field is the same as that shown in (4.2.11); therefore it follows that: "surface A area = surface B area".

With reference to mode I, this new condition allows us to obtain the value of the virtual crack extension δ, by means of simple operations (see, e.g. Ref. 1). By applying the plastic zone correction to the expression of K in mode I, we get:

$$K = C(a)\ \sigma \sqrt{\pi\left(a + \frac{K^2}{2\pi\sigma_{ys}^2}\right)} \quad .$$

This relationship shows that K must be evaluated by an iterative process, but, owing to the small influence of $(K^2)/(2\pi\sigma_{ys}^2)$ on the final value of K, the usual procedure is to add this contribution to the usual expression of K given by $K = C(a)\ \sigma\sqrt{\pi a}$, where C(a) takes the influence of the geometrical configuration into account.

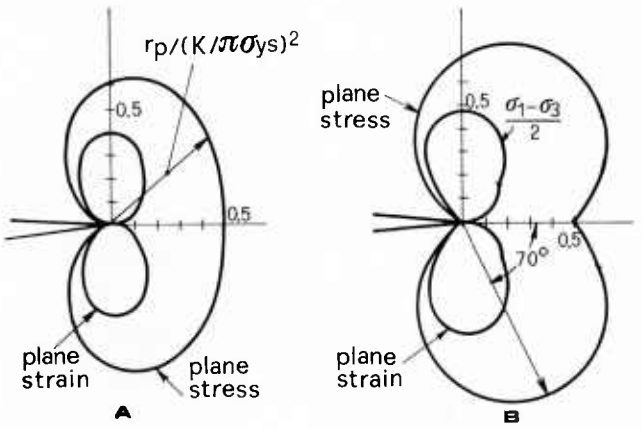

Fig. 4.2.B-1 Plastic zone shape according to:
a) Von Mises criterion,
b) Tresca criterion.

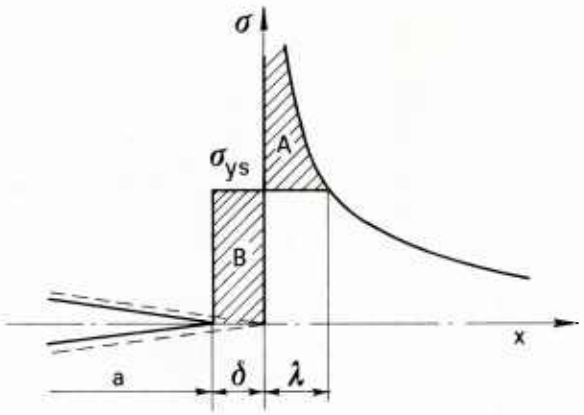

Fig. 4.2.B-2 Crack length increment.

APPENDIX 4.2.C

Requirements for the determination of the Plane Strain Fracture Toughness K_{Ic}

Assessment of F.T. in plane strain state must be carried out so that the plastic zone is small with respect to crack length.

The criteria proposed for judging the reliability of F.M. plane strain tests are formulated so that limits are evaluated for the plastic zone size.

For this purpose, it may be useful to introduce the following non-dimensional parameter:

$$\beta = \frac{1}{B}\left(\frac{K}{\sigma_{ys}}\right)^2 = \frac{1}{B}\,2\pi r_y \qquad (4.2.C\text{-}1)$$

where B is the specimen thickness and r_y is the dimension of the plastic zone along the crack line; in critical conditions and plane strain state, (4.2.C-1) becomes:

$$\beta_{Ic} = \frac{1}{B}\,2\pi r_{y_{Ic}} \qquad (4.2.C\text{-}2)$$

When $\beta = 2\pi$, that is $B = r_y$, experimental data of the type in Fig. (4.2.C-1) shows that the fracture surfaces are almost completely flat; then the stress state is highly triaxial on the basis of the conclusions stated previously.

Certain authors assume that the plane strain condition is satisfied when:

$$B \geq 40\ r_{y_{Ic}}\ , \qquad (4.2.C\text{-}3)$$

that is

$$B \geq \frac{40}{6\pi}\frac{K_{Ic}^2}{\sigma_{yS}^2} = 2.1\,\frac{K_{Ic}^2}{\sigma_{ys}^2}\ . \qquad (4.2.C\text{-}4)$$

A.S.T.M. and B.S. requirement for the plane strain condition is:

$$B \geq 2.5\left(\frac{K_{Ic}}{\sigma_{yS}}\right)^2\ ; \qquad (4.2.C\text{-}5)$$

this requirement is more conservative than that relevant to (4.2.C-4).

Specimen geometry does not influence the results of F.M. tests on the whole, but for obvious practical reasons, two types of specimens are required: the well-known "Compact Tension Specimens" and the "Flexure Specimens"; certain limitations are imposed on the dimensions and depth of cracks (see, e.g., Appendix II of Ref. 29).

F.T. plane strain tests must only be carried out in laboratories fitted with suitable equipment. Methodologies were then developed to correlate K_{Ic} value to other simpler parameters, which can be assessed by means of non-cracked specimens and simple rigs; a review of these methodologies is reported in Ref. 38. Many uncertainties exist at present concerning the reliability of such correlations.

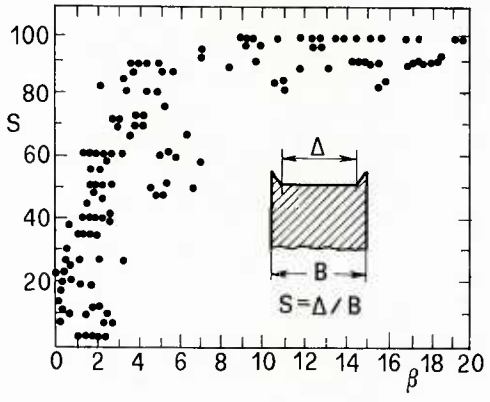

Fig. 4.2.C-1 Experimental data on fracture surface.

LIST OF SYMBOLS

a - Half-crack length
da/dn - Crack growth rate
K - Stress intensity factor
K_{Ic} - Critical value of the stress intensity factor in plain-strain condition
K_c - Critical value of the stress intensity factor
K_{th} - Threshold value of the stress intensity factor
n - Number of load cycles
R - Stress ratio, $\sigma_{min}/\sigma_{max}$
J - J-Integral
σ - Stress
σ_{ys} - Yielding stress
ΔK - Stress intensity factor range
ΔK_{th} - Range of the threshold value of stress intensity factor

SUB-CHAPTER 4.3
FATIGUE STRENGTH IMPROVEMENT AND DETERIORATION

by

Ferdinand F. LIARD
Former Scientific Department head
Société Nationale Industrielle Aérospatiale
B.P. 13 – 13725 MARIGNANE CEDEX
FRANCE

CONTENTS

4.3.1 Introduction

Aircraft designers know that each gram saved on empty weight means more than two grams gained on useful load. This is even truer for helicopters where hovering requires a larger power-to-weight ratio then it is for fixed-winged aircraft.

It is then obvious that the best part is the lighter one. It must be able to sustain safely no more than the load spectrum to which it is submitted in service.

This is the reason why, apart from the best possible choice of shape and material, they sometimes use the latest improvements in fatigue behavior coming from laboratory research.

But there is often better reasons to look for fatigue strength improvement :

After certification a noticeable drop in fatigue strength may come from unnoticed variations of the material production process, the manufacturing of parts or the actual environmental conditions in service. This may lead to unsafe operation or premature retirement of parts and actions must be taken to restore their fatigue strength.

A strengthening of some fatiguewise critical parts may also be needed when engine power increases or aerodynamic refinements allow a greater gross weight for a helicopter type.

In both cases the improvement must, for economic reasons and as far as possible, be made using the old part or at least without increasing the space needed for its operation. A redesign of mating parts is necessary when this is not the case.

The easiest way to describe the methods used to increase fatigue strength is to review the different causes for its deterioration and explain the various means to avoid it. This is what is done in the following subchapters together with some advice to design, manufacture and inspect in order to get the best possible fatigue results.

As very little has been done for composites and as crack propagation is dealt with in chapter 4.2, this chapter is limited to crack initiation in metallic materials.

4.3.2 Influent parameters

For several reasons : Fatigue failures usually originate near the surface of the parts the maximum stress is often located in this area where a plane state of stress exists, it is where the environment acts and where different types of incidents like scratches or static cracks can occur during manufacturing, handling or operation which affects fatigue strength.

As fatigue develops by plastic shear around internal defects such as voids, flaws or inclusions acting as stress raisers, the choice of clean materials is important.

However, for the same shape and material fatigue strength depends on the state of static stress existing in the critical area : As shown by the GOODMAN diagram of Fig. 1, a mean tensile stress lowers fatigue strength while a mean compressive stress increases it.

Thus, internal stresses generated during the processing of the material or the manufacturing of the part can have a major effect.

The main causes of poor fatigue performance for a given design are then mainly related to the state and working conditions of the surface of the part.

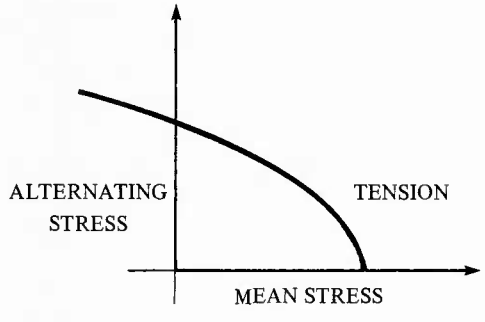

Fig. 1 – Example of GOODMAN diagram

4.3.3 Fatigue strength deterioration

Even brand new parts may have low fatigue strength due to the selected manufacturing process. They can also sustain a lower alternating stress than expected because of their friction on the mating parts during operation or because of the environmental conditions in service.

This leads us to consider separately the effects of manufacturing and operation.

4.3.3.1 Effect of manufacturing process

4.3.3.1.1 Grinding

This type of machining is required for making parts out of hard materials when dimensional precision and low roughness are necessary. Owing to the type of material removal - abrasion at high speed - small areas of the surface reach high temperatures which can induce large and variable internal stresses causing a wide fatigue scatter.

In fact, this is caused by «grinding burns» producing local heat treatments ranging, for steel, from tempering at various temperatures to requenching.

Tempering creates soft zones of smaller strength and requenching hard spots where high tensile stresses and microcracks are present.

According to W.G. BARROIS (Ref. 1), the average fatigue loss for steel between a «good» grinding and a «bad» one is of 23 % and, for titanium, the fatigue loss between lathe-turned and ground specimen can reach 33 %.

One must,however,keep in mind that these are average values and cases are known where strength losses are much higher :

For instance, investigations into a tooth failure in a main gear box, before the development of inspection methods to detect burns, showed that the fatigue limit was divided by a factor greater than 3.

Also, this degradation of fatigue strength is not limited to high strength steels. Some unexpected failures occured in rotor shafts or landing gear spindles tempered above 500 deg. C for which grinding burns were not detectable. In these cases, grinding of critical zones was made only to ease production and, for one of the rotor shafts, a sharp angle in the shoulder fillet caused by the wear of the shaped grinding wheel was an aggravating factor.

It is then very important to avoid grinding the critical areas unless it is quite necessary and, in this event, to closely control the process.

4.3.3.1.2 Heat treatment of steels

On some cases the atmosphere of the heat treatment furnace can produce surface decarburization which decreases the hardness abd the fatigue strength of the surface where the cracks initiate.

Ref. 1 quotes the results of JACKSON and POCHAPSKY on notched and unnotched specimen. The fatigue limit of well treated specimen is divided by the following factors when a deep decarburization (.2 to .25 mm) occurs :

U.S. AISI Alloys 2340, 4140 and 5140 heat treated at more than 1600 N/mm^2 :

- unnotched specimen : factor 3.35 to 4.3
- notched specimen : factor 2.75 to 3.5.

This large loss is not only caused by the softening of the surface but by the decrease of the compressive stresses generated by the transformation of austenite into martensite during heat treatment.

Another cause of fatigue deterioration caused by heat treatment is the presence of quenching cracks generated when too small internal radii are machined on the rough part (Fig. 2).

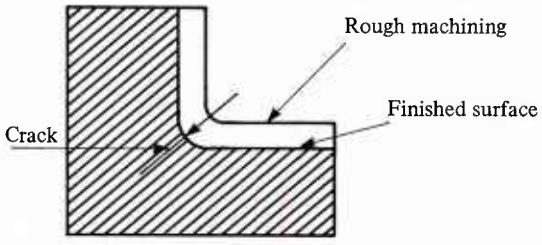

Fig. 2 — Quenching crack

4.3.3.1.3 Plating - anodizing

It is well known that plating generally lowers more or less the fatigue strength of the unprotected part tested in dry air but that it can have a beneficial effect when this part is operated in severe environmental conditions.

This may be caused by the fact that the fatigue strength of the coating is smaller than that of the core or that internal tensions are present in the coating. In this case, cracks initiate in the coating and extend into the parent metal.

The case may also be that fatigue cracks initiate in the parent metal when plating produces tensile stresses in the parent metal or hydrogen embrittlement of the latter.

The loss of fatigue strength varies widely according to the plating process and has to be evaluated in each case. It is greater for chromium and nickel plating for which residual stresses are high than for cadmium or zinc plating generating small internal stresses.

Chemical plating is generally less detrimental than electrochemical plating.

As an example, here are a few figures extracted from the work of W.J. HARRIS (Ref. 2).

Plating	Parent metal	
	Cr-Ni steel	Al. Alloy
Chromium	15 to 75 % *	48 to 63 %
Nickel	7 to 33 %	
Cadmium	20 %	
Zinc	5 to 15 %	

loss of fatigue strength in % of basic figure in dry air.

* According to heat treatment for thick deposits.

For high strength Ni cr. Mo steel, the loss of fatigue strength at 10^5 cycles for thick coatings (.5 mm) is of 16 % for chromium deposits and 22 % for mixed nickel and chromium deposits (Ref. 3).

Thinner deposits are generally less detrimental. For instance, a .1 mm chromium deposit on a high strength Ni cr steel lowers the fatigue strength by 10 % and a .01 mm cadmium plating gives a loss of only 2.5 % on the same steel (Ref. 4).

In the two latter examples the specimen are shot peened before plating and the comparison is made with shot peened unplated specimen.

Anodizing also lowers the fatigue strength of aluminium alloys by some 10 to 30 % according to the type and thickness of anodization. It seems that hard anodizing is more detrimental.

4.3.3.1.4 Contour etching

Chemical milling of aluminium alloys produces sharp surface micro-notches that decrease the fatigue strength of the sheets or the forgings as delivered by some 30 % (W.J. HARRIS - Ref. 2).

However, the original fatigue properties can be easily restored by vapor or vacu blasting.

4.3.3.1.5 Welding

Welding is generally detrimental to fatigue strength of jointed parts for several reasons :

- The weld is a cast metal, the mechanical properties of which are often very different from those of jointed metals.
- The heat treatment produced by the process varies according to the distance from the weld generating large internal stresses.
- The weld causes by itself a geometric stress concentration and contains usually stress raisers such as inclusions or voids in the cast area.

This is why the ratios of cast to wrought properties of welded chromium nickel steels or heat treatable aluminium alloys are about one half.

4.3.3.1.6 Surface finish

As fatigue cracks generally originate at the outer surface of the part, it is quite understandable that machining striations act as stress raisers and that surface finish is an important parameter for fatigue strength.

However, surface finish is not easy to quantify and equal roughness values can correspond to quite different surface profiles and hence fatigue limits.

In fact, fatigue strength depends not only on the roughness but on the state of internal stresses varying with the machining process. It is well known that lathe turning gives compressive internal stresses while grinding is generally the cause of surface tensions. This is why a relatively rough turned part can show a better fatigue strength than the very smooth one ground to the same shape.

However, for a given type of machining, fatigue strength decreases when the roughness increases, R. CAZAUD (Ref. 5) showed for instance that the ratio of rough to fine milling bending fatigue strengths was 2/3 for flat specimen of AU4G1 (24 ST) aluminium alloy.

It is then very important not to vary the condition of machining of a part after its fatigue qualification is done.

4.3.3.2 Effect of service usage

4.3.3.2.1 Fretting corrosion

The first attempts to evaluate the fatigue behaviour of joints such as lugs from the fatigue strength of the materials and stress concentration factors showed that the laboratory results were worse than expected by a factor of 3 to 7.

In the meantime, the examination of the fracture revealed the presence of surface oxydation and micro cracks at the nucleous of the fatigue failure.

This physico-chemical phenomenom caused by the rubbing of the mating parts under elastic deformations and involving transient welded junctions of asperities, oxydation of finely divided particules and wear, is called fretting corrosion.

WATERHOUSE (Ref. 6) studied the effect of fretting on the fatigue limit of various metals. The tests were carried out on rotating bending specimens subjected to fretting in their middle and gave the results of the following table. The reduction factor is the ratio of the fatigue limit without fretting to the fatigue limit with fretting.

MATERIAL		VICKER'S HARDNESS NUMBER	REDUCTION FACTOR
Carbon steel	. 1 % C	137	1.41
Carbon steel	. 33 % C	165	1.48
Carbon steel	. 4 % C	420	2.00
Carbon steel	. 7 % C Normalized	270	2.08
Carbon steel	. 7 % C Cold worked	365	3.18
Steel alloy	. 6 % cr, 2,5 % Ni, . 5 % Mo	330	4.38
Steel alloy	. 1.4 % cr, 4 % Ni, . 3 % Mo	510	3.55
Al. Alloy	4 % Cu	117	1.59
Al. Alloy	4.4 % Cu, . 5 % Mn, 1.5 % Mg	140	1.92
Al. Alloy	4.4 % Cu, . 8 % Mn, 7 % Mg	160	2.72
Cu Alloy	30 % Zn	175	1.50

He also studied the influence of parameters such as pressure of contact, amplitude of relative displacement or frequency.

As far as the first two parameters are concerned, they are of little influence above a given threshold.

On the contrary the fatigue limit decreases when the frequency decreases.

4.3.3.2.2 Chemical corrosion

Chemical corrosion is responsible for a number of fatigue fractures specially after several years of service in severe environmental conditions. It has been shown that in some cases (steel rotor spindles for instance), the fatigue strength was divided by a factor close to 3.

In fact, apart from mild uniform corrosion typical of some light alloys and having little influence on the fatigue strength, corrosion produces pits or intergranular cracks acting as stress raisers. However fatigue tests performed in dry air after chemical corrosion do not show a large enough decrease in fatigue strength to explain field failures.

It is now well known that simultaneous action of corrosion and alternating stress, a phenomenom called corrosion fatigue, has a much more detrimental effect on fatigue strength.

As an example CAZAUD (Ref. 5) quotes the results obtained by MAC ADAM on a Ni-cr heat treated steel for which the following fatigue limits were obtained.

Without corrosion	:	49 kg/mm^2
Test in air after 10 days in pure water	:	32 kg/mm^2
Test in air after 10 days in pure water and alternating stress of 6 km/mm^2	:	22 kg/mm^2
Fatigue strength in pure water	:	11 kg/mm^2

It is then very important to correctly protect helicopter parts against corrosion.

4.3.3.2.3 Ageing of composites

It has been shown that the loss of fatigue strength of coupons of composites was directly related to the percentage of moisture absorbed by the material.

This is true for glass or carbon fibers with usual plastic cores were losses of properties up to 50 % were noticed. However high modules carbon composites with resins cured at high temperatures are practically insensitive to moisture (Ref. 7).

The same reference shows that thick parts such as glass composites blades submitted to natural ageing without protection for several years kept their fatigue strength in spite of visible external degradations.

This is due to the fact that the outer layers of the skin, although altered, protected the internal frame essential to fatigue strength. It shows that there is little to fear for parts of composites incorporating a well studied and maintained protection.

4.3.4 Fatigue strength improvement

A part may have too low a fatigue strength either because of a poor design or manufacturing process which will be dealt with in the following subchapters, or just because its size does not allow a better performance with usual production techniques.

In the latter case it is useful to improve its fatigue strength without changing its dimensions.

The possible solutions depend on the location of the crack initiation : if it is located at an external stress raiser, the cancellation of tensions by using pre-stretched materials or the generation of local surface compressions are generally used ;

When the fatigue crack is induced by fretting corrosion, one can try to prevent or reduce the micro motions of the mating parts by using interference fits, to prevent the formation of fretting micro cracks by interposing anti-fretting screens or coatings or to combine the various preceding means.

4.3.4.1 Improvement at external stress raisers

When the weaker cross section of a part is located at a stress raiser - a shoulder fillet for instance - and when the fillet radius has been given the larger possible dimension, the improvement in fatigue strength is generally done through some form of local cold working.

It is well known that cold working produces surface compressions raising the fatigue limit in accordance with the Goodman diagram. The beneficial effect of hand polishing has been known for ages and gives high compression in a very thin layer of the material. Unfortunately it varies with a lot of parameters and is difficult to define and to reproduce. It is the reason why controllable processes such as shot peening or cold rolling are preferred.

In both cases caution shall be taken to stop the cold work sufficiently away from the stress raiser at a point where the stresses have lowered. In fact, the internal equilibrium of the part requires that, at short distance from the border of the cold worked area, the surface internal stresses reverse and become tensions which can lower the fatigue strength.

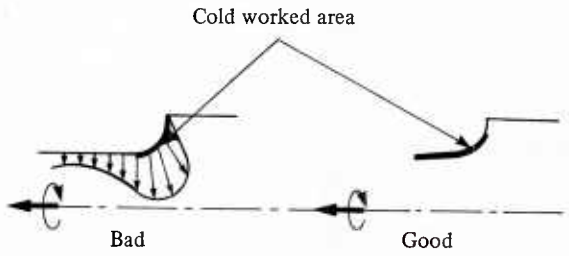

4.3.4.1.1 Cold rolling

Cold rolling is not used very often in helicopter manufacturing probably because it is limited to turned parts and may require several tool changes even for the different areas of the same item.

The advantage of this method however is its good reproducibility when the pressure of the roller and the number of revolutions have been established.

It is popular in the engine field where large production of simple parts incorporating small fillets of the same size and submitted to complex vibrations can be easily cold rolled if necessary.

It can be seen in Ref. 2 that the fatigue strength of crankshafts was improved by 50 to 60 % in bending and 100 % in torsion by cold rolling.

Another application of this technique is the production of dynamically loaded bolts. Most helicopter manufacturers require cold rolled threads and head fillets for all bolts of the rotating components and the main structural assemblies.

Here again Ref. 2 shows a 41 % improvement in fatigue strength for cold rolled threads compared to machine-cut threads. This is true for medium strength steel bolts and it is recommanded not to exceed 115 hbar ultimate strength to obtain good results.

4.3.4.1.2 Shot peening

Shot peening is widely used in the helicopter field either to improve the fatigue strength of parts already made or to prevent its deterioration by other operations of the manufacturing process.

Shot peening before chromium or nickel plating avoids the internal tensions generated by these platings and is an example of the latter case.

To obtain good results, it is necessary to closely control the numerous parameters involved : type and size of the shot, speed and flow, position and orientation of the nozzles in relation to the part, percentage of broken shot, time of shot peening, etc . . .

In fact the final results are tested on Almen specimen distributed in the critical areas of a dummy part which is shot peened in exactly the same manner as the actual one.

This does not exclude a close inspection of each part for lack of coverage that may be due to obstruction of the nozzles or to surface contamination by broken shot.

For steels CAZAUD (Ref. 5) quotes fatigue limit improvements of 27 to 49 % in rotating bending and 42 to 49 % in torsion, the latter being related to piano wire and stainless steel 18.8. To my knowledge a 25 % improvement can be obtained by shot peening on actual parts of currently used Ni-Cr and Ni-Cr-Mo steels.

For light alloys Ref. 8 shows a fatigue strength improvement of 10 to 20 % when the alloy remains untreated after shot peening and of 30 to 45 % when shot peening is followed by chromic anodization, the comparison being made with the same process with or without shot peening. Shot peening with glass balls with an Almen deflection of .19 mm gives slightly better results than steel balls shot peening with Almen deflections of .32 and .42 mm.

It seems that steel balls are preferable to broken wire shot, cases are known of failures in service at notches caused by broken wire shot.

For titanium, shot peening seems to have no effect in tension probably because turning generates surface compression which causes sub-surface nucleation like for shot peened specimen. However, it improves the rotating bending fatigue strength by 24 to 34 %.

4.3.4.1.3 Surface treatments

Carburizing, Nitriding or carbonitriding induce high surface compression (on the order of 100 bar) that leads to a substancial improvement in fatigue strength. It has even been shown in some cases (Ref. 5) that nitriding completely attenuates stress concentrations.

It is not usual to decide the application of such treatments just to improve the fatigue strength of steel parts not only because it generally necessitates a change of material but because the fragility of the case may be a drawback.

However when a part such as a gear or shaft is already case hardened, the extension of surface treatment to a zone incorporating a stress raiser and protected in the previous process can leat to improvement.

4.3.4.2 Attenuation of fretting corrosion

Fretting corrosion is a major cause of fatigue failures of mechanical parts of transmission and of airframe joints, where this phenomenom occurs at peak stress locations.

In order to allow the calculation of lugs, AEROSPATIALE analysed a number of fatigue tests of helicopter parts, writing that the average number of cycles to failure at a given load corresponds to the fatigue stress on the mean fatigue curve of the material. The calculated stress was adjusted to this value considering an overall concentration factor product of the geometric concentration factor by a fretting concentration factor given by the following table :

	MATERIAL	CONDITION OF LOADING	
		REPEATED LOAD	ALTERNATING LOAD
FRETTING FACTOR	STEEL	3.5	6
	LIGHT AND ULTRA LIGHT ALLOYS- TITANIUM	4	7

Such a drastic reduction in fatigue strength is the reason why considerable work has been directed towards an attenuation of fretting corrosion.

4.3.4.2.1 Interference fit

This technique is applicable to lugs or bolted joints, the idea being to reduce the motion between bolt or pin and part by application of pre-strain.

In case of fixed joints the bolts can be press fitted into the holes,an example being the well known taper pins or the multi-bolts cuff to spar assembly of a number of metallic blades.

The drawback of this method is that a rather large interference is needed and that the corresponding tensions around the hole can reduce the profit.

When the pin has to be frequently removed or when it must be free to rotate, a good solution is to press fit a bush inside the hole, thus shifting the fretting zone from the hole to the bush.

The fitting must be tight enough; to prevent the bush from becoming free under the maximum load expected in service.

The best design is obtained for a bush thin enough to minimize the tension in the lug and thick enough to prevent its buckling.

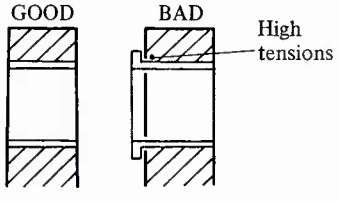

With usual interferences, bushing improves the high cycle fatigue strength of lugs by a factor of 1.1 to 2.

Caution must be taken to obtain cylindrical bushes : a polygonal external shape caused by vibrations during centerless grinding of a thin bush led to very low fatigue results.

Collared bushes are also to be avoided because the stiffness of the collar induces very high permanent tensions at one side of the hole that may cancel the improvement due to bushing. If the sides of the lug have to be protected against fretting, other solutions such as coating or bonding of separate shims are preferable.

4.3.4.2.2 Cold working

The surface compressions produced by work hardening can also prevent or delay micro-cracks caused by fretting.

Different processes are used for holes according to their sizes and the thickness required for the work hardened layer. Roller burnishing gives thin hardened layers while bore sizing or ballizing allow larger ones. Shot peening is only used for large holes.

For external parts such as bearing journals, the same techniques as in para. 4.3.4.1.1 are used.

Here again an improvement of 20 to 30 % is easily achievable on actual parts and this profit adds to the one given by interference bushing as shown by the following table giving the fretting factors (see 4.3.4.2.1 above) :

HOLE PROTECTION / LUG MATERIAL	NONE (reference)	BUSHING	COLD WORK AND BUSHING
Steel	Load : alternated : 6 repeated : 3,5	3	2
Light alloy ultra Light alloy Titanium	Load : alternated : 7 repeated : 4	3,6	2,4

Special caution is to be taken for bore sizing titanium lugs for which scratches produced by seizure during the process reduce fatigue strength. The best results were obtained using large interferences producing thick work hardened layers followed by final machining to remove scratches.

4.3.4.2.3 Surface protection

As fretting involves oxydation and punctual welds one can think of protecting the surface by coating it with other metals insensitive to oxydation or welding by friction or with the same kind of protective film having low friction coefficient.

The technique of thick metallic coating is also very interesting for the salvation of worn-out parts during overhaul.

It is the reason why a number of tests has been carried out by different authors. Unfortunately, the number of parameters to cover is so large that the precise case one may need is often lacking or unprecisely defined.

The comparison is often made on rotating bending specimens in the center of which a metallic shoe is pressed to produce fretting corrosion. These tests results are to be used with caution because the stress gradient and fretting conditions are not representative of aircraft parts. They may however be used to select a process and test it at full scale.

As an example, the following table givespart of the rotating bending tests carried out in France, where the figures are the mean fatigue limits or mean fatigue strengths at 2.10^7 cycles in hbar and the percentages of the reference.

Ni Cr Mo steel .3 % C			Ni Cr Mo steel .12 % C		
Coating	S_∞	%	Coating	S_∞	%
Without	21,2	100	Case hardening	45	100
Ni Sulfamate	12.4	58.6	Case hardening + Tungsten carbide	69.5	154
Ni Dalic	31.6	149			

7075 T73			TA6V		
Coating	S_∞	%	Coating	S_∞	%
Without	5.4	100	Sulfuric anodizing	38.6	100
Ni chemical	8.9	165	Ni Dalic	50.5	131
Ni dalic	8	148	Tungsten carbide	54	140
Chromic anodizing	6.1	113			
Chromium plating + grinding	4	74			

More representative fatigue tests have also been carried out on lug specimens. Unfortunately many of the results are not precise enough for lack of a sufficient number of representative test points.

The following table gives the order of merit of a few protections obtained in repeated tension on lugs :

6061		TA6V	
Configuration of lug	S_∞ / S_∞ ref	Configuration of lug	S_∞ / S_∞ ref
Unbushed	1	Sulfuric anodizing	1
Bushed	1.7	Coating with polyamide lacker	4
Bushed Nylon screen between bush and hole	1.9		

It is clear that protection by screens or lackers are very promissing because they eliminate fretting corrosion. However it must be shown that they do not wear out or creep in service on actual parts.

4.3.5 Design to fatigue

Each helicopter structural part is designed using the best possible material and protection according to the known working conditions.

Its shape is also studied to minimize stress concentrations and the use of loaded resin mockups coated with photoelastic lacker films is very useful to achieve this aim.

The interest of this method is to easily allow modifications of shape by addition or removal of material.

But the designer must also keep in mind the ease of manufacturing an inspection in order to get reproducible results. For instance, it is strongly recommended not to grind fillets when unnecessary for fear of grinding burns or cracks but when the adjacent journal must be very smooth, one must think of releasing the fillet :

Bad Good

Following this idea, some firms have found valuable the examination of drawings, before manufacturing, by a team of design, stress, manufacturing and inspection specialists.

4.3.6 Manufacturing and inspection to fatigue

The analysis of a number of catastrophic accidents in the helicopter industry has shown that, as far as fatigue is concerned, relatively small manufacturing modifications can lead to large losses in fatigue strength (factors of 3 are not infrequent).

For metallic parts where fatigue starts at the surface or in the zone of contact of mating parts, the main causes are heat treatment (internal stresses), final machining, surface protection and jointing conditions (tolerances, surface finish, etc .. . .)

For composites, apart from ambient conditions (cleanliness, controlled moisture) and polymerization conditions (pressure, temperature, time, etc . ..) the materials themselves are of primary importance. Very minute variations in the composition of resins or in the preparation of fiber surface can result in drastic fatigue strength variations while the same batch exhibits small scatter.

Ageing of raw materials during storing is also important.

The now well known vital parts procedure and statistical fatigue quality control can be used to avoid unexpected fatigue strength deteriorations.

4.3.6.1 Vital parts procedure

A «vital part» is a part the failure of which may cause a serious accident and that does not incorporate a safety margin large enough to tolerate the variations related to its type of manufacturing without its risk of failure becoming unacceptable.

The procedure consists in freezing the manufacturing an inspection processes in the state used for making the parts for fatigue qualification. Any further modification must be analysed and may lead to the repetition of fatigue tests.

4.3.6.2 Statistical fatigue quality control

The vital parts procedure is generally sufficient to insure a good level of fatigue strength for simple parts of aeronautical quality. It is not the case for complex assemblies such as blades, the manufacturing of which involves unusual contingencies. In this case, a periodical quality control fatigue testing is done, the results of which are analysed to validate the parts made during the corresponding period.

The specimen may be :

a) Complete parts as is the case for metallic blades in which two specimens are cut for subtantiation of the inboard or outboard critical zones. It is also the case for simple metallic parts the manufactirung of which involves unusual risks.

b) Specially selected coupons. It is the case of parts made of composites for which only the initial qualification or the qualification of variants are made on actual parts. In this case, the coupons follow the polymerisation cycle used during the period and the substantiation is done for each material and each critical zone. Furthermore, any change of batch inside a given period of manufacturing must be tested separately.

The specimen are taken haphazarilly during the period of manufacturing - generally one month - and fatigue tested to failure or to a high enough number of cycles (10^7 for instance) at a given load.

Notice is taken whether the failure is a conform or a non conform one (it does or does not occur according to the critical mode). A non conform failure cancels the test which has to be done again.

The statistical processing of test results is made using the SNP curve (load, number of cycles, probability) taken for fatigue qualification and altered, if necessary, when the number of tests increases.

It is performed using a parameter 1 which is a function of the number of cycles N_t obtained in the test and which is supposed to be gaussian.

For instance, if it has been shown that the fatigue properties are such that, at a given number of cycles N, V = Log. S_N is gaussian, 1 is non other than the difference, measured in number of standard deviations q , between the value of V given by the test and the average value $\bar{V}$ of the population (Ref. 9).

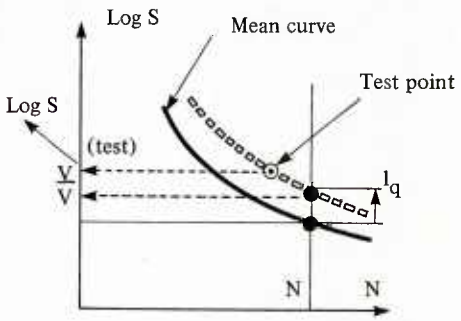

Just like for the statistical control of dimension of parts in mass production, the following variables are inspected simultaneously :

- the parameter 1
- the mean value of the last 3 tests $\frac{1 + 1' + 1''}{3}$
- the range of those 3 parameters, i.e. the larger of $|1 - 1'|$, $|1 - 1''|$, $|1' - 1''|$.

and, for each of them, warning limits are fixed, the probability of which to be exceeded is generally 5 % for the parameter and 2.5 % for the mean value and the range.

Control limits are also calculated, the probability of which to be exceeded being generally . 2 % for the parameter and . 1 % for the mean value and for the range.

3 cases can occur :

a) The 3 variables are within warning limits :

the production is considered satisfactory.

b) One at least of these variables is outside control limits :

the production is supposed to be defective and an inquiry is open during which appropriate measures are taken such as :
- improvement of manufacture,
- life reduction,
- alteration of statistical control limits.

c) One at least of the variables is between warning and control limits :

a new test is run with a part of the same period of manufacturing. According to the result of this test, one comes back to a) or b), the production being supposed to be defective if the result of the previous test is confirmed.

4.3.7 Conclusion

There would be much more to say about this chapter, every new incident bringing some additional knowledge about what to do and what not to do in order to obtain safe and reliable helicopters. For this, it is important that a free exchange of information exists between helicopter manufacturers and official services, which is one of the aims of AGARD.

4.3.8 References

1. Manuel sur la fatigue des structures. II Causes et prévention de l'endommagement.
   AGARD MANUAL, 1978
2. Metallic Fatigue by W.J. HARRIS.
   Pergamon Press, 1961
3. Influence de l'épaisseur de chrome sur la tenue à la fatigue du 35 NCD16.
   Rapport CEAT N° N4 4975.00
4. Etude de l'influence des revêtements de surface sur la tenue en fatigue de l'acier NC 405W.
   Rapport CEAT N° M9 525800
5. La fatigue des métaux.
   R. CAZAUD - Dunod, 1969
6. WATERHOUSE : The effects of fretting corrosion in fatigue crack initiation. Corrosion fatigue.
   The university of Connecticut
7. Matériaux nouveaux et certification des hélicoptères.
   F. LIARD - 14ème Congrès Aéronautique de la A.A.A.F. - Paris, 1979
8. Etude sur alliages d'aluminium de divers modes de grenaillage suivis ou non d'une protection de surface.
   Rapport CEAT N° M7 677400
9. Note STAe/VT N° 165 par Jean SOULEZ-LARIVIERE.

SUB-CHAPTER 4.4

STATISTICAL BASIS OF DATA PROCESSING

by

A.Facchin and M.Raggi
Costruzioni Aeronautiche Giovanni Agusta
21017 Cascina Costa di Samarate (VA)
Italy

CONTENTS

4.4.1 MATHEMATICAL DESCRIPTION OF FATIGUE STRENGTH

The general result of a fatigue test consists of a pair of values, one of which is related to the applied load and the other to the number of cycles.

In the strict sense the load definition in fatigue tests requires two values to be used: mean and oscillating load; but the mean load is held at a constant level while the oscillating load is changed from one test to another and we can choose the oscillating load as a variable quantity.

The trend of a set of tests carried out with different oscillating loads but with the same mean load can be interpreted by the relationship $S = f(N)$ with S = oscillating load and N = number of cycles to failure.

The first problem we meet is the definition of the function $f(N)$ on the basis of some test results (S_i, N_i). The solution of this problem is carried out in two steps:

a. definition of the mathematical equation $f(N)$
b. calculation of the parameters contained in $f(N)$.

The type of the equation $f(N)$ can be stated by a qualitative examination of test data: the calculation of the parameters, on the other hand, requires a numerical analysis of test data.

The trend of the physical behaviour of fatigue failure is quite well interpreted by a curve with two concavities as shown in fig. 44.1.

For this kind of curve the Weibull four parameters equation is commonly used:

$$S = S_L + A\,(N+B)^c \qquad (4.4.1)$$

But in the field of helicopters, where the attention is mainly focused on high numbers of cycles ($N \geqslant 10^4$) this equation is used in the reduced type with three parameters:

$$S = S_L + AN^c \qquad (4.4.2)$$

The calculation of the parameters of Eq (4.4.1) and (4.4.2) is based on a statistical analysis of experimental data.

This statistical analysis is carried out by different methods depending on the size of the sample used to represent the fatigue behaviour of the whole population.

4.4.2 STATISTICAL ANALYSIS ON LARGE SAMPLES

4.4.2.1 Best fit technique

The calculation of the parameters of the equation (4.4.1) and (4.4.2) is carried out by fitting the curve to the experimental data according to certain conditions.

The most widely used condition for this purpose is to minimize the sum of the squares of the differences between the experimental data and the corresponding values of the curve.

This technique is well known as "the best fit" with least squares analysis and is generally used in the linear form, which requires a previous transformation of variables in order to make the problem linear.

In the case we are dealing with, it can be obtained from equation (4.4.1):

$$S - S_L = A\,(N+B)^c$$

$$\log\,(S - S_L) = \log A + c \log\,(N + B)$$

and putting

$$Y = \log\,(S - S_L)$$

$$X = \log\,(N + B) \quad \text{and} \quad a = \log A$$

then

$$Y = a + cX.$$

The transformation of variables is also required by other reasons: the correct use of the best-fit techniques requires that the following assumptions should be satisfied:

1. the scatter of the experimental data must not be due to systematic errors in the tests, but has to depend on the real characteristics of the phenomenon under examination
2. the scatter of the experimental data must be constant along the whole curve.

This last hypothesis is satisfied quite well by choosing the logarithm of the load (log S) as statistical variable.

However, the scatter of the endurance (log N), that could be the other statistical variable to define the fatigue behaviour, increases for low loads, and it can approach infinity for loads close to the fatigue endurance limit where run-outs can be obtained.

Thus log N is not suitable for a "best fit" technique.

The curve obtained by calculating the values of the parameters from the "best fit" technique has the following properties:

I It is satisfied by the couple of values $(\overline{X}, \overline{Y})$ that are mean values of the data (X_i, Y_i)

II The test data (X_i, Y_i) lie half over and half under the curve.

From these properties it follows that an endurance prediction based on this curve is not always conservative because of the following reasons:

1. the calculated parameters are strictly valid only for the tested sample: the extention of them to the whole population involves an uncertainty factor connected with the size of the sample

2. even if the curve were valid for the whole population of samples, it would assure the survival of only a half of the elements.

In order to make a safe prediction it is necessary to use a reduced curve obtained from the mean curve through a statistical analysis of the experimental data.

4.4.2.2 Evaluation of the reduced curve

On the basis of the observations made in the previous paragraph, in order to have a safe working curve it is necessary:

a) to define the maximum difference, for a given confidence level, between the characteristics of the sample and those of the whole population

b) to calculate the amount of the reduction to be applied to the mean curve so that a stated proportion of the population has a life greater than or equal to that calculated on the basis of the curve so reduced.

The object of a) is generally defined in statistics [1] as "estimate by intervals" and consists of determining, on the basis of the sample values, an interval that contains with a given uncertainty the population parameter that has to be estimated.

Such an interval is called the "confidence interval"; α, the uncertainty, is called the "significance level" and $\gamma = 1 - \alpha$ the "confidence level".

At this point we must devote our attention to the kind of statistical distribution that better represents the behaviour of the chosen variable.

It is generally recognised [2] that such behaviour is quite well described by a normal distribution of the variable "log S" or a log normal distribution of the variable "S".

The typical pattern of a normal variable distribution is the Gaussian "bell-shaped" curve of fig. 44.2 in which the two basic parameters of the distribution are:

μ = mean value

σ = standard deviation

The most common confidence interval is the interval related to the mean value.

For a population with normal distribution of unknown parameters μ and σ, the population mean value can be estimated by the sample characteristics using the relationship:

$$\mu = \overline{x} \pm t_{\alpha} \frac{s}{\sqrt{n-1}} \qquad (4.4.3)$$

where:

$$\overline{x} = \sum_{i=1}^{n} \frac{x_i}{n}$$ mean value of the sample

n = number of sample elements

$$s = \sqrt{\frac{\sum_{i=1}^{n} (x_i - \bar{x})^2}{n}}$$ standard deviation of the sample

t_α = value of the Student variable T for which the probability that T is contained in the interval $[-t_\alpha, +t_\alpha]$ is equal to $1 - \alpha$.

The variable T is defined as follows:

$$T = \frac{\bar{x} - \mu}{s}\sqrt{n - 1} \qquad (4.4.4)$$

and plotting its distribution on a graph we have the typical shape of figure 44.3.

In fig. 44.3 we can see that the probability that T is contained in the interval $[-t_\alpha, +t_\alpha]$ is equal to $1 - \alpha$. So from equation (4.4.4) it follows that the probability that the (4.4.3) is true is exactly $1 - \alpha$.

The above mentioned case represents a symmetric confidence interval called in statistics the "two-sided confidence interval".

As far as fatigue problems are concerned, where it is important to assure that the mean value is greater than a stated minimum value, we need refer only to the lower limit of the confidence interval.

This case in statistics is known as the "one sided confidence interval".

With reference to fig. 44.3 we can state that in $100 \cdot (1 - \alpha/2)\%$ of the cases the mean value μ is greater that $(\bar{x} - t_\alpha \frac{s}{\sqrt{n-1}})$.

So we can say that $(\bar{x} - t_\alpha \frac{s}{\sqrt{n-1}})$ is an estimate of the lower limit of the mean value with a confidence level μ equal to $1 - \alpha/2$.

If the standard deviation of the population is known, an estimate of the mean value is:

$$\mu = \bar{x} \pm z_\alpha \cdot \frac{\sigma}{\sqrt{n}} \qquad (4.4.5)$$

where:

$\bar{x}$ = mean value of the sample

n = number of sample elements

σ = standard deviation of the population

z_α = value of the standard normal variable Z for which the probability that Z is contained in the interval $[-z_\alpha, +z_\alpha]$ is equal to $1 - \alpha$.

The previous considerations are still valid for the definition of confidence intervals (two-sided and one-sided).

It is worthwhile to remark that for $n > 20$ the estimate of mean value made with known or unknown standard deviation of the population is exactly the same.

So for $n > 20$ it makes no difference whether equation (4.4.3) or (4.4.5) is used.

The object of b) is the definition of tolerance limits.

We have to determine an interval, in which we can say that a stated proportion of the elements of the population is contained with a given confidence level.

If the mean value and the standard deviation of the population are not known, which is the most common case, an estimate of the tolerance limits can be made using the mean value and the standard deviation of the sample.

The relationship used for two-sided tolerance limits is:

$$x_p = \bar{x} \pm K(n, \alpha, p)\, s$$

where:

$\bar{x}$ = mean value of the sample

s = standard deviation of the sample

K = factor depending on the number of elements (n) on the significance level (α) and on the required tolerance limit (p).

The formula of K (function of n, α and p) is obtained through a complex analysis reported in technical literature [3] .

Values of K for the most common cases are given in table 44.1.

As far as fatigue behaviour is concerned,only the lower tolerance limit of the fatigue strength is of interest and it has to be exceeded by a stated proportion of elements.

In this case we have a one-sided tolerance limit, whose relationship is as follows:

$$x_L = \bar{x} - K\,s$$

appropriate values of K are again given in table 44.1.

4.4.3 STATISTICAL ANALYSIS ON SMALL SAMPLES

4.4.3.1 Standard shape curves

The most frequent case in the analysis of fatigue test data is that of tests on real components.

The costs of such tests are so high that the manufacturers tend usually to reduce them to a minimum meaningful number (4 or 6).

In this case it is impossible to use a meaningful"best fit" technique because of the small sample. Curves of fixed shape are therefore used, depending on geometry (K_T) and loading environment.

These curve-shapes are obtained on the basis of the methodology given in the previous paragraph, by conducting a large number of tests on coupons.

The S/N curve shape obtained from coupon is then extended to the real components on the basis of the assumption that the fatigue behaviour of coupons and real components is the same.

4.4.3.2 Mean curve evaluation

The mean curve evaluation is made according to the hypothesis of isoprobability of the points on the same S/N curve.

Such a hypothesis is equivalent to saying that the statistical distribution of S, and hence its scatter, are constant in all the lives field. This assumption, discussed already for the "best-fit" method, allows one to state a statistical correspondence between each testing datum and a point at a reference number of cycles at which the statistical analysis is made.

The standard shape equation is:

$$S = E + g\,(N)$$

with E = endurance limit (for $N = \bar{N} = 10^7 \div 10^8$ cycles)

By fitting this standard shape to each testing point, several values for E can be found.

Each E value is given by:

$$E_i = S_i - g\,(N_i)$$

A mean curve(of 50% probability) is then associated to the mean value (E_M) from E_i values. Its equation is:

$$S = E_M + g\,(N)$$

4.4.3.3 Working curve evaluation

The reduction of the mean curve is made by determining a factor F to be applied

to the E_M value from tests:

$$E_{red} = F \cdot E_M$$

The equation of the reduced working curve will be:

$$S = E_{red} + g(N)$$

On the basis of a normal or log-normal distribution hypothesis on the E_M values, it is possible to determine an F value exactly such as we can predict with a given confidence level that a proportion p of the population of the endurance limit E_i will lie above $F \cdot E_M$. Such exact analysis, based on tolerance limits concepts, was examined in the previous paragraphs.

On that basis we have:

$$E_{red} = E_M - K\ (n, \alpha, p)\ s$$

s = standard deviation of the E_i sample from the tests

K (n, α, p) = factor depending on the number of tests, confidence level and requested tolerance limit.

Because of the small size of the sample, while the estimate of the mean value (E_M) is reasonably good, the estimate of the standard deviation is not quite so and the use of the previous exact method causes a too large a reduction of the mean curve.

It is common practice to use alternative methods, less exact, but nevertheless used systematically.

A few manufacturers, for example, use the standard deviation obtained from tests of coupons of the same material or from previous tests on similar components instead of the standard deviation of the actual component tests. The reduction factor is in this case less severe [2] .

The assumption that the standard deviation of the coupons is equal to that of the components takes into account the scatter due to the material properties and the manufacturing procedures, but it disregards the scatter effect due to the testing machines, which is different for coupons and for components.

To overcome this disadvantage a factor has been proposed taking into account both effects [2] .

The second assumption of keeping the same standard deviation from previous tests on similar components must be demostrated by an investigation on several samples.

However, very often manufacturers use the so called "three sigma" level in which the K value is assumed to be constant and taken equal to 3, regardless of the number of tests.

In this case, to safeguard against a fortuitous low value of the standard deviation, a maximum limit for F is used ($F \leq F_{max}$).

This method has not an exact statistical basis and can be justified only by its long use without many serious accidents.

4.4.4. START-STOP CYCLE

The "start-stop" cycle, also called "ground-air-ground" cycle, takes into account the greatest excursion of the loads from the start to the stop of the rotor.

The components most influenced by this cycle are the rotor components.

The start-stop loads have high oscillating values and low frequency (1 cycle per flight).

In fatigue testing, the start-stop cycle may be taken into account three different ways:

1. by inserting a certain number of such cycle into constant amplitude fatigue tests
2. by evaluating it separately by appropriate tests
3. by taking into account the actual load conditions in flight by flight tests

In the last case, of course, the problem is not evaluated separately.

In the first case, to safeguard against the possible scatter, a few manufacturers increase the number of start-stop cycles per flight hour according to a K factor depending on the number of tests to be done. (see fig. 44.5)

In the second case the problem is evaluated by testing a given number of components at a constant amplitude level equal to the maximum flight excursion.

In the region of interest for the start-stop cycles the S/N curves usually used (see previous paragraph) are not very meaningful.

A few manufacturers then use a statistical evaluation assuming as a variable the lives in cycles that are considered to have a log normal distribution.

In this case the reduction can be based on the scatter of the tests or on the data from previous experience, as was already seen.

4.4.5 ANALYSIS OF DATA USING PROBABILITY PAPER

The use of probability paper is quite common and convenient either to see if a given physical phenomenon follows a certain kind of statistical distribution or to obtain graphically the characteristic values of the distribution.

Given a random variable X with probability density function p (x) (p(x) is the probability that X assumes the x value) it is possible to define:

$$P(x) = \int_{-\infty}^{x} p(x) \cdot dx$$

where P (x) is the cumulative probability distribution function i.e. the probability that a random value is equal to or less than x.

For a normal distribution the shape of p(x) and P(x)is that of fig. 44..6.

To obtain a probability graph, a transformation of variable must be made to change the S-shape of the cumulative probability function P (x) into a linear one.

In other words, if the values of the cumulative probability function are plotted on the appropriate transformed scale of the probability paper a straight line can be drawn.

The linear abscissae scale is for the random variable X.

To use the graph and fit the points (x_i, P_i) some assumption must be made about the P_i values (also called plotting positions) that are attributed to known x_i.

For example, after having arranged the x_i values in ascending order, it may be assumed that:

$$P_i = \frac{i}{n}$$

n = number of all x_i elements of the sample

i = integer number corresponding to the order of x_i

Several other plotting positions have been proposed in order to better represent the probabilities corresponding to testing data x_i [4].

In practice, the sample data are plotted on the probability paper against their assigned cumulative frequency and a curve is drawn through the points. If a reasonably straight line fits the points, then the random variable has a statistical distribution of the same type as the probability paper.

In this case the desired statistical parameters can be read directly from the graph.

For a normal distribution the mean value is found at the intersection of the data line and the 50% value of the cumulative frequency; the standard deviation is the difference between the mean value and the abscissa corresponding to the 84,13% of cumulative frequency (or 15,87%).

The normal and log-normal probability papers [3] are shown in fig. 44.7 and 44 .8.

4.4.6 REFERENCES

1. CIAMPI DEL CORSO "Metodi di Osservazione e Misura"
2. R. NOBACK "State of the art and statistical aspects of helicopter fatigue substantiation procedures.
   AGARD CONFERENCES PROCEEDING N° 297
3. The analysis of normally distributed data
   ENGINEERING SCIENCES DATA UNIT item N° 68014
4. W. WEIBULL "Fatigue Testing and Analysis of results. PERGAMON Press 1961
5. AMCP 706-110 "Engineering design handbook
   Experimental statistics - Section 1 "
   U.S. ARMY MATERIAL COMMAND DEC. 1969

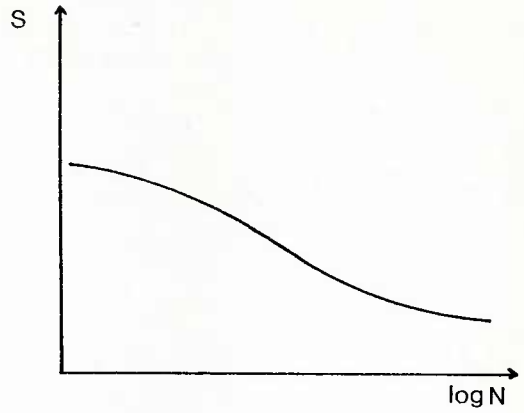

fig 4 4.1

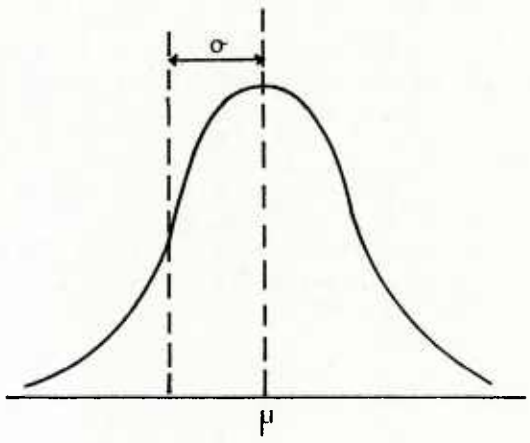

fig 4 4.2

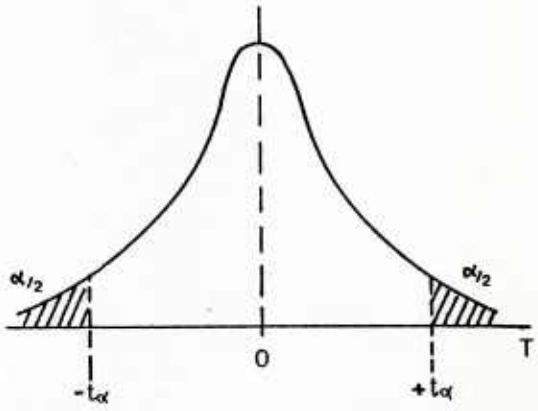

fig 4 4.3

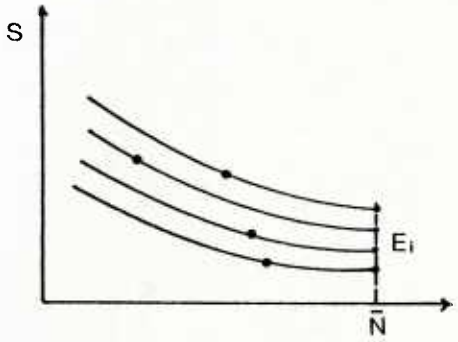

fig 4 4.4

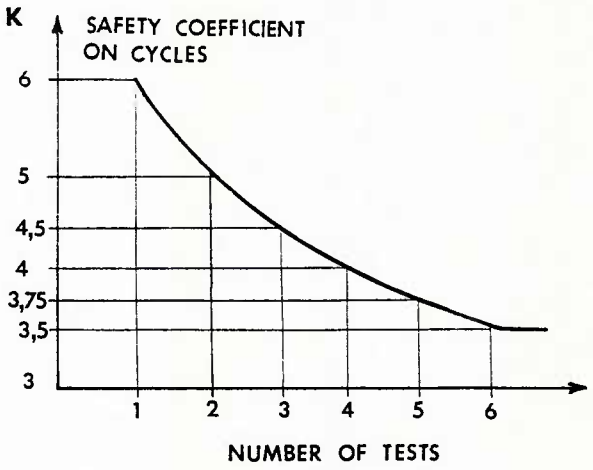

fig 44.5

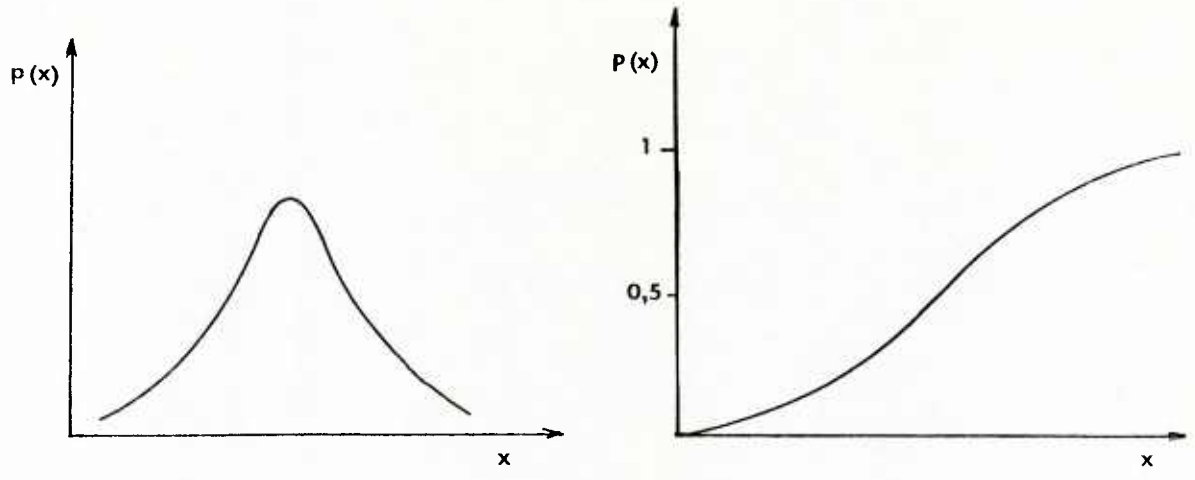

fig 44.6

TABLE 44.1
Tolerance limit factors

Confidence	γ = 0.90			γ = 0.95			γ = 0.99		
Proportion	p=0.90	p=0.95	p=0.99	p=0.90	p=0.95	p=0.99	p=0.90	p=0.95	p=0.99
N									
2	10.253	13.090	18.500	20.581	26.260	37.094	103.029	131.426	185.617
3	4.258	5.311	7.340	6.155	7.656	10.553	13.995	17.370	23.896
4	3.188	3.957	5.438	4.162	5.144	7.042	7.380	9.083	12.387
5	2.742	3.400	4.666	3.407	4.203	5.741	5.362	6.578	8.939
6	2.494	3.092	4.243	3.006	3.708	5.062	4.411	5.406	7.335
8	2.219	2.754	3.783	2.582	3.187	4.354	3.859	4.285	5.812
10	2.066	2.568	3.532	2.355	2.911	3.981	3.497	3.738	5.074

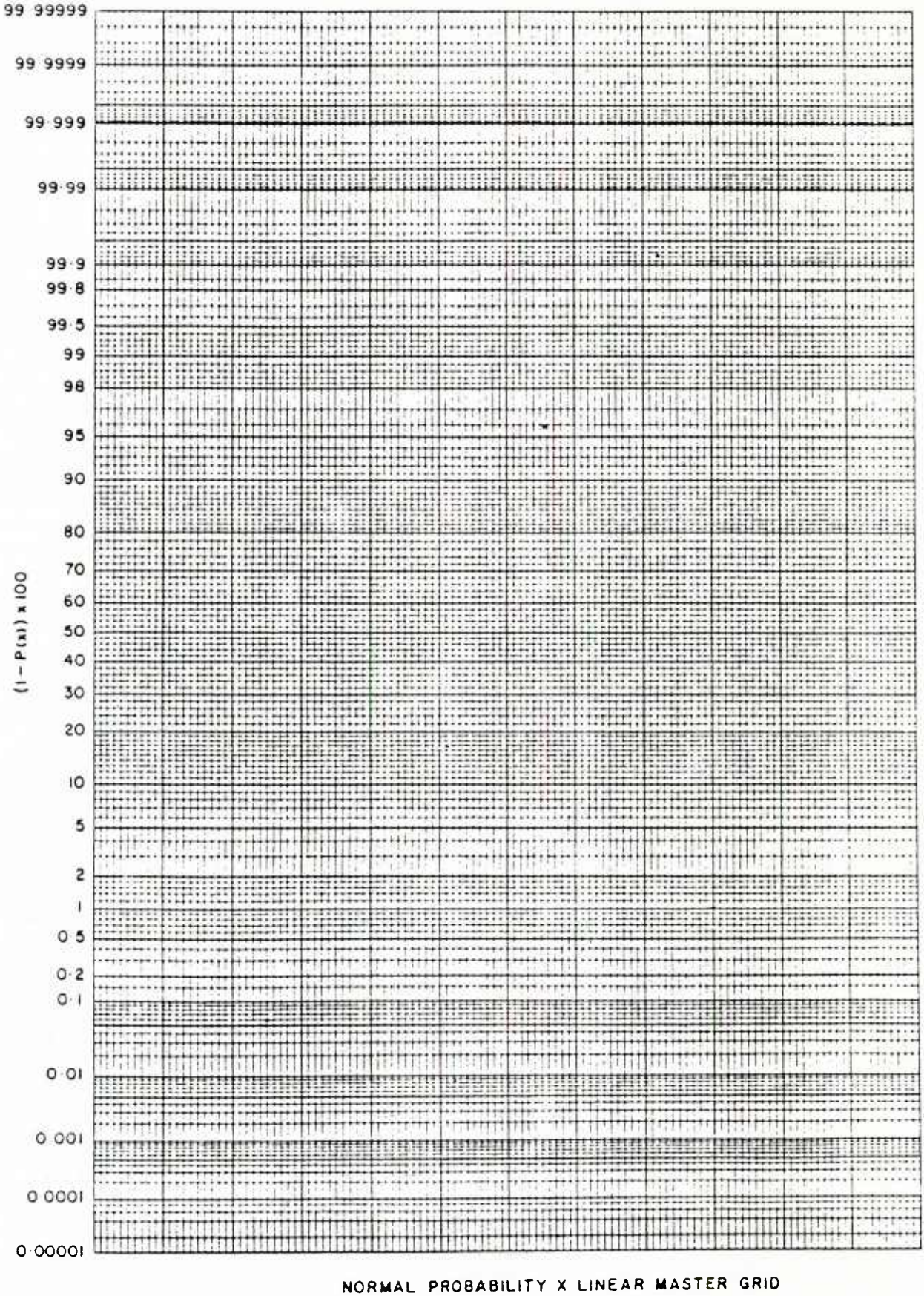
99 99999
99 9999
99·999
99·99
99·9
99·8
99·5
99
98
95
90
80
70
60
50
40
30
20
10
5
2
1
0 5
0·2
0·1
0 01
0 001
0 0001
0·00001
(1 – P(x)) x 100
NORMAL PROBABILITY X LINEAR MASTER GRID

fig 44.7

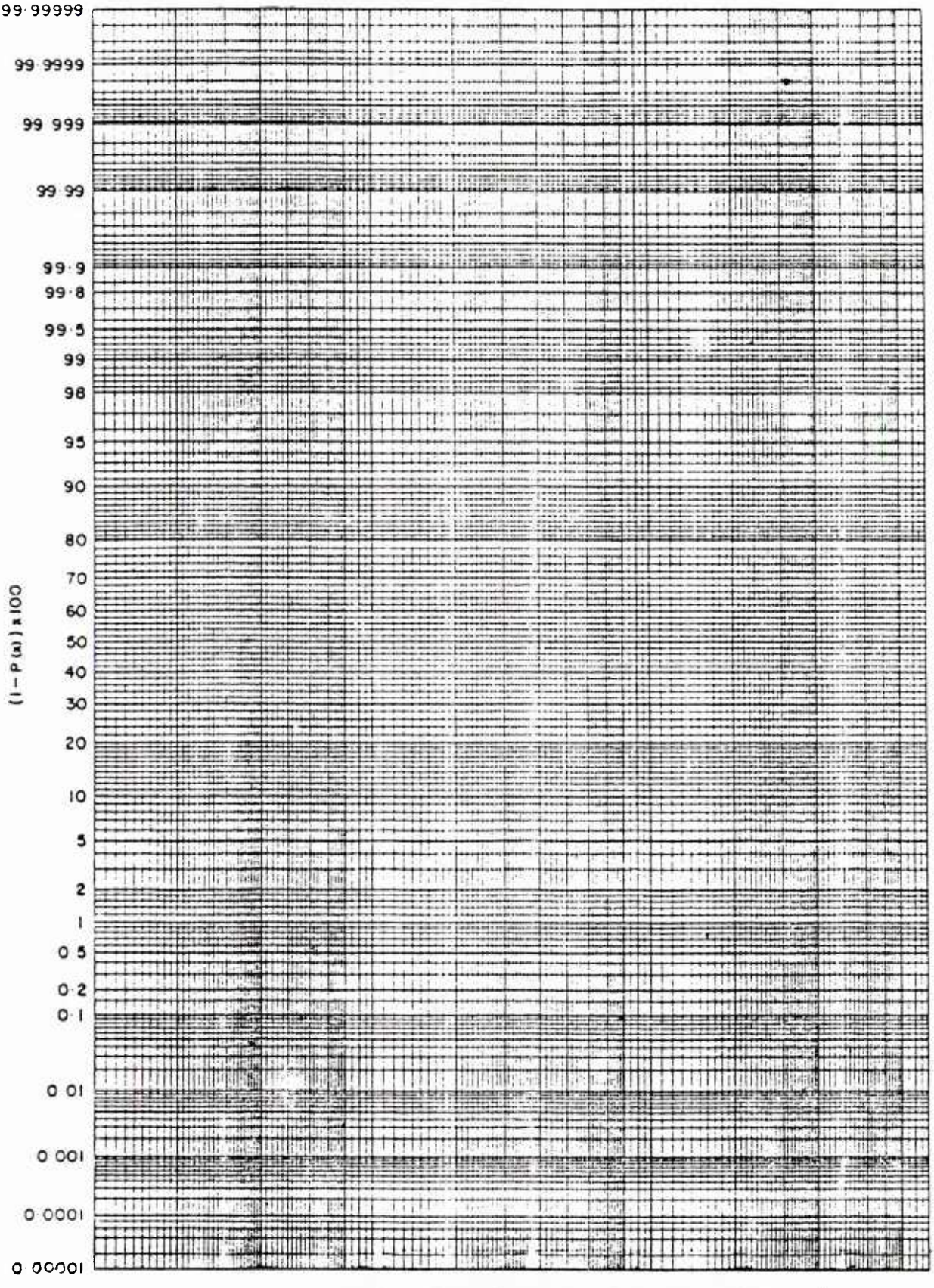

NORMAL PROBABILITY X LOGARITHMIC MASTER GRID

fig 44.8

CHAPTER 5

DEVELOPMENT AND QUALIFICATION PROCEDURES

BY

R.W. ARDEN
DEVELOPMENT AND QUALIFICATION DIRECTORATE
HQ, US ARMY AVIATION RESEARCH AND DEVELOPMENT COMMAND
ST. LOUIS, MISSOURI 63120
USA

D.P. CHAPPELL
HQ, US ARMY RESEARCH AND TECHNOLOGY LABORATORIES
MOFFETT FIELD, CALIFORNIA 94035
USA

H.K. REDDICK
APPLIED TECHNOLOGY LABORATORIES
US ARMY RESEARCH AND TECHNOLOGY LABORATORIES
FT. EUSTIS, VIRGINIA 23604
USA

CONTENTS

5.1 INTRODUCTION

5.1.1 SUMMARY

Chapters 2, 3, 4 and 6 have provided, from the viewpoint of the manufacturer, a general survey of current procedures and detailed discussions of the processes required to generate the data needed to substantiate the fatigue life of helicopter components. Airworthiness qualification of fatigue components, however, is generally conducted under the auspices of a government agency which is responsible for the qualification of aircraft systems. This chapter discusses, from the point of view of the Qualifying Agency, the current requirements for qualification of fatigue critical structures and the substantiation of those requirements as a function of the various phases in the development of an aircraft system. Where possible, the risks inherent in the various qualification methodologies are included.

The chapter covers, for flight critical helicopter structures, a broad spectrum of fatigue qualification topics including:

- Safelife and damage tolerant methods
- Metallic and composite structures
- Military and civilian requirements
- S-N and spectrum testing
- Airframe and dynamic (rotor) system qualification

Also presented is an overview of the substantiation process including a historical perspective, a review of the major events in the process, a listing of the physical requirements for ground and flight fatigue testing and a discussion of the importance of structural classifications. Examples of safe life and damage tolerant methods are provided and discussed in terms of potential risks or uncertainties. Comments are provided regarding special criteria such as post-ballistic damage flight requirements and the effects of extreme environments on component fatigue strength.

5.1.2 SPECIFICATIONS AND CERTIFICATING AGENCIES

The following is a list of the principal agencies which certify helicopters. The usage of various certification documents by these agencies is summarized in Table 5.1. The certification documents are incorporated as References 5.1 through 5.21. In every case, the system specification for the particular aircraft constitutes the primary source of requirements for development and qualification, whereas the other documents may be incorporated in whole or in part, or may serve as guides.

United Kingdom

Ministry of Defence (Procurement Executive)

Civil Aviation Authority (CAA)

France

Service Technique Aeronautique (STAe)

Direction Generale De l'Aviation Civile (DGAC) who delegate part of their powers to:

-Service Technique Aeronautique (STAe) for the technical side and flight testing,

-Bureau Veritas for the inspection side.

Germany

Bundesamt fur Wehrtechnik und Beschaffung, Leiter des Musterprufwesens fur Luftfahrtgerat der Bundeswehr (BWB-ML)

Luftfahrtbundesamt (LBA)

Italy

"Direzione Generale delle Costruzioni, Armi ed Armamenti Aeronautici e Spaziali", briefly Costarmaereo (General Direction of Aeronautical and Space Constructions, Weapons and Armaments)

R.A.I. (Registro Aeronautico Italiano)

Netherlands

Aeronautical Inspection Directorate of the Department of Civil Aviation (Directie Luchtvaartinspectie, Rijksluchtvaartdienst).

United States

U.S. Army

U.S. Navy

Federal Aviation Administration (FAA)

	ENGLAND	FRANCE	GERMANY	ITALY	NETHERLANDS	U.S.
F.A.R. PART 27		X	X	X	X	X
F.A.R. PART 29		X	X	X	X	X
CAM-6 APP. A						X
AC20-95			X			X
C.A.R. PART 6						X
C.A.R. PART 7						X
F.A.R. PART XX						X
AMCP 706-201						X
AMCP 706-202						X
AMCP 706-203						X
AR 70-10						X
AMCR 70-32						X
AMCR 70-33						X
DI-E-1134						X
MIL-S-8698 (ASG)						X
MIL-T-8679						X
Av. P. 970 VOL. 1	X					
Av. P. 970 VOL. 3	X					
BCAR SECTION A	X					
BCAR SECTION G	X		X			
BCAR SECTION R	X					
JAR 25	X					
NORMES AIR		X				
SYSTEM SPEC. OR PRIME ITEM DEVEL. SPEC.	X	X	X	X	X	X

TABLE 5.1 USAGE OF CERTIFICATION DOCUMENTS BY GOVERNMENT AGENCIES

5.2 SUBSTANTIATION PROCESS

5.2.1 HISTORICAL

Although the lifting airscrew concept dates back indefinitely, the intensive development of today's rotorcraft began in the 1930's. During this time, there was a vast proliferation of ideas, concepts, and configurations in the US and Europe. The fundamental problems of control and torque counteraction superseded structural fatigue problems in importance during this period. Fatigue loadings were accounted for in a relatively simple manner. Only the most critical conditions were investigated by strain surveys in flight or in wind tunnel tests.

Finite life predictions based on a complete flight spectrum were not generally performed. Instead, an attempt was made to design the components so that the endurance limits were not exceeded under the critical conditions investigated. To determine the allowable stresses, full scale parts as well as elements and material specimens were tested to 10 million cycles or so of constant amplitude periodic loading to estimate the endurance limit. The number of full scale specimens was small, and it would not have been extraordinary to find a rotor blade S-N curve constructed through a single data point.

Efficient analytical methods of load prediction were available-notably, the normal mode expansion analysis of rotor blade periodic motions. However, digital computers were not in use prior to around 1950, and earlier analyses were restricted by the time required for hand-calculation procedures.

In the case of these experimental aircraft not intended for general use by the public, it was appropriate that the methods of fatigue qualification were left largely to the manufacturers. The methods were satisfactory, partly because of the simplicity of the structures being analyzed, and partly because of their limited exposure to the loading environment - the accumulated flight times of early helicopters did not exceed 100 to 150 hours per ship. In addition, prior to 1944, helicopters were not produced in large numbers, and as has been ably pointed out by some authors, the probability of fatigue failure in service is proportional to the size of the fleet.

The era of series production began with Sikorsky's manufacture of helicopters for military use in the early 1940's. In 1946, the Bell Model 47 was awarded the world's first commercial helicopter license and certificate by the US Civil Aeronautics Administration. By this time, the experiments which began in the 1930's had brought about the helicopter's evolution into a few basic configurations: primarily the single main rotor with tail rotor and the tandem types.

The universal use of digital computers, beginning in the 1950's, then led to the development of current flight simulation and load prediction computer programs: C81, REXOR, NASTRAN, and 2G-CHARLIE.

Fatigue qualification requirements imposed by governmental agencies were initially loose and general, and remain so to the present. The regulations state simply that the structures shall be designed to withstand the fatigue loads throughout the flight envelope, and that when the safe-life criterion is applied, the service life shall be established by tests or other methods. In addition, they require flight strain measurements as a basis for the fatigue strength analysis. Appendix A to CAM-6, dated January 1963, and the ensuing FAA AC20-95, dated May 1976, supplied guidelines in the form of a typical flight spectrum for fatigue qualification of civil helicopters and also guidelines for safety factors to be applied to fatigue test data depending upon the number of specimens and other factors.

Considerations regarding the actual statistical significance of the test data and the resulting service life predictions have not been dealt with to any significant extent in the regulatory or advisory documents, although it is sometimes stated that for certified aircraft, the proability of failure shall be extremely small. Although the required probability of safety may be stated in the system specification for an individual aircraft, the full demonstration of compliance is outside the scope of any development and qualification program.

In the absence of more specific directives, the detailed procedures for aircraft qualification remain largely under the control of the manufacturers to the present time. The overall approach, on the other hand, has been effectively dictated in the advisory documents: by showing "an acceptable method", the regulating agencies early indicated their consent to accept finite life calculations based upon Miner's Theory of cumulative damage. This approach, through its simplicity and adaptability to computerized bookkeeping techniques, and most of all through its acceptability to the regulatory agencies, has come to be the method most commonly used for rotor systems, controls, and related structure.

Even after the most scrupulous safe-life analyses have been performed, occasional random failures continue to occur in large fleets of aircraft, even in parts for which infinite life has been predicted. Therefore, it would theoretically be better to provide structures in which defects, both manufacturing and service induced, are detected prior to catastrophic failure. FAR Part 29, Amendment 29-4, October 1968 opened the way for this alternative design approach by allowing certification under the fail-safe criterion. FAA Advisory Circulars 20-95, 1976 and 20-107, 1978 provided further guidelines for fail-safe qualification. Fail-safe applications, still in the minority, are gaining headway through the use of materials and structures which exhibit gradual failure modes in lieu of catastrophic cracking properties.

5.2.2 MAJOR EVENTS

5.2.2.1 Program Activities

The so-called Development Phase is an arbitrarily defined portion of a continuous process as illustrated in Figure 5.1. Decisions which strongly govern the conduct and outcome of the Development Phase are established in the nominally earlier, but partly concurrent, Design Phase.

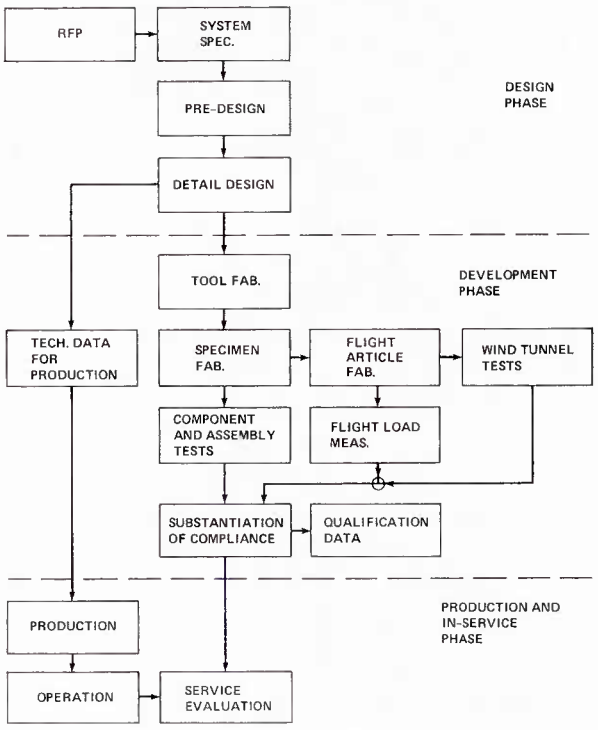

FIGURE 5.1 MAJOR EVENTS IN LIFE CYCLE OF FATIGUE-CRITICAL STRUCTURE

During preparation of the Request For Proposal (RFP) and the System Specification, basic requirements and criteria are established which control the execution of the Development Phase. These include the applicable documents, safety goals and requirements, methods of qualification, performance requirements (speeds, flight envelope and maneuver spectrum), criteria to be used: safe life and/or damage tolerant, service life requirements, methods of demonstration of compliance, and the number and usage of test specimens and flight articles.

As a result of the Preliminary Design activity, the structural arrangement, material selections, and manufacturing approach are established.

During the Detail Design stage, the initial sizing of the critical fatigue-loaded structural members takes place, as well as the design of tooling in accordance with the selected manufacturing approach. Design support testing during this stage consists of tests of coupons and small specimens to verify the material selections, structural configurations and the performance of key structural elements.

Analytical studies are performed during this phase to predict the aircraft performance, dynamic characteristics, applied loading environment, fatigue strength and the internal member loads and strains.

The Development Phase may nominally be considered to begin with the commitment of resources to the production of hardware, specifically to hard tooling and full-scale specimens for laboratory fatigue tests. As the fabrication, instrumentation, and laboratory testing of full-scale specimens progresses, the fabrication and instrumentation of the flight and wind-tunnel test aircraft proceeds concurrently. Completion of the full-scale fatigue tests and completion of the flight strain survey are the two most significant milestones in Development, since they provide the inputs for the final analytical demonstration of compliance with the requirements of the RFP and the System Specification.

The concurrency approach outlined here inherently contains some degree of risk, since necessary design changes revealed during laboratory and flight tests may require re-tooling and fabrication of new specimens with attendant costly program delays. If resources are strictly limited, abandonment of the program may result. On the other hand, the conservative approach of delaying major development activities until the results are in from other activities would probably result in a program so protracted as to be even more costly.

As a prolongation of the Design Phase, the preparation of technical data for production proceeds in parallel with development. These data consist of production drawings, quality control plans, manufacturing plans, materials and processes qualification data, and inspection and maintenance procedures.

Figure 5.2 illustrates the overall sequence of events leading to the analytical substantiation of compliance for certification purposes, including the application of the laboratory test and flight strain survey results. The figure illustrates the continuity between the design and development phases.

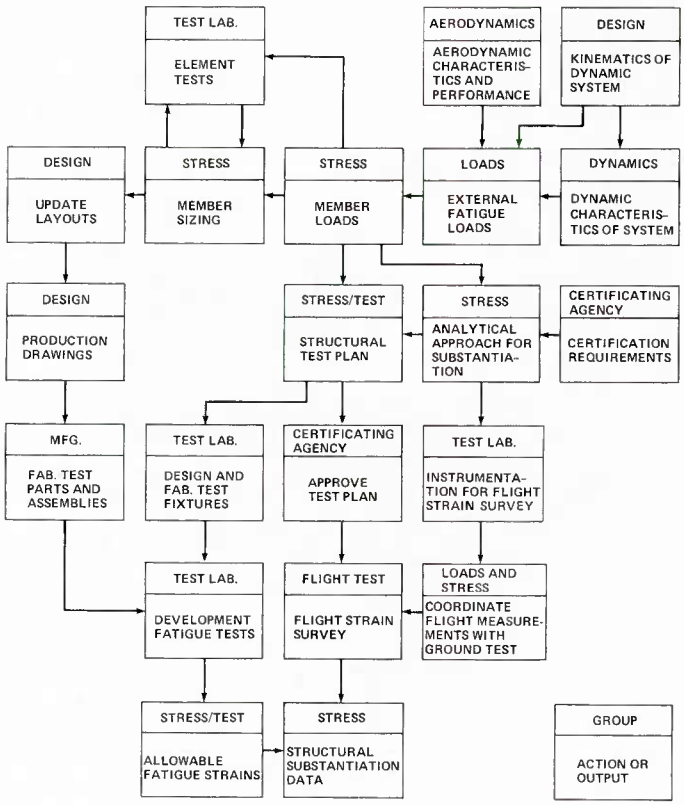

FIGURE 5.2 STRUCTURAL SUBSTANTIATION APPROACH

Unfortunately, the substantiation as outlined above for the purposes of certification of aircraft cannot be considered as final. Especially where large numbers of aircraft are involved, a prolongation of Development, i.e., the Service Evaluation Phase, must be carried past Production into the Operational phase for the purpose of confirming and revising the operating flight spectrum and determining the actual performance of the fatigue-critical components.

5.2.2.2 Procurement/Qualification Activities

The following defines the Procurement and Qualification Activities which parallel the major program events. These activities require significant interface between the manufacturer and the Qualifying Agency. Included also are the competitive selection phases of the process which are unique to the qualification of US Army helicopters.

Requirements Definition

The process originates in a user command where it is perceived that some form of aircraft is required to perform a specified mission or to counter an enemy threat. These needs are documented in a

Mission Element Needs Statement (MENS). Further evaluation of the battlefield scenario results in the writing of a Required Operational Capability (ROC) document which defines the operational capability required to meet the needs of the MENS. At this point, the fatigue requirements are only implicitly stated in the operational capability and are therefore rather general in nature. These general requirements are converted into specific engineering requirements in the Request For Proposal (RFP). This document is then provided to all qualified manufacturers who are interested in the specific competition.

For military helicopters, fatigue requirements are normally defined by a military agency and may include:

- Mission profile/Operational Usage
- Minimum fatigue life
- Number of specimens to be tested
- Minimum reductions from mean S-N curves
- Life reductions for spectrum tests

Table 5.2 presents a summary of current fatigue requirements for military helicopters. Fatigue requirements for civilian helicopters are similar to their military counterparts in that a usage spectrum is defined and agreements are reached regarding the number of specimens to be tested, reductions from mean S-N curves and life reductions for spectrum tests. Civilian agencies do not, in general, specify a

TABLE 5.2 CURRENT MILITARY FATIGUE REQUIREMENTS

REQUIREMENT	FRANCE	GERMANY (BO 105, REF. 1.3)	ITALY	UNITED KINGDOM	UNITED STATES ARMY
MISSION PROFILE	DEFINED INITIALLY BY MILITARY USER (STAe). LATER REVISED BY MEASUREMENT OF ACTUAL SERVICE USAGE	US F.A.A. SPECTRUM WITH MINOR MODIFICATIONS	DEFINED BY MILITARY USER	DEFINED BY MILITARY USER (RAF, RN)	DEFINED BY MILITARY USER (TRADOC) AND ARMY R&D COMMAND (AVRADCOM)
MINIMUM FATIGUE LIFE (HOURS)	1000		3600	VARIES, DEFINED IN AIRCRAFT SPECIFICATION	4500 TO 5000
NUMBER OF FULL SCALE S-N SPECIMENS TESTED	6		6	6	6
REDUCTIONS FROM MEAN S-N CURVES	2.00 FOR LIGHT ALLOYS AND 1.67 FOR STEELS	SURVIVAL PROBABILITY OF 99.9%	LOWER OF 3σ OR 20% FOR STEELS AND 3σ OR 25% FOR LIGHT ALLOYS	SEE TABLE 5.3	M-3σ OR FIXED PERCENTAGE REDUCTION DEPENDING ON MANUFACTURER (SEE NOTE)
LIFE REDUCTIONS FOR SPECTRUM TESTS OF FUSELAGE, EMPENNAGE AND WINGS	5 FOR CONVENTIONAL MATERIALS, 10 FOR COMPOSITES		SPECTRUM TESTS NOT CONDUCTED	5 FOR ONE TEST SPECIMEN, 3.9 FOR THREE SPECIMENS, 3.6 FOR SIX SPECIMENS	4 BASED ON ONE TEST SPECIMEN

NOTE: WHEN LESS THAN 6 SPECIMENS ARE TESTED, THE REDUCTIONS ARE:

$$\text{REDUCTION FROM MEAN (\%)} = \frac{(3)\,(COV)\,(1+\frac{1}{\sqrt{N}})}{1+\frac{(3)\,(COV)}{\sqrt{N}}} \times 100$$

WHERE: COV = POPULATION COEFFICIENT OF VARIATION (IN DECIMAL FORM)
N = NUMBER OF SPECIMENS TESTED

TABLE 5.3 U.K. REDUCTION FACTORS

NUMBER OF SPECIMENS TESTED	REDUCTION FACTOR	
	ALUMINUM ALLOYS	STEEL AND TITANIUM
1	1.72	1.49
3	1.63	1.42
6	1.60	1.40

minimum fatigue life as this is considered a prerogative of the manufacturer. These agencies do, however, place requirements on the final calculated fatigue lives as shown in this example from the US F.A.A. for a specific helicopter program:

Calculated Fatigue Life (Hours)	Maximum Allowable Service Life
< 3350	0.75 x Calculated Life
> 3350	0.375 x Calculated Life + 1250

Initial Competitive Selection

This initial phase of the competition may involve from 2 to 5 manufacturers whose proposals are thoroughly evaluated by the Source Selection Evaluation Board (SSEB) which consists of specialists in every engineering discipline obtained from throughout the Army technical community. Since the US has no standardized fatigue methodology, the SSEB must evaluate the approach of each manufacturer to determine compliance with minimum requirements. Also reviewed are the preliminary fatigue life estimates which are based entirely on analytical component strength and predicted loads. This phase of the competition ends when the SSEB selects two manufacturers for the initial development phase.

Initial Development

Since the flight spectrum will have been defined in an earlier phase, the primary tasks during initial development are:

- Identify fatigue critical components
- Conduct initial component S-N tests
- Conduct coupon tests (S-N curve shapes) for unique material such as composites
- Develop load spectrum based on analytical predictions
- Redesign components, if necessary, based on preliminary life calculations

Fatigue critical components are initially identified by preliminary analysis and experience with previous aircraft systems. This list of components, however, must be treated as preliminary since it is likely that additional fatigue critical items will be discovered once flight testing has begun. Using this initial list as a guide, S-N tests are begun on the most critical of the fatigue components.

Since most manufacturers have an extensive data base for metallic curve shapes, it is unlikely that coupon testing of metals would be necessary. However, with the advent of composite materials having almost unlimited variability in fatigue characteristics, it is almost a certainty that coupon testing of composite substances will be required. Of particular importance are the effects of natural environments (principally temperature and humidity) on the fatigue strength of composite materials. Current US Army helicopters have an operational temperature range of - 65°F (-54°C) to + 125°F (52°C) and humidity requirements up to 95%. Recent experience, however, has shown that composite materials with certain exterior coatings will absorb large amounts of solar energy and reach temperatures of 220°F (104°C). For these reasons, it is likely that future coupon tests of composite materials will be conducted over a wider range of temperatures.

Using a conservative analytical load spectrum and the results of the initial S-N tests, a preliminary calculation of fatigue lives can be conducted. Components having marginal fatigue lives are redesigned and returned to fatigue testing.

Final Competitive Selection

At this stage of the competition, both manufacturers will have accomplished the following:

- Built three or more prototype aircraft
- Conducted initial required coupon tests
- Conducted limited flight tests to a restricted envelope
- Established a load spectrum based on analysis and limited flight test
- Conducted S-N tests of at least 1 specimen of all flight critical fatigue components
- Redesigned components where necessary
- Performed preliminary fatigue life calculations

In addition to the above, each manufacturer provides two documents which are the basis for the contract between the manufacturer and the US Army. These documents are the System Specification (SS) which contains the fatigue requirements and the Airworthiness Qualification Specification (AQS) which defines the testing which will be performed to substantiate the requirements of the SS. All of the above data are reviewed by the SSEB for compliance with the requirements of the RFP and one manufacturer is selected to proceed into the final development phase.

Final Development

This phase requires a substantial amount of interfacing between the manufacturer and the Qualifying Agency. The Agency is responsible for the following actions:

- Review and approve all component S-N test plans
- Issue airworthiness releases for all flight testing
- Review and approve all design changes to fatigue critical components
- Insure manufacturer compliance with development phase minimum fatigue requirements

The development phase is essentially an iterative process (Figure 5.3) leading to the full qualification of the aircraft for production. Flight tests using heavily instrumented aircraft (see Chapter 5.2.3) are conducted to succeedingly larger flight envelopes. These flight tests provide actual loads measurements which replace the analytical value contained in the load spectrum. Component S-N testing is continued and working curves are less conservatively defined based on increased numbers of specimens. The result of these two actions (flight and S-N tests) is to provide an improved estimate of component fatigue lives and an indication of any necessary component redesign. The iterative cycle is continued until the aircraft reaches the limits required for qualification.

Qualification/Substantiation for Production

The fatigue qualification of an aircraft requires completion of the tasks that were begun in the preliminary design phase. Component S-N tests for all production parts must be completed, working curves are established in accordance with required reduction factors and test results approved by the Qualifying

Agency. A flight loads survey must be conducted to the full aircraft specification flight envelope. This is an extensive flight test program requiring that each condition in the flight spectrum be flown to provide actual loads data for all points in the load spectrum. If required, spectrum tests are conducted using loads obtained during the flight loads survey. Spectrum tests are normally used for the fatigue substantiation of the complete fuselage or major aircraft sections such as the tailboom, empennage and wings.

The final step in the qualification process is the documentation of the fatigue life calculations in a fatigue substantiation report. This report contains, in addition to the calculated lives, the manufacturers recommended service retirement lives. The Qualifying Agency reviews these recommendations based on the field service history of similar components and accepts or amends the service retirement lives which are then documented in the operator's manual.

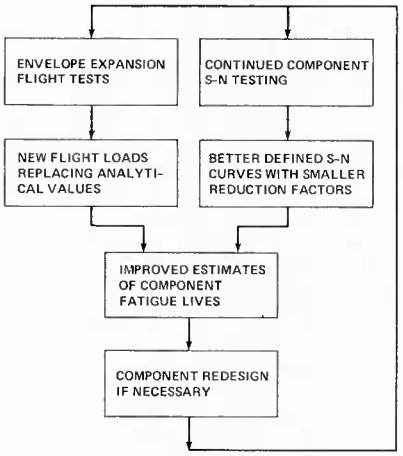

FIGURE 5.3 DEVELOPMENT PHASE ITERATION OF COMPONENT FATIGUE LIVES

Quality Control Fatigue Tests

To insure the quality of fatigue components throughout the production process, quality control fatigue tests are conducted. The procedure used by the U.K. is typical and is presented here as an example. Two components are selected from the production line on a regular basis such as one out of 40 items or once a month. One component is tested in a simplified version of the full production fatigue test. The results of the test are compared to a "warning limit" and an "action limit" which have been determined statistically from previous tests. If all required parameters are within the warning limit, the results are satisfactory and the second specimen is returned to production. If any parameter exceeds the action limit, production must cease until the cause is determined. Parameters falling between the warning and action limits will require the second specimen to be tested.

Quality control fatigue testing has increased significantly as a result of the general application of composite materials. It is especially critical when, as is common in the U.S., attempts are made to qualify additional vendors for a specific production component. Experience has shown that small differences in seemingly identical manufacturing processes can result in unexpected variations in fatigue properties.

Service Load Monitoring

The initial qualification of fatigue components is based either on a standardized flight spectrum for a particular class of helicopter or on a spectrum which is tailored for a specific helicopter application. In either case, the spectrum is, at best, an analyst's estimate of the eventual usage of the aircraft. Although the initial design spectra are constructed in a conservative manner, the constant evolution of battlefield tactics and commercial applications creates the possibility that the actual usage spectrum is significantly different. To investigate this problem, several agencies have begun to monitor aircraft within the operational fleet.

The U.K. has conducted the initial work required to show that parameters (such as aircraft accelerations and velocities, control inputs and altitude) measured in-flight as a function of time can be converted into recognizable maneuvers. Current plans are to instrument several aircraft within the fleet and compare the derived spectrum with the spectrum used in the initial qualification.

The US Army has accumulated an extensive amount of in-service flight data for all classes of helicopters, particularly during the conflict in Southeast Asia. Portable flight recorders with varying degrees of sophistication are in existence and the computer tools necessary to translate flight recorded data into mission spectra are available. At the present, however, there are no active programs to monitor the current service fleet. Although merit is recognized in using flight monitoring systems, this present trend has been prompted by two factors:

. Economic - the fatigue lives of modern technology helicopters are very large ($\geq$ 5000 hours) and at current aircraft usage rates will require component replacement only after many years of service.

Safety - the excellent safety record of modern technology helicopters has demonstrated that, although the design spectrum may not reflect actual aircraft usage, there is sufficient conservation within the entire fatigue qualification process to preclude premature fatigue failures.

US Army interest in service load monitoring is limited at the present to Service Life Extension Programs for older aircraft within the current fleet.

France is currently using service load monitoring to the maximum extent possible. Current practice is to initially qualify fatigue components to a design spectrum. When the aircraft system is fielded, sufficient flight data are recorded to derive an actual usage spectrum and final fatigue lives are recalculated on this basis. In this manner, service load monitoring becomes the final link in the chain of the fatigue qualification process.

5.2.3 PHYSICAL REQUIREMENTS

The first major physical requirement is the laboratory testing facilities and full scale specimens used to establish component fatigue strength (or life in the case of spectrum tests). The most common laboratory test is the constant amplitude S-N test. Although the test set-up will depend to some degree on the size and complexity of the tested component or subassembly, these tests are routinely conducted using simple load application/monitoring and crack detection systems. The difficulty with S-N testing is not in the test itself, but in the sheer number of tests to be conducted. A modern helicopter may have from 75 to 100 fatigue critical components with 6 specimens of each component to be tested. The end result is that testing will require tens of thousands of hours and the entire test program may extend over several years. A further complication is the emergence of environmental requirements (such as high temperature and humidity) in the testing of composite structures. Conducting a fatigue test in an environmental chamber will require additional test facility equipment, instrumentation and monitoring devices and more time will be required to conduct the test due to the presence of such things as heat-up and cool-down cycles.

A spectrum test is generally more difficult to conduct than an S-N test. Test specimens are usually large, complex structures up to the size of an entire helicopter airframe requiring an equally complex test facility. Since the purpose of the test is to apply a quasi-random load spectrum to the structure; load application, phasing and monitoring will normally require the use of a computerized system. Instrumentation and the detection of crack initiation will also be more difficult due to the size and complexity of the test specimen. Although a spectrum test may require only one test specimen, the test duration can be quite lengthy since the response of many large scale structures will force a rather low ($2\ H_z$) rate of load cycle application.

The second important physical requirement is the flight test facility and aircraft used in the acquisition of component loads data by means of the Flight Loads Survey (FLS). Within the U.S., the FLS is normally conducted by using a single, heavily instrumented test aircraft. Although the use of only one aircraft prevents an evaluation of the variations between aircraft and pilots, the cost associated with instrumentation and flight testing normally precludes the use of additional test vehicles. The two factors which create difficulty within the FLS are the number of instrumentation parameters which must be maintained throughout the flight program and the number of flight conditions required to provide the necessary data for the design flight spectrum. Table 5.4 presents a typical instrumentation list for a flight program recently conducted for the US Army. Although most of these parameters will be recorded on magnetic tape for subsequent analysis, 20 to 30 flight safety critical parameters will be relayed via telemetry to the ground station for real-time presentation. With regard to the number of flight conditions, a typical program might consist of 500 conditions considering all the combinations of weight, center of gravity, altitude and rotor RPM. The scope of the FLS will depend to a large extent on the complexity of the aircraft system and its mission profiles. A current program in the US Army involves an aircraft with several different external store configurations. Preliminary analysis shows that nearly 400 instrumentation parameters will be required and that the FLS will consist of nearly 1000 flight conditions.

	NUMBER AND TYPE OF MEASUREMENT		
LOCATION OF MEASUREMENT	STRUCTURAL LOADS	VIBRATION AND ACCELERATIONS	POSITIONS AND DEFLECTIONS
MAIN ROTOR SYSTEM	17		3
TAIL ROTOR SYSTEM	14		1
CONTROLS	12	8	11
AIRFRAME	20	35	1
DRIVE SYSTEM	17	9	
WEAPONS SYSTEM	1	3	
SUBTOTALS	81	55	16

TOTAL	152
AIRCRAFT PARAMETERS	36
ENGINE PARAMETERS	8
GRAND TOTAL	196

TABLE 5.4 TYPICAL INSTRUMENTATION LIST

The French approach to FLS testing is somewhat different from that of the U.S. Two or three instrumented aircraft are used in the survey and these are flown by several different pilots. The number of flight conditions investigated ranges from 40 to 55 and a typical instrumentation package averages 48 channels with a maximum of 84 channels.

5.2.4 STRUCTURAL CLASSIFICATIONS

Fatigue design must be accomplished on all safety of flight critical structural components which are those whose failures would result in loss of the aircraft. These components are generally classified as safe life or damage tolerant.

Safe life structures are designed to a specific service life and are removed from service at or before this elapsed time so that the probability of failure is remote. Damage-tolerant structures are designed to have the ability to successfully contain damage over a specified increment so that the damage may be detected and corrective action taken before the residual strength of the structure is reduced below a safe value. This design approach is generally achieved in one of two methods -- failsafe or safe crack growth. Failsafe structures are usually comprised of multiple elements or load paths such that damage can be safely contained. Safe crack growth structures are sized using fracture mechanics or empirical data such that initial damage will grow at a stable, slow rate and not achieve a size large enough to fail the structure prior to detection.

5.3 QUALIFICATION OF SAFE LIFE STRUCTURES

5.3.1 CURRENT ANALYTICAL PROCEDURES

The principal elements comprising the safe life structural fatigue analysis procedures are outlined in Figure 5-4. Each element defined in the blocks is treated in depth in other chapters of this manual; however, the elements are frequently referred to throughout this chapter and so are presented herein for ready reference.

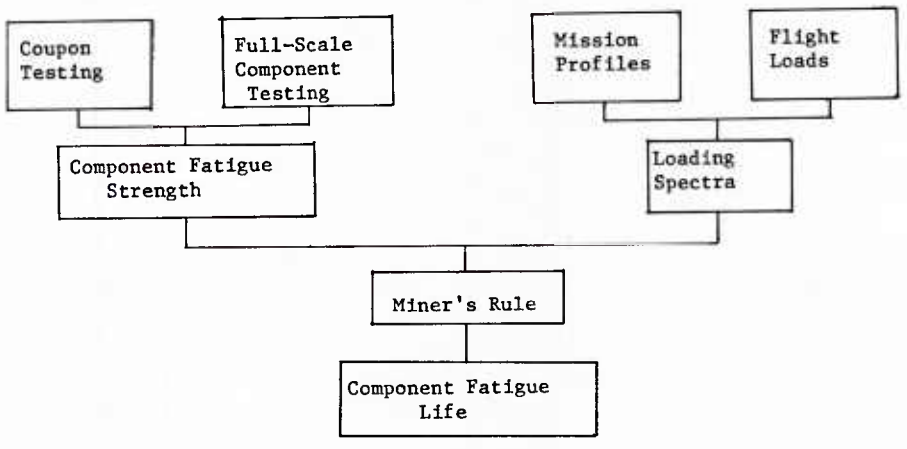

FIGURE 5.4 SAFE LIFE METHODOLOGY

The component fatigue strength is developed from coupon and full-scale component data. The mission loading spectrum is developed from the mission profiles for the helicopter and the loads for all flight conditions comprising the profile. Initially these loads are calculated using analytical programs or empirical data based on flight loads of similar aircraft. Following a flight strain survey, they are updated with measured flight loads for the aircraft. With the component fatigue strength and a loading spectra the component fatigue life is developed using Miner's cumulative damage theory.

5.3.2 UNCERTAINTIES IN ANALYSIS

Uncertainty in the Definition of Fatigue and Fatigue Failure

The fracture mechanics theory of crack propagation rests upon a relatively sound theoretical and experimental base involving the physical parameters of crack length and strain history, and the material property of fracture toughness. By contrast, the engineering concept of cumulative fatigue damage during crack initiation (i.e., most of the safe-life period for a metal structure) is based upon the assumed gradual accumulation of a hypothetical property--the so-called fatigue damage--or conversely, the degradation of the fatigue strength. On investigation, the fatigue damage is found to be simply the ratio of the time spent in a defined fatigue environment to the total time expected to elapse prior to the occurrence of a detectable crack or some other event by which failure is defined. This is a circular concept, since in the absence of the final event, the progressive nature of the damage cannot be detected or determined. Although physical changes which are related to crack initiation are known to occur at the microscopic and molecular level, the relationship of these changes to the crack initiation time is undefined.

The difficulty in characterizing the crack initiation stage has led to imprecision in the concept of fatigue. From the materials science point of view, it can be stated that all materials contain crack-like discontinuities, and that the likelihood of fatigue failure is the likelihood that such

discontinuities will occur or be created at critical locations where the strain levels are such that the discontinuities are likely to grow. From this definition, it follows that fatigue life in a given environment is as much a property of the individual part (or the aggregate of the parts) and the strain within the part as of the material itself.

The lack of characterization of the fatigue process leads to a difficulty in identifying a specific stage of the process with which failure can be associated. For the purpose of qualification of aircraft, a definition of failure is required for each component being qualified, and fatigue testing and analysis should be conducted in accordance with the definition. The definition may be modified as development progresses. The failure or end-of-life may be defined as a barely detectable crack, a large crack, a degradation of static strength, or a degradation of stiffness.

Newly-manufactured metal parts in which cracks are detected are generally considered to be failed or at the end of their life, even though their service time is zero. Metal parts in the dynamic system will be retired from service when cracks are detected, even though their static strength may not be measurably degraded. The practice of immediately retiring metal parts with known cracks follows from the fact that with the relatively rapid accumulation of loading cycles in helicopters, catastrophic failures can occur after a few hours of operation at stresses above the crack propagation threshold.

Composite materials generally have more gradual modes of failure than metals and are more tolerant toward manufacturing defects and various forms of damage. At the operating strain levels typically found in helicopter rotor blades, relatively large defects may be tolerated, so that the practice of retiring parts with small defects no longer applies. Because of the anisotropy of these structures, and the complex interactions between the matrix and fiber materials, the definition of failure is more uncertain, and may only be obtainable through arbitration based upon the full-scale test results.

Uncertainty in the Sources of Random Fatigue Loads

Since all fatigue loads are dynamically amplified in an aircraft system, the analytical determination of the loads through flight simulation models requires that both the applied airloads (the forcing function) and the structural response are accurately known. Analytical models which use a deterministic estimate of the airloads and the structural response can be used to estimate the mean, expected value of the oscillatory loads. However, when the same loads are determined experimentally, large components of loading are measured which are random, intermittent, and unpredictable. A careful analysis of the flight data always reveals that there are variations in both the airload forcing function and in the structural dynamic response which are beyond the scope of any deterministic analytical model. These effects, which are found even in hover or steady flight, or in a stabilized test condition in a wind tunnel, are referred to under the general category of statistical variations of the applied loads.

Loading variations of this type are always found to exist between one aircraft and another, between identical components on a given aircraft, from one day to the next, and with different pilots. They are correctly attributed to the following factors: variations in rotor blade contours and mass distributions, within acceptable manufacturing tolerances; atmospheric changes from day to day and from test point to test point; variations in pilot technique - rapidity and excursion of control movements, phasing of cyclic and collective controls; variations in aircraft dynamic and kinematic properties - structural damping, clearances, wear and looseness of parts; and variations in drag and trim attitude between aircraft of the same type.

Although these phenomena are significant and well documented as to their existence, the quantitative evaluation of the variation of the applied loads resulting from these factors is beyond the scope of the development program for a new aircraft type. A research program directed towards quantification of the statistical variations of the applied loads would present unique requirements in terms of extensive duplication of instrumentation on numerous aircraft and parts of aircraft, and repetition of flights and flight conditions. In the case of a U.S. Government-sponsored research program of this type, the applied loads were found to be from 50% to 75% higher at the .999 (approximately 3 sigma) probability of non-exceedence than at the .50 (expected value) level. It may be anticipated that in view of the more limited amount of statistical data obtained during an aircraft certification program, the loads measured in the flight strain survey will be nearer to the .50 probability values. A risk of unknown magnitude is thus entailed in the application of the flight strain survey data to the prediction of flight safety.

Uncertainty of Statistical Distribution of Allowable Strains

All certificating agencies require substantiation of allowable strains through full-scale fatigue testing of major components and assemblies. In view of the costly nature of full-scale tests, the testing of a sufficient number of specimens for the results to have any true statistical significance is beyond the scope of all development programs. As far as practical application of the data is concerned, and at the level of safety required, i.e., one failure over ten years of operation in a fleet of one thousand aircraft, small sample statistical methods remain almost a contradiction in terms. Attempts have been made to assess the probable scatter in the allowable strains for apparently identical parts on the basis of previous experience. On the basis of development tests within an aircraft program, the standard deviation of the allowable strain is found to be itself a stochastic quantity which varies among the various components. If a log-normal distribution is used to fit the test data for each component, the scatter below the mean is of the order of 10 to 15 percent at 50% confidence level, but at 90% confidence the scatter below the mean is of the order of 50 to 60 percent of the mean.

Methods used to allow for the scatter are: (a) an assumed typical or maximum value of the scatter is applied to estimate the safe operating stress from the test mean, (b) the 3-sigma scatter of the actual test data is used, assuming a normal or log-normal distribution, to establish the working stress boundary, or (c) some estimate of the distribution function of the allowable strains is entered into a Monte Carlo analysis along with another distribution function for the applied strains, to develop a probabilistic estimate of the predicted service life. However, the tails of the statistical distribution functions, at which the required high probability levels exist, are outside the data sample for both the

applied and allowable strains, and the distributions in these regions are always assumed rather than empirically demonstrated. Further, there is no reason to assume that the empirical data, even if it were available, would match the assumed distribution functions in these regions. Under the circumstances, a risk of unknown magnitude is inherent in the application of any of these methods. Unfortunately, the theoretical computation of "3-sigma" or "five nines" probability of non-failure does not alleviate the uncertainty of the underlying assumptions.

5.3.3 AREAS OF POTENTIAL STANDARDIZATION

Philosophy of Standardization

Standardized methods of qualifying safe-life structures are subject to certain restrictions and limitations. Even though the life estimation procedures are universally understood in principle, their practical use requires the application of a formidable background of engineering judgement based upon experience, without which serious errors may result. As the conditions are approached where the computed finite life lies in the region of interest, i.e., predicted lifetimes of zero to 30,000 hours, small variations in the defined relationships between the applied load spectra and the allowable S/N data may result in large variations in the predicted life. Such variations may correspond to anticipated random or statistical variations due to uncertain or unknown causes, or to deliberate selection of input factors based upon the analyst's judgement. In addition, these critical variations in the applied and allowable strain data are likely to lie within the tolerance band of acceptable values based upon a reasonable interpretation of the available data.

In view of the many uncertainties involved in the safe-life analysis, it is not intended that standardized methods shall be used to replace the individual manufacturer's judgement in those areas for which judgement and experience are essential, or to reduce the manufacturer's liability or responsibility in developing airworthy structures. In fact, it shall always be a major duty of the manufacturer to detect and point out any unique design features, or any phenomena such as non-linearity, fretting, friction, relative motion, alternative failure modes, or environmental effects which may tend to invalidate the use of standardized methods.

In spite of these limitations, it is still desirable to standardize as many portions of the safe-life analysis as feasible. Such standardization will provide the certificating agencies with an equitable basis for comparison and evaluation of proposals, reduce the review burden, and minimize incidental or gratuitous differences between contractor's life predictions. Obviously, the most practical areas in which to standardize initially are those in which an essential consensus already exists among the contractors and among the certificating agencies.

The following recommendations are made with respect to some of the areas of potential standardization.

S/N Curve Shapes for Specific Materials

In performing the safe-life stress analysis, each helicopter manufacturer employs the S/N curve shapes which are considered in his judgement to be the most suitable for the purpose. The data base on which the curve shapes rest may be obtained from tests of both material coupons and production parts, and may include information from the manufacturer's own in-house tests as well as from outside agencies and sources. The ability to justify the use of certain curve shapes for life prediction becomes a key item for the aircraft manufacturer in the defense of product liability suits. For this reason, and because of the sensitivity of the life prediction to the shapes selected, it is in the contractor's interest to maintain control over the data and methods used, subject to the final approval by the certificating agency.

It is recommended that proposed standardized S/N curve shapes for the commonly used materials initially be supplied by the certificating agencies as a guide to manufacturers. These shapes would be intended to be used to the maximum extent feasible, but would be subject to deviation at the manufacturer's request. The justification of the final selection of S/N curve shape for each life prediction calculation would remain the responsibility of the manufacturer, subject to agency approval.

Reduction Factors for Working Curves

In the U.S. Army's comparative study of various manufacturers' life predictions for a hypothetical pitch link, conducted in 1980, the selected reduction factor from the mean of the test data was found to have a greater impact on the predicted life than the S/N curve shape, the material considered (steel or aluminum), or the degree of analytical or statistical refinement of the analysis. The selected reduction factor varied widely among the companies represented, and was mainly a reflection of each company's policy and tradition regarding the degree of conservatism desired. Although the Army's study was simplified and idealized, the importance of the reduction factor as well as the lack of a consensus on the method of selecting it were shown graphically. In spite of this, each manufacturer appeared to have high confidence in his own individual approach.

Various statistical analyses of test data, both full scale and coupon, are performed to establish the appropriate reduction factors. For correctness, these analyses would have to allow for the uncertainty of the mean of the total population as estimated from the test population, as well as the uncertainty of the scatter of the total population. The shape and magnitude of the empirical distribution/density functions near the tails of the functions would also have to be estimated. It is extremely unlikely that any statistical analysis of six to twelve specimens will produce a high confidence in any of these quantities. It is altogether more likely that in case of doubt, the allowable strains will be directly or indirectly based upon accumulated experience with similar parts in similar environments, with partial verification being obtained from development tests on the current model.

As compared to the S/N curve shapes, the reduction factors from the mean have an equal or greater impact in the area of product liability. They are even more uncertain, since the majority of test data clustered near the mean tend to establish the curve shape, whereas the reduced working curve by its nature lies in the region where the data are most sparse. It is likely that the manufacturers will wish to retain some degree of control over these particularly sensitive inputs to their analyses.

On the other hand, a strong precedent exists for the selection of standardized working stress reduction factors in structural design. The traditional 1.5 factor of safety for ultimate strength is such a factor which covers all uncertainties, both defined and undefined. Since it is desirable to standardize the fatigue strength reduction factors to the extent that is feasible, it is recommended that the Structures and Materials Panel of AGARD conduct a poll of manufacturers, analogous to the study of factors of safety for static strength which was conducted in 1980-81, with emphasis on determining the magnitude of reduction factors from the mean which are currently in use or are recommended. This information may then be used by the certificating agencies as a basis for developing some form of standardization, although further negotiations may be required before a consensus is reached. It is understood that all manufacturers will wish to reserve the right to deviate from these factors where justified, and also that some manufacturers may use alternative statistical analysis methods in lieu of the type of reduction factor under discussion.

Use of Standardized Mission and Loading Spectra

Diverging possibilities exist regarding the definition of the applied loads. One trend is toward a very detailed definition of the flight envelope, supported by research into actual operating histories of various types of aircraft such as observation, utility, attack, crane, and transport, taking account of many permutations of the flight parameters, and producing an operating spectrum unique to each helicopter type. The flight spectrum emanating from this approach may contain hundreds of segments and may require a very extensive flight strain survey to satisfy the requirements of certification. In view of the inherent uncertainty of the safe-life prediction process, the use of highly detailed and specialized flight and loading spectra may imply a degree of refinement which in fact does not exist. In addition, the need for versatility of aircraft, as mission requirements change with time, implies that a flight spectrum of a composite character, corresponding to a variety of applications, is more likely to be realistic and practical.

As opposed to the use of very rigorous and detailed spectra, some manufacturers and agencies have shown a trend towards a more simplified and generalized approach, notably Bell, Sikorsky, and the U.S. Army R&T Laboratory. Simplified methods of life prediction which employ standardized loading spectra are discussed in References 5.22 and 5.23. In both of these references, the load level versus probability of occurrence spectra for the complete flight envelope and characterized by only two parameters, one of which represents the absolute load level at a reference probability, while the other represents the extent of the scatter of the loads about the same reference point. Under this method of Reference 5.22, empirical loading spectra were implicitly included in the analyses which led to the working curves of life versus the spectrum parameters, for various materials. In the method of Reference 5.23, the applied loading spectra for rotor systems and related components were assumed a priori to be defined by log-normal functions. The two methods were then shown to be equivalent within a few percent, which lent credence to the log-normal assumption.

Although the methods of References 5.22 and 5.23 were only proposed for flight load monitoring of experimental aircraft and for use in preliminary design and development of new models, there appears to be little or no practical loss of accuracy resulting from their application. A critique of the short-cut method versus the more traditional certification approach, given in Reference 5.24, implies that in the case of the Bell YAH-63, a satisfactory design result would probably have been reached by either method. Under the circumstances, it can be postulated that the requirement for very detailed spectral analyses is based as much upon ready acceptance by the certificating agencies as upon the need for greater accuracy.

It is recommended that the manufacturers as well as the certificating agencies give further consideration to the use of standardized loading spectra which are capable of representation as continuous functions of a few parameters, similar to the manner in which the S/N curves are represented as analytic functions, even though the data base which they characterize consists of many discrete points. In this form, the characteristic features of the loading spectra could be more easily grasped conceptually, and the functions could be manipulated to account for changes in the mission spectra, the severity of usage, and the loading scatter. It is understood that if simplified and standardized flight and loading spectra are eventually used, it will still be the manufacturer's responsibility to identify any deviations which are necessitated by conditions which are unique to the aircraft and its operation.

Acquisition, Evaluation, and Treatment of Flight Strain Data

Certain activities related to the conduct of the flight strain survey and the ensuing analysis of the flight data are amenable to standardization, whereas other activities are by necessity flexible and must be dealt with differently for each aircraft program. Areas which do not appear to be readily subject to standardization are those which involve the general conduct of the flight strain survey, as follows: the number of test aircraft to be used; the number of different pilots used; the number of repetitions of flight test points; and the number of flight conditions and maneuvers required to be flown in order to explore the flight envelope adequately. Other areas not amenable to standardization are those unique to each aircraft; e.g., the selection of the critical locations to be instrumented, and the need to test under different atmospheric conditions, which depends upon the sensitivity of the particular aircraft to turbulence.

Activities which are more readily subject to standardization are those which relate to the analysis of the flight data leading to certification. It appears that one or more algorithms used for fatigue load cycle counting may conscientiously be selected as standard. Since a scientific basis for these algorithms has not yet been established, it is recommended that those automated methods be selected which count the amplitude of the major stress reversals in the manner which best replicates the judgement of an

experienced stress analyst. It is recommended that methods which select the maximum oscillatory strain in a given record as being representative of the entire maneuver, or similar methods, not be selected, since these introduce a conservatism of an unknown magnitude, contributing to further uncertainty in the life predictions.

Providing the continuous loading spectra of the type recommended above are used, the method of converting the aggregate of the flight strain survey data to an integral loading spectrum, representing the load level versus probability of occurrence for the complete flight envelope, should be standardized. Such a method should provide for the inclusion of all load levels, not just the damaging ones, so as to correctly establish the shape of the spectrum, and should also include the means of accounting for ground-air-ground loading cycles and of correcting for variations in the mean loads which coincide with the oscillatory loads. The method should include the means of accounting for anticipated loading scatter which is not directly measured because of the limited nature of the flight strain survey.

Although these and other subjects involving the applied loads may be amenable to standardization, the resolution of the many alternatives in these areas will require extensive negotiation, and is therefore beyond the scope of this report.

Conduct of Full-Scale Specimen Tests

It appears that only general rules governing good practice can properly be standardized in the area of full-scale development testing. Because of the complexity of modern structures, and the unique interactions of materials, design details, and manufacturing processes, the best course of development testing for a new design cannot necessarily be predicted by standardized methods. Until the number and type of probable failure modes have been identified, one does not have sufficient resolution to specify the requisite number of test specimens in advance. A cost versus benefit tradeoff, either expressed or implied, will be performed to determine the practical extent of testing for each of the major components. Major decisions, such as the application of spectrum loading versus constant amplitude loading, will be based upon considerations which are unique to the individual program. The following general rules regarding good testing practices are therefore presented.

(a) The design of the test specimens and the test apparatus should be such that all pertinent loading effects are included. These include the dynamic amplification and phasing of the applied airloads; oscillatory loading components due to relative motions in combination with steady or oscillatory loads, with or without friction effects; and centrifugal forces and other inertia forces acting upon the masses of the components themselves.

(b) The physical environment which surrounds the specimen under test should be the same as that found in the aircraft. This includes the geometric and stiffness properties of the mating parts as well as any conditions of fretting, wear, or other phenomena which affect the fatigue strength. To achieve this objective, it may be necessary to test the specimen as part of a larger assembly rather than individually in a test rig.

(c) Specimens should be tested at a number of different load levels so as to explore all failure modes and so as to produce failures throughout the range of the S-N curve which will be used for life prediction purposes.

(d) Atmospheric extremes of temperature and humidity, within the scope of the aircraft specification, should be applied in combination with the test loadings.

(e) The aircraft program schedule should not be set up so as to preclude the incorporation of design corrections necessitated by the outcome of the development tests.

5.3.4 EXAMPLES

In order to illustrate the manipulation of the applied and allowable strain data in the manner discussed above, a sample data base is taken from CAM-6 Appendix A, January 15, 1963. The applied stress portion of this data base is tabulated below.

Flight Condition	Percent Occurrence	Oscillatory Stress
I (a)	.5	1900.
(b)	.5	2100.
(c)	.5	2300.
II (a)	.5	2600.
(b)	.5	9600.
(c)	.5	10500.
(d)	.5	3400.
III (a)	1.	6500.
(b)	3.	5100.
(c)	18.	7700.
(d)	25.	8100.
(e)	15.	8380.
(f)	3.	8900.
(g)	.5	9100.
(h)	3.	11200.
(i)	3.	11400.
(j)	2.	10900.
(k)	4.	9900.
(l)	1.5	7800.
(m)	2.	6700.
(n)	1.	9700.

	(o)	.5	7800.
	(p)	.5	7900.
	(q)	.5	7300.
	(r)	3.	6700.
	(s)	.5	6700.
	(t)	.5	7900.
IV	(a)	2.	7100.
	(b)	.5	9700.
	(c)	1.	9300.
	(d)	1.	9900.
	(e)	.5	6800.
	(f)	.5	6100.
	(g)	.5	5900.
	(h)	1.	7600.
	(i)	2.	7900.

The applied stress spectrum above is shown as a density function in Figure 5.5(a), and in its integral form in Figure 5.6(a). These functions were obtained by taking arbitrary 3% increments of load from zero to the maximum and accumulating the probability of occurrence in each loading window. The discontinuous nature of the spectrum is apparent from the gaps in the density function and from the regions of zero slope in the integral function. This situation is unsatisfactory, since actual flight loading spectra are always continuous by nature. The assumption of constant loading in individual flight conditions is also non-representative of actual data.

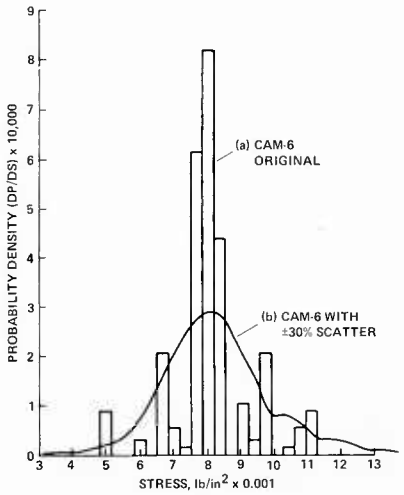

FIGURE 5.5
APPLIED STRESS DENSITY FUNCTIONS

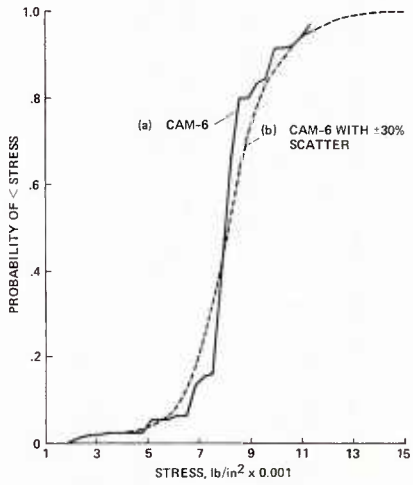

FIGURE 5.6
INTEGRAL APPLIED STRESS SPECTRA

The allowable stress in the CAM-6 example is based upon the results of four hypothetical specimen tests, as follows:

Specimen	Failure Stress	Cycles to Failure	Log (n)
1	21450	758578	5.88
2	13000	2884032	6.46
3	11400	12011644	7.08
4	10150	52480746	7.72

In CAM-6 Appendix A, a curve was faired through these test points to represent the mean of the test data. For the purposes of the present example, this curve is represented by the Weibull equation

$$N = 831800./((S/10000.)-1.)^{1.0564}$$

The working curve for life estimation is

$$N = 831800./((S/(10000. \times REDFAC))-1.)^{1.0564}$$

Where REDFAC is the reduction factor applied to the mean. In CAM-6 Appendix A, REDFAC = .8.

Effect of Strength Reduction Factor

The reduction factor applied to the mean of the test data is a semi-arbitrary factor having a large impact on the outcome of the life prediction calculation. As long as factors of this type are implicit in the analysis, the efficacy of refinement in other areas is questionable. The variation of the predicted life based upon the CAM-6 Appendix A data is shown in Figure 5.7(a) with the reduction factor as the independent variable. The factor of .80 selected by CAM-6 is seen to be on the steep part of the curve. A factor of .70 or less, nearer the knee of the curve, would appear to be safer under the circumstances. However, with a factor of .70, the life would probably be considered inadequate and a

redesign of the part would be required. This illustrates the sensitivity of the design and qualification process to the selected value of the reduction factor.

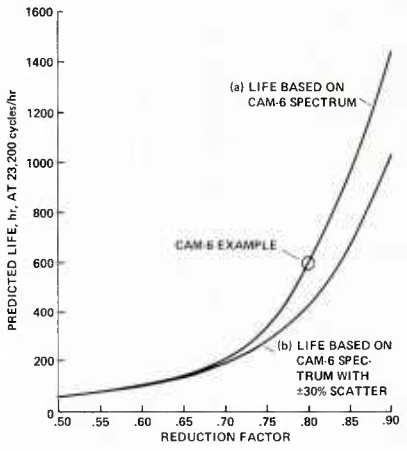

FIGURE 5.7
EFFECTS OF RED FACT & SCATTER

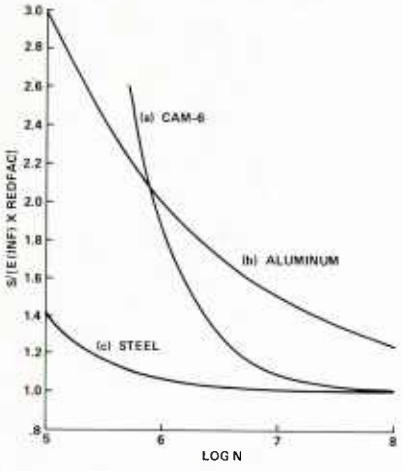

FIGURE 5.8 S-N CURVE SHAPES

Effect of S-N Curve Shape

The choice of S-N curve shape affects both the interpretation of the full-scale test data and the subsequent safe-life estimation. The curve shape used in the CAM-6 example appears to have been based upon the test results for the four specimens. This method is no longer used, the current practice being to project each test point separately to an endurance limit or to a reference number of cycles, using a curve shape based upon prior and more extensive data. The final mean curve passes through the mean of the projected points.

In order to explore the impact of the curve shape on the life prediction, the method described above was applied to the CAM-6 hypothetical test data using two additional alternate curve shapes, which are considered to be representative of steel and aluminum. The corresponding Weibull equations are as follows:

$$\text{Steel:}\quad N = 33497./((S/(E(\text{inf}) \times \text{REDFAC}))-1.)^{1.2402}$$

$$\text{Aluminum:}\quad N = 998670./((S/(E(\text{inf}) \times \text{REDFAC}))-1.)^{3.3184}$$

Where E (inf) is the endurance limit and REDFAC is the reduction factor applied to the mean. The curve shapes, normalized to the endurance limit times reduction factor, are shown in Figure 5.8. Based upon the four test points, the endurance limits are as follows:

Steel 12892. lb/in^2
Aluminum 8336. lb/in^2 (10,416 lb/in^2 at 10^8 cycles)
CAM-6 dashed curve 10000. lb/in^2

The predicted lifetimes at Σ (n/N) = 1. based upon the various curve shapes along with the CAM-6 block spectrum are presented in Figure 5.9, again as functions of the strength reduction factor from the mean. This figure illustrates the sensitivity of the life prediction calculation to both the S/N curve shape and the strength reduction factor. The uncertainty of both these inputs contributes to the indeterminacy of the life prediction process.

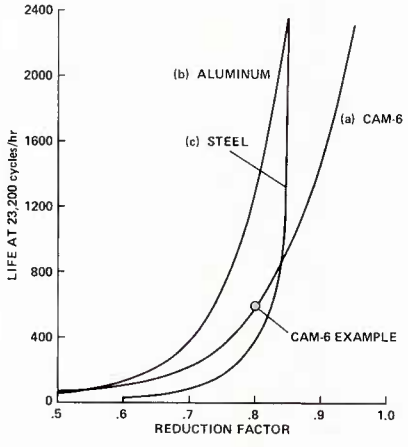

FIGURE 5.9 EFFECTS OF REDUCTION FACTOR AND S-N CURVE SHAPE

Effect of Scatter in the Applied Loads

The uncertainty in the life predictions resulting from random scatter in the applied loads was discussed in 5.3.2. Although the damage rate is sensitive to changes of stress level under constant amplitude loading for most materials, the probable effect of random variation of stress level throughout the flight spectrum is not intuitively obvious.

To investigate the possible effect of scatter using the CAM-6 data as an example, the loads within each flight condition were assumed to follow a log-normal distribution with an approximate 3-sigma scatter of ± 30% above and below the original CAM-6 loads. The probabilities of occurrence for the overall flight envelope were obtained by computerized numerical integration using small intervals of stress from the minimum to the maximum.

The resulting composite spectrum is shown as a density function in Figure 5.5(b) and in its integral form in Figure 5.6(b). This spectrum provides a more satisfactory simulation of an actual flight load spectrum. The tails of the distribution functions are better defined than they were by the original data and extend farther into the high and low probability regions. The overall spectrum is smooth and continuous and follows essentially a log-normal distribution. Except in the region of the tails, the loads under the composite spectrum do not differ greatly in magnitude from the original ones at the same probability levels.

The theoretical fatigue damage rate under the new spectrum was calculated by computerized numerical integration. As shown in Figure 5.7(b) the predicted life is reduced from approximately 600 to approximately 400 hours if the reduction factor is .80, and the cycling rate is 23200 cycles per hour, as in the original CAM-6 example. However, as the reduction factor approaches .70, a more probable value for most manufacturers, the effect of the scatter becomes virtually negligible.

Effect of Fatigue Strength Improvement

The effect of the S-N curve shape, though significant, can be nullified by relatively small changes in the allowable stresses as determined from the test data. Although none of the example materials achieved a 600-hour predicted life with a .70 reduction factor from the mean, small improvements in the test results would enable any of the materials to meet this objective. Figure 5.10 shows the effects of 5.7% improvement in the aluminum, 14.4% improvement in the CAM-6 sample, and 17.3% improvement in the steel, which are the changes required to meet the 600-hour life requirement in the example problem. Improvements of this order of magnitude are often achievable in practical designs through small design changes such as a localized increase of cross-section, and increased fillet radius, or by processing such as shotpeening. The corresponding improvements in the predicted life are 60% (aluminum), 190% (CAM-6 material), and 645% (steel).

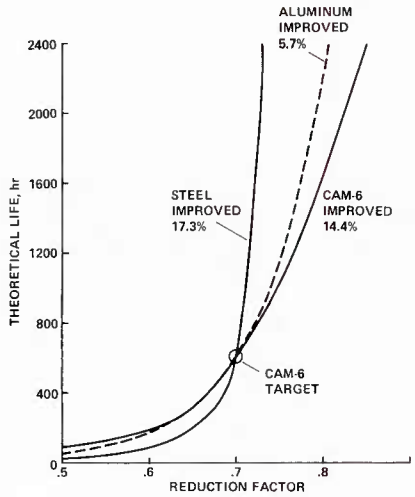

FIGURE 5.10 EFFECT OF FATIGUE IMPROVEMENT

5.4 FAIL-SAFE AND DAMAGE-TOLERANT STRUCTURES

5.4.1 INTRODUCTION

The fail-safe and damage-tolerance approaches for helicopter structures are intended to ensure that the structure maintains a sufficiently high proportion of its design structural integrity even after damage has occurred. Although these approaches have become a necessity in the design of modern aircraft, their importance was recognized as long as four centuries ago. Near the end of the 15th century, technical notes were written on what must have been one of the first requirements for damage-tolerant design. These were in the notebook of Leonardo da Vinci in which he discussed the physics of flight and the design of "flying machines". He wrote (Reference 5.25):

> "In constructing wings one should make one cord to bear the strain and a looser one in the same position so that if one breaks under strain, the other is in position to serve the same function."

For many years the fatigue critical components of the helicopter have been designed to the safe-life philosophy discussed in the earlier sections of this chapter. This approach, wherein all fatigue

critical components are designed to a specific service life and are removed from service at or before this elapsed time so that the probability of fatigue failure is remote, applies only to statistically predictable failures which are those occurring from the random combination of fatigue strength and applied fatigue loads. The safe-life philosophy therefore does not quantitatively address flaws which may be present. Over the years operational experience has shown (References 5.26 through 5.28) that the safe-life approach by itself is not adequate because of fatigue failures caused by unpredicted factors such as manufacturing defects, maintenance errors, and service-induced damage. Furthermore, review of this operational history has shown the number of these unpredictable failures to be considerably higher than the predictable ones. Consequently, in the early 60's a fail-safe design philosophy began to evolve within the rotary-wing industry that has been used in numerous applications (References 5.29 through 5.32). The safeguard in the fail-safe approach is that damage, induced or fatigue, will be detected by inspection procedures before the damage grows to such an extent that the residual strength of the structure is reduced below a safe level.

In the early 70's a third design philosophy - damage tolerance - began to evolve. This philosophy is similar to the fail-safe approach but addresses the ability of a structure to successfully contain damage over a specified time increment without adversely affecting safety of flight. The damage is most commonly characterized as a crack from flaws originating during manufacture or service usage. The most detailed example of this design approach is in the US Air Force's MIL-A-83444 (Reference 5.33). Fundamental to the damage-tolerant approach is an understanding of structural performance in the presence of defects or damage, hence, this approach relies heavily on the technology of fracture mechanics. For metallic structures, this technology is reasonably well established. For fibrous composite material structures, which are generally forecasted for extensive application in future helicopter systems, the fracture mechanics technology is still under development. Most damage-tolerance assessments of composite structures to date have been primarily empirical based upon component and full-scale testing. Nonetheless, it is important to realize that the general damage-tolerance philosophy of inspecting critical regions, detecting damage, and maintaining residual strength certainly applies to composite structures.

The objectives of this section are to define in detail the philosophy for fail safety and damage tolerance as it has been developed and applied to helicopter structures, and to identify and discuss the essential elements required for the development and qualification of these structures. As will be discussed in the ensuing sections, the damage-tolerance approach has been applied within the rotary-wing industry in much the same manner as fail safety, that is, as a complement to safe-life design. It has not yet been applied as a replacement to safe-life design, as has been done by the US Air Force for fixed-wing aircraft. Irrespective of the extent to which damage tolerance is eventually applied to helicopters (complement or replacement), there still remains considerable work to be accomplished in developing specification requirements and procedures for the design approach.

5.4.2 FAIL-SAFE AND DAMAGE-TOLERANCE APPROACHES

The fail-safe and damage-tolerance design philosophies each have the common objective of providing integrity at a reasonable level of assurance for all safety-of-flight structures, that is, structures whose failure could cause direct loss of the aircraft. Reference 5.27 points out a subtle but important distinction between fail safety and damage tolerance. Fail safety as it was defined prior to the evolution of damage-tolerance is based upon the premise that one cannot be certain that cracks (or damage) will not initiate at some time during the aircraft life, and these cracks must be detected before the strength drops below a certain level. Damage-tolerance, on the other hand, assumes the existence of initial flaws in the structure and the structure is designed to retain adequate residual strength until damage is detected and corrective actions taken. Although damage-tolerance contains fail safety as one of its two categories for qualifying a structure (such as in MIL-A-83444), this category still assumes that a flaw is present in each structural member. This is done mainly to assure good durability characteristics, i.e., low incidence of cracking. Fail-safe structures, as they have generally been treated within the helicopter industry, have not been assumed to have initial defects. Thus, by the strict definition they have not been damage tolerant but rather solely fail-safe by the definition established in the 1960's. This is not to say, however, that these fail-safe designs have not possessed good durability features. As is seen later in this section, continuing with a sound safe-life design approach has provided reasonable assurance of good durability characteristics. As the specification documents for rotary-wing aircraft are revised to include damage-tolerance requirements, or as new specifications evolve, clearer cut definitions and associated required approaches will undoubtedly result.

5.4.2.1 Damage-Tolerance Philosophy

The basic philosophy of damage-tolerant design is based on:

- The acceptance that damage will occur for one reason or another despite all precautions taken.

- An adequate system of inspection prescribed so that the damage (cracks) may be detected and repairs made at a proper time.

- An adequate strength maintained in the damaged structure so that, during the period between inspections when damage is undetected, ultimate failure of the structure will not occur.

In designing to this philosophy, the criteria must address both the static residual strength and the damage propagation for the structure under consideration. The residual strength is the amount of static strength available at any time during the service exposure period with damage present.

Figure 5.11 illustrates these elements of the philosophy. Upon nucleation of a crack and the subsequent propagation under repeated loading, the residual strength of the structure decreases as shown by the residual strength diagram. The corresponding crack (damage) growth curve begins at an initial

crack size and subsequently propagates to fracture which is the critical crack size for static strength. Note that the rate of growth of a crack is directly related to the rate of loss of residual strength, thus forming a basis for the selection of the crack to quantify structural fatigue damage. The crack growth time to failure obviously depends upon the size of the initial crack - if the initial crack were larger, the time to failure would be foreshortened. Also shown on the crack growth curve is the minimum crack size that allows detection. The period of time required for the crack to grow from the minimum detectable crack size to the critical crack size is the detection period.

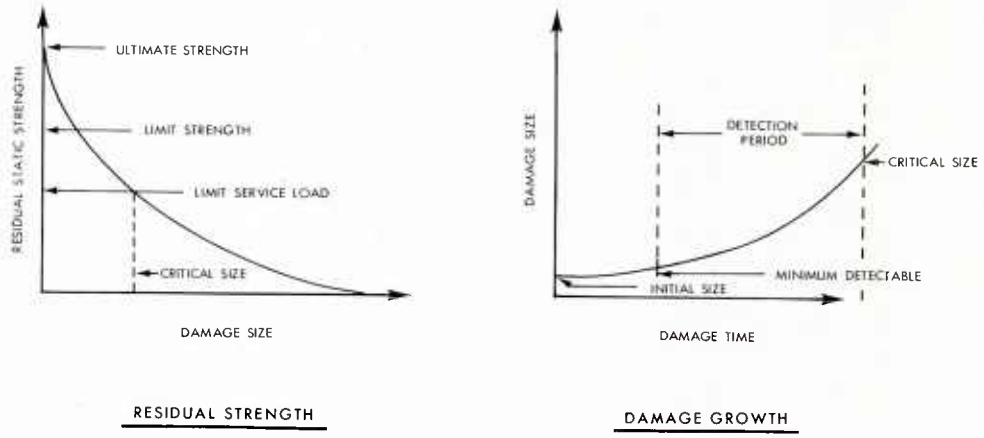

FIGURE 5.11 RESIDUAL STRENGTH AND DAMAGE GROWTH

These residual strength and propagation diagrams are for a single load path configuration structure. These diagrams would change for other structural arrangements such as multiple load paths and structures with crack-arrest features; however, the principle presented is still valid. References 5.34 and 5.35 present these diagrams for a variety of structural configurations. It is important to point out here that although Figure 5.11 is constructed for metals, the philosophy also applies to composites. In such case the "damage size" could include damage corresponding to the critical failure mode of the structure (fiber breakage, delamination, etc.). Along this same line the critical damage size for composites need not be based upon residual static strength, but could be based upon stiffness loss to a critical value.

Damage in the sense that it is considered herein is generally categorized as either "initial", as resulting from material defects or manufacturing-induced anomalies; "in-service", as resulting from environment, handling, or foreign object damage (FOD); or ballistic. Ballistic damage obviously occurs in-service; however, because of the extreme nature of this damage and its associated differing requirements and means of treatment, it is generally addressed separately.

Although the safe life is based upon time to crack initiation and damage tolerance is based upon crack growth to failure, both are "life" approaches. Damage tolerance can be looked upon as a safe-life approach of the cracked or partially failed structure. The real difference in the two concepts is that with damage tolerance an inspection is added and it is related to the crack propagation time. Thus, the damage-tolerance concept is an active procedure requiring action related to service use, whereas the safe-life crack initiation approach tends to be a passive one, which trusts that nothing will happen prior to repair or replacement of the structure.

5.4.2.2 Means of Achieving Damage Tolerance

Damage tolerance may be achieved in one of two different methods, as shown in Figure 5.12. In fail-safe structures, damage tolerance (and safety) is assured by the allowance of partial structural failure, the ability to detect this failure prior to total loss of the structure, the ability to operate safely with the partial failure prior to inspection, and the maintenance of specified static strength throughout the period. Fail-safe structures are usually comprised of multiple elements or load paths such that damage can be safely contained by failing a load path, as by arrestment of a rapidly running crack at a tear strap, or by other deliberate design failure. In safe crack growth structures, damage tolerance is achieved by sizing the structure by using fracture mechanics or empirical data such that initial damage will grow at a stable, slow rate and not achieve a size large enough to fail the structure prior to detection. A special case within this category is nonpropagating defect structures wherein the structure is designed to sufficiently low stress levels for virtually no propagation of the largest defect that would not be detected during a production inspection or that could be incurred in this service.

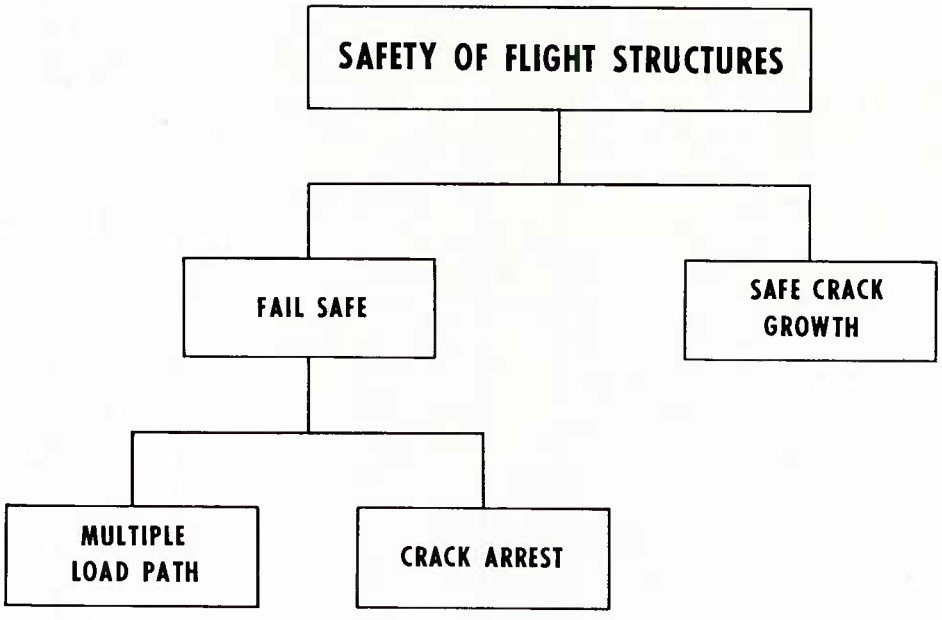

FIGURE 5.12 DAMAGE TOLERANCE APPROACHES

5.4.2.3 Durability

Durability is an economic requirement and is intended to assure that the fleet of helicopters can operate effectively with a minimum of structural maintenance, inspection and downtime costly retrofit and repair and replacement of major structure due to the degrading influence of cracking, delamination moisture and thermal effect, during a service lifetime. If damage tolerance is viewed as an added feature to safe life, the aircraft must still have a good safe-life design. If it does not, then although flight safety may not be compromised because of the damage-tolerance feature, the durability - rate of crack initiation or partial failures - may be unacceptably low, resulting in frequent repair or replacement requirements, and hence significantly more expense than a structure having a longer crack-free life.

This can best be illustrated with an analysis performed in the development of the fail-safe structural design criteria for the US Army's Heavy Lift Helicopter prototype program. The logic diagram for the analysis for a singly redundant structure is presented in Figure 5.13. The failure rate for the

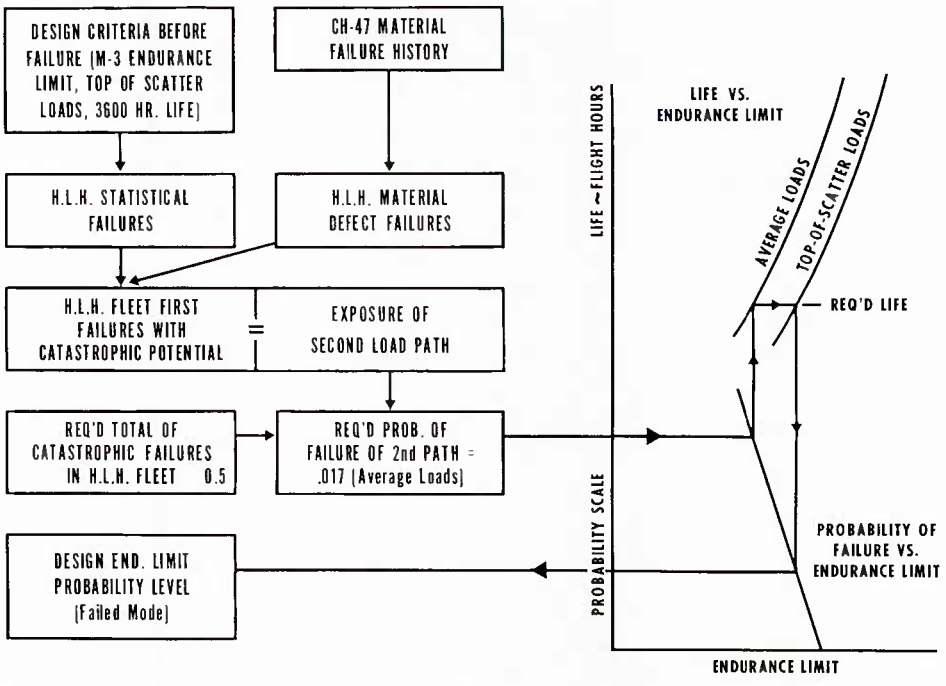

FIGURE 5.13 DERIVATION OF HLH COMPONENT DESIGN FATIGUE STRESS FOR SINGLY REDUNDANT STRUCTURES AFTER FIRST FAILURE

HLH critical components was predicted based upon failure rates (failure/per flight hour) of a predecessor helicopter, projected fleet statistics for the HLH, and an average component retirement life of 3600 flight hours. The basic fatigue reliability objective was that the expected number of component failures in the fleet life be less than 0.5. This, combined with the safe-life criterion that each component be designed in safe life to a M-3σ fatigue endurance limit and top-of-scatter flight loads, produces a failure probability of the first load path. This value is then used in the following relationship:

Probability of complete failure of one fail-safe component = [Percentage of components with no material or manufacturing defects in either load path] x [Probability of complete failure of a component which has no material or manufacturing defects]

+ [Percent of components with a material or manufacturing defect in one load path] x [Probability of complete failure of a component which has failed in one load path due to a material or manufacturing defect]

From this relationship the probability of failure of the second load path is determined. Using this value and top-of-scatter flight loads for the partially failed mode shows that the structure must be designed to a mean (M) endurance limit for the failed mode. For conservatism, all structures were designed to a M-1σ endurance limit for the failed mode. This diagram may be used to demonstrate the ramifications associated with relaxing safe-life requirements. For example, if the safe-life endurance limit criteria were a M-1σ endurance limit rather than M-3σ and top-of-scatter flight loads, the overall reliability objective of less than 0.5 failure in the fleet life could still be satisfied using top-of-scatter loads and a M-1σ endurance limit for the partially failed mode. However, the rate of partial failures could increase eightfold to, for this example, over 200 partial failures. This is not to say that safe-life requirements cannot be relaxed, and such recommendations have been made. However, it does point the durability impacts associated with doing so.

5.4.3 DAMAGE-TOLERANCE REQUIREMENTS

While the US Army in their more recent major helicopter system procurements, such as for the UH-60 BLACK HAWK (Reference 5.36), has addressed damage tolerance for the primary helicopter structure, no specification document such as MIL-A-83444 for airplanes has been written to define in detail the specific requirements for damage-tolerant helicopter structures. Rather, these requirements have been stated in general terms as follows:

"The primary structure (as defined in MIL-A-008866) shall incorporate materials, stress levels, and structural configurations that will minimize the probability of loss of the aircraft due to damage of a single structural element (including control system or dynamic components), or due to propagation of undetected flaws, cracks, or other damage. Slow crack growth, crack arrestment, alternate load paths and systems, and other available design principles shall be used to achieve this capability. --"

It has been left up to the helicopter manufacturer to define the specifics such as damage or flaw sizes, inspection intervals, etc., subject, of course, to Government approval.

5.4.4 DESIGN PROCEDURES

The following three-element approach may be used in the design and verification of helicopter structures for damage tolerance: the development of damage tolerance criteria, the establishment of design and analytical methodologies, and testing to demonstrate compliance with the criteria.

5.4.4.1 Development of Damage-Tolerance Criteria

Using system or component specification requirements as a basis, definitive damage-tolerant criteria should be developed for the design of flight critical components. Table 5.5 presents typical criteria

Defect Tolerant System Description		Design Parameters for Structure				
		Design Fatigue Criteria		Propagation Criteria	Ultimate Load Factor	
Failure Detection	Defect Tolerant Technique	Before Failure	After Initial Failure	From Detection of Initial Failure to Complete Failure	Before Failure	After Initial Failure
Indicator	Redundant load path	Mean-3σ endurance limit 5,000-hr life Top-of-scatter flight loads	M-1σ endurance limit Mean flight loads 30-hr life	Not applicable	1.5	1.0
	Slow crack growth		N/A	30-hr Mean flight loads		
Visual	Redundant load path		M-1σ endurance limit Mean flight loads 30-hr life			
	Slow crack growth*		N/A	30-hr Mean flight loads		
None	Redundant load path		M-1σ endurance limit Mean flight loads 5,000-hr life			
	Nonpropagating defect		N/A	5,000-hr Mean flight loads		
*Used for composites only						

TABLE 5.5 DAMAGE TOLERANCE DESIGN CRITERIA

developed by Boeing Vertol for their UTTAS aircraft (Reference 5.37). These criteria should address:

Damage Characterization: The size, configuration and location of damage, both manufacturing and in-service induced, are very pertinent parameters in the damage tolerance analysis. As discussed earlier, very detailed criteria for damage size have been established in Reference 5.33 for fixed-wing metal structures. Here the maximum undetectable flaw size is specified along with a probability of detecting the flaw and the confidence level associated with the probability. A comparable specification does not exist for rotary-wing aircraft; therefore, such criteria must be either established by the procuring authority and set forth as a part of the systems specification, or by the manufacturers and presented to the procuring agency for approval. In either case the assumed damage requirements should be rationally determined and should take into account the type of damage that has historically led to catastrophic failure of helicopter structures, inspection techniques during manufacture and in-service inspection procedures, and should be supported, when possible, with appropriate analyses.

In the case of composite structures, because of their different constituent materials (fiber and matrix) and the fact that they are generally considered to be nonhomogeneous and anisotropic, their damage (or flaw) characterization is far more complex than for metals. It is therefore improbable that a single parameter characterization of damage in composites analogous to crack length in metal will be possible. Typical sources for damage to composite structures are listed in Table 5.6.

- **DESIGN ERRORS**
- **MATERIAL—AND MANUFACTURING—INDUCED DEFECTS**
  - IMPROPER LAYUP
  - INCORRECT/INCOMPLETE CURING
  - MACHINING ERRORS
  - HANDLING/ASSEMBLING AREAS
- **SERVICE INDUCED DAMAGE**
  - FOREIGN OBJECT DAMAGE (FOD)
  - MAINTENANCE ERRORS
  - GROUND HANDLING
- **BALLISTIC DAMAGE**
  - SMALL ARMS PROJECTILES (7.62mm & 12.7mm)
  - HIGH EXPLOSIVE INCINDIARY (23mm HEI-T)

TABLE 5.6 SOURCES OF STATISTICALLY NON-PREDICTABLE FAILURES

Inspection Requirements: An essential element in damage-tolerant design is the detection of cracking or damage within the structure. This is accomplished through inspection programs which must be employed when the component is being manufactured and when the component has been fielded into service.

During manufacture of a structural component, nondestructive inspection (NDI) and material control must be established and enforced to determine, with a high level of assurance, that the component meets an established criterion of acceptable defect/anomaly and contains none that would preclude its meeting this criterion. Typical NDI techniques are listed in Table 5.7 (Reference 5.38). Figure 5.14 presents the sensitivity levels for surface flaw detection for the more widely used techniques.

X-RAY RADIOGRAPHY	
ULTRASONICS	WIDE
EDDY CURRENT	APPLICATION
LIQUID PENETRANTS	
MAGNETIC PARTICLE	
ACOUSTIC EMISSION	
THERMAL	
OPTICAL HOLOGRAPHY	SELECTED APPLICATION
MICROWAVE	AND
BARKHAUSEN EFFECT	DEVELOPMENT
NEWTRON RADIOGRAPHY	
SONICS	
NUCLEAR MAGNETIC RESONANCE	
EXO-ELECTRON EMISSION	NEW
POSITRON ANNIHILATION	CONCEPTS

TABLE 5.7 NDE METHODOLOGIES

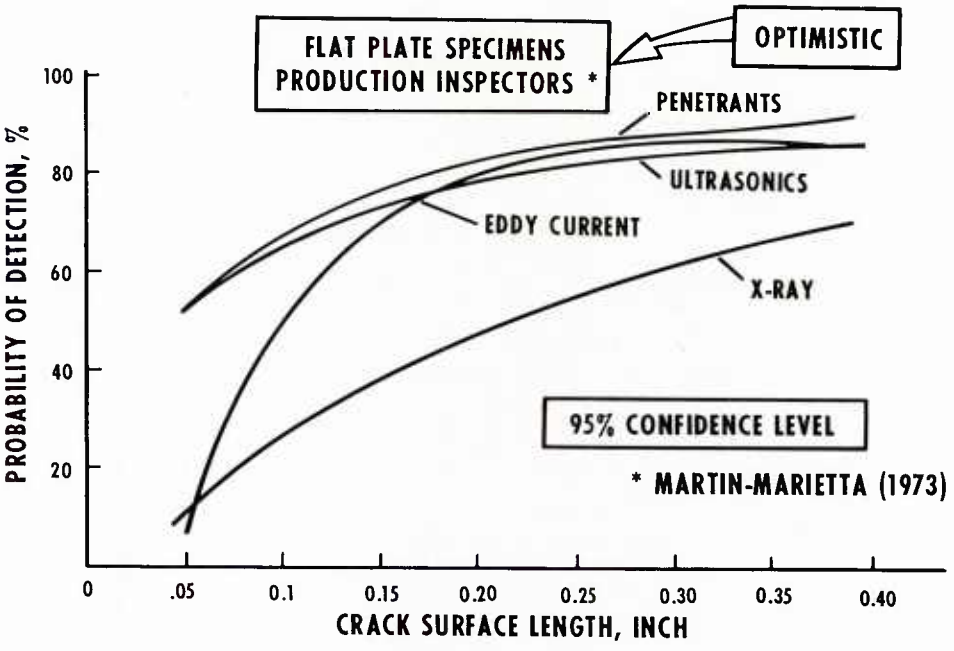

FIGURE 5.14 ESTIMATED METHOD SENSITIVITY LEVELS - SURFACE FLAWS

The basis for the in-service inspection program is the difference between the time at which the damage becomes detectable and the time at which the extent of damage reaches the value critical for residual strength. This is graphically illustrated with the residual strength/crack growth diagrams in Figure 5.11. The key here is to define the condition (or conditions) that indicates this damage growth and to devise an inspection system and procedure to reliably measure the condition. An inspection procedure must thereby be devised, based upon damage growth time and inspection technique, so that the probability of detecting damage is acceptably high before associated structural degradation reaches a critical value. The damage growth time depends upon the damage growth characteristics, which in turn are a function of the structural configuration, materials, and loading state. The inspection approach depends upon the inspectability of the structure, inspection methods, sensitivities of the methods, and inspection interval. There is an obvious interdependence between the damage growth time and the inspection technique, with the latter generally becoming more sophisticated as the growth time decreases.

In developing damage-tolerant structures, strong consideration should be given to design configuration that, in the remote event of failure, do so in a manner that produces a high likelihood of being revealed. The more amenable a structure is to its failure being revealed in a routine manner, such as through ground inspections and pilot feel of the aircraft, the more desirable a damage-tolerant structure it is.

In principle, the structure can be made damage tolerant even when cracks or flaws propagate rapidly if the inspection interval is made short enough. The shorter inspection periods, of course, have an economic impact. Interestingly also, as the inspection period is made shorter, the likelihood of the aircraft experiencing a high load is lessened and hence the retardation benefits associated with the high load. Crack propagation rates within the interval will be higher.

Improvement of the inspection technique is a better guarantee for safety than an increase of the critical crack length. As can be seen from the crack growth curve in Figure 5.11, doubling the critical crack length has far less effect on the detection period than reducing the minimum detectable crack length. Brock (Reference 5.39) points out the importance of more than one inspection during a damage-tolerant inspection period. This is necessary since a crack of the minimum detectable length may just escape detection during one inspection. Although the crack may have an appreciable length at the end of the "failed" period, it is much smaller during the greater part of the time, since the high growth rates occur at a longer crack length. This can mean that relatively small cracks have to be detected, even if the maximum tolerable crack is relatively large. The damage tolerance criterion presented in Table 5.5 specifies 30 flight hours remaining from time of damage detection. Based upon planned 10-hour ground inspection intervals for the UTTAS, this allows three attempts to detect failure. Time for detection of course depends upon several variables such as sophistication of the detection system, complexity of the structure and degree of analysis and testing.

Over the years several detection techniques have been employed in the design of fail-safe and damage-tolerant structures and have included visual, condition indicating systems, and in-flight detection (References 5.40 through 5.42). These have been employed especially in the helicopter dynamic system where growth rates tend to be rapid.

Visual Detection - has generally been relied upon for redundant fail-safe structures wherein the time between partial failure (failure of one load path), which is detectable, and complete failure is reasonably high, thus enabling several attempts at detection. A redundant structure is considered

visually inspectable if, at complete failure of one of the load paths, the failure can be seen without disassembly of any of the structure. For most dynamic system components such as blade and hubs, this inspection is a part of the ground crew preflight inspection.

Condition Indicating Systems - have typically been used on components designed for controlled crack propagation rates and have included crack wires, structures with dye-filled cavities, and differential pressure indicating systems. The differential pressure failure warning system has been the most commonly used and relies upon the principle of creating a pressure differential (pressure or vacuum) between a sealed cavity within the structure and its outer surface. In the event of a fatigue failure, a propagating crack develops into a through (the wall thickness) crack, thus providing a leak path and causing a loss in pressure differential. This causes an indicator display, either mounted on the structure on in the cockpit, to change from a "safe" to "unsafe" condition. This concept has been used on metal rotor blades such as Sikorsky's Blade Indication Method (BIM) on the CH-53 and UH-60 helicopters, and Boeing's Integral Spar Inspection System (ISIS) on the CH-46 and CH-47 helicopters. These failure warning systems in general have been successful but not without maintenance and reliability problems, not to mention the initial costs of the systems themselves. Admittedly, in certain applications such as main rotor shafts, where inspection is not easy and damage growth can be rapid, indication systems have a place. Even here, however, every effort should be made to minimize their sophistication and reduce high cost.

In-Flight Detection - can be achieved through a change in in-flight vibration levels of the helicopter, which would be noticeable to the pilot but still within a safe operating range. This detection method has appeared especially suitable for composite structures. Investigations have shown that initial deterioration of composites under repeated loading is manifested in a gradual loss of stiffness which is attributable to failure or breakdown within the resin. This is presented quantitatively in Figure 5.15. This stiffness loss, combined with the feature that it can occur, depending upon the stress level, many thousand cycles before static failure, yields the possibility of inherent damage tolerance for many composite structures.

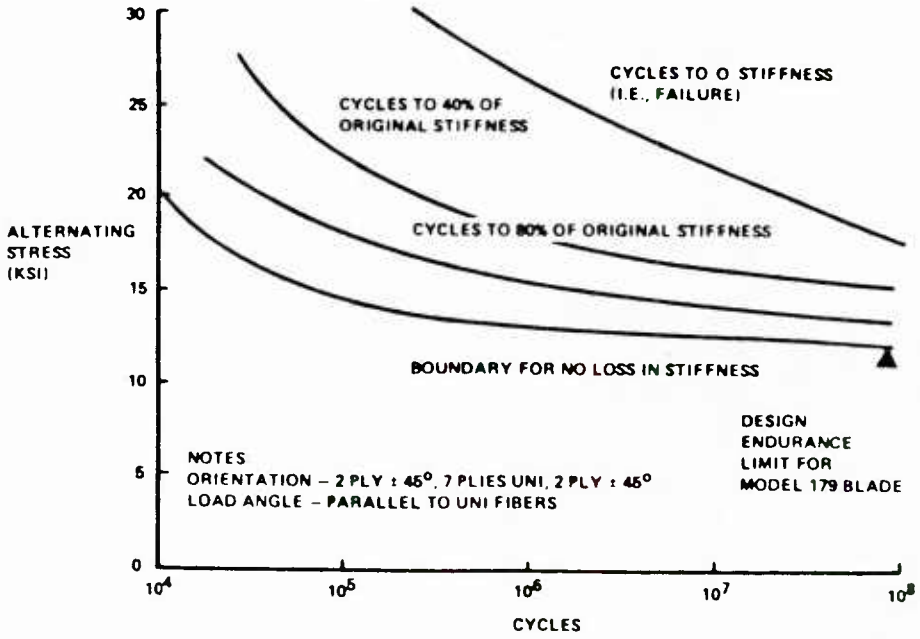

FIGURE 5.15 FAILURE MODE DESIGN CURVES FOR S-GLASS EPOXY

This detection method has been demonstrated on full-scale fatigue testing of fiberglass rotor blades. Reference 5.41 reports that during fail-safe testing of the Boeing Vertol UTTAS rotor blade root end, which was fiberglass/epoxy construction, there was a noticeable decrease in torsional stiffness after approximately 2 x 10^6 cycles at elevated test loads. Although the blade still retained its full structural integrity, the change in stiffness was deemed a failure. The loads were dropped to high speed level flight values and the equivalent of 30 flight hours were run, with no further measured degradation. Test loads were then increased to the originally high level and testing continued until blade deflections exceeded machine capability. Even here, there was no structural failure. Dynamic analyses, based upon reduced stiffness values (at 2 x 10^6 cycles), showed that the vibrational levels would have risen to a level noticeable to the pilot but would still have been within a safe operating range. Additionally, regions of surface delamination became visible along with stiffness loss. A key issue that must be addressed with this detection procedure is tying the indication, such as increased vibration level, to the correct source.

Residual Strength Requirements: Required residual strength is that strength available at any time during the exposure period, considering damage present and accounting for the growth of damage as a function of service exposure time. It has generally been the requirement that all damage-tolerant structures have residual strength capability up to design limit load at all times through the service life of the structure. This allows for unrestricted operational usage. Consideration should also be

given to residual stiffness as a function of damage growth, for in certain instances this can be a more limiting consideration than residual strength.

For composite structures, Liard (Reference 5.44) has presented an approach for quantitatively relating the inspection interval to the component retirement life. This is accomplished by first testing a structure under constant amplitude loading until the first perceptible deterioration appears. A relationship between retirement life and risk R1 (see Figure 5.16a) is then established, where the risk is a function of standard deviation values at a given confidence level. Fatigue testing of the component is then continued at normal flight loads and the time between perceptible deterioration and failure of the component is recorded. A statistical survey is then performed on this latter test. Assuming a fixed inspection interval, the risk R2 is calculated for a deterioration, initiated after any number of flying hours between two inspections, to propagate catastrophically in-flight before the next inspection. This risk R2 is then plotted against inspection interval as shown in Figure 5.16b. Assuming the deterioration, initiation and fracture propagation are independent, the total failure probability is the product of R1 and R2. Then, for a selected value of risk deemed acceptable (i.e., 10^{-6}), the retirement life can be expressed as a function of inspection interval.

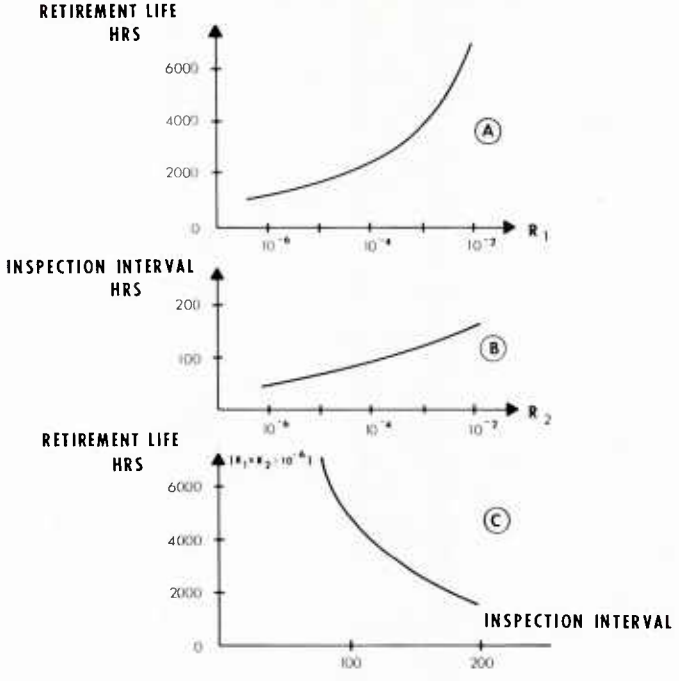

FIGURE 5.16 COMBINATION OF FAIL SAFE AND SAFE LIFE

5.4.4.2 The Establishment of Design and Analytical Methodologies

In order to design components to possess desired damage-tolerance characteristics, it is necessary to employ a sound analytical methodology based on an empirical data base and/or fracture mechanics analysis techniques. Weiss and Zola in Reference 5.40 present a sequence of operations and calculations for predicting damage growth in helicopter metallic structural components. It is illustrated in diagram form in Figure 5.17. The methodology employs the following three step procedure:

Step 1 - Structural Idealization

Step 2 - Computation of Crack Growth

Step 3 - Determination of Limit Loss Capability (Residual Strength)

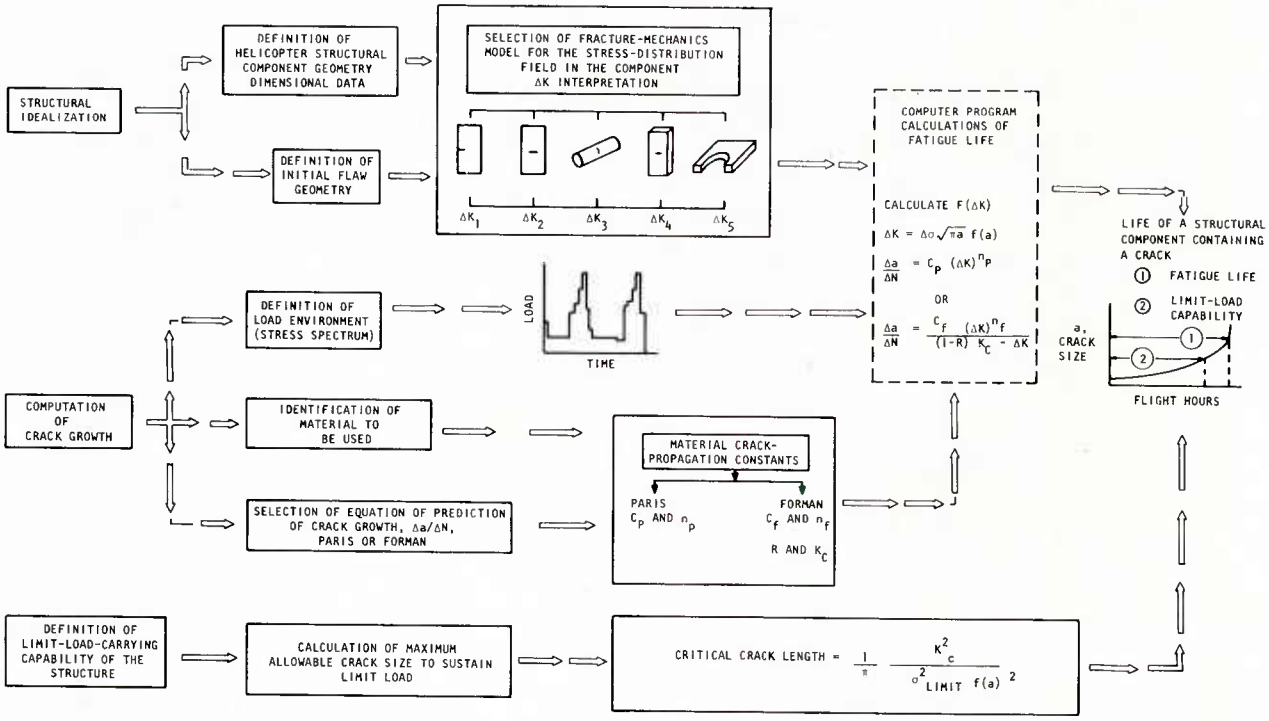

FIGURE 5.17 METHODOLOGY FOR PREDICTING LIMITED DAMAGE GROWTH IN HELICOPTER STRUCTURAL COMPONENTS

Step 1 - Structural Idealization - This step entails defining the initial flaw geometry and the geometry of the component to be analyzed. The flaw geometry shall have been developed as a part of the damage criteria and it should be assumed to exist in the most critical locations as determined from experience with similar structures and analysis of the current structure. The component geometry is idealized using fracture mechanics models which simulate the stress field around the crack. From these models, the correction factors to account for components and crack geometry and loading state for the stress intensity factor, K, and stress intensity factor range, ΔK, are derived and applied in the following manner:

$$K = \sigma\sqrt{\pi a}\quad f_1(a).f_2(a).--f_n(a)$$

σ = net area stress

a = crack length parameter

$f_1(a)$, $f_2(a)$, $--f_n(a)$ = geometric correction factors

Step 2 - Computation of Crack Growth - The essential elements for the calculation of crack growth are the loading spectrum, the material crack propagation constants, and the crack growth equation. The loading spectrum is developed based on the mission profiles for the aircraft. Caution must be exercised in developing this spectrum, for if crack retardation is considered it can be unconservative to include the maximum expected peak loads (or limit load), since they may not actually occur within the inspection interval. The maximum expected load level is therefore a function of the likelihood of detection and the inspection interval. Reference 5.43 has shown that comparing test results from a spectrum containing only level flight stresses indicate that crack growth times determined for aircraft not experiencing high maneuver stresses would be unconservative if this crack growth time were based on test data taken under spectra containing both maneuvers and level flight stresses.

The crack-propagation rate characteristics vary with material, loading condition, and environment and are generally presented in the form da/dN vs ΔK. These characteristics are defined quantitatively, depending upon the crack growth equation used for analysis. Either the Paris or Forman crack growth equation is typically used, the choice depending upon the particular application.

Step 3 - Determination of Residual Strength (Limit Load) Carrying Capability

The limit load carrying capability of the damage-tolerant structure is determined by assuming that the material critical stress intensity factor K_c is reached as the limit load stress in the component. From this, the critical crack length is determined. This critical crack size establishes the upper limit on fatigue crack life. If the required life is not achieved, that is, if the crack reaches the critical length before the required life, then resizing or material change would be required.

Since the aforementioned methodology is based upon linear elastic fracture mechanics (supplemented with appropriate tests), it is generally applicable only to metal structures. Even though the ability to

predict the behavior of flaws in composites is being gradually achieved, it is not currently at a sufficiently mature stage to warrant the methodology approach just described. Thus, damage-tolerance analysis for composites must currently be based upon empirical tests.

5.4.4.3 Testing to Demonstrate Compliance

Testing to demonstrate compliance with the damage-tolerance design requirements must be performed. The test program should be defined based upon the damage-tolerant features of the structure (fail safety, slow crack growth, etc.) and the number of fracture critical areas that it contains. In developing detailed test requirements, the following must be considered:

- Number of tests
- Choice of specimen
- Precrack/flaw characteristics, to include simulation of initial crack (or flaw) and location(s)
- Test load spectrum
- Static load verification

It has generally been the practice within the United States to perform damage tolerance bench testing on a minimum of two full-scale specimens. These specimens may be those used for safe-life fatigue strength testing. If at all possible, the test spectrum should be based upon flight test measured loads. If the structure employs a condition indicating system for failure warning, the system should be operative and damage-tolerance verification should begin at failure indication. If the structure has not failed upon completion of the required spectrum testing, the maximum flight load (generally limit) for damage tolerance design should be applied to demonstrate residual strength structural integrity.

Although damage tolerance testing generally does not entail as many loading cycles as for safe-life demonstration, it can in fact be more involved. The testing is conducted with spectrum rather than constant amplitude loads, and it is often desirable to periodically perform NDE on the specimen during testing to monitor crack/flaw growth as a function of applied cycles. In the case of composite structures, the loading rates should be real-time to preclude unrepresentative heat buildup in a damaged region, and stiffness checks should be periodically performed to determine any change as a function of cycles.

Post-test inspection and analysis should include fractographic analysis to verify analytical crack growth predictions and compliance with damage-tolerance requirements, and assessment of the adequacy of the inspection techniques and procedures.

REFERENCES

5.1 FAR Part 27 Airworthiness Standards: Normal Category Rotorcraft

5.2 FAR Part 29 Airworthiness Standards: Transport Category Rotorcraft

5.3 CAM-6 Appendix A - Main Rotor Service Life Determination

5.4 FAA Advisory Circular AC 20-95 - Fatigue Evaluation of Rotorcraft Structures

5.5 Civil Aeronautics Board Civil Air Regulations Part 6 - Rotorcraft Airworthiness; Normal Category with amendments

5.6 Part 7 - Rotorcraft Airworthiness; Transport Categories with amendments

5.7 FAR Part XX Tentative Airworthiness Standards, Powered Lift Transport Category Aircraft, August 1970

5.8 AMC Pamphlet AMCP 706-201 Engineering Design Handbook, Helicopter Engineering, Part One, Preliminary Design, August 1974

5.9 AMC Pamphlet AMCP 706-202 Engineering Design Handbook, Helicopter Engineering, Part Two, Detail Design, January 1976

5.10 AMC Pamphlet AMCP 706-203 Engineering Design Handbook, Helicopter Engineering, Part Three, Qualification Assurance, April 1972

5.11 AR 70-10 Test and Evaluation During Research and Development of Materiel

5.12 AMCR 70-32 Aeronautical Design Standards (ADS) for U.S. Army Aircraft Systems and Subsystems

5.13 AMCR 70-33 Airworthiness Qualification of U.S. Army Aircraft System and Subsystems

5.14 Data Item Description DI-E-1134 Airworthiness Qualification Data

5.15 System Specification or Prime Item Development Specification for the Specific Aircraft, based upon the Documents above

5.16 MIL-S-8698 (ASG) Structural Design Requirements, Helicopter

5.17 MIL-T-8679 Helicopter Ground Test Requirements

5.18 U.K. Ministry Documents Aviation Publications:

Av. P. 970 Vol. 1 (Fixed Wing)

AV. P. 970 Vol. 3 (Rotorcraft)

5.19 British Civil Airworthiness Requirements (BCAR):

Section A Certification and Approval Procedures

Section G Rotorcraft

Section R Radio

5.20 JAR 25 (Fixed Wing)

5.21 Normes AIR of "Bureau de Normalization de l'Aeronautique" (BNAe) when applicable to helicopters. (They are the French equivalents to US MIL specs or HDBKs)

5.22 G.L. Graham and M.J. McGuigan, Bell Helicopter Company, Ft. Worth, Texas, "A Simplified Empirical Method for Rotor Component Fatigue Design", 25th Annual Forum of the American Helicopter Society, May 1969

5.23 David P. Chappell, Research and Technology Laboratories, USAAVRADCOM, Moffett Field, California, "Monitoring of Fatigue Loading on Rotor Systems and Related Components", Journal of the American Helicopter Society, Volume 24 - Number 2, April 1979

5.24 John P. Norvell, Bell Helicopter Textron, Ft. Worth, Texas, "Application of an Empirical Fatigue Design Method to Predict Fatigue Life During a Development Program", 33rd Annual National Forum of the American Helicopter Society, Washington, D.C., May 1977, Preprint No. 77.33-83

5.25 Toor, P.M. and Payne, B.M., "Damage Tolerance Design and Analysis of a Typical Aircraft Wing Structure (New or Existing)", Case Studies in Fracture Mechanics, AMMRC-MSN 77-5, June 1977

5.26 Immen, F.H., "Fail Safe vs Safe Life Philosophy in V/STOL Design," Journal of the American Helicopter Society, Vol 14, No. 4, October 1969

5.27 Cansdale, R., "An Evaluation of Fatigue Procedures for UK Military Helicopters", AGARD Conference Proceedings No. 297, Helicopter Fatigue Life Assessment, March 1981

5.28 Polley, I.M., "Damage Tolerant Design for Helicopter Structural integrity", Presented at the Second European Rotorcraft and Power Life Aircraft Forum, Buckeburg, Germany, September 1976

5.29 Smith, H.G., "Fail-Safe Structural Features of the Hughes OH-6A, Presented at the 22nd Annual AHS Forum, Washington, D.C., May 1966

5.30 Weiss, W.L. and Thompson, G.H., "Fail-Safety for the H-46 Rotor Blade, Presented at the 27th Annual AHS Forum, Washington, D.C., May 1971

5.31 Field, D.M., "Achieving Fail-Safe Design in Rotors", Presented at the 28th Annual ASH Forum, Washington, D.C., May 1972

5.32 Reddick, H.K., McCall, C.D. and Field, D.M., "Advanced Technology as Applied to the Design of the H.L.H. Rotor Hub", Presented at the 29th Annual AHS Forum, Washington, D.C., May 1973

5.33 "Airplane Damage Tolerance Requirements", Military Specification MIL-A-83444 (USAF) July 2, 1974

5.34 Wood, H.A., and Engle, Robert M., "USAF Damage Tolerant Design Handbook: Guidelines for the Analysis and Design of Damage Tolerant Aircraft", AFFDL-TR-79-3021, March 1979

5.35 Feldt, G.W. and Russell, S.W., "Fail-Safe/Safe-Life Interface Criteria", USAAMRDL-TR-75-12, April 1975

5.36 "Prime Item Development Specification (PIDS) for UH-60A Utility Tactical Transport Aircraft System", Spec No. AMC-CP-2222-S10000B, November 1976

5.37 Hoffrichter, J.S. and McCracken, C.M., "Damage-Tolerant Design of the YUH-61A Main Rotor System", Presented at AHS/NASA-Ames Conference on Helicopter Structures Technology, November 16-18, 1977

5.38 "Analysis of USAF Aircraft Structural Durability and Damage Tolerance", Lecture and Workshop Program, April 1978

5.39 Brock, D., Elementary Engineering Fracture Mechanics, Presented at the 29th Annual AHS Forum, Washington, D.C., May 1973

5.40 Weiss, W.L. and Zola, A.C., "The Application of Fracture Mechanics to the Design of Damage-Tolerant Structures", Presented at the 30th Annual AHS Forum, Washington, D.C., May 1974

5.41 Scarpati, T.S., Feenan, R.J. and Stratton, W.K., "The Results of Fabrication and Testing of the Prototype Composite Rotor Blades for HLH and UTTAS, AIAA 1975 Aircraft Systems and Technology Meeting, Los Angeles, CA, August 1975

5.42 Needham, James F., "Failsafe/Safe-Life Interface Criteria", USAAMRDL-TR-74-101, Hughes Helicopters, January 1975

5.43 Boeing Vertol Inner Office memorandum 8-7451-5-65, "ISIS Program - Effect of a Spectrum of Loads - Analysis of Data Obtained in Crack Propagation Tests of Coupons", August 1970

5.44 Liard, F., "Fatigue of Helicopters - Service Life Evaluation Method", AGARD Report No. 674, Helicopter Fatigue - A Review of Current Requirements and Substantiation Procedures

CHAPTER 6

SERVICE LOAD MONITORING AND STRUCTURAL INTEGRITY EVALUATION

by

R Cansdale

Royal Aircraft Establishment
Farnborough, Hants
United Kingdom

CONTENTS

6.1 MONITORING OF MISSION PROFILES

6.1.1 Missions for which Profiles Produced

The helicopter started out as a multi-purpose vehicle and to a large extent still is. However more specialized types such as gunships and cranes are produced and even the more utility designs may be assigned to a dedicated role such as search and rescue. Some of these roles may differ sufficiently in the time spent in damaging flight regimes to make it necessary to define a specific mission profile.

Of land based helicopters, the utility types would mostly have a transport function but the more specialized missions include:-

Underslung load carriage or crane.
Search and rescue (SAR).
Anti-tank.
Battlefield radar surveillance.
Air-to-air combat.

Naval helicopters also can have a transport role and do SAR work but they too have specialized missions such as:-

Anti-submarine warfare (ASW).
Replenishment at sea (VERTREP).
Minesweeping.
Commando assault.

Training for a particular role can often be more severe than the role itself and the training spectrum needs to be known. This is particularly important if specific aircraft have been designated solely for training.

6.1.2 Examples of Different Mission Profiles

The mission profile for a particular aircraft will depend not only on the intended role but to some extent on the capabilities of that aircraft. Nevertheless there are a number of standard spectra which are commonly used as a basis for the derivation of new ones.

Perhaps the most widely used are those contained in AR56[1]. These US Navy requirements give examples of profiles for cargo, crane, ASW, utility, attack, training and transit missions. They give values of percentage time in various speed bands and flight conditions and numbers of events such as landings and autorotations, but they must be combined with a rational distribution of other significant parameters affecting fatigue life. These include cg position, altitude, gross weight, and have to be provided by the designer and user.

The US Army Material Command Pamphlet 706-203[2] also defines a typical manoeuvre spectrum but this is more of a general example to illustrate the flight conditions in which load measurements should be made rather than a definitive guide to usage in a specific role.

On the civil side both the US FAA Civil Aeronautics Manual 6[3] and the British Civil Airworthiness Requirements[4] contain mission profiles which could be relevant to military helicopters. However the BCARs do say that the table is only a guide.

6.1.3 Means of Monitoring Profiles

The simplest way of recording mission profiles is a manual exercise in which pilots record after landing their estimates of time spent in various flight conditions. Clearly the number of parameters must be limited and a considerable degree of inaccuracy is inevitable. However this may be acceptable if the previous state of knowledge of the aircraft's usage was very low.

Such an exercise was undertaken in 1974 by the UK Armed Forces. Data was logged for virtually every helicopter flight over a whole year[5]. The forms given to the pilots asked for:-

Sortie airborne time.
Number of rotor starts.
Maximum all-up-weight.
Number of landings.
Number of flares (automatic or manual)
Time of torque above 90%.
Time in hover.
Time above 0.95 V_{max}.
Ground OAT
Sortie code (covering some 40 different military sortie types).

This manual recording exercise provided valuable data but it was recognised that more detailed information could only come from a fully instrumented recording exercise.

Such exercises, of varying degrees of sophistication, have been performed in a number of countries. If all that is required is the amount of time spent in bands of speed, altitude, load factor etc, the task is not too complicated provided that suitable recording gear is available. Such programmes have been mounted by the US Navy[6], UK[7] and others, and modern digital tape recorders have overcome many of the previous problems such as the effects of angular vibration on FM and digital systems (nevertheless, tape speeds below $\frac{7}{8}$ in/s continue to present problems of data integrity). However mission profiles usually include details of the numbers of turns, pull ups, autorotations and other manoeuvres and the recognition and recording of these is a much more complex task.

The first step is to identify which are the manoeuvres and flight regimes of structural interest. As well as an operational manoeuvre recording programme this may require a flight load measurement programme during which strain gauge measurements and flight parameters will be recorded whilst the aircraft is flown through a range of standard, and hopefully operationally typical, conditions and manoeuvres. Having identified the regimes of interest it is then necessary to devise ways of recognising them from the flight parameters, whose choice is therefore crucial to the success of the programme[8]. Doing this reliably may pose severe problems, but if it can be done these key combinations of parameters can then be applied to the recordings made in service to compile the real mission profile. It is important to concentrate on the structurally relevant features of the manoeuvres rather than pilot oriented descriptions, eg the relative merits of defining spot turns as angular acceleration or angular velocity and turns as bank angle, normal g or lateral g need careful consideration.

The volume of data recorded in such an exercise means that 'manual' flight condition recognition analysis is quite impractical and a computer must be used. This can either be interposed between the transducers and the flight recorder or used on the ground when the recording is replayed. The former method will reduce the amount of data needing to be recorded but the latter will offer more flexibility since the raw data will be retained for further analysis if necessary.

6.2 QUANTITATIVE MONITORING

6.2.1 Monitoring Flight Parameters

The methods mentioned in the previous section for developing mission profiles can also be used to monitor fatigue life consumption on individual aircraft with varying degrees of accuracy and confidence, provided that structurally relevant parameters are being measured.

This has been done for many years on fixed wing aircraft by using counting normal accelerometers or 'fatigue meters'. These of course take no account of the effects of asymmetric manoeuvres, which must be estimated separately, and are totally inadequate for helicopters in which the number of damaging fatigue cycles will depend not only on how often manoeuvres occur but how long they last and the associated airspeed, altitude, weight etc.

One of the best documented attempts at usage monitoring is the US Army's Structural Integrity Recording System (SIRS)[9,10]. This was developed for the Bell AH-1 Cobra with the aim of reducing cost and improving effectiveness by measuring the fatigue life consumption of components in the dynamic system. Parameters monitored were:-

Rotor speed.
Roll angle.
Pitch angle (rudder position on the AH-1S).
Torque.
Vertical acceleration.
Pressure altitude.
Airspeed.
Outside air temperature (OAT).
Gross weight.

These inputs were used to compute, within the airborne SIRS equipment, % V_L airspeed, % V_H airspeed and density altitude. The equipment then recorded time during which the parameters fell in certain ranges which were used to identify flight conditions such as Full Power Climb, Asymmetric Pullouts, Autorotative Turns. It also recorded occurrences of landings, high normal acceleration (n_z) manoeuvres, rotor start/stop and maximum % V_L and maximum n_z. The store capacity was such as to require data retrieval on the ground only once a month.

The system was not without problems. Gross weight estimation by measuring strains in the under-carriage or lift links proved unreliable and difficulty was experienced in detecting accurately take-offs and landings. There were also software problems of identifying some flight conditions and the resolution of parameters into appropriate bands was fairly coarse. Nevertheless the SIRS is an impressive demonstration of the potential of micro-computers to do real-time in-flight data analysis.

The use of manoeuvre recognition potentially has the ability to enable the user of the aircraft to identify types of operation causing excessive fatigue life consumption and to modify the way of flying to reduce it. This ability may be lose if the parameters are used directly in flight to calculate loads in components. Nevertheless this more direct approach may be easier to implement and more accurate since it removes one step from the process and enables some account to be taken of a manoeuvre's intensity rather than just recording it as, say, an autorotation. An example of this approach has been implemented on a UK Sea King aircraft. Six accelerometers placed at strategic positions on the airframe enable the three linear and three angular* accelerations of the fuselage to be derived. Using the known fuselage inertias, the main rotor shaft bending moment needed to produce the angular accelerations can be calculated. This has shown widely differing values for what were nominally similar manoeuvres; these differences were not readily detected by studying the original basic accelerometer traces.

6.2.2 Monitoring Flight Loads

A further step may be removed if loads are measured directly rather than calculated from flight parameters. The advantages are that variation of all-up-weight does not need to be accounted for and that the effects of non-standard flight conditions such as unusual underslung load carriage or icing are automatically assessed.

---

* These accelerations, being derived from the outputs of a pair of linear accelerometers do contain an extra component which in, say, the case of pitch acceleration is proportional to the product of roll and yaw velocities.

The drawbacks are that loads may have to be measured in many components and that the long-term reliability of strain gauges may be a problem. For rotating components the use of slip rings may lead to difficulties and some alternative means of signal transfer would be essential. Very high information bandwidth is also needed from strain gauges and some data analysis in the air becomes essential.

One of the few attempts at direct load measurements was the system tried by the Canadian Forces on their Boeing Vertol CV 113 aircraft. A single channel recorder was used in conjunction with a microprocessor to do a real time two dimensional rainflow count on strains measured in the fore and aft rotor longitudinal pitch links; these strain signals were previously provided for the cruise guide indicator so no additional transducers were needed. The results of the rainflow count were used to calculate fatigue life consumption in 12 critical components in the rotor systems. However the correlation between the strains in the links and those in the other critical components was somewhat uneven.

There are indications that direct strain measurement may replace the use of the counting accelerometer type fatigue meter on some fixed wing aircraft. If it is possible to find a component on the airframe of a helicopter in which the strains can be correlated with those in the rotor, this type of system would seem to hold considerable promise for helicopters as well. However there would appear to be severe problems of data rate and long-term reliability for strain gauges and slip rings on rotor components.

6.2.3 Identification of Structurally Relevant Events.

The use of mission and manoeuvre spectra for design, and the use of manoeuvre recognition systems for fatigue monitoring both rely on the assumption that damaging flight regimes can be identified. Because of the very large number of rotor-induced loading cycles that are experienced by many of the critical components, the design must be such as to ensure that the loads in most flight conditions are non-damaging if a reasonable fatigue life is to be achieved. Thus damage will only be accumulated during the rarer, more extreme flight conditions or during the transition from one manoeuvre to another.

Current safe-life substantiation methods do not normally recognize the possibility that some of the more damaging loading cycles may have a peak during one manoeuvre and a trough during another. This possibility can only be accurately accounted for by range-mean-pairs counting of actual strain measurements. However if this is not being done it is still important to establish which flight regimes are the most damaging in their own right. The parameters which need monitoring in service will depend to some extent on the aircraft type (eg it may be important to be able to identify sideways flight or lateral acceleration if the tail rotor is critical) but the major aircraft motions will have to be characterized, together with rotor speed, engine torques and control inputs. Identification of the damaging conditions will probably initially have to be done by visual inspection of records by experts in flight mechanics and fatigue familiar with the characteristics of the aircraft type. Operational data has often been found to contain flight conditions not previously covered by flight test, eg landings with one engine out with rotor speeds as low as 70% normal.

6.2.4 Processing and Presentation of Data

It is unlikely that direct recording of flight parameters or strain gauge signals at rotor order frequencies, for subsequent analysis on the ground, will ever be a feasible proposition for whole life fatigue monitoring due to the shear volume of data generated.

Some form of data preconditioning will be needed and fortunately the microprocessor has the speed and capacity to do it. Rainflow counting has already been mentioned and such a system has been flown on an RAF C130 aircraft to monitor strain gauges mounted on the wing. The American SIRS unit totalled up the occurrences of various flight conditions which it was programmed to identify and only needed interrogation every 4 to 6 weeks. The data was then further processed on the ground with the intention of obtaining the fatigue life consumption of critical components in the rotor systems.

6.2.5 Direct Structural Integrity Monitoring

All the monitoring techniques discussed so far have been aimed at reducing the unknowns associated with aircraft usage. Variations in the strength of components still have to be allowed for statistically and defects due to manufacturing or in-service damage are not taken into account.

To be able to use to the full the strength and potential life of each individual component it is necessary to monitor its actual structural integrity. This is the basis of the 'damage tolerant' fatigue philosophy in which defects are assumed to be present in the structure which then has to be designed so that they will not propagate to failure before being detected by inspection. This requirement has two immediate and clearly desirable effects - the structure must be designed for easy inspection and slow crack growth.

Non-destructive testing (NDT) is a large and well documented subject in its own right and the reader is referred to the literature for details of methods.

In general helicopter airframes present no more problems of inspection than do fixed wing aircraft. However components in the rotor system tend to be highly stressed and subject to high frequency loading. Thus any degradation in strength may cause a dramatic reduction in life. This can cause inspection problems since a component whose mean life might be infinite could require inspection every few hours if there was a possibility of, say, corrosion. If the component was something large like a rotor blade this would be an impossible servicing burden.

To cope with this problem on tubular metal spar rotor blades, self-inspection schemes have been devised. The spar is sealed and pressurized with gas and a pressure indicator is fitted. Cracking of the spar then allows the gas to escape and inspection is then a simple matter of checking the pressure

indicator. Normally these are fitted to the blade itself but for cases where propagation times to failure are very short systems have been devised which give a direct indication in the pilots cockpit without the need to stop the rotor. The system has been widely used on metal rotor blades and has detected many cracks which could otherwise have caused catastrophic failure.

In principle this type of crack detection system could be applied to any hollow structure capable of being pressurized; indeed there are stories, possibly apocryphal, of cracks being found in the pressure cabins of passenger airliners thanks to the nicotine stains left on the outside of the fuselage by air leaks from the interior.

For the detection of fibre cracking in glass fibre reinforced composites it has been suggested that fibre optic principles could be used. Thus a beam of light shone down a length of fibre could be detected at the other end as long as the fibre was intact. Such a scheme might be applicable to rotor blades.

The main hope for composite rotor blades however is that there will be sufficient margins of strength to allow failures to propagate enough to produce stiffness and detectable vibration changes without risking complete failure. There seems to be a good prospect that this may be the case, particularly if the blades have been designed to withstand ballistic damage. The same may apply to rotor head components made from composites.

Elastomeric bearings also seem to offer slow and detectable failure modes which should make possible easy inspection and on-condition lifing.

The use of composites and elastomerics may well prove to be a more cost effective route to damage tolerance than the use of a multiplicity of add-on inspection systems. These would only be effective if they were of adequate reliability; in the past this has not always been the case.

6.3 STRUCTURAL INTEGRITY EVALUATION

6.3.1 Expected Standards of Safety

Although individual countries and companies have sets of requirements for fatigue substantiation, they seldom define the overall standard of safety which they aim to achieve. One set which does is the British Civil Airworthiness Requirements (BCARs) where it is stated in Chapter G3-1, Paragraph 5.1:

> 'The strength and fabrication of the rotorcraft shall be such as to ensure that the possibility of disastrous fatigue failure of the Primary Structure and other Class 1 Parts under the action of the repeated loads of variable magnitude expected in service, is Extremely Remote throughout its operational life'.

Extremely Remote is normally associated with a probability of occurrence of less than 10^{-7} per hour of flight. This is also the sort of figure aimed at by designers of aircraft systems, failure of which would hazard the aircraft.

In fact 10^{-7} failures per hour appears to be broadly compatible with the aims of most substantiation methods even if not explicitly stated.

6.3.2 Number of Fatigue Failures in Service

Although accident rates due to fatigue failures on aircraft designed to current procedures are difficult to establish, it seems clear that in the past at least, the rates have been considerably higher than the 10^{-7} per hour suggested. Le Sueur[12] mentions a figure of 3×10^{-5} per hour for civil twin-engined helicopters and Cansdale[13] reports 24 major fatigue related accidents in the last 20 years of flying by British military helicopters, which would give a not dissimilar rate. American sources give similar figures, which do though, happily, show a downward trend[14]. Nevertheless accidents due to structural causes account for only a small proportion, less than 10%, of all accidents, and not all structural failures are due to fatigue.

However, the cost of fatigue cannot be counted merely in terms of aircraft and lives lost. The users of helicopters have to spend a great deal of time and money to maintain the current levels of safety because the safe-life assurance has in many areas to be supplimented by inspection and repair procedures. This sort of husbandry is as much a part of flight safety as is production quality control or the fatigue substantiation process. Ways of reducing the costs of ownership due to fatigue are perhaps as important for the military user as means for improving safety. Certainly the cost of safety improvements ought to be offset by increased lives and lower maintenance.

6.3.3 Assessment of Potential Errors in the Safe Life Process

The vast majority of fatigue induced accidents in the past will have happened due to failure of parts designed on safe-life principles. Most of these are dynamic components in the transmission and rotor systems; relatively few accidents appear to be caused by helicopter airframe failures[13]. Although it is not possible to associate quantitative risks with all the various stages of safe-life determination, it is essential to be aware of the possible sources of error.

6.3.3.1 Mission Spectra Definition

The mission spectra presented to the designer represent the best estimate of how the aircraft will be used, based usually on past experience. However in an evolving military scenario the role of the aircraft may end up being very different from what was originally envisaged. Since it is not normally

feasible to design for zero fatigue damage under all flight conditions, the change in usage may have safety implications. One example quoted from the civil world was of a machine being used for logging operations in which the number of transitions to and from the hover was greatly in excess of the design spectrum, leading to a catastrophic fatigue failure.

Mission spectra normally only quote times in various flight conditions and numbers of simple events such as landings, turns etc. The really damaging flight regimes may involve more complicated manoeuvres whose occurrence is impractical to predict. Indeed if the rainflow counting techniques are used, the largest cycles of loading could have a peak in one manoeuvre and a trough in a completely different one.

There is much to be said for regarding spectra just as an input to the design as a standard against which compliance with specification fatigue lives may be demonstrated. Actual service lives should be based on measured service usage, which should be periodically updated.

6.3.3.2 Flight Load Measurement

A major part of the flight test programme of a new design is the measurement of loads in components in the various flight regimes specified in the mission spectrum. Since the same manoeuvre is never flown exactly the same way they must be repeated to give some statistical validity to the loads. However they are standard manoeuvres flown by test pilots and may not be the same as those flown in service.

It is British practice to apply a stress factor of 1.2 to the typical loads in each flight condition to cover variability of flight loading due to piloting, blade tracking etc if the loading is not monitored or limited in service. Alternatively some firms use the maximum load measured in a test flight condition for substantiation.

Since it is clearly impossible to strain gauge every area on the aircraft, stress analysis has to be relied upon to indicate the most critical areas. Accidents have happened due to unpredicted dynamic behaviour causing high loads which were missed or may not have been produced in the load measurement programme.

6.3.3.3 Fatigue Strength Testing

Tests are normally done on typical as-manufactured components. Many of the accidents in service are caused by problems, such as corrosion, manufacturing or servicing defect or accidental damage, which degrade the fatigue strength and which are not taken into account in the initial fatigue testing. This is probably the biggest shortcoming of the safe-life substantiation process.

It is not possible to simulate exactly on test the loads which a component will see in service. Much of the testing is in fact done under constant amplitude loading, though there are moves to use a realistic spectrum of loads applied either randomly or as a block programme.

If it were possible to achieve failures in a reasonable time using unfactored loading the case for using realistic loading spectra would be overwhelming. In the fixed wing world for example it is accepted that retardation of crack growth will be caused by the residual compressive stress left by occasional high-g manoeuvres[15].

There is also some evidence to suggest that the beneficial effects of interference fits of fasteners and bushes may be reduced by high peak loads in a spectrum[16]. Whether these mechanisms are equally important for helicopter dynamic components is less clear; the fact that they are designed to withstand perhaps 10^9 cycles of loading reduces the chances of local stresses reaching a proof condition even when loads are factored to achieve practical testing times. However other evidence[17] suggests that even in the absence of peak loads that cause tensile or compressive yield effects the very mixing of amplitudes is more damaging than would be estimated from constant amplitude tests.

If a fully representative programme of flight-by-flight loading can be used it should be possible to derive the life directly, bypassing doubts about S-N curve shapes and cumulative damage theories. Such tests though are generally too lengthy and expensive and require detailed knowledge of the flight spectrum; should this subsequently be changed, the assessment of the new life presents difficulties and the designer will have to resort to cumulative damage calculations again using available S-N curves.

In fact constant and variable amplitude loading both have their uses and should be seen as complementary, the one to provide data on S-N curve shapes and the other to account for loading interaction effects.

6.3.3.4 Derivation of Factors

The derivation of factors to allow for fatigue strength variation is a fruitful area for the statistician and many papers have been written on the subject[18,19,20]. The basic problem is that one is trying to make predictions about members of a population on the basis of a sample which is usually too small to enable the characteristics of that population to be accurately defined (Ref 21 is a useful summary of the situation). Consequently the actual level of assurance provided by the factors is not clear. For instance it is common practice to speak of the mean-minus-three-standard-deviation level of strength as providing a $1/740$ chance of failure; this assumes a normal distribution of strength. If a Weibull or other truncated distribution is used, that same level of strength can be claimed to give a very much higher level of assurance.

In many cases the factors used have little real statistical justification. For instance some companies do tests on six specimens and set the working fatigue strength at the mean-minus-three-standard-deviation value derived from the six test results (there is usually an upper limit set at about 80% of the mean).

Although six results should give a reasonable estimate of the mean, the standard deviation is likely to be greatly in error and indeed less reliable than standard deviations derived from greater numbers of previous tests of similar but non-identical components. The latter method is used by many firms and it does perhaps offer a greater consistency and a lower chance of being caught out by a freak series of test results. It also enables non-failure results to be used which are a problem with the other method.

Of course if there is inadequate past experience as in, for example, the case of some composite materials, variability has to be derived from tests. The numbers of tests though must be statistically meaningful, so simpler and cheaper specimens representing the correct failure mode may have to be devised.

In practice the factors on stress used to produce allowable values from the mean, whatever the method of derivation, tend to lie somewhere between 1.5 and 2 and the usual justification for the particular method of derivation is that it has produced an adequate level of safety in the past. Danger lies though in the possibility that an inadequate factor may be masked by some unidentified conservatism elsewhere in the fatigue substantiation, which could be lost if, say, there was a change in the system.

6.3.3.5 Damage Summation Methods

The Palmgren-Miner hypothesis[22] is almost universally used in cumulative damage calculations. Although other methods have been proposed, eg by Corten and Dolan[23], Freudenthal and Heller[24], Richart and Newmark[25], none have gained wide acceptance. This is largely because none of the alternative methods appears to offer much consistent improvement in accuracy over the range of applications that must be considered in design and they all tend to be more complicated. Miner's hypothesis at least has the merit of simplicity. In most cases[26] it tends to underestimate the life which is safe although wasteful. There are however cases where the life is overestimated[17]; this fact is recognised to some extent in the British requirements which call for $\Sigma \frac{n}{N}$ to equal 0.75 if only a constant amplitude test is done.

6.3.4 Possible Means for Improvement

Clearly the different substantiation methods and factors used by the various companies must produce somewhat different levels of safety; this is difficult to quantify but comparisons of fatigue lives can be made. The US Army produced a test case[27] for which seven different companies calculated lives; these differed by more than two orders of magnitude. This result should perhaps be viewed with some caution though, since there does not appear to be any evidence that the products of the low-life company are grossly overweight, nor that those of the high-life one are particularly unsafe.

It seems clear that, on the whole, the fatigue substantiation methods currently used continue in service for pragmatic reasons - ie they work tolerably well even if they do not have a particularly rigorous scientific basis. Dabbling in the statistics of fatigue factor determination or producing more precise cumulative damage rules is unlikely to have a major impact on flight safety. The things that cause most fatigue related accidents - manufacturing defects, corrosion, misuse of the aircraft etc, are not covered by the safe-life process. Increasing the scatter factors to give a larger margin of safety would mean that even more serviceable components were thrown away than at present and could lead to even greater cost of ownership.

Some of the uncertainties in the safe-life process can be reduced, as mentioned in the previous sections, by monitoring flight parameters to reduce errors in the mission spectra, or by monitoring flight loads thereby cutting down errors in the load measurement programme as well, or ultimately by monitoring structural integrity directly by systems such as BIM (Blade Inspection Method). If this last sort of system is adopted the fatigue philosophy has essentially moved from "safe-life" towards "damage tolerance".

It seems to be generally agreed that the best hope for improvement in safety, and also for making best use of components' available life, lies with the adoption of "damage tolerant" design methods. It is important to distinguish between ballistic or battle damage tolerance and defect tolerance. Only the latter is being addressed here, although clearly battle damage requirements should provide a spin-off in improved safety in peace-time operation.

Although not all components lend themselves to damage tolerant design and the substantiation process may be more expensive this approach has already been adopted for features of helicopters such as the Boeing YUH 61A[28]. In fact as long ago as 1959 Raoul Hafner was proposing what were then called "fail safe" components for helicopters[29]. As yet formal damage tolerant design requirements for helicopters are not generally in use although they are being actively discussed. Fatigue substantiation of vital parts will therefore probably continue to be done on a safe-life basis for some while yet. There is nevertheless a potential improvement in safety to be gained by adopting elements of damage tolerant design such as easy inspectability and slow crack growth (as distinct from slow initiation in the safe-life process). Features of modern helicopters such as composite blades and elastomeric bearings are being adopted partly for these reasons.

On the airframe side there is an increasing emphasis on low vibration for reasons of better crew environment and improved equipment reliability. This should also have a beneficial effect in reducing airframe fatigue problems; these may not be a great safety hazard but cost money to repair.

Improvements in safety and reductions in fatigue life consumption are potentially possible if means can be devised of warning the pilot when he is entering a damaging flight regime. This may perhaps be done by monitoring loads in some critical component. Such systems, known as Cruise Guide Indicators are in service on some aircraft. Care must be taken though to ensure that the instrument does identify damaging loads correctly. For some duties also, such as nap of the earth flying, it is not reasonable to ask the pilot to continuously monitor yet another instrument.

This is in fact a problem common to all active monitoring systems such as the Cruise Guide Indicator or cockpit-indicating BIM which are, in a sense, analogous to the thing called pain which monitors our own personal structural and systems integrity. The modern pilots' workload is such that very careful thought will need to be given to the method of presentation of the information. Perhaps a computerized central warning system linked to a voice synthesizer might be an answer.

REFERENCES

1		Structural Design Requirements (Helicopters) AR56 US Naval Air Systems Command. February 1970.
2		Engineering Design Handbook. Helicopter Engineering Part 3. Qualification Assurance AMCP 706-203.
3		Civil Aeronautics Manual 6. US Federal Aviation Agency.
4		British Civil Aviation Requirements, Section G. Rotorcraft. Civil Aviation Authority. September 1977.
5	A D Hall	Helicopter Design Mission Spectra. AGARD Conf Proc No 206. April 1976.
6	R E Malatino	US Navy helicopter operational flight spectrum survey program - Past and present. AGARD Conf Proc No 206. April 1976.
7	P B Hovell D A Webber	Operational flight data from a helicopter in the training role. RAE TR 78014 January 1978.
8	P B Hovell J R Sturgeon	Operational data for service life predictions of helicopter components. RAE TM Structures 861. April 1975.
9	T H Farrell R B Johnson M C Tyler	Structural Integrity Recording System for US Army AH-1G helicopters. USAAVRADCOM-TR-80-D-15. March 1981.
10	J G Dotson A W Kolb	Structural Integrity Recording System for US Army AH-1S helicopters. USAAVRADCOM-TR-81-D-6. March 1981.
11	Susan D Ellis	A combined range-mean-pairs rainflow count of load time histories for use in the formulation of structurally relevant cost functions and fatigue analysis. RAE TR 81122. October 1981.
12	H E Le Sueur	Helicopter fatigue - a civil view. AGARD Conference Proceedings No 297. September 1980
13	R Cansdale	An evaluation of fatigue procedures for UK military helicopters. AGARD Conference Proceedings No 297. September 1980.
14	L L Douglas	Fatigue methodology - a technical management system for helicopter safety and durability. AHS Helicopter Fatigue Methodology meeting, St Louis, March 1980.
15	L F Impellizzeri	Cumulative damage analysis on structural fatigue. American Society for Testing and Materials STP 462, 1970.
16	J E Moon	Fatigue behaviour of BS2L65 aluminium alloy pin loaded lugs with interference fit bushes. R&M 3835, 1977.
17	A W Cardrick M L Meyer	Elastic and plastic interactions - their influence on the validity of the Palmgren-Miner hypothesis. Proc I Mech E Conference - 'Designing against fatigue' 9 October 1974, London
18	R J Atkinson	Permissible design values and variability test factors. R&M No 2877, July 1950.
19	N I Bullen	A note on test factors. RAE Report Structures 215, September 1956.
20	A M Stagg	The philosophy of test factors. RAE Technical Report 76113, August 1976.
21	Carl E Nord	Estimating the reliability of fatigue loaded rotorcraft structures. American Helicopter Society, Proceedings of 23rd Annual National Forum, May 1967.
22	M A Miner	Cumulative damage in fatigue. Journal of Applied Mechanics, Vol 12, No 3, September 1945.

23	H T Corten T J Dolan	Cumulative fatigue damage - proceedings of International Conference on Fatigue of Metals. Institution of Mechanical Engineers & American Society of Mechanical Engineers, New York, November 1956.
24	A M Frendenthal R A Heller	On stress interaction in fatigue and a cumulative damage rule. Journal of Aeronautical Sciences, Vol 26, No 7, July 1959.
25	Richard F E Newmark N M	An hypothesis for the determination of cumulative damage in fatigue. Proceedings of American Society for Testing and Materials, Vol 48, 1948.
26	Herbert F Hardrath	Fatigue and fracture mechanics. Journal of Aircraft, Vol 8, No 3, March 1971.
27		Proceedings of the American Helicopter Society Specialists Meeting on Helicopter Fatigue Methodology, St Louis, March 1980.
28	Jack S Hoffrichter Charles M McCracken	Damage tolerant design of the YUH 61A main rotor system. American Helicopter Society/NASA Ames Conference on Helicopter Structural Technology, November 1977.
29	R Hafner	Safe mechanisms. RAe S Journal Vol 63 No 581, May 1959.

APPENDIX A

HELIX AND FELIX: LOADING STANDARDS FOR USE IN THE FATIGUE EVALUATION OF HELICOPTER ROTOR COMPONENTS

by

A.A. ten Have
National Aerospace Laboratory NLR
THE NETHERLANDS

CONTENTS

A.1 INTRODUCTION

At present it is generally accepted that tests under constant amplitude or blocked loading insufficiently represent the interaction effects between individual load cycles which occur during a more complex loading. This may lead to inaccuracies in the prediction of the fatigue behaviour. As a consequence, the use of more realistic load sequences has found wide application in fatigue testing. It was realised, however, that if realistic but different load sequences are being applied by different investigators the test results cannot be compared. Therefore a demand grew for standardisation of load sequences that could be considered as representative for a specific type of loading.

As result of an international program two standardised fatigue test load histories for helicopter rotors have been developed which will be described in this appendix.

The two loading standards pertain to two different rotor designs, namely:

- Helix: a loading standard for hinged or articulated rotors with the point of maximum flapwise bending moment at about half rotor radius.
- Felix: a loading standard for fixed or semi-rigid rotors which are of a more recent design. The point of maximum bending is located at the blade root.

The aim of this cooperative work is to assess the suitability of using standard flight simulation loading instead of constant amplitude loading in the fatigue evaluation of helicopter main rotor parts.

This appendix is not intended to fully describe all aspects concerning Helix and Felix but mainly to introduce the new standards and to provide a summary with some qualitative data for potential users. Because the subject of loading standards is not yet very familiar within the helicopter world it was considered worthwile to include a discussion on already existing loading standards for fixed wing aircraft being used in many laboratories all over the world.

The development of Helix and Felix is the result of collaboration between:

- Fraunhofer-Institut für Betriebsfestigheit, LBF, Darmstadt-Kranichstein, West Germany.
- Industrieanlagen-Betriebsgesellschaft mbH, IABG, Ottobrunn, West Germany.
- Royal Aircraft Establishment, RAE, Farnborough, England.
- National Aerospace Laboratory, NLR, Amsterdam, The Netherlands.
- Messerschmitt-Bölkow-Blohm, MBB-UD, West Germany.

A.2 PROPERTIES OF STANDARD LOAD SEQUENCES

By definition, standard load sequences consist of well defined load time histories that may be considered as typical or representative for the service loading in a specific type of structure. Essential properties may be defined as follows (Ref. A.1):

- relevancy: a relevant loading standard can only be defined for those types of loading that are characterised by a specific spectrum shape, reflecting specific features of the original signal such as the number and severity of high loads, the mission-mix and flight length variability.
- applicability: in order to be easily applicable a loading standard should be kept as simple as possible and should be fully documented and uniquely defined.

Application of such a loading standard is not intended for the fatigue testing of components for a specific aircraft, because in that case actual load collectives which reflect that aircraft's usage would be more appropriate.
The main areas of application are the evaluation of materials properties, fabrication techniques, structural details and analytical prediction techniques.

With the above in mind the usefulness of a loading standard for the evaluation of helicopter parts has to be investigated.

In fact, helicopter configurations and helicopter loading environment are highly different from their fixed-wing aircraft counterparts for which loading standards are being applied successfully. To illustrate this some features will be discussed of two loading standards which have found wide application already, namely FALSTAFF and TWIST pertaining to fighter and transport fixed-wing aircraft respectively.
The topics of feasability and use of standard load sequences for helicopter rotor parts will be discussed furtheron.

A.2.1 The Fighter Aircraft Loading Standard For Fatigue Evaluation FALSTAFF

In order to determine features that are common to fighter aircraft the loading environment for fighters may be roughly characterised as follows: loading is primarily due to manoeuvres causing upward bending moments with wing tension skins often being fatigue critical. Usually, the mean flight stress level is relatively low and the ground-air-ground transition is relatively small because of the high load factor capability of fighters. Often, the subsequent manoeuvre loads appear in a systematic manner, contrary to the random order which is typical for gust loading.
As common features for a fighter aircraft loading standard can be defined:

- a limited number of mission types and each mission type consisting of a logical sequence of exercises;
- these basic exercises show irregular but characteristic loading patterns;
- a recurrence period in accordance with the yearly aircraft utilisation.

A detailed description of FALSTAFF has been given in references A2 and A3. Some essential points are summarised below.

FALSTAFF is a loading standard considered representative for the load time history in the lower wing-skin near the wing root of a fighter aircraft. It represents a block of 200 flights which is the average

european annual fighter utilisation. The data used was selected from actual loading data pertaining to five different fighter aircraft types operated by three different Air Forces.
Figure A1 shows the overall manoeuvre spectrum of the 200 flights, which is pronouncedly asymmetric (far more positive than negative load increments) with the upper part having a convex shape. Loading spectra derived for different fighters usually have this characteristic shape but differ mainly in severity.
From the loading data a stress history was derived such that the final result consisted of a uniquely defined sequence of 35966 peaks and troughs, ranging from 1 to 32. This sequence length was set by selecting a range-filter with a magnitude of appr. 10 % of the highest positive stress level reached, the one exceeded once per hundred flights. Variability of flight load severity was simulated by the definition of three different groups of mission types (see fig. A1) and three different flight lengths per mission group. Ground loads are represented by insertion of two full cycles before and after each set of airborne loads. A sample of the FALSTAFF loading sequence is given in figure A2.

Generation of FALSTAFF was accomplished by classifying the history contents into three bivariate distributions of stress-ranges and corresponding stress-range means, one load matrix for each mission group. The final FALSTAFF was defined by these bivariate distributions in conjunction with a uniquely defined random draw process. It must be realised that this generation method is incapable of simulating logical manoeuvre and load cycle sequences. Nevertheless, FALSTAFF has proven to be very useful and is being used extensively. A recent application, sponsored by AGARD, is mentioned in chapter A.2.3.

A.2.2 The Transport Wing Standard TWIST

The TWIST standard represents the loading environment of lower wing skins of transport aircraft due to gust loading. General features of this type of loading are that the flight load cycles are superimposed on a tensile one-g flight stress. Taxi load cycles are superimposed on a compressive ground stress giving rise to a pronounced ground-air-ground cycle. Measurements on a variety of transport aircraft showed the symmetric gust load spectra with concave shape of figure A3, indicating small differences between the loading spectra of a variety of transport aircraft.
Evidently, the stress experiences of tension skins of transport aircraft have sufficiently typifying features in common to establish a relevant standard. The development of TWIST is fully described in reference A.4 and included the following basic steps.

A load spectrum was established pertaining to 40.000 flights, which may be considered as an average design life for transport aircraft. The standardised and continuous spectrum, being the average of the scatterband shown in figure A3, was normalised (all stresses divided by the one-g stress level) and converted into a stepped test load spectrum. The highest load to be included (the truncation level) is the load that is exceeded 10 times per aircraft life of 40.000 flights or once per 4000 flights. The load spectrum for 4000 flights is shown in figure A4. Taxi loads are represented by one transition only to a "severe" ground level. A sequence length of 4000 flights was thought to be sufficiently large to ignore any sequence effect. The loads were distributed over 10 different flight types varying from very smooth ("J"-FLIGHT) to extremely rough ("A"-FLIGHT). Each of them having loading spectra which have similar shape but differed in severity. The final TWIST sequence consists of 398665 gust load cycles plus 4000 ground-air-ground cycles and is uniquely defined by its spectrum content from figure A4 plus a sequence generation algorithm. The average flight length is about 100 cycles per flight. A sample of the TWIST standard is given in figure A5.
Since the number of 100 cycles per flight was sometimes considered as relatively long a shortened version was created, called MINITWIST (Ref. A5). Omission of most of the cycles of the smallest amplitude resulted in MINITWIST having ca 15 cycles per flight which gives much shorter testing times.

A.2.3 The use of standard load sequences

As mentioned previously, the standards TWIST and FALSTAFF have found worldwide application. Various examples have been presented in reference A1.
A recent example is the so-called Fatigue Rated Fastener Evaluation Program, sponsored by the AGARD SMP. In this program seven laboratories and industries in Europe and America cooperate in a systematic evaluation of the fatigue properties of different fastener systems by means of comparative fatigue testing. Obviously a common load standard is indispensable in such a case. As the typical application of the considered fastener systems is in fighter aircraft, FALSTAFF has been chosen as the loading to be used in the program.
Apart from tests on structural details and components, the standard sequences have been applied successfully in the evaluation of materials properties. In reference A6 tests were reported to compare the crack propagation properties of four different aluminium alloys.
Three types of loading were considered, namely simple program loading, gust spectrum loading (TWIST) and manoeuvre spectrum loading (FALSTAFF).
Some of the results obtained have been reproduced in figure A6; it appears that the relative ranking of the materials depends on the type of loading. In other words, the material that may be the best choice for say a transport aircraft wing is not automatically the most appropriate one for a fighter structure.

These findings underline the necessity to do comparative fatigue tests under loading conditions that are representative for the anticipated structure and its loading environment.

A.2.4 Standard load sequences and future indications

It was mentioned above that development of standard load sequences is useful for those types of loading that show typical features with regard to spectrum shape and load cycle appearance.
The loading standards described above have been defined in order to reflect these features by defining the sequences of load reversals without consideration of frequency effects and influences of the environment.
However, it is generally believed that the relevance of standardisation applies to the same extent for loading patterns which are not purely mechanical. It is expected that within the near future loading standards will be developed that take into account not only mechanical loading but also factors such as temperature profiles and humidity cycles. A recent initiative is the definition of a flight-by-flight environment simulation standard based on FALSTAFF for which several proposals are being investigated. The intention is

to use such a standard for the evaluation of fibre reinforced composites as a material for application in primary structures. Typical applications for these types of standards which are not only defined by a mechanical loading history are envisaged for the evaluation of non-metallic materials and the turbojet engine. Very recently, in fact, an international working group has initiated work to arrive at a standardised load sequence for gas turbine discs. In this working group a collaboration is established between engine manufacturers, universities and laboratories.
It must be realised that these loading standards have a limited applicability and are more expensive to apply than the standards which employ mechanical loads only.

It is important that each sophistication to be included in a standard should be developed for maximum simplicity.

A.3 STANDARD LOAD SEQUENCES FOR HELICOPTER COMPONENTS

In a feasability study produced by the Helix/Felix working group the relation between loading standards and helicopter practice is considered. From this discussion two main topics emerged which will briefly be outlined here.

- Feasability: A necessary prerequisite for establishing a relevant standard pertaining to a specific type of loading is that this type of loading shows some typifying characteristics. The question rises whether helicopter loading has such characteristics. As seen before this applies in particular to an adequate simulation of spectrum shape and specific load cycle sequences.

To answer the above question it is worthwile to consider the helicopter loading in some detail.
The forces acting on a blade consist of a lift force, a dragmoment and a centrifugal force resulting in a variable bending moment along the blade axis. It is shown in figure A7 that there is some difference between a hinged (articulated) and a hingeless (semi-rigid) rotor. The hingeless rotor type has no bearings in the flap and lag sense but only retains a bearing along the longitudinal blade axis.
Near the rotor head the bending moment in the hinged blade is zero whereas the maximum bending moments in the hingeless case are situated there. At half span radius the situation may be not too different for both rotor types and may be represented by the loading in the standards.
In general, each rotor revolution gives one basic load cycle. Normal rotor speeds are in the order of 3 to 7 cps yielding 10 to 25 million cycles per 1000 flights. Thus, the dynamic loading may be characterised by a large number of flight load cycles with relatively small amplitude, superimposed on a constant tensile stress due to centrifugal forces. Compared to the rotor speed the amplitude of these cycles varies slowly so that a sample of a load-time trace has the appearance of a sequence of different blocks representing periods spent in discrete manoeuvres, with each of those blocks containing cycles with relatively constant amplitude. Between the flights pronounced ground-air-ground cycles occur associated with rotor stop and downward bending of the blades under their own weight. From the above it follows that there are some typifying features with regard to actual helicopter loading on which the similarity between actual and standardised loading could be based. From measurements it appeared that variations in mean stress were larger for the rigid rotor type. Also it was expected that manoeuvres significant to fatigue damage on an articulated rotor would not necessarily be significant in fatigue for the rigid rotor and vice versa. For these reasons it was decided to define a standard for each of the rotor types.

The reproduction of a representative spectrum shape is more complicated. Apart from the wide variety of helicopter types which are used for completely different roles even helicopters of the same type may experience a very different mission usage. Any loading standard representative for a general usage should take account of all relevant sorties performed by the helicopter. The literature indicates, however, that the majority of sorties can be categorised into a limited number of sortie-types. This will be discussed furtheron in the appendix.

Since the standard should reflect the different loading and usage of both articulated and hingeless rotor types it was felt necessary to develop two standards, viz. Helix for articulated rotors and Felix for hingeless rotors.

- Usefulness: Once established that the development of a helicopter loading standard is feasable the question rises concerning its usefulness for helicopter applications.

It should be kept in mind that loading standards are primarily intended for comparative tests, to evaluate the relative merits of design details or different materials. The higher relevancy of such tests if carried out under realistic loading sequences also applies in the case of helicopter applications.
However, because of the high cycle character of helicopter fatigue it must be expected that a relevant standard must have an extensive sequence length.
Doubts may exist with regard to the practical applicability of such standards because of the necessarily long test durations. It was the opinion of the working group that in order to be able to check this practical use and relevancy a helicopter standard should be available in the first place and that for this reason alone the development of Helix and Felix appeared to be useful.

A.4 HELIX AND FELIX

A.4.1 General

In this chapter the fundamentals of Helix and Felix are described. Some basic data is given from which they have been derived, the method of generation and additional information concerning their spectrum content. In this appendix the intention is not to present all data which is necessary for the complete generation of both loading standards. Since the generation method makes use of rather extensive data in tabular form presentation of these tables seems not very illustrative within the present discussion. Basic considerations and definition of Helix and Felix have already been published in reference A7. The final report of the working group including the results of evaluation tests has been scheduled for autumn 1982. The Helix/Felix survey given in this appendix intends to be a further introduction to the subject, linked to the already existing interest in standard loading sequences for fixed-wing aircraft.

A.4.2 Load spectra assessment

A first step in the development of a helicopter standard is the demonstration of similarity between the loading experience of different helicopters of the same rotortype. This was accomplished by a comparison between Sea King and Sikorsky CH-53 transport spectra for articulated rotors and MBB BO-105 and Lynx average usage spectra for hingeless rotors.

Sea King data was available consisting of stress histories for most manoeuvres flown by this helicopter, measured on the lower surface of the blade at about half rotor radius where the maximum flapwise bending moment occurs. From these blade loads the Sea King spectrum for the transport role was constructed by combining the individual manoeuvres in the appropriate ratio for a transport role. From CH-53 measurements the overall loading spectrum of a transport sortie was extracted. The transport spectra are given in figure A8 indicating that both curves have a shape that is representative for a helicopter spectrum and that they are quite similar, despite the big differences that exist in data sources, aircraft weights and usage, number of rotor blades and the fact that the Sea King spectrum was synthesised whereas the CH-53 transport spectrum was actually measured.
From this it was concluded that a standard loading sequence for an articulated rotor could be defined and that the available data could be used in its development.

The situation for hingeless helicopters was different in that no recent Lynx measurements were available. MBB provided flight load measurements taken from the lower surface of a BO-105 blade root for a pattern of manoeuvres that describes the design mix of manoeuvres. Design mixes of manoeuvres, as used for development and certification purposes, of both BO-105 and Lynx are similar and may be considered as representative for the helicopter type. In figure A9 the measured BO-105 spectrum is compared with a calculated design spectrum that describes an average sortie of the Lynx. In the high stress region substantial differences can be observed. However, it must be recognised that differences should be expected due to both the differences in rotor construction and the origin of the basic loading data. It was decided to base Felix entirely on the measured BO-105 data.

A.4.3 Definition of Helix and Felix

In the development of a loading standard the available data are generally not the only determining factors. The method of generation is also very important. Features that are specific for the type of loading must be generated adequately, while on the other hand the generation procedure is to be kept as simple as possible to ease frequent application. By a generation method through loading matrices and a rather complex random drawing technique, analogue FALSTAFF and TWIST, it is impossible to recognise individual manoeuvres, even in a sortie-wise generation procedure.

In order to maintain the identity of separate manoeuvres and to simulate actual load interaction effects between subsequent load cycles as much as possible it was decided to generate the helicopter standards in a deterministic way. The method uses a predetermined sequence of sorties, a predetermined sequence of manoeuvres within each sortie and a fixed load cycle sequence within each manoeuvre. Four sortie types were defined and three flight lengths for each sortie. By generation along these lines there is no need for a more or less sophisticated generation algorithm which generally improves the handling and application capacity of a standard. In the present generation method the necessary computer memory capacity to store all tabular information turned out to be rather limited. The number of integers to be stored is less than 5000. Simulation of four separate sortie-types within the standards was chosen in preference to one average sortie because of the importance attached to realistic modelling of the complex load interactions. The resulting standards Helix and Felix are similar in that there exists no difference in sortie-mix, flight length variability and total number of flights simulated by both standards. The differences lie in the discrete manoeuvres that make up each sortie and in the different load cycles occurring within each manoeuvre.

Definition of the final standards required the establishment of a sortie-mix, a series of discrete manoeuvres for both helicopter types and time spent in each of them to perform the various sorties. In helicopter loading the number of load cycles accumulated by the blade is related to the flying time, contrary to the situation under manoeuvre loading, e.g. FALSTAFF, in which the number of load cycles depends on the number of flight phases with significant loading. Vital steps in the generation of Helix and Felix are shortly discussed below.

Examination of a variety of sorties, as reported in a survey of UK service use of military helicopters revealed that the majority of sorties could be categorised under four main headings, namely Training, Transport, Anti-Submarine Warfare (ASW) and Search And Rescue (SAR). The total number of sorties (= flights to perform a certain role) to be contained in the standards has been derived on the basis of a given sorti-mix and a given set of flight length data. The number of occurrences per flight hour of each sortie was calculated from this data and the overall number of sorties was found by stating that the most infrequent sortie was to be represented in the sequence once. The standard sortie-mix used for Helix and Felix is the average of all sorties from the survey. The percentage time spent in each of the four sortie types is: training 33.0 %, transport 48.5 %, ASW 9.0 % and SAR 9.5 %. To account for realistic flight length variability the Sea King data have been used for both standards. The result of the above analysis was that Helix and Felix comprise a total of 140 flights pertaining to 190.5 flight hours, with a mixture of flight durations of 0.75, 2.25 and 3.75 hours for each of the four sortie types. Table A1 lists the number of flights of each duration for each of the four sorties that are required to achieve the desired mission mix. Thus, each of the standards consists of a sequence of 12 discrete sorties, created by a once and for all random draw. This sequence, identical for Helix and Felix, is listed in table A2.

As indicated before the generation method also required the establishment of individual manoeuvres that make up the various sorties. For this purpose design mixes of manoeuvres are used that had already been defined. The sets of manoeuvres that build up Helix and Felix are given in tables A3 and A4. The Sea King versus BO-105 loading data did not correlate completely. In particular control reversals performed on BO-105 helicopters find no equivalence in the Sea King data. However, a sufficient analogy of both helicopter mission profiles could be established.

The technique to describe the sorties by logical sequences of manoeuvres employed a common-sense consideration of the flight profiles and the objective of the sorties because no operational statistics were available. In the simplest form this approach says that for example the helicopter cannot perform a landing without first having taken off. In the development of the standards the four sortie types are generally described as follows:

Transport: this sortie represents take-off and low-speed manoeuvres away from the terminal area, flight at cruising speed while manoeuvring to take into account terrain and air-traffic control restrictions and finally low-speed manoeuvres and landing in the terminal area.

ASW : in this sortie the helicopter repeatedly decelerates to allow deployment of a sonar buoy and accelerates to another search area.

SAR : the essential part of this sortie is low -speed manoeuvring to execute a rescue.

Training : this was the most difficult sortie to describe because of the wide-ranging operations that are flown. The assumption was made that this sortie should simulate the essential aspects of flight needed to perform the other sorties with additional training exercises.

The result of the above procedure was the definition of four tables for each of the four sortie types, pertaining to the longest flight length of 3.75 h. In these tables all discrete manoeuvres are listed one by one in their sequence of appearance with the associated number of applications to represent the adequate time spent in the particular manoeuvres, as given by the design mix of manoeuvres. To illustrate this table A5 presents the manoeuvre-mix applied in the 3.75 h Felix sorties, thus simulating as much as possible the basic design manoeuvre-mix. The 0.75 h and 2.25 h sorties are found by taking fractions of the 3.75 h sorties.

The final step was the derivation of the loading within the manoeuvres. Since the loading spectra compared favourably (see A.4.2) it was considered reasonable to base Helix on Sea King measurements and Felix BO-105 measurements. The available flight records were analysed by the rainflow counting technique to form mean-alternating stress (BO-105: strain) matrices for each manoeuvre, taking into account a certain range-filter magnitude to reduce the number of cycles. An average mean stress for each manoeuvre was estimated and counts of cycles in the same amplitude counting interval were summed. The results of these analyses are also listed in the load matrices in tables A3 and A4 which give for each manoeuvre the mean stress and number of stress cycles at each stress amplitude. The number of cycles in each manoeuvre has been reduced by dividing by the highest common factor; the number of applications of each manoeuvre has been adjusted accordingly. The tables indicate that a few manoeuvres do not contain significant stress cycles. They are still presented in the tables to illustrate equivalency between Helix and Felix, but in the final generation these manoeuvres have been ignored.
Since the load cycles appeared in the measurements in a random way it was considered justified to define all load cycles within the manoeuvres by a once and for all random draw.

Originally, the counting intervals in the mean-alternating stress matrices (pertaining to Helix) have been made equivalent to 250 psi (1.72 MPa) which equals half the stress interval for the amplitudes in the Sea King data. The Felix levels have been allocated to the BO-105 data such that the largest strain value from these recordings coincides with the maximum Helix level found above.
Finally, the number of discrete load levels defining Helix and Felix has been reduced by a factor 3 through an increase of the class widths. As a result, the stress levels, which are expressed as percentages of the maximum load, are presented in tables A3 and A4.
Note that the Helix load matrix defines 6 different alternating stress levels (with magnitudes varying from 20 to 40 percent max. load) against 9 different alternating stress levels (with magnitudes from 16 to 60 percent max. load) for the Felix load matrix. Also, the mean stress levels in the Helix manoeuvres are, in general, higher than the mean stress levels in the Felix manoeuvres.

The standards are completed by positioning of the ground load levels between the flights. For Helix the stress at the lower side of the blade at about half rotor radius was measured as -27 MPa which is equivalent to -20 percent maximum load. This value has also been adopted for Felix since the maximum occurring bending moments by the dead weight of the blades are comparable for both helicopter types.

A.4.4 Analysis of Helix and Felix

In this appendix no quantitative Helix/Felix data are presented concerning the generation method, basic loading data, flow charts etc. Additional information about the subject may be gathered from the main reports.
At this stage it is assumed that the generation procedures have been performed and that the complete Helix and Felix sequences are available, expressed in percentages of maximum load.

The above discussion indicates that both Helix and Felix simplify to a large series of individual manoeuvres which are separated by ground loads. Each manoeuvre, in its turn, is defined by a mean-load and a series of amplitudes. These manoeuvres and their load cycle contents are already shown in tables A3 and A4. The characteristic nature of the helicopter load time histories is illustrated by samples of the Helix and Felix sequences in figures A10 and A11. From the figures it can be seen that in general the manoeuvre mean loads are lower for Felix, whereas the alternating stresses within the Felix manoeuvres clearly illustrate the larger number of alternating stress levels, as compared to Helix. The final Helix and Felix have been analysed with the rain-flow counting technique. The resulting distribution of the ranges is given in tables A6 and figure A12. The range-means are ignored in fig. A12. The postive level cross count of Helix and Felix is shown in fig. A13. The largest range-size in Helix is 120 percent max. load with peak- and through-values varying from -20 (ground load) to +100 (max. stress). Since the landing manoeuvre in Felix generates loads deeper into the compressive region than -20 the largest range present in Felix is greater than that in Helix, namely 128 percent max. load, with peaks and troughs varying from -28 to +100 percent max. load.
The tables indicate that the standards are relatively long, with more than 2 million cycles representing 140 flights. With a testing frequency of 20 Hz application of one sequence has a duration of more than 30 hours.

A.4.5 Evaluation of Helix and Felix

Within the present program the usefulness of the helicopter standards is to be demonstrated by the work depiced in table A8. All cooperating institutes are involved in the testing program which includes Ca-, block- and spectrum loading on three materials: aluminium, titanium and glass fibre reinforced plastic. The relative severity of the block spectra, which are simple three stepped approximations of the Helix- and Felix-spectra, is illustrated in fig. A14. At the time of writing some of the work is still going on and most of the test results are not yet presented in a final format. Some preliminary Helix test results on aluminium are shown in fig. A15. Development tests with a reduced Helix standard spectrum are envisaged in order to determine the effect of omission of the small load cycles. These tests possibly indicate to what extent the sequence length could be shortened in order to arrive at shorter and thus more economical test durations.

A.5 FINAL REMARKS

In the foregoing paragraphs an impression is given of collaborative work with respect to loading standards and their application in helicopter fatigue evaluation. Two basic loading standards have been derived from available data with some simplifications being assumed. In order to demonstrate their usefulness a test program has been defined which is not yet completed. In this program tests are envisaged that must answer the question whether the proposed standards may be simplified without loosing their significance. This simplification mainly concentrates on two topics: omission of small load cycles to arrive at shorter testing times and a decreased number of discrete stress levels to ease handling.

Resuming, two loading standards have been derived that are typical for the present usage of articulated and hingeless helicopters, resp. Helix and Felix and the final reports will be published within the near future. The contributors to this collaborative work may be contacted whenever some information is needed. To overcome the effort of generation the contributing institutes are willing to provide the complete standards, say, by means of magnetic tape or by sending the standardised computer programs.

A.6 REFERENCES

A.1. de Jonge, J.B., The use of standardised fatigue load sequences in coupon and component tests. NLR MP 80001 U, 1980.

A.2. van Dijk, G.M., de Jonge, J.B., Introduction to a fighter aircraft loading standard for fatigue evaluation (part I). Proceedings of the VIIth ICAF Symposium, Lausanne 2-5 June, 1975. Also published as NLR MP 75017 U.

A.3 Various authors., FALSTAFF. A description of a Fighter Aircraft Loading Standard for Fatigue Evaluation. Jount Publication of F + W (Switserland), LBF and IABG (Germany) and NLR (Netherlands). March, 1976.

A.4 de Jonge, J.B., Schütz, D., Lowak, H. and Schijve, J., A standardised load sequence for flight simulation tests on transport aircraft wing structures. NLR TR 73029 U, LBF-Bericht FB-106. March, 1973.

A.5 Lowak, H., de Jonge, J.B., Franz, J. and Schütz, D. Minitwist. A shortened version of TWIST. NLR MP 79018 U, LBF-Report TB-146. May, 1979.

A.6 de Jonge, J.B., Review of aeronautical fatigue investigations in the Netherlands during the period March 1979-February 1981. NLR MP 81006 U, 1981.

A.7 Darts, J., RAE UK., Schütz, D., LBF Germany. Development of standardised fatigue test load histories for helicopter rotors - Basic considerations and definition of Helix and Felix. (Paper 16 of reference 1.4).

TABLE A1

Number of flights of each sortie for the three flight durations in HELIX and FELIX

Flight duration (h)	Number of flights			
	Training	Transport	ASW	SAR
0.75	47	38	2	5
2.25	11	20	4	4
3.75	1	5	2	1

TABLE A2

Sequence of sorties for 140 flight sequences of HELIX and FELIX

(1 block = 140 flights)

21, 11, 43, 11, 21, 12, 22, 11, 11, 21, 21, 21, 23, 42, 23, 21, 12, 11, 21, 22, 11,
42, 22, 21, 32, 21, 11, 22, 32, 22, 11, 31, 21, 22, 11, 11, 42, 42, 21, 21, 33, 12,
31, 22, 22, 11, 11, 11, 11, 11, 21, 21, 11, 41, 11, 12, 22, 22, 22, 11, 21, 11, 21,
11, 21, 21, 21, 21, 11, 11, 22, 21, 21, 21, 11, 21, 11, 12, 12, 21, 11, 11, 22, 11,
41, 21, 11, 11, 11, 23, 11, 21, 11, 21, 11, 21, 11, 22, 32, 23, 11, 12, 22, 22, 23,
12, 21, 11, 22, 11, 11, 41, 33, 22, 32, 21, 11, 21, 21, 22, 21, 21, 12, 21, 11, 21,
21, 13, 11, 11, 12, 11, 11, 11, 41, 11, 22, 11, 41, 12.

Key: Training - 10
Transport - 20
ASW - 30
SAR - 40

Shortest flight duration - 1 (0.75 hour)
Middle flight duration - 2 (2.25 hours)
Longest flight duration - 3 (3.75 hours)

therefore 23 is a transport flight of the longest duration

TABLE A3

Load matrix of HELIX

ALTERNATING STRESS			20	24	28	32	36	40
NO.	MANOEUVRE	MEAN STRESS	NUMBER OF CYCLES					
1	Take-off	44	2	-	-	-	-	-
2	Forward flight 20 kn	72	13	-	-	-	-	-
3	Forward flight 30 kn	68	-	12	2	-	-	-
4	Forward flight 40 kn	60	4	9	1	-	-	-
5	Forward flight 60 kn	60	11	2	-	-	-	-
6	Forward flight 103 kn	64	2	4	12	-	-	-
7	Max power climb 70 kn	68	1	-	-	-	-	-
8	Shallow approach to hover	56	12	5	6	8	4	-
9	Normal approach to hover	60	11	2	4	3	5	1
10	Hover	-	-	-	-	-	-	-
11	Bankturn port	68	-	1	20	1	-	-
12	Bank turn starboard	68	-	1	16	1	-	-
13	Sideways flight port, 30 kn	56	3	-	-	-	-	-
14	Recovery from 13	52	11	5	9	1	2	-
15	Sideways flight starboard	60	3	3	3	-	-	-
16	Recovery from 15	52	11	2	3	2	4	1
17	Rearwards flight 20 kn	68	1	-	-	-	-	-
18	Recovery from 17	60	4	-	9	10	1	-
19	Spot turn port	64	30	8	2	-	-	-
20	Spot turn starboard	68	3	-	-	-	-	-
21	Autorotation	60	19	-	-	-	-	-
22	Recovery from 21	60	-	2	10	4	1	-
23	Descent	60	11	2	-	-	-	-
24	Landing	72	1	3	1	-	-	-

All stresses are expressed as percentages of the maximum load.

TABLE A4
Load matrix of FELIX

NO.	MANOEUVRE	MEAN STRESS	ALTERNATING STRESS 16	24	28	32	36	44	48	52	60
			NUMBER OF CYCLES								
1	Take-off	32	7	13	11	1	-	-	-	-	-
2	Forward flight 0.2 VNE	48	11	2	-	-	-	-	-	-	-
3	Forward flight 0.4 VNE	-	-	-	-	-	-	-	-	-	-
4	Forward flight 0.6 VNE	48	2	-	-	-	-	-	-	-	-
5	Forward flight 0.8 VNE	-	-	-	-	-	-	-	-	-	-
6	Forward flight 0.9 ÷ 1.1 VNE	48	24	1	-	-	-	-	-	-	-
7	Max power climb 70 kts	-	-	-	-	-	-	-	-	-	-
8	Transition to hover	40	10	1	-	-	-	-	-	-	-
9	Hover	36	10	1	-	-	-	-	-	-	-
10	Cruise turns 0.4 ÷ 0.8 VNE	60	20	4	-	-	-	-	-	-	-
11	Cruise turns 0.8 ÷ 1.0 VNE	64	14	13	1	-	-	-	-	-	-
12	Sideways flight portside	36	11	3	-	-	-	-	-	-	-
13	Sideways flight starboard	36	10	19	13	1	-	-	-	-	-
14	Rearwards	36	10	9	1	-	-	-	-	-	-
15	Spot turns	36	16	2	-	-	-	-	-	-	-
16	Autorotation (AR)	40	32	21	9	3	1	1	-	-	-
17	AR incl. large amplitudes	40	32	21	9	3	1	1	3	1	3
18	Recoveries from AR	36	32	2	-	-	-	-	-	-	-
19	Control reversals 0.4 VNE	36	32	12	5	3	1	-	-	-	-
20	Control reversals 0.7 VNE	44	36	13	5	3	2	-	-	-	-
21	Descent	36	-	1	26	2	-	-	-	-	-
22	Landing	8	-	-	-	-	2	-	-	-	-

All stresses are expressed as percentages of the maximum load.

TABLE A5
Duration of FELIX manoeuvres for the 3.75 h missions

NO.	MANOEUVRE	TRAINING	TRANSPORT	ASW	SAR
1	Take off	0.26	0.26	0.12	0.26
2	Forward flight 0.2 VNE	2.25	0.38	2.67	0.22
3	Forward flight 0.4 VNE	1.62	0.38	2.67	0.22
4	Forward flight 0.6 VNE	1.54	0.38	2.67	0.22
5	Forward flight 0.8 VNE	3.04	8.22	5.72	24.89
6	Forward flight 0.9 ÷ 1.1 VNE	60.51	79.22	34.31	62.21
7	Max. power climb	0.49	0.42	1.28	0.42
8	Transition to hover	0.74	0.16	1.33	0.08
9	Hover	18.74	2.74	31.53	4.67
10	Cruise turns 0.4 ÷ 0.8 VNE	3.07	1.23	8.42	0.69
11	Cruise turns 0.8 ÷ 1.0 VNE	0.77	0.31	2.10	0.17
12	Sideways flight portside	0.32	0.30	0.30	0.30
13	Sideways flight starboard	0.31	0.30	0.30	0.30
14	Rearwards	0.50	0.30	0.30	0.30
15	Spot turns	1.03	0.42	0.42	0.42
16/17	Autorotation (AR)	0.42	0.42	0.42	-
18	Recoveries from AR	0.04	0.04	0.04	-
19	Control reversals 0.4 VNE	2.00	2.00	2.00	2.00
20	Control reversals 0.7 VNE	2.00	2.00	2.00	2.00
21	Descent	0.50	0.26	1.28	0.51
22	Landing	0.12	0.26	0.12	0.12
	Σ	100%	100%	100%	100%

TABLE A6

HELIX rainflow analysis

a) distribution of the ranges

RANGE SIZE (PERC.)	NUMBER	CUMUL. NUMBER	AVERAGE MEAN (PERC.)
4	2994	4264048	65.5
8	656	4258060	62.3
12	277	4256748	66.0
16	69	4256194	64.0
20	140	4256056	62.0
24	0	4255776	-
28	277	4255776	66.0
32	0	4255222	-
36	232	4255222	59.2
40	479542	4254758	62.2
44	369	3295674	62.4
48	455327	3294936	63.6
52	3588	2384282	65.4
56	1168181	2377106	64.2
60	2226	40744	65.7
64	10329	36292	61.8
68	271	15634	57.2
72	5898	15092	57.7
76	415	3296	58.4
80	942	2466	58.5
84	10	582	58.0
88	141	562	56.0
92	0	280	-
96	0	280	-
100	0	280	-
104	0	280	-
108	0	280	-
112	0	280	-
116	140	280	40.0

b) Peak/trough count and count of positive level crossings

LEVEL (PERC.)	NUMBER PEAKS	PEAKS CUMUL.	NUMBER TROUGHS	TROUGHS CUMUL.	POSITIVE LEVELCR.
-20	0	2132024	140	140	140
-16	0	2132024	0	140	140
-12	0	2132024	0	140	140
-8	0	2132024	0	140	140
-4	0	2132024	0	140	140
0	0	2132024	0	140	140
4	0	2132024	0	140	140
8	0	2132024	0	140	140
12	0	2132024	281	421	421
16	0	2132024	1668	2109	2109
20	0	2132024	2233	4342	4342
24	0	2132024	10412	14754	14754
28	0	2132024	7093	21847	21847
32	0	2132024	16898	38745	38745
36	0	2132024	1163994	1202739	1202739
40	0	2132024	676930	1879669	1879669
44	0	2132024	210951	2090620	2090620
48	0	2132024	5651	2096271	2096271
52	0	2132024	32039	2128310	2128310
56	141	2132023	88	2128398	2128257
60	160	2131883	1010	2129408	2129107
64	1834	2131723	2283	2131691	2129556
68	2798	2129889	333	2132024	2127091
72	7012	2127091	0	2132024	2120079
76	6346	2120079	0	2132024	2113733
80	248246	2113733	0	2132024	1865487
84	253998	1865487	0	2132024	1611489
88	382222	1611489	0	2132024	1229267
92	1150931	1229267	0	2132024	78336
96	73302	78336	0	2132024	5034
100	5034	5034	0	2132024	0

TABLE A7

FELIX rainflow analysis

a) distribution of the ranges

RANGE SIZE (PERC.)	NUMBER	CUMUL. NUMBER	AVERAGE MEAN (PERC.)
4	687	4570144	41.9
8	416	4568770	43.4
12	1841	4567938	50.0
16	1036	4564256	51.9
20	1688	4562184	50.8
24	1231	4558808	49.1
28	910	4556346	35.3
32	2027902	4554525	47.6
36	827	498721	39.2
40	5258	497066	49.4
44	480	486550	39.1
48	171388	485590	45.9
52	1592	142814	50.2
56	52518	139630	36.9
60	1965	34594	48.7
64	10264	30664	38.7
68	1079	10136	50.3
72	3378	7978	38.9
76	117	1222	41.9
80	156	988	40.2
84	34	676	41.4
88	25	608	40.0
92	90	558	45.0
96	9	378	40.0
100	8	360	42.0
104	8	344	40.0
108	7	328	34.0
112	6	314	29.8
116	0	301	-
120	142	301	32.9
124	0	16	-
128	8	16	36.0

b) Peak/trough count and count of positive level crossings

LEVEL (PERC.)	NUMBER PEAKS	PEAKS CUMUL.	NUMBER TROUGHS	TROUGHS CUMUL.	POSITIVE LEVELCR.
-28	0	2285072	406	406	406
-24	0	2285072	0	406	406
-20	0	2285072	164	570	570
-16	0	2285072	0	570	570
-12	0	2285072	8	578	578
-8	0	2285072	24	602	602
-4	0	2285072	40	642	642
0	0	2285072	1472	2114	2114
4	0	2285072	9442	11556	11556
8	140	2285072	49938	61494	61354
12	0	2284932	55619	117113	116973
16	0	2284932	9146	126259	126119
20	0	2284932	157152	283411	283271
24	0	2284932	81595	365006	364866
28	0	2284932	43200	408206	408066
32	0	2284932	1760246	2158452	2158312
36	140	2284932	17641	2176093	2175813
40	354	2284792	14290	2190383	2189749
44	470	2284438	77633	2268016	2266912
48	3196	2283968	17056	2285072	2280772
52	141552	2280772	0	2285072	2139220
56	8836	2139220	0	2285072	2130384
60	99165	2130384	0	2285072	2031219
64	1796322	2031219	0	2285072	234897
68	22370	234897	0	2285072	212527
72	83615	212527	0	2285072	128912
76	80940	128912	0	2285072	47972
80	17408	47972	0	2285072	30564
84	15500	30564	0	2285072	15064
88	13960	15064	0	2285072	1104
92	1080	1104	0	2285072	24
96	0	24	0	2285072	24
100	24	24	0	2285072	0

TABLE A8

Survey of the joint test programme

Material	Ti 6 Al 4 V		Al Cu Mg 2 (eq. 2024)		unidir. GFRP		multidirectional GFRP	
Specimen Type	open hole, K_t = 2.5		open hole, K_t = 2.5		unnotched		lugs, 10 mm hole dia	
Thickness	2 mm	5 mm	5 mm		10 mm		10 mm	
Loading Type	axial		axial		4-point bending		axial	
Laboratory	RAE	NLR	IABG	LBF	RAE	IABG	IABG	LBF
Testing Type								
Constant Amplitude		x	x	x		x	x	x
HELIX Standard	x			x	x			
HELIX Reduced	x				x			
HELIX Block			x	x		x		
FELIX Standard		x	x			x		x
FELIX Block		x	x			x		x

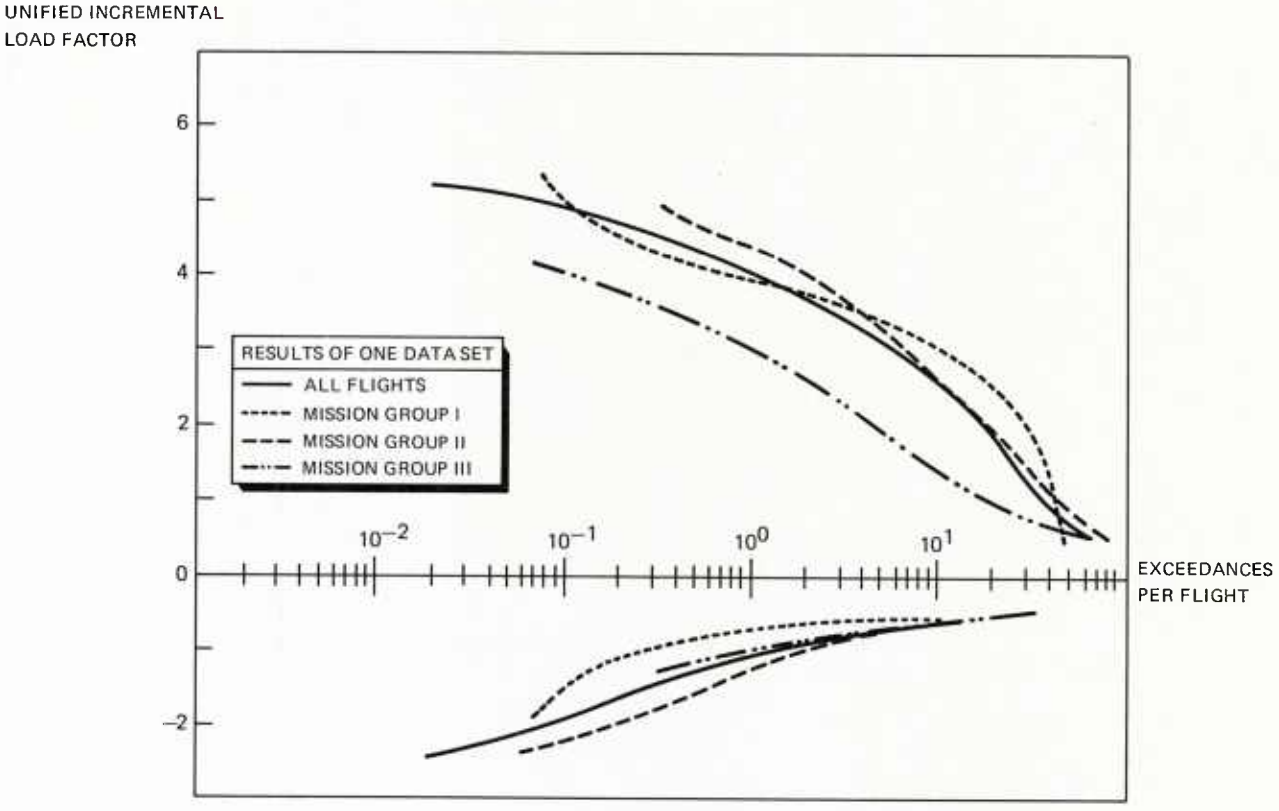

Fig. A1 Mission-group classification and sub-spectra of FALSTAFF

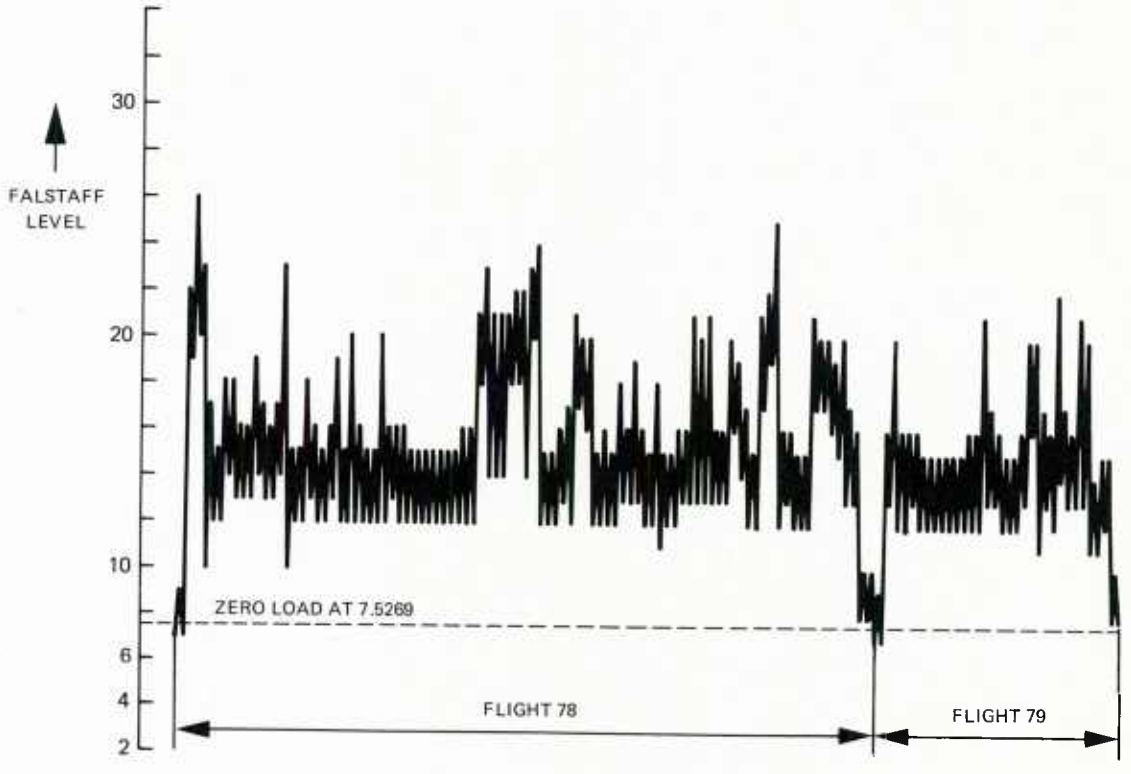

Fig. A2 Part of FALSTAFF sequence

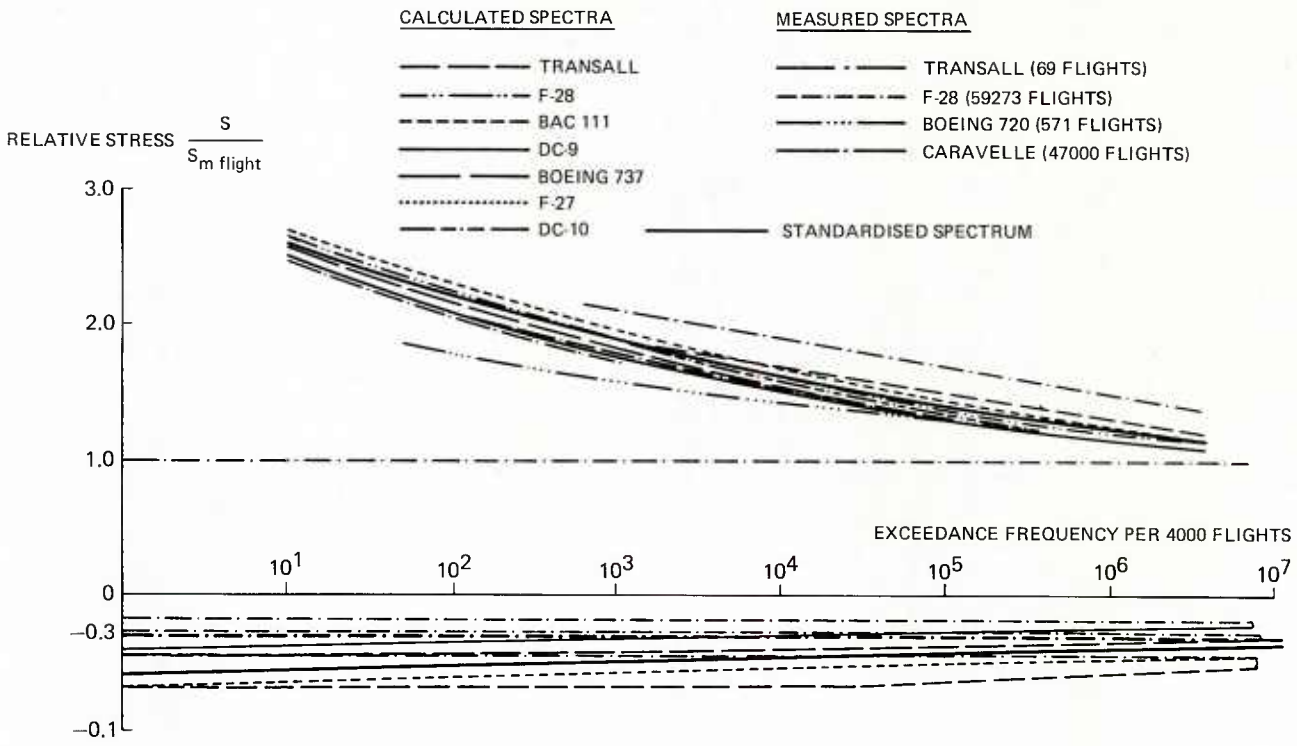

Fig. A3 Load spectra pertaining to 40,000 flights for different aircraft

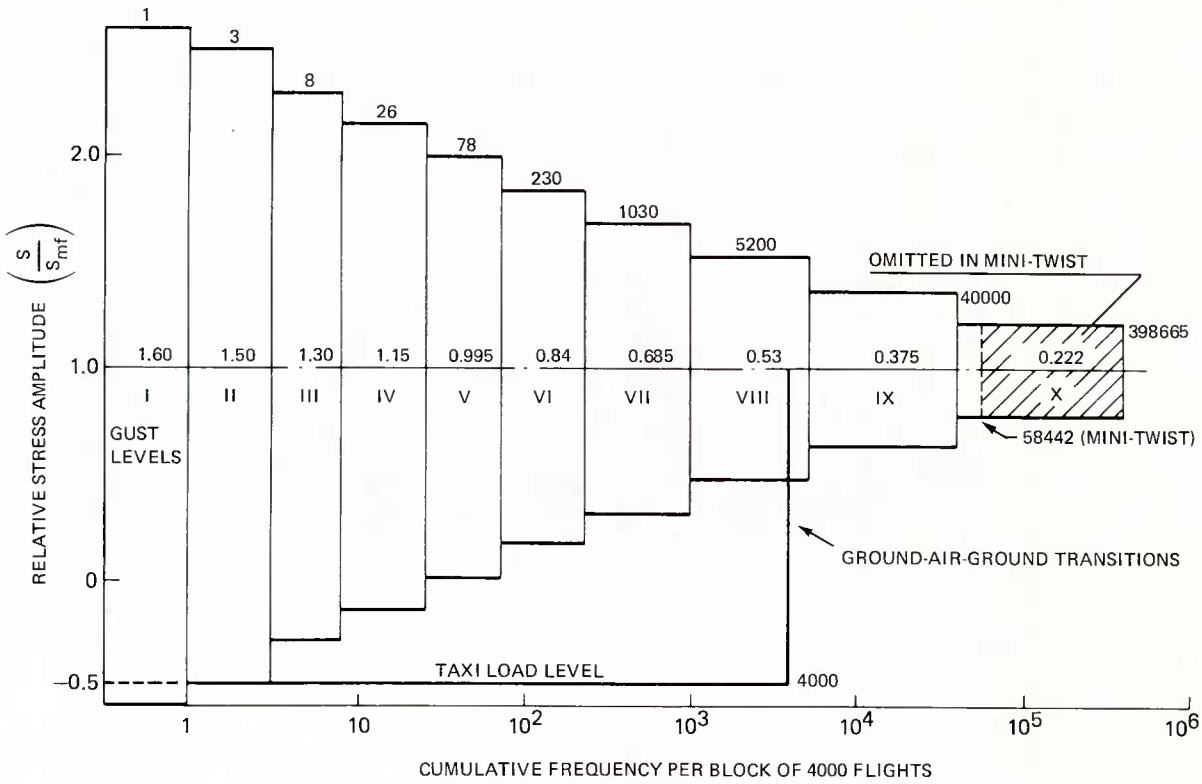

Fig. A4 The test load spectrum pertaining to TWIST and MINI-TWIST

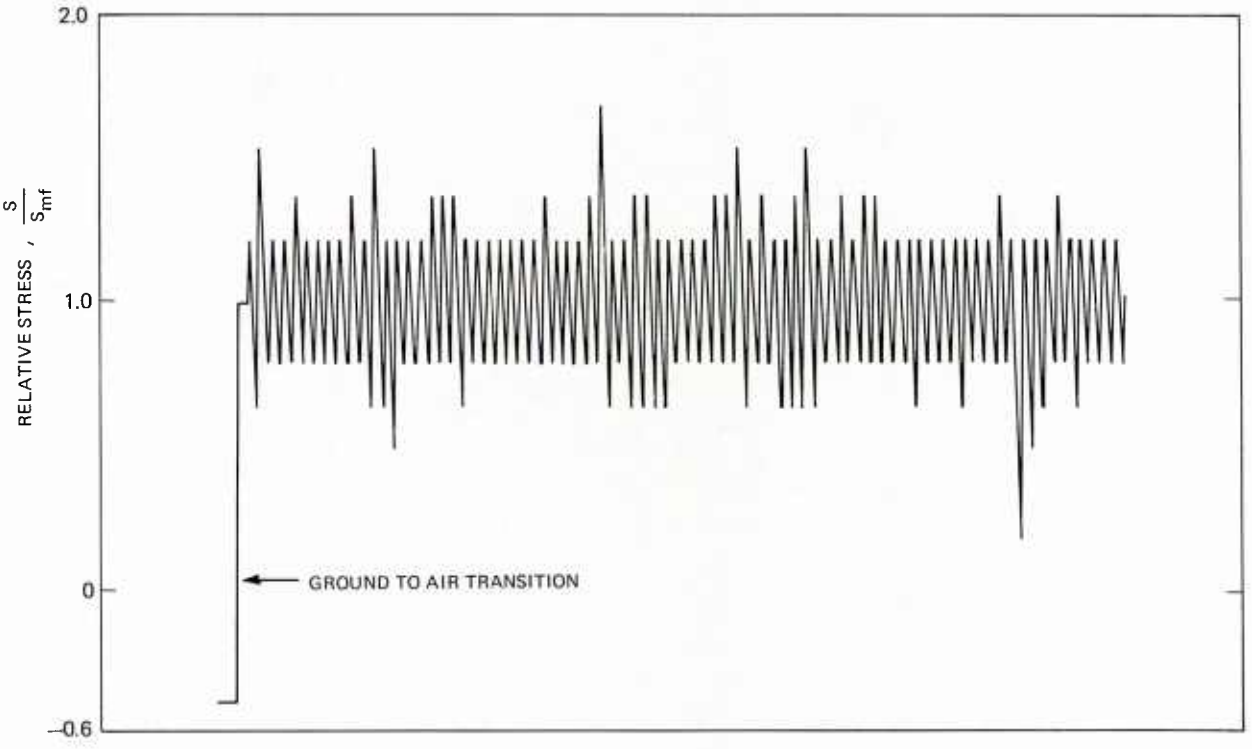

Fig. A5 Cutout of a "D"-flight loading trace within TWIST

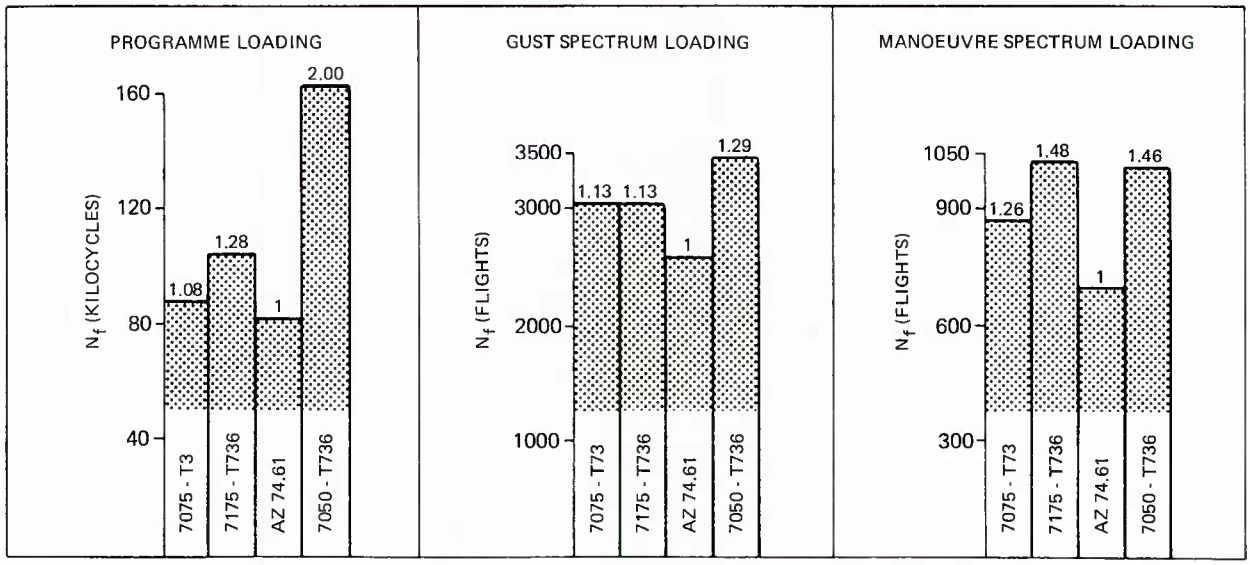

Fig. A6 A survey of mean fatigue crack propagation lives of four aluminium alloys

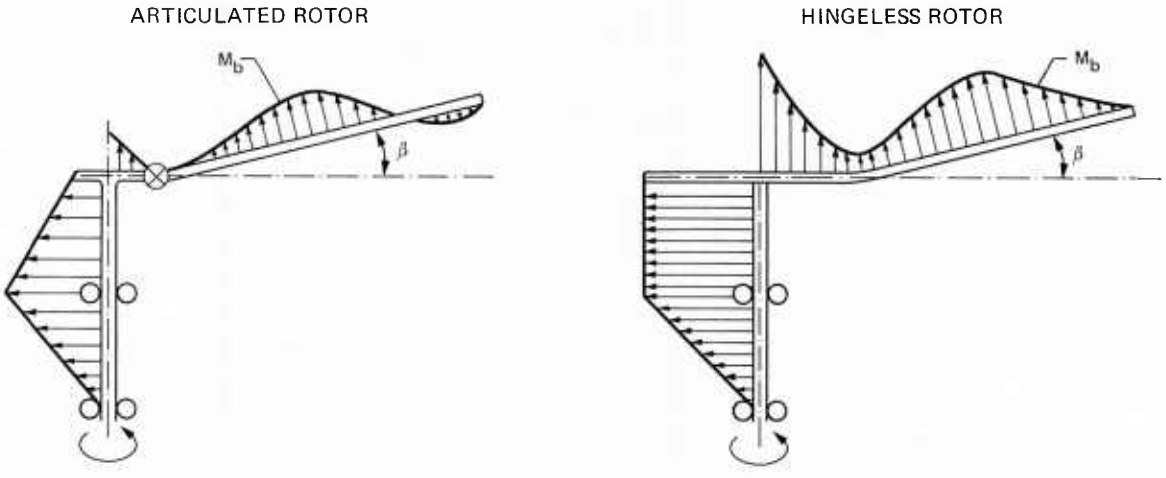

Fig. A7 Loading situation of a hingeless rotor in comparison to an articulated rotor

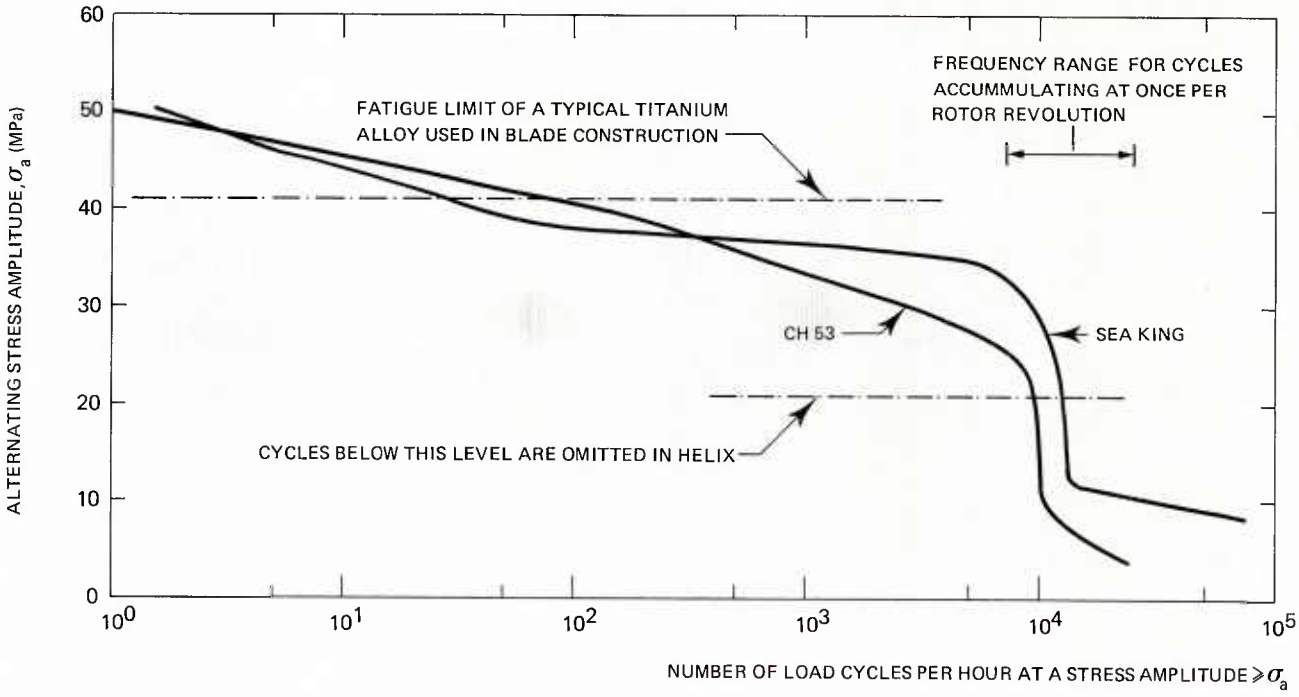

Fig. A8 Comparison of stress spectra at half rotor radius for CH 53 and Sea King transport sorties

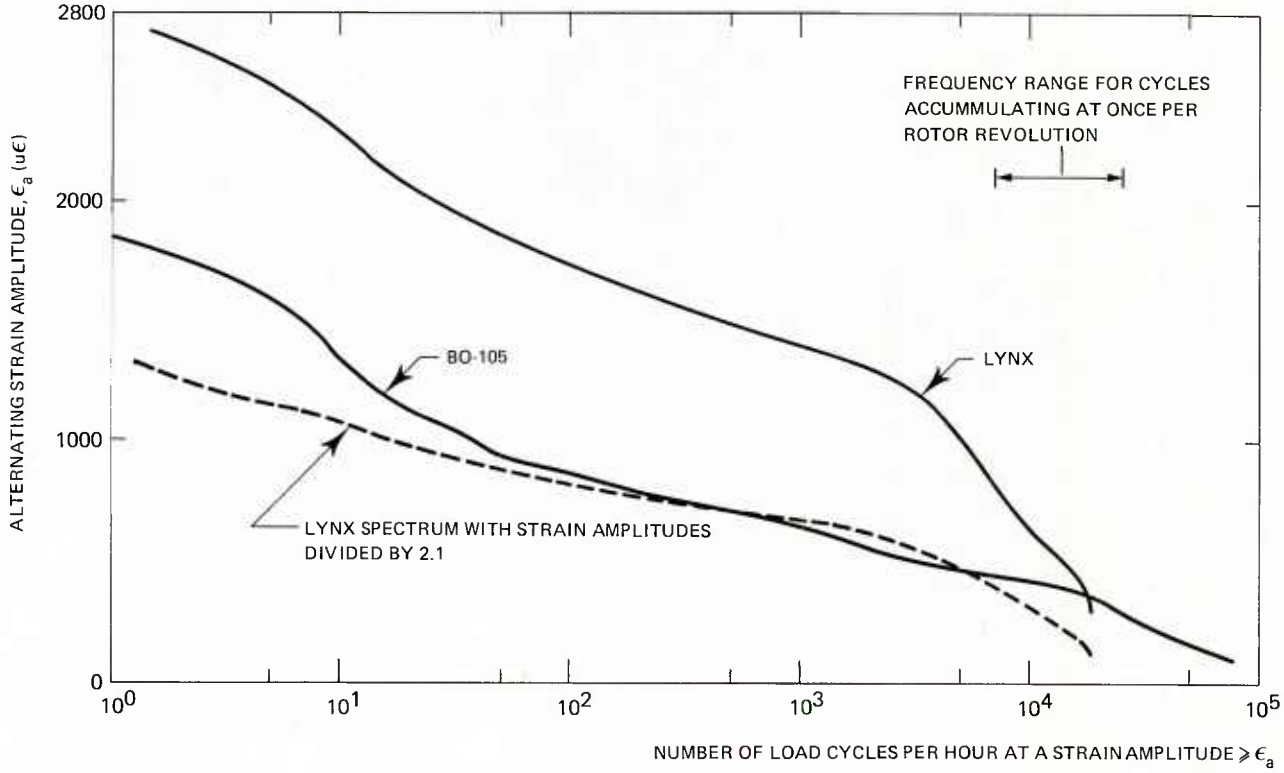

Fig. A9 Comparison of strain spectra for BO-105 and Lynx design sortie

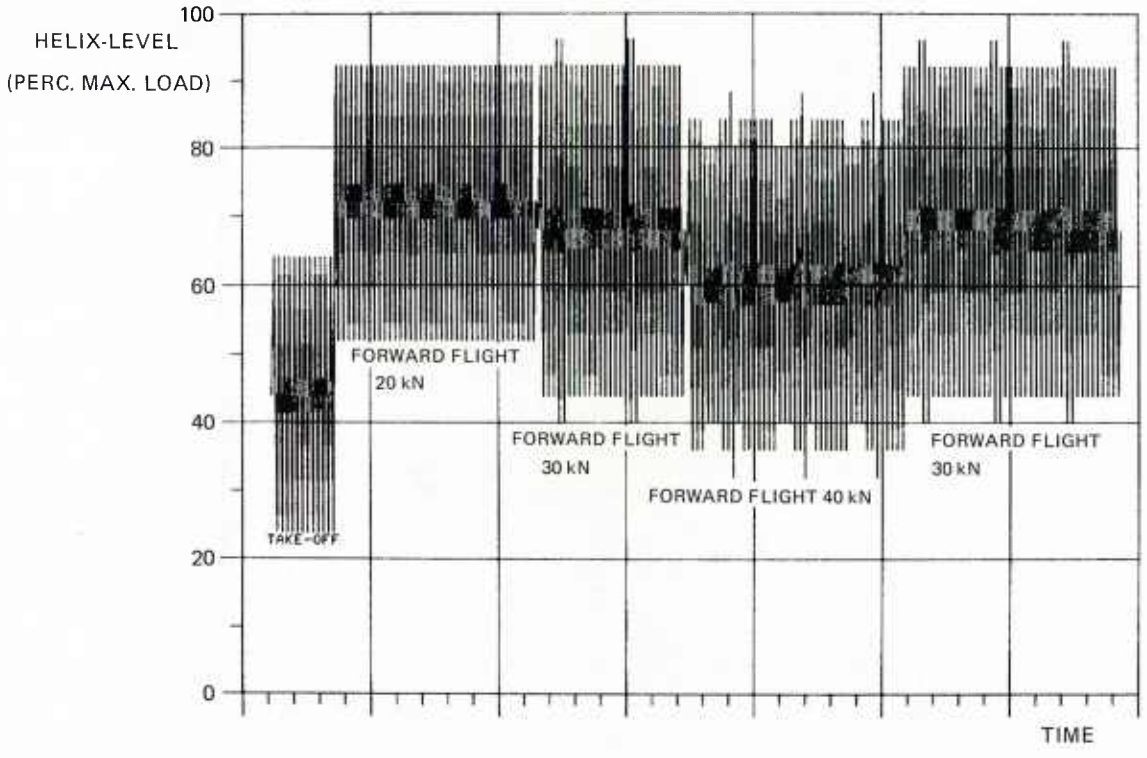

Fig. A10 Beginning of HELIX training-flight (representing 90 seconds flight time)

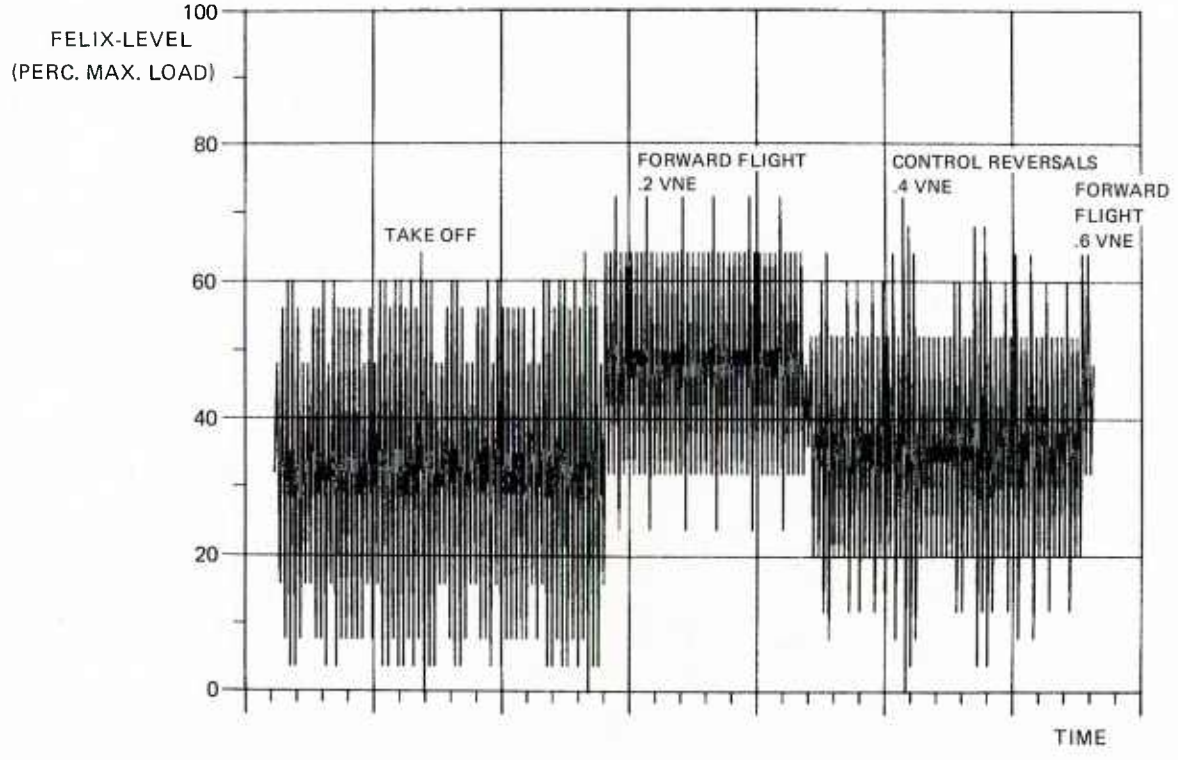

Fig. A11 Beginning of FELIX training-flight (representing 84 seconds flight time)

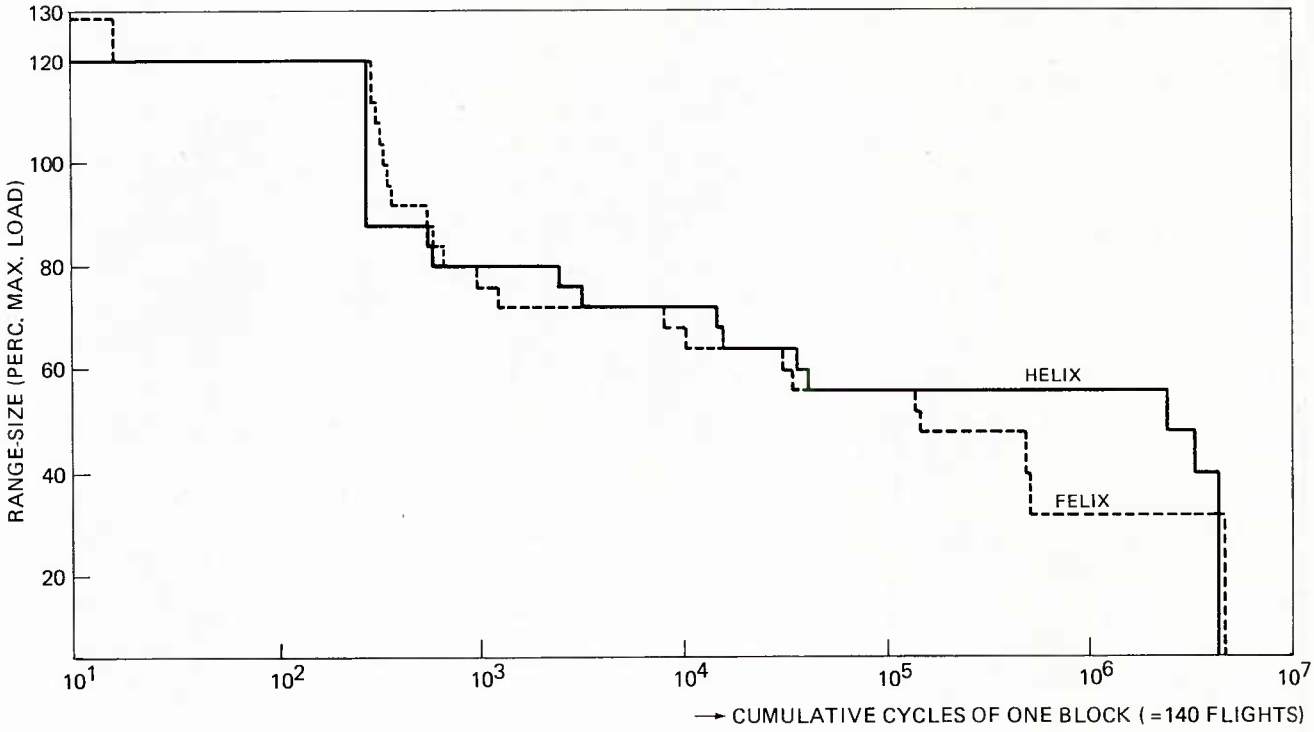

Fig. A12 Comparison of HELIX and FELIX overall spectra (full cycles, rainflow counting technique)

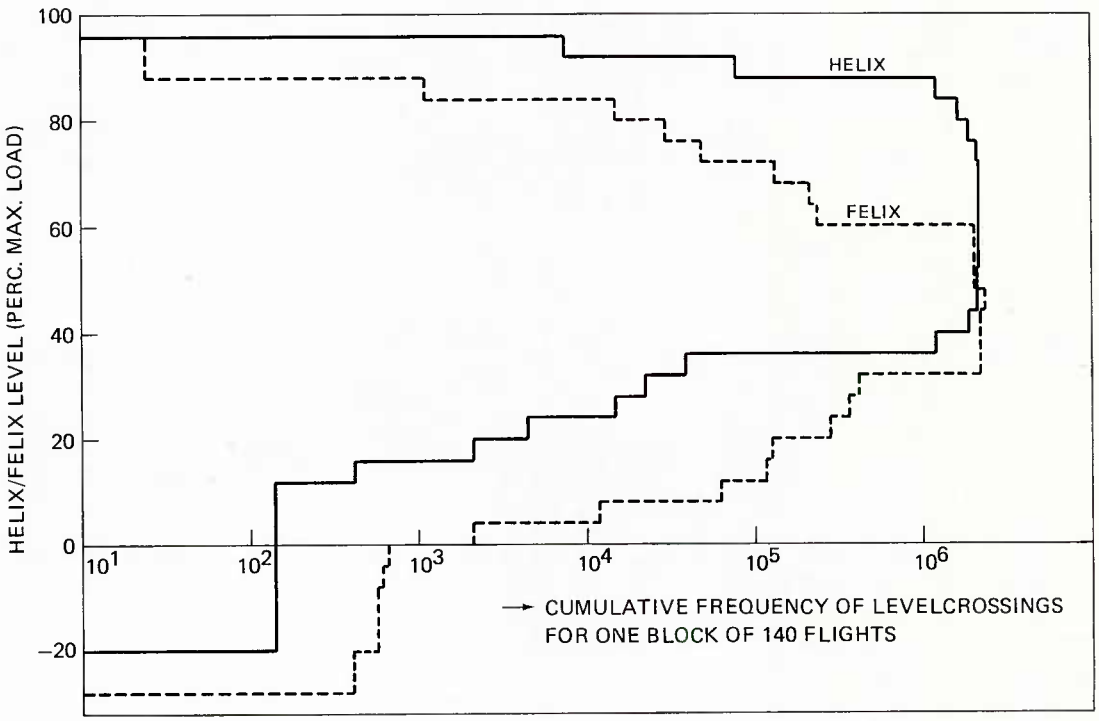

Fig. A13 HELIX/FELIX level cross counting

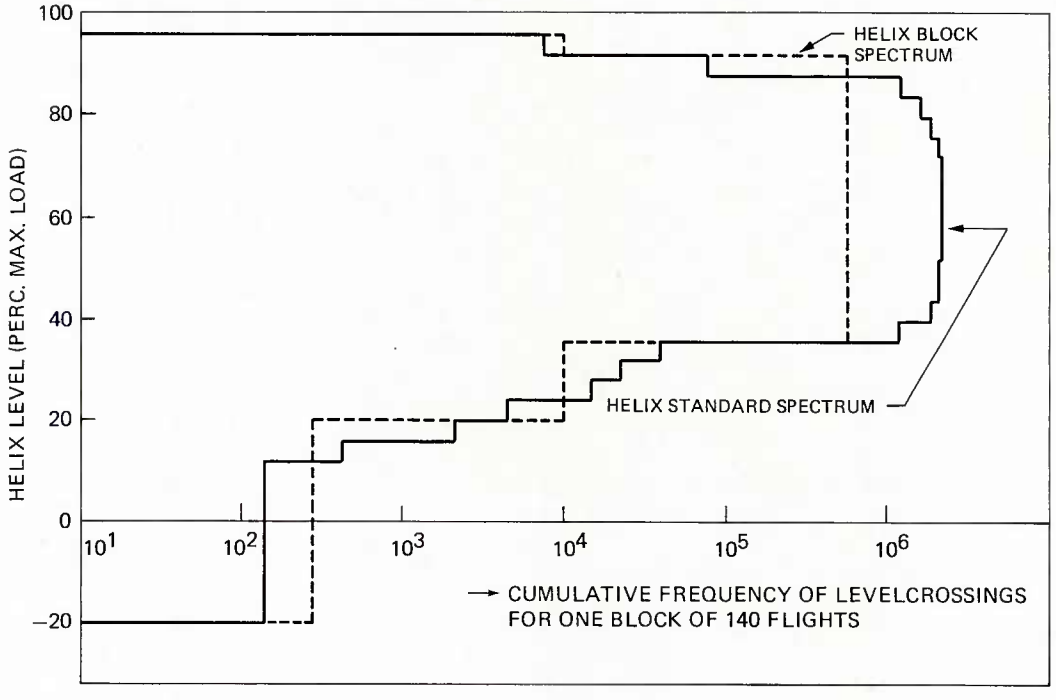

a) HELIX

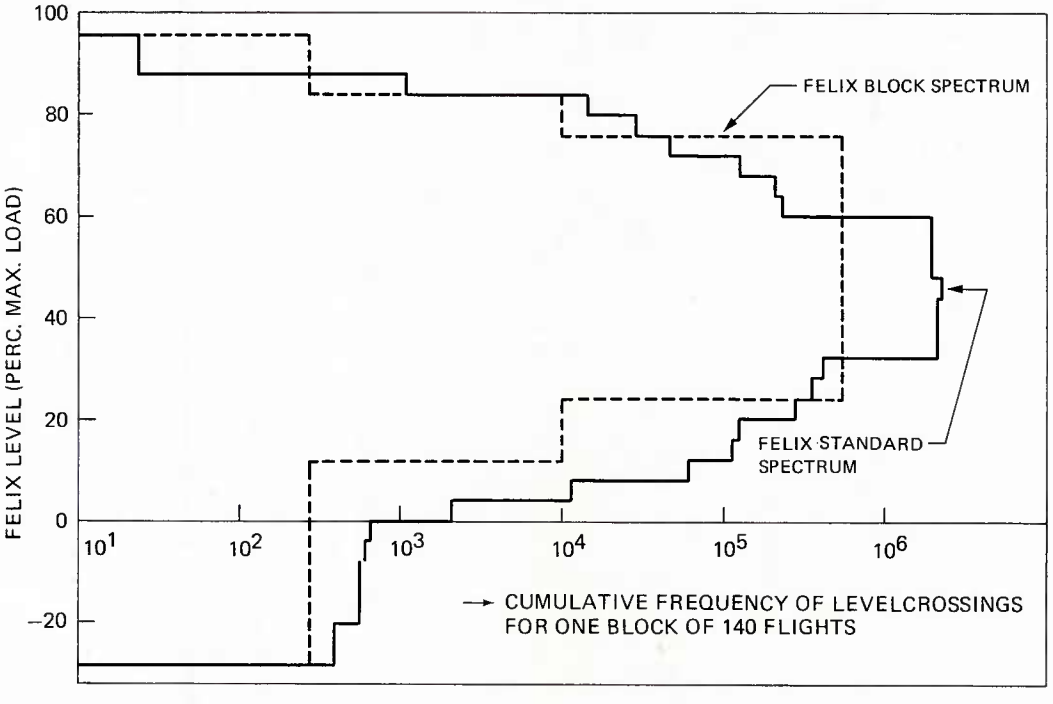

b) FELIX

Fig. A14 Standard spectra versus blocked spectra in the HELIX/FELIX evaluation test program

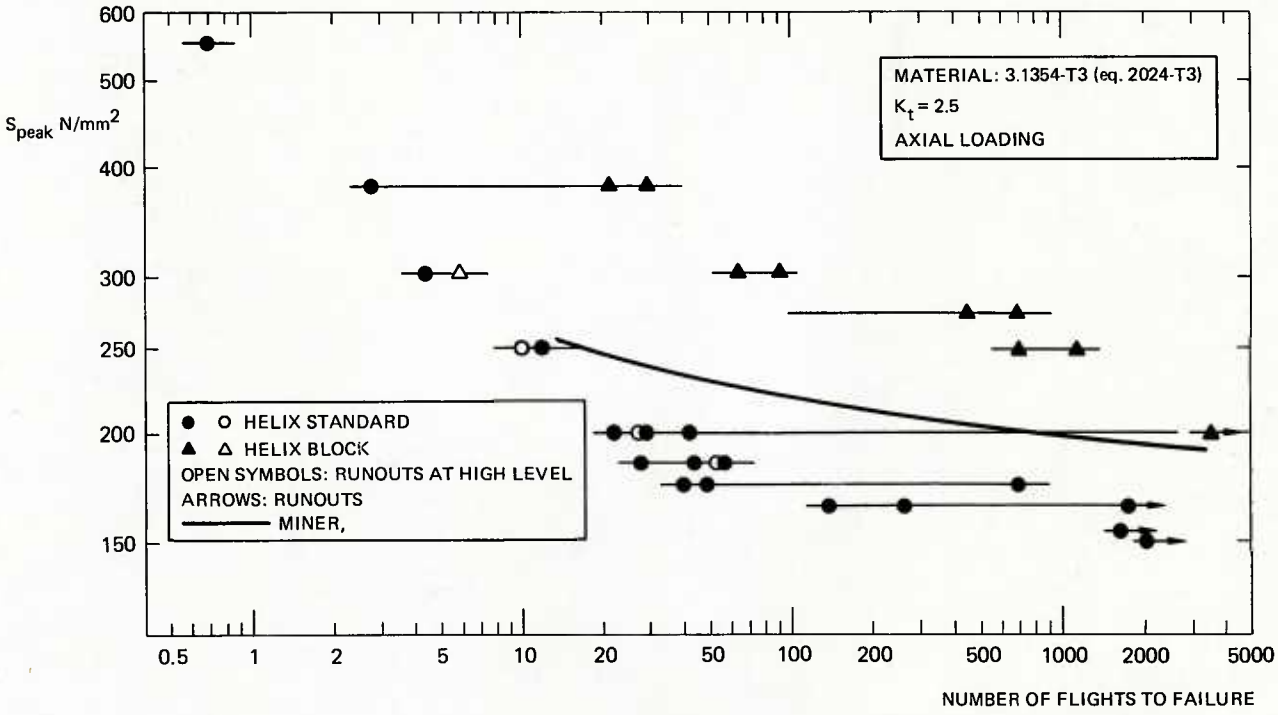

Fig. A15 Preliminary test results

AGARDograph No.292 Advisory Group for Aerospace Research and Development, NATO HELICOPTER FATIGUE DESIGN GUIDE Edited by F.Liard Published November 1983 278 pages In the course of the past few years the Structures and Materials Panel of AGARD has considered a number of aspects of the fatigue problem as it affects helicopters. The present publication constitutes a review document in which is distilled the experience of specialists from amongst the helicopter manufacturing nations of NATO. It is aimed especially at those in design offices and test houses who undertake rotary wing aircraft P.T.O	AGARD-AG-292 Helicopters Design Fatigue (materials)	AGARDograph No.292 Advisory Group for Aerospace Research and Development, NATO HELICOPTER FATIGUE DESIGN GUIDE Edited by F.Liard Published November 1983 278 pages In the course of the past few years the Structures and Materials Panel of AGARD has considered a number of aspects of the fatigue problem as it affects helicopters. The present publication constitutes a review document in which is distilled the experience of specialists from amongst the helicopter manufacturing nations of NATO. It is aimed especially at those in design offices and test houses who undertake rotary wing aircraft P.T.O	AGARD-AG-292 Helicopters Design Fatigue (materials)
AGARDograph No.292 Advisory Group for Aerospace Research and Development, NATO HELICOPTER FATIGUE DESIGN GUIDE Edited by F.Liard Published November 1983 278 pages In the course of the past few years the Structures and Materials Panel of AGARD has considered a number of aspects of the fatigue problem as it affects helicopters. The present publication constitutes a review document in which is distilled the experience of specialists from amongst the helicopter manufacturing nations of NATO. It is aimed especially at those in design offices and test houses who undertake rotary wing aircraft P.T.O	AGARD-AG-292 Helicopters Design Fatigue (materials)	AGARDograph No.292 Advisory Group for Aerospace Research and Development, NATO HELICOPTER FATIGUE DESIGN GUIDE Edited by F.Liard Published November 1983 278 pages In the course of the past few years the Structures and Materials Panel of AGARD has considered a number of aspects of the fatigue problem as it affects helicopters. The present publication constitutes a review document in which is distilled the experience of specialists from amongst the helicopter manufacturing nations of NATO. It is aimed especially at those in design offices and test houses who undertake rotary wing aircraft P.T.O	AGARD-AG-292 Helicopters Design Fatigue (materials)

design and who need information by which to determine fatigue strength and behaviour.

This AGARDograph was sponsored by the Structures and Materials Panel of AGARD.

ISBN 92-835-0341-4

design and who need information by which to determine fatigue strength and behaviour.

This AGARDograph was sponsored by the Structures and Materials Panel of AGARD.

ISBN 92-835-0341-4

design and who need information by which to determine fatigue strength and behaviour.

This AGARDograph was sponsored by the Structures and Materials Panel of AGARD.

ISBN 92-835-0341-4

design and who need information by which to determine fatigue strength and behaviour.

This AGARDograph was sponsored by the Structures and Materials Panel of AGARD.

ISBN 92-835-0341-4

AGARD
NATO OTAN
7 RUE ANCELLE · 92200 NEUILLY-SUR-SEINE
FRANCE
Telephone 745.08.10 · Telex 610176

DISTRIBUTION OF UNCLASSIFIED AGARD PUBLICATIONS

AGARD does NOT hold stocks of AGARD publications at the above address for general distribution. Initial distribution of AGARD publications is made to AGARD Member Nations through the following National Distribution Centres. Further copies are sometimes available from these Centres, but if not may be purchased in Microfiche or Photocopy form from the Purchase Agencies listed below.

NATIONAL DISTRIBUTION CENTRES

BELGIUM
Coordonnateur AGARD – VSL
Etat-Major de la Force Aérienne
Quartier Reine Elisabeth
Rue d'Evere, 1140 Bruxelles

CANADA
Defence Science Information Se
Department of National Defenc
Ottawa, Ontario K1A OK2

DENMARK
Danish Defence Research Boar
Østerbrogades Kaserne
Copenhagen Ø

FRANCE
O.N.E.R.A. (Direction)
29 Avenue de la Division Lecl
92320 Châtillon sous Bagneux

GERMANY
Fachinformationszentrum En
Physik, Mathematik GmbH
Kernforschungszentrum
D-7514 Eggenstein-Leopoldsh

GREECE
Hellenic Air Force General St
Research and Development D
Holargos, Athens

ICELAND
Director of Aviation
c/o Flugrad
Reykjavik

ITALY
Aeronautica Militare
Ufficio del Delegato Nazionale all'AGARD
3, Piazzale Adenauer
Roma/EUR

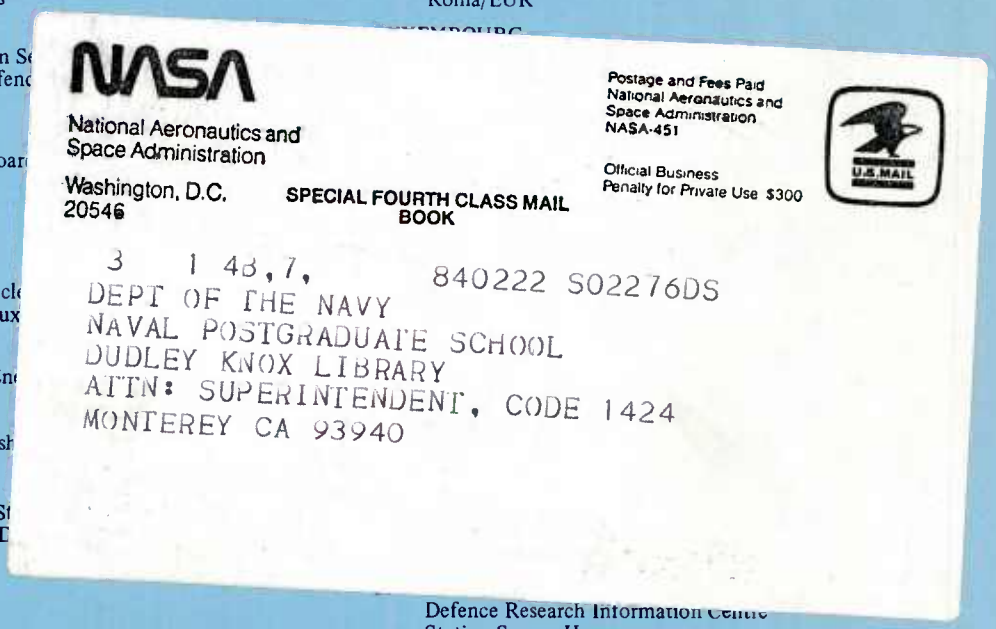

Defence Research Information Centre
Station Square House
St. Mary Cray
Orpington, Kent BR5 3RE

UNITED STATES
National Aeronautics and Space Administration (NASA)
Langley Field, Virginia 23365
Attn: Report Distribution and Storage Unit

THE UNITED STATES NATIONAL DISTRIBUTION CENTRE (NASA) DOES NOT HOLD STOCKS OF AGARD PUBLICATIONS, AND APPLICATIONS FOR COPIES SHOULD BE MADE DIRECT TO THE NATIONAL TECHNICAL INFORMATION SERVICE (NTIS) AT THE ADDRESS BELOW.

PURCHASE AGENCIES

Microfiche or Photocopy
National Technical
Information Service (NTIS)
5285 Port Royal Road
Springfield
Virginia 22161, USA

Microfiche
ESA/Information Retrieval Service
European Space Agency
10, rue Mario Nikis
75015 Paris, France

Microfiche or Photocopy
British Library Lending
Division
Boston Spa, Wetherby
West Yorkshire LS23 7BQ
England

Requests for microfiche or photocopies of AGARD documents should include the AGARD serial number, title, author or editor, and publication date. Requests to NTIS should include the NASA accession report number. Full bibliographical references and abstracts of AGARD publications are given in the following journals:

Scientific and Technical Aerospace Reports (STAR)
published by NASA Scientific and Technical
Information Branch
NASA Headquarters (NIT-40)
Washington D.C. 20546, USA

Government Reports Announcements (GRA)
published by the National Technical
Information Services, Springfield
Virginia 22161, USA

Printed by Specialised Printing Services Limited
40 Chigwell Lane, Loughton, Essex IG10 3TZ

ISBN 92-835-0341-4